Dotto Ring Evaluation for Nadia

John Smigel

23 August 2024

Table Of Contents

Introduction

This paper analyzes the technology proposed by the "Dotto Ring."

The Dotto ring works based on thermoelectric and electromagnetic effects.

For general references on topics related to the Dotto ring, see Appendix A. I avoid including links for references because they often go away or change. There are many more private references that are only available for a fee. I have not yet evaluated all the Appendix A references for scientific data supporting Dr. Dotto's claims or for their accuracy.

Some basic reference information from various sources is included in the appendices for convenience. All the specific Dotto ring information I have is included in Appendix J. For background on thermoelectric effects and thermocouples, see Appendices B and C. For electromagnetic fields, electromagnets, and magnetism background, see Appendix G.

NOTE: I am doing this for fun and to learn more about science. I do not feel much of what Dr. Dotto describes as his theory about what the ring does or how it works is accurate. I do want to investigate how strong of an electromagnetic field can be generated using just heating and cooling sources. I consider the Dotto ring a "Rube Goldberg" way of generating an electromagnetic field. There are much easier ways (directly apply a voltage to make current flow through wire rings). I can't directly address any potential biological effects, but will try to evaluate what the Dotto ring will do electrically (and look for any signs of antigravity).

Ring Evaluation Status – 4 July 2024

I am calling this approximately ¼ scale model "Nadia's Improved Dotto Ring (NIDR)." Most of the mechanical design and construction is complete. The biggest challenge so far has been getting the holes for mounting parts in the right places. It is also hard to mount flat cooling and heating surfaces to a circular ring. Dr. Dotto did not give details on how it is heated or cooled. Also, no Dotto detail is given on constantan connection size/length/resistance. This has been mostly a mechanical design/construction project so far. Electrical details will follow. Here are a few early photos:

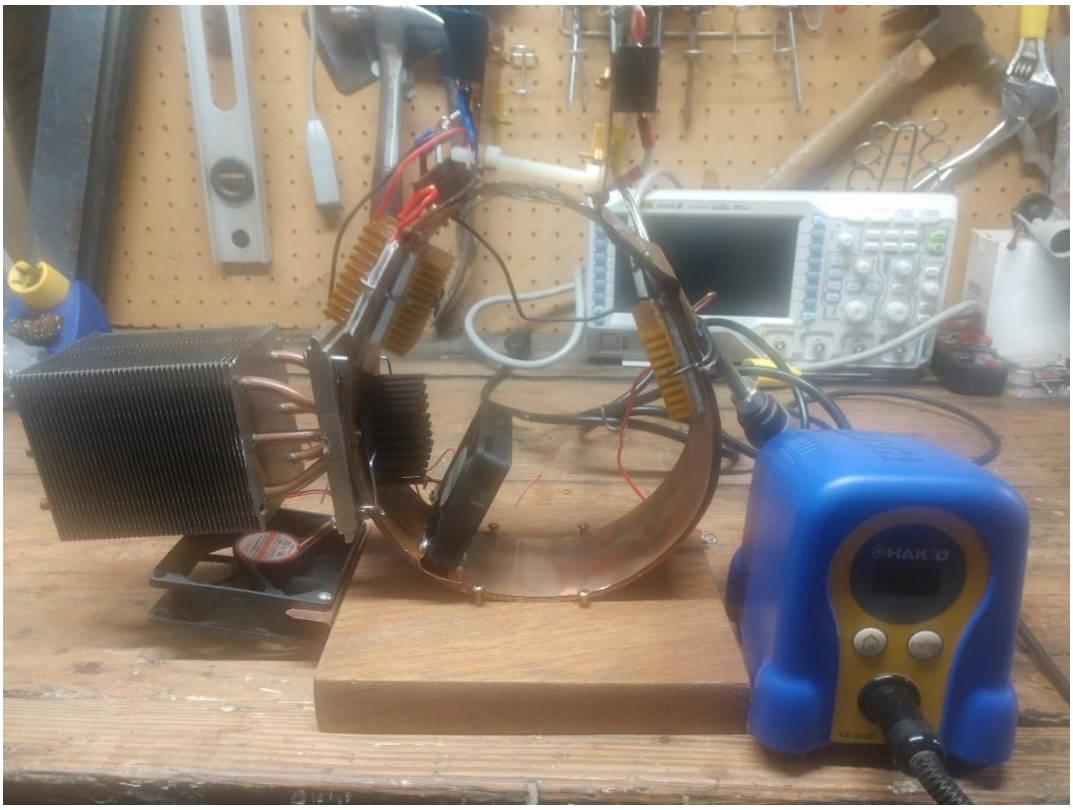

Figure 1*. Front View – cooling system on the left, heating system on the right. Note: I may try to get this to look more like a ring, but it is hard to do that and maintain the flat surfaces to mount the TEC's and heat sinks.*

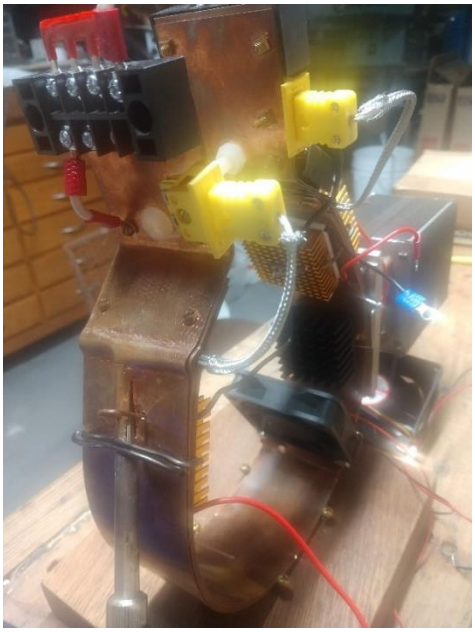

Figure 2*. Heating Side of Ring with 3 Potential Heat Sources (1. Direct heater, 2. Type E Thermocouple, and 3. Thermo-electric Cooler (TEC) configured as either heater or ring gap voltage source.)*

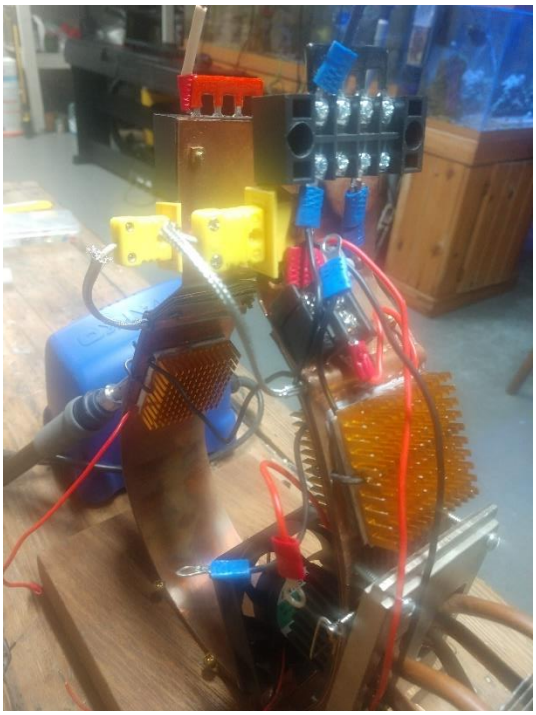

Figure 3*. Cooling Side – Active cooling near gap: 2 TEC's on both sides of the ring, Passive cooling: Large capacity heat sink with fans to intercept heat from hot side of ring. Also has a thermocouple to measure temperature or provide an additional voltage source.*

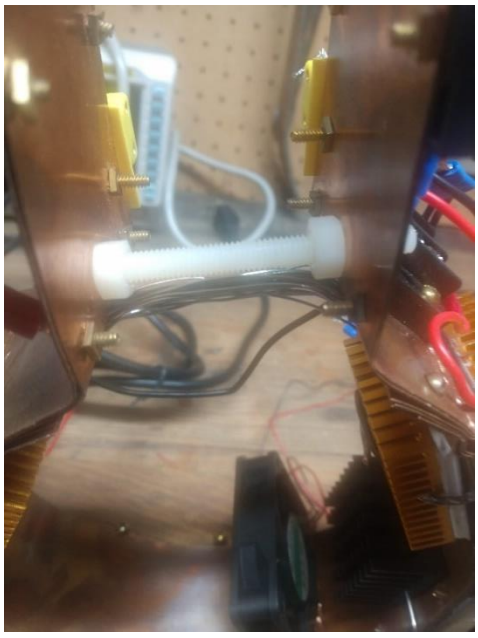

Figure 4*. Ring Gap Detail – Adjustable gap distance with Constantan wire thermocouples mechanically connected to the ring. Non-conductive bolt/nuts adjust the gap and stabilize the ring.*

I have measured the voltage vs temperature today with just the direct heating subsystem set to 750 deg F and no cooling. The type-E thermocouple produces higher voltage, as expected, since it is higher efficiency. It is slightly closer to the heat source than the gap thermocouple (type T), so it gets a little hotter. The thermocouples do not reach the set temperature of the heat source (750 deg F) due to the heat transfer/cooling of the copper and constantan. Copper is one of the most thermally conductive materials after diamond and silver. The hot junction gets to about 220 deg F. The corresponding open-circuit voltages were about 3 and 5 mV for the Type-T and Type-E thermocouples respectively. Direct heating of the Type-E thermocouple can produce at least 7 mV at a higher temperature. The adjustable heat source has a capacity of about 65W.

I have not tested my improved cooling side (original design was clearly inadequate). I'm still waiting for a few new parts for finishing the cooling components/power supply and instrumentation.

Misc. status:

- Started collecting data on scientific knowledge in areas relevant to the Dotto ring. I collected most of the freely-available books and articles and have started reviewing/cataloging them. I am weak in biology knowledge so I started taking an MIT course on biology (lectures and reading textbook (had to buy, but not expensive used)). Fascinating. This course seems to emphasize biology and biochemistry related to cancer. Also viewed a lecture on cancer.
- Remaining construction/design: details of electrical power supply to cooling system and instrumenting device (on/off, measured voltages, currents)
- Will test/measure voltage/current achieved and calculate electro-magnetic field strength. Will try to determine if alternating voltage/current can be produced by adjusting gap size/resistance (as claimed by Dotto).
- Document design, results, references found.

Status – 18 July 2024

- Tested the primary cooling subsystem yesterday with Facetime link to Nadia. Cooled down to about 62 deg F with 77-78 deg F ambient temp.
- Finished secondary cooling and TEC heating subsystems today. Wired hot temp control gauges for TEC and secondary cooling fan.
- Tested with just TEC heat source and with both TEC and Hakko Soldering Station set to 750 deg F. Not calibrated though, ordering new temp sensor to calibrate. Broke my thermometer.

Status – 28 July 2024

Have been writing the documentation (this document) while waiting for a few more parts to upgrade the analysis. I ordered ceramic insulation for the hot side of the ring (found out Styrofoam melts), a high-precision voltmeter for more-

easily measuring voltage across the constantan/gap, and a remote infrared (IR)/laser temperature sensor to help determine heating and cooling characteristics. The temperature sensor has both remote and contact (thermocouple probe) modes. It listed a capability to measure up to 1000 deg F, but I found out this was only for the IR mode. The probe mode only measures to 500 deg F. I already had a better probe sensor accurately measuring to almost 500 deg F. My new temperature sensor is not very accurate at lower temperatures. I have not been able to find an inexpensive thermocouple-based temperature probe that goes above 500 deg F.

I want to be able to predict how much energy and power are required to heat and cool the ring to a particular steady-state temperature difference. If I develop mathematical equations for this, I can determine the best ring configuration (maximize current with some constraint on ring diameter). This is complicated by the need to both heat and cool the copper ring at the same time.

The measured results with just the single inside TEC as a heat source and the combined TEC and Hakko Soldering station are shown in the results section here.

Note that the terms “hot” and “cold” are usually used for the thermocouple temperature differences. I’m using the term “cool” instead of “cold” because the “cold” side in this application may only be less hot and not really cold.

I get significantly lower voltage measured around the ring when the wires are connected to copper on both sides. This means the copper resistance, Rcu, is significantly less than the constantan resistance, Rcon, as expected.

The predicted ring resistance for a solid copper ring with the NIDR dimensions is about 51.8 uOhms. This is quite a bit less resistance than the 235 uOhms I am measuring. As long as all the layers have good electrical contact at the beginning and end, the multiple-layer construction should not increase resistance. Putting the constantan wires between the copper layers may have increased the resistance at the beginning and end. My copper is only 99.95% pure compared with Dotto’s spec of 99.99%, but hard to believe that makes much difference. Perhaps my voltage and current measurements are not accurate enough. I checked the current measurement with a different (admittedly inexpensive) hall-effect current meter and it agreed. I’ll work on making sure my measurements are accurate.

I’m measuring a lower-than-predicted resistance for the constantan wires. I’m not sure about the exact number of wires, might be more than estimated 20. I should have counted accurately when I put them in.

Status – 29 July 2024

Finished the documentation except results, discussion, and lessons learned. After mounting the precision voltmeter above the current gap meter, I found the heating TEC controller was broken. I took it apart and tried to fix it, but no luck. Also, was getting a short across the 12v supply and it was shutting off immediately for protection. This problem seems to have gone away. May have been caused by the broken controller? I ordered another pair of controllers that should come in a couple of days. Finished all the other wiring and adding the ceramic insulation to the hot side. Had to move the voltage reference to the left ear (point B). The soldering iron grounds this point anyway.

Fired it up this morning with just the soldering iron source. Did not get as hot, as expected. The max hot temperature was 195 deg. Note that this is still above the operating temp range for the TEC. Current, voltage and temperature readings seemed consistent with previous measurements. Checked the new precision voltmeter voltage across the constantan with the Fluke meter and they matched (was 0.4mV). I soldered some wires to the ends of the constantan wires to make sure the voltage is measured across the constantan (this is another thermocouple – so how does this change things?).

Status – 1 August 2024

I finished making the custom heat shield yesterday from ceramic insulation with a polyurethane coating. It doesn't look pretty, but should be less annoying and protect the temperature controller that got toasted. I was going to try to run the hot side even hotter by using the heat shield and increasing the soldering iron temp up to 850 deg F. Even though I'm not using the TEC as a cooling device, I don't want to break another one by overheating it. The max operating temperature of the device is 181 deg F. I already destroyed one thermocouple by overheating it. I tried to solder larger conductors to see if I could increase the current capability, but I just melted the solder holding the thermocouple wires together. So, I guess I'll set the shutoff temp on the replacement controller that burned up at about 180 to 200 deg F. It may still break if the temperature gets much above this. Not sure what the storage/survival temperature is.

The original voltmeter of the combined volt/current meter used to measure the gap voltage and current can't measure low-enough voltages (a few millivolts). I switched to a high-precision voltmeter that I added on top instead. Since I wasn't using other the voltmeter for anything anymore, I decided rather than just showing 0.0 volts all the time, I would try to use it for something. I have been considering trying to use one of the TEC thermopiles to generate more current in the ring. I have not figured out a good way to do this or if it is possible. The main problem is that the internal resistance of the device is relatively high, about 2 to 4 ohms. The resistance of the constantan gap wires is only about 3.25 mOhms. Also, the max rated current of the TEC is about 6 amps.

Status - 2 August 2024

I burned out the primary heating TEC. The problem is that I can only get the hot side thermocouple junction up to the max TEC operating temperature without burning it out. The maximum operating environment temp spec is 181 deg F. The maximum working temperature is 248 deg F. The most common solder melts at about 360 deg F. Not sure exactly what temperature breaks it.

I decided to give up on using the soldering iron to heat. The power and connection area are too low. The iron tip is mounted on top of the primary TEC chip and I have been setting the temp to between 750 deg F and 850 deg F (Has not been able to get above 750 deg F). It is not surprising that the TEC chip burned out. I'm not sure the ring will provide enough cooling to the TEC used as a heater while trying to get above 200 deg F. For now, I plan to stick with the TEC chips to heat because: 1) they are inexpensive (about $4.30 each), 2) I prefer to use the same component for both heating and cooling to minimize the number of different components, and 3) I'm familiar with them now. There are more powerful TEC's available, but they may not have a higher operation temperature.

I modified the heating design to allow adding up to two TEC chips for heating. They are still turned on and off by the temperature-based controller. A single controller will control both TEC's. I ordered more TEC's. They should come tomorrow. I also ordered a higher power TEC, TEC1-12615, with a max current of 15 amps instead of 6. Cost < $4. Not sure what I'll get. Coming directly from China by Sept 13Update: Not surprisingly, what I received was not really a 15-amp chip, but a lower-cost and power chip labelled as the 15-amp part. Not worth arguing over. At least the chip somewhat worked, which is better than some past experiences.

Using a higher power heating TEC might cause even more overheating problems. It also might start to exceed the 20A max (240W) of the power supply I'm using. I have a 30A supply, if I really need more power.

I plan to put a heating TEC on both ring sides near the top. I finished most of the modifications today. I'm just waiting for the replacement TEC.

Status – 4 August 2024

Well, yesterday was challenging. I was hoping it would go better. I finished the new heating subsystem design that uses two TEC devices (heat pumps) and no longer uses the Hakko soldering station for heating. I removed the Hakko from the design because: 1) Small tip area is ineffective at transferring enough heat fast enough to the ring, 2) Small tip at high temperature makes local hot spot that burns out TEC device connected to the other side of the ring, 3) Hakko is expensive, 4) prefer a solution that does not required a separate heating device. However, it will not be possible to get a hot

temperature above the max operating temperature of the TEC device, somewhere between 181 deg F and 248 deg F for the TEC1-12606.

I made a new heat shield for the bottom heating TEC, but have not used it yet. It will be challenging to install.

I ordered replacement TEC's from a different source in a package of 5 TEC's without the heat sinks. I already have enough inadequate heat sinks. The new devices are slightly less expensive, so that is a risk. The first new problem, so far, is that I installed the TEC devices backwards with the cooling side against the ring, instead of the heating side. This was not all my fault. You are supposed to be able to tell the hot side from the cold side based on which side has the device model printed on it. Printing is supposed to be on the hot side, according to the instructions. I found out that the new devices have the printing on the cool side! Not a good sign for the new device quality. The new TEC's are also a little thicker than the first ones. One of the 5 TECs had a cracked corner. Not sure if that will impact performance. Decided to use the cracked one first in case I burn the first ones out. A better way of determining the hot side (than side with writing): place the device on a flat surface with the wires down and the black wire on the right – the top side is hot.

Remaining problems:

1) Not getting the hot side temperature as high as I would like. It is also taking a long time to heat up. I would like to get back to at least the 213 deg F max temperature I achieved with one TEC plus the Hakko. At a minimum would like to get above ¼ of the 800 deg F Dotto max temperature (since this is a ¼ scale model). Reached about 130 deg F with a single heating TEC and about 170 deg F with two TECs. The 130 deg F with a single TEC is consistent with the previous measurement. I was expecting to get higher than 170 deg F with 2 TEC's. Also not getting as much current drawn from the 12v supply as I expect. Only drawing about 9 amps with all 3 TECs and the 2 fans all running. The TECs are supposed to draw 4-5 amps each so 3 running is expected to draw 12 to 15 amps. The fans and meters are another couple amps. The resistance and power drawn by the TEC must depend on the temperature. The new TEC's might not be as powerful as their spec. Also, should check that voltage to TECs is not dropping significantly below the nominal 12v. On the plus side, I might be able to use higher-power TECs without exceeding the 12v, 240W power supply's limit.
2) It's not clear the inside cracked TEC is fully working. When operated with both TEC's running, the heat sink attached to the cold side is getting hot instead of cold. I ran with just the inside TEC powered and the cold side did get a little cold. The total current drawn was a little above 6 amps. The TEC not getting cold when both are on might be because I don't have the heat shield installed on the inside TEC. Will try installing a heat shield on the inside TEC.
3) The precision voltmeter is not reading the voltage across the constantan accurately. When I tested with just the outside heating TEC (see video), the gap

voltage measured was about 5.9 mVolts when the cooling TEC was on and then dropped down to 3.2mVolts when the cooling TEC shut off. This is clearly a problem: 1) 5.9 mVolts is way too high for the constantan voltage (should be <1 mVolts at these temps). Also, the constantan voltage should not instantly have a large drop when change when the cooling TEC shuts off. For my new configuration, I am attaching the precision voltmeter (need easier name) negative reference (black wire) to the B? negative source connection on the terminal strip. Ideally, all the negative terminal strips should be at the same voltage and this should be the negative voltage of the 12v supply. But since current is flowing through the power strip and it has significant resistance of the connections between the terminals, not all the B (negative) terminals are at the same voltage. I verified that the 9mVolt measurement was the correct measurement using the Fluke meter, so the meter is working (could be worse). I determined that the negative (B) voltage terminal strips vary in voltage by about 9 mVolts from one end of the terminal strip to the other. The voltage measured by the precision voltmeter was being dominated by the voltage drop in the terminal strip. I tried to move the meter negative reference to the negative end of the constantan gap and learned another lesson (see next problem). I'm not sure how or why I was getting a good precision voltmeter measurement on 29 July – see status writeup above.

4) Accurately measuring the small voltage across the constantan wires is difficult. The Fluke meter seem to work, but I need to manually touch the meter probes to each end of the constantan wires, not easy. I could just use the previously-measured constantan resistance (approximately constant) and multiply by the Hall-sensor-measured current that appears accurate to about 0.1 amp. But I bought and installed the precision voltmeter, so I want to get it working. My goal was to enable videoing the ring operation and being able to see the changes in temperature, voltage, and current just by watching the video. I think I understand the problem. I soldered thick copper wires to the ends of the constantan gap to make a place to connect the precision voltmeter. However, using thick copper wires to make the connection was a mistake. The thick copper wires connected to the constantan makes 2 additional thermocouples that are activated by the hot temperature of the constantan wires, at least on the hot side. I verified that the voltage at the copper wire output is different from the voltage measured by directly connecting the probes to the ends of the constantan. The negative voltage reference for the meter needs to be attached to the negative side of the constantan gap, the hot side. Connecting the precision voltmeter through 2 thermocouple junctions with changing temperatures is clearly not a good solution for gap voltage measurement (I'm going to call the voltage across the constantan the "gap voltage"). Note that if you connect a voltmeter across the copper ears of the ring, you measure what I call the "copper voltage." This is the voltage across the copper side of the ring. This is equal to the ring current times the copper resistance. This is typically much lower than the gap voltage.

Planned solutions attempts:

1) Inadequate hot temperature problem: Try installing inside heat shield and alternate TEC on inside (not cracked and higher power, when received)
2) Gap voltage measurement problem: Connect the voltmeter to constantan using constantan wires instead of the copper wires. Remove the copper wires soldered to the constantan.
3) Inside TEC not getting cool problem: Same as 1) above.

Status – 5 August 2024

I completed the planned changes to fix the gap voltage measurement problem, replaced the inside TEC, and added thermal insulation to the inside TEC. The device seems to be fully working now, but only reaches a maximum steady-state temperature of 189 deg F after about 10 minutes. The TEC heater is not as effective as the soldering iron set at >750 deg F, but I'm not going back to using the soldering iron. The soldering iron by itself only achieved a 178 deg F maximum temperature. To increase the temperature back above the 200 deg F goal, I plan to upgrade the heating TECs to 10-amp or 15-amp devices. I'm not yet sure how hot they can get before they burn out. Probably somewhere between the 181 and 248 deg F listed as the max environment and operating temperatures for the 6-amp device.

I took 4 videos:

1) Cooling only
2) Inside heating TEC only powered
3) Both heating TECs powered
4) Both TECs powered with digital oscilloscope measurements

The videos are too large to directly include in this document without breaking it. Here's a link to the bottom video:

a. 4 – Both heating with scope.

Ring Analysis

Ring Electrical Circuit

The Dotto ring is a simple device that consists of two connected thermocouples, a heat source, and a cooling source. The Dotto design uses a type-T thermocouple with copper and constantan as the two different metals. Heating the copper-constantan junction produces a voltage across the junction. The copper becomes a positive voltage source (anode) and the constantan is a negative voltage (cathode) relative to the copper. Note that electrons flow from negative to positive voltage, but by convention, positive current flows from positive voltage to negative voltage. The resulting voltage produces current through the copper and constantan.

An electrical circuit for the device is shown in Figure 5. You can't get much simpler.

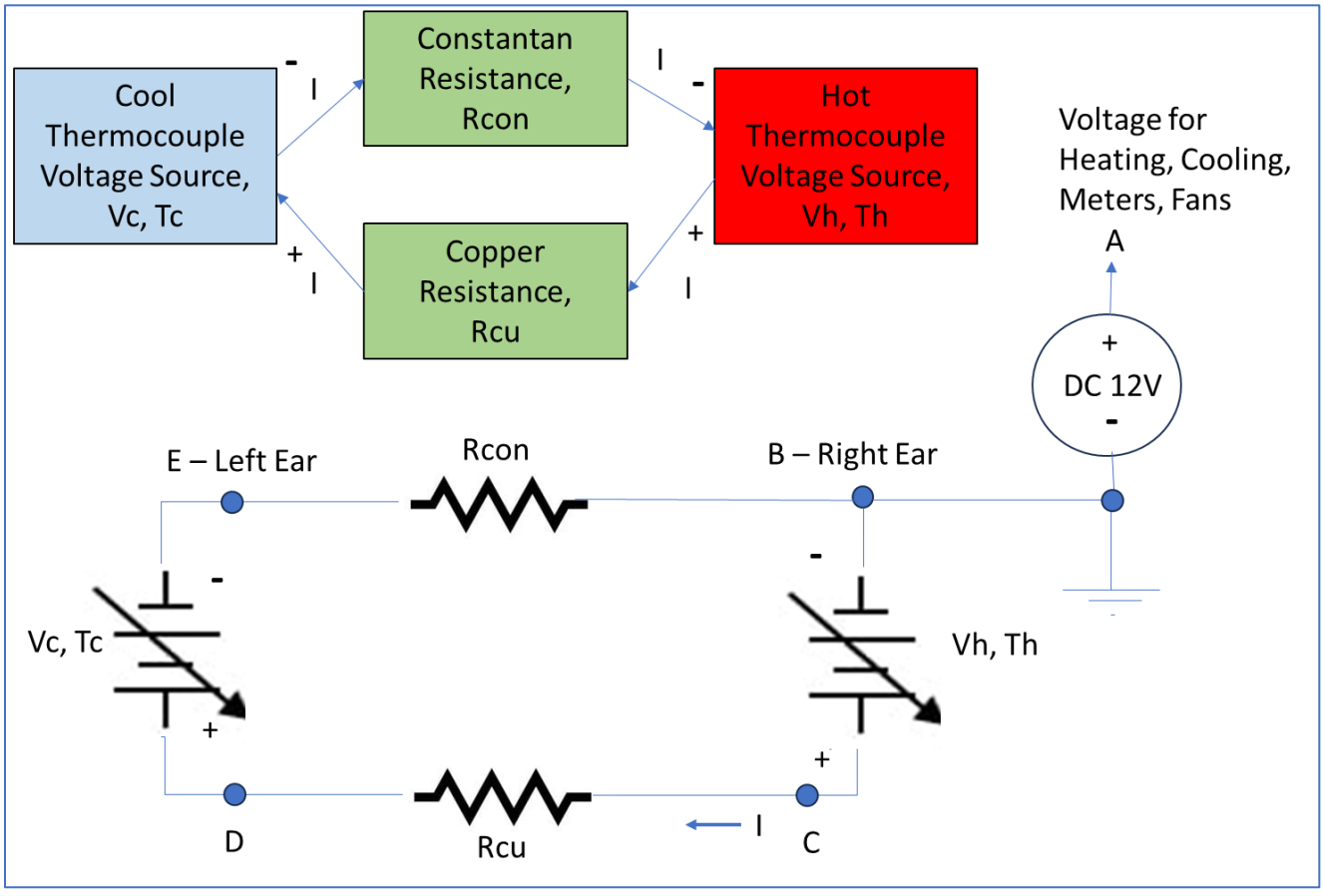

***Figure 5**. Electrical Circuit for Dotto Ring*

The variable DC voltages from the thermocouple junctions, Vc and Vh, depend on the temperatures at the junction and wires connected to the junction. There is only one path for the current, I. The thermocouple voltages will try to drive current in opposite directions so the current, I, is given by

$$I = (Vh-Vc)/(Rcon+Rcu). \quad (1)$$

Or using

$$Vnet = Vh-Vc \quad (2)$$

and

$$Rtot = Rcon+Rcu \quad (3)$$

then

$$I = Vnet/Rtot. \quad (4)$$

Note that a positive current is defined as going around clockwise from the positive side of Vh. This is the expected current direction when Vh is larger than Vc and Th is hotter than Tc. Heat will tend to flow from the Vh junction to the Vc junction through both the copper and constantan connections. As heat flows from Vh to Vc, Th and Tc will become closer, making the current decrease. With no additional heating or cooling, eventually Vh will equal Vc and the current will stop (I=0).

Figure 6 lists the expected type T thermocouple voltage versus junction temperature.

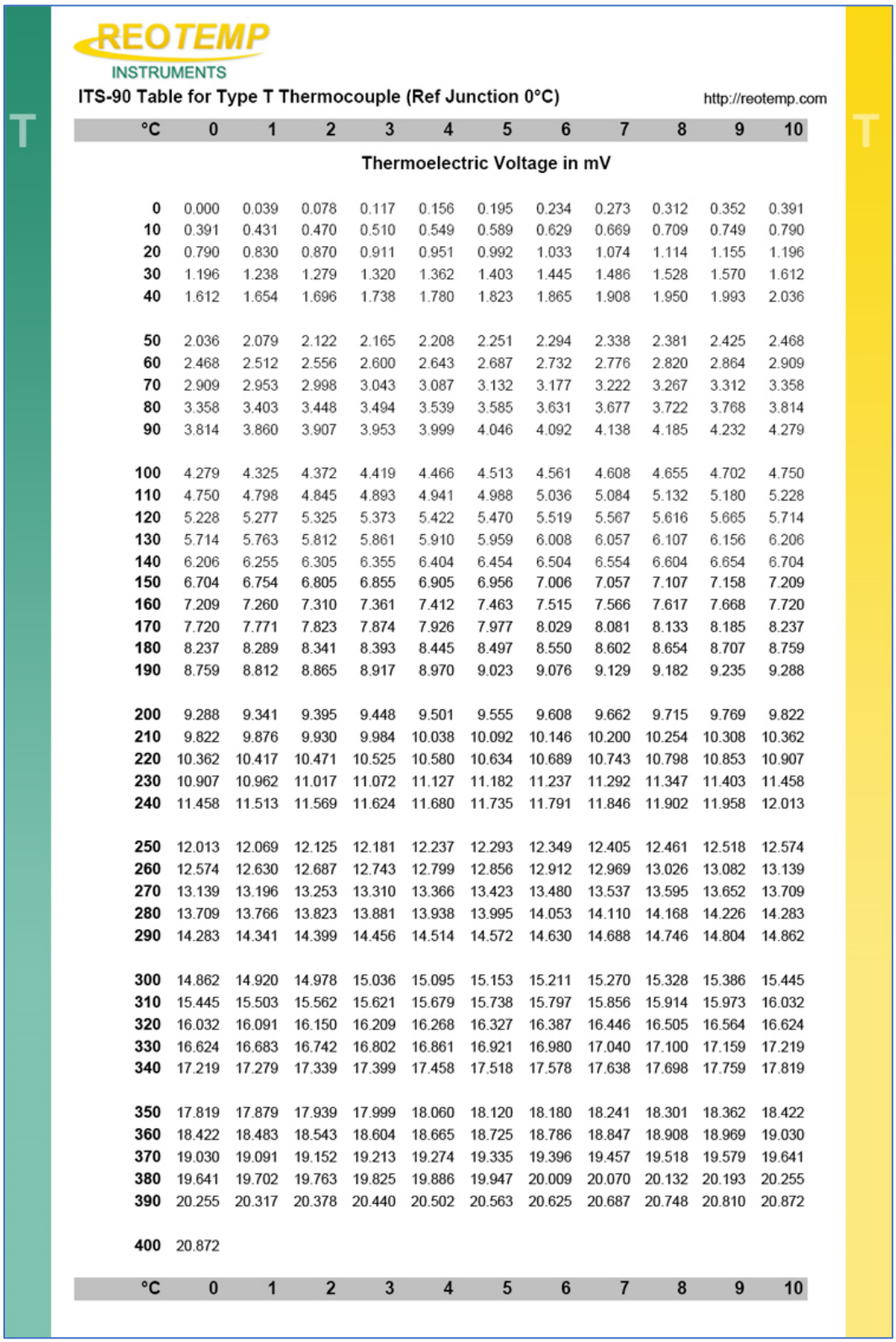

REOTEMP INSTRUMENTS

ITS-90 Table for Type T Thermocouple (Ref Junction 0°C) http://reotemp.com

T T

Thermoelectric Voltage in mV

°C	0	1	2	3	4	5	6	7	8	9	10
0	0.000	0.039	0.078	0.117	0.156	0.195	0.234	0.273	0.312	0.352	0.391
10	0.391	0.431	0.470	0.510	0.549	0.589	0.629	0.669	0.709	0.749	0.790
20	0.790	0.830	0.870	0.911	0.951	0.992	1.033	1.074	1.114	1.155	1.196
30	1.196	1.238	1.279	1.320	1.362	1.403	1.445	1.486	1.528	1.570	1.612
40	1.612	1.654	1.696	1.738	1.780	1.823	1.865	1.908	1.950	1.993	2.036
50	2.036	2.079	2.122	2.165	2.208	2.251	2.294	2.338	2.381	2.425	2.468
60	2.468	2.512	2.556	2.600	2.643	2.687	2.732	2.776	2.820	2.864	2.909
70	2.909	2.953	2.998	3.043	3.087	3.132	3.177	3.222	3.267	3.312	3.358
80	3.358	3.403	3.448	3.494	3.539	3.585	3.631	3.677	3.722	3.768	3.814
90	3.814	3.860	3.907	3.953	3.999	4.046	4.092	4.138	4.185	4.232	4.279
100	4.279	4.325	4.372	4.419	4.466	4.513	4.561	4.608	4.655	4.702	4.750
110	4.750	4.798	4.845	4.893	4.941	4.988	5.036	5.084	5.132	5.180	5.228
120	5.228	5.277	5.325	5.373	5.422	5.470	5.519	5.567	5.616	5.665	5.714
130	5.714	5.763	5.812	5.861	5.910	5.959	6.008	6.057	6.107	6.156	6.206
140	6.206	6.255	6.305	6.355	6.404	6.454	6.504	6.554	6.604	6.654	6.704
150	6.704	6.754	6.805	6.855	6.905	6.956	7.006	7.057	7.107	7.158	7.209
160	7.209	7.260	7.310	7.361	7.412	7.463	7.515	7.566	7.617	7.668	7.720
170	7.720	7.771	7.823	7.874	7.926	7.977	8.029	8.081	8.133	8.185	8.237
180	8.237	8.289	8.341	8.393	8.445	8.497	8.550	8.602	8.654	8.707	8.759
190	8.759	8.812	8.865	8.917	8.970	9.023	9.076	9.129	9.182	9.235	9.288
200	9.288	9.341	9.395	9.448	9.501	9.555	9.608	9.662	9.715	9.769	9.822
210	9.822	9.876	9.930	9.984	10.038	10.092	10.146	10.200	10.254	10.308	10.362
220	10.362	10.417	10.471	10.525	10.580	10.634	10.689	10.743	10.798	10.853	10.907
230	10.907	10.962	11.017	11.072	11.127	11.182	11.237	11.292	11.347	11.403	11.458
240	11.458	11.513	11.569	11.624	11.680	11.735	11.791	11.846	11.902	11.958	12.013
250	12.013	12.069	12.125	12.181	12.237	12.293	12.349	12.405	12.461	12.518	12.574
260	12.574	12.630	12.687	12.743	12.799	12.856	12.912	12.969	13.026	13.082	13.139
270	13.139	13.196	13.253	13.310	13.366	13.423	13.480	13.537	13.595	13.652	13.709
280	13.709	13.766	13.823	13.881	13.938	13.995	14.053	14.110	14.168	14.226	14.283
290	14.283	14.341	14.399	14.456	14.514	14.572	14.630	14.688	14.746	14.804	14.862
300	14.862	14.920	14.978	15.036	15.095	15.153	15.211	15.270	15.328	15.386	15.445
310	15.445	15.503	15.562	15.621	15.679	15.738	15.797	15.856	15.914	15.973	16.032
320	16.032	16.091	16.150	16.209	16.268	16.327	16.387	16.446	16.505	16.564	16.624
330	16.624	16.683	16.742	16.802	16.861	16.921	16.980	17.040	17.100	17.159	17.219
340	17.219	17.279	17.339	17.399	17.458	17.518	17.578	17.638	17.698	17.759	17.819
350	17.819	17.879	17.939	17.999	18.060	18.120	18.180	18.241	18.301	18.362	18.422
360	18.422	18.483	18.543	18.604	18.665	18.725	18.786	18.847	18.908	18.969	19.030
370	19.030	19.091	19.152	19.213	19.274	19.335	19.396	19.457	19.518	19.579	19.641
380	19.641	19.702	19.763	19.825	19.886	19.947	20.009	20.070	20.132	20.193	20.255
390	20.255	20.317	20.378	20.440	20.502	20.563	20.625	20.687	20.748	20.810	20.872
400	20.872										
°C	0	1	2	3	4	5	6	7	8	9	10

***Figure 6**. Type T Thermocouple Voltage vs Junction Temperature*

Figure 7 plots the thermocouple voltage versus temperature, called the characteristic function, for different types of thermocouples. Figure 8 shows a similar chart with linearized characteristic functions.

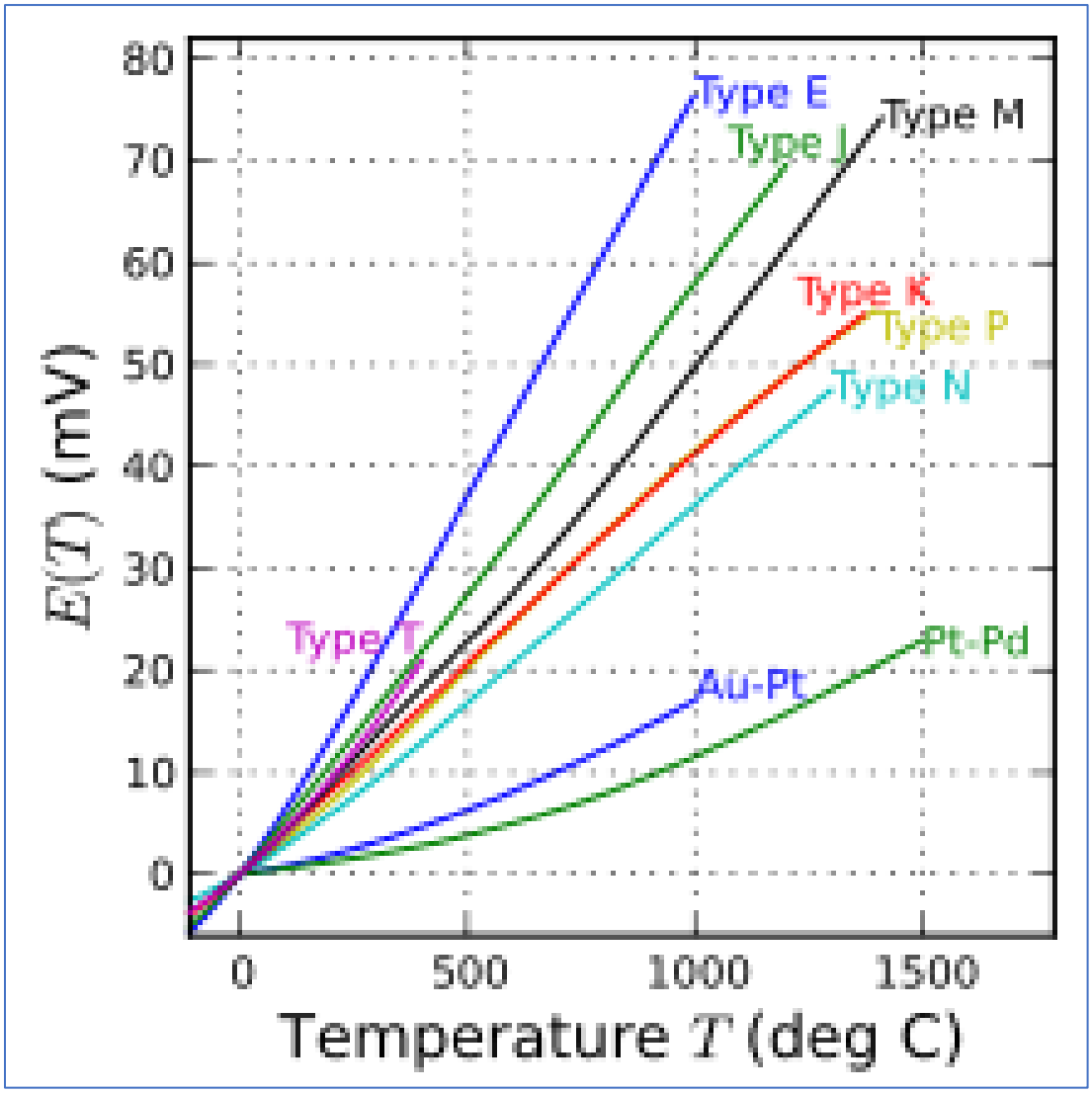

Figure 7*. Characteristic functions for thermocouples that reach intermediate temperatures, as covered by nickel-alloy thermocouple types E, J, K, M, N, T. Also shown are the noble-metal alloy type P and the pure noble-metal combinations gold–platinum and platinum–palladium.*

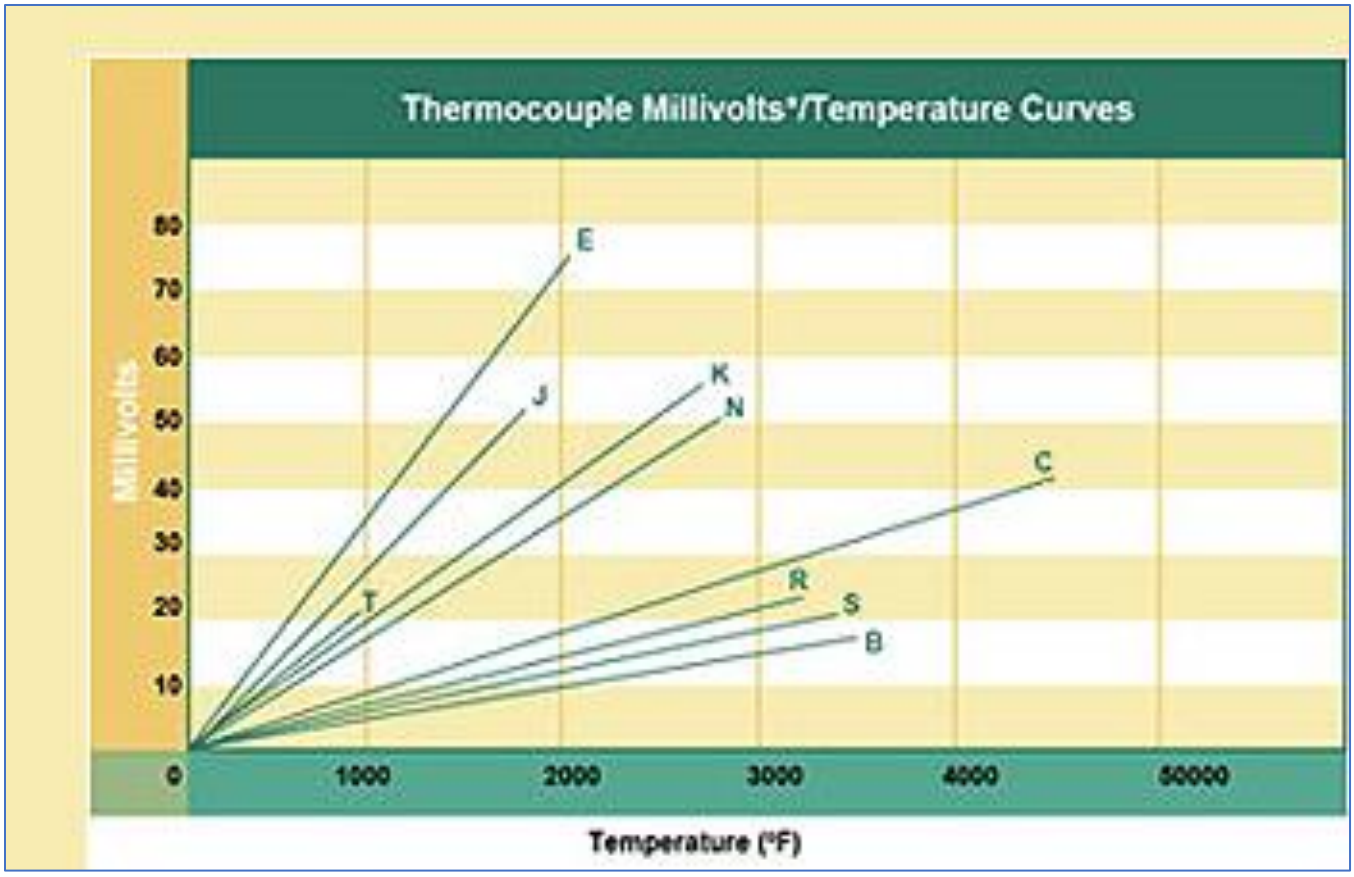

***Figure 8**. Linearized Thermocouple Voltage vs Temperature Curves*

Electrical and Thermal Properties of Copper and Constantan

Constantan:

- Electrical resistivity: 50.8 microhm·cm (micro Ω cm; micro = 10^{-6})
- Temperature coefficient of resistivity: **+-0.00004 1/K** (± 30 PPM/°C)
- Thermal conductivity: 21.2 W/m**K**

Copper:

- Electrical resistivity of annealed copper at 20°C: 1.72 micro Ω cm
- Temperature coefficient of resistivity (near room temperature): **0.393% per degree Celsius (C)** (0.00393 1/K)
- Thermal conductivity of pure copper: about 401 watts per meter kelvin (W/mK)

The relationship for resistance vs temperature can be expressed in the formula:

$$R = R_{ref}[1 + \alpha(T - T_{ref})] \quad (5)$$

where,

R	=	Conductor resistance at temperature "T" in Ohms
Rref	=	Conductor resistance at reference temperature (Tref) in Ohms
α	=	Temperature coefficient of resistivity for the conductor material
T	=	Conductor temperature in degrees C
Tref	=	Reference temp at which α is specified for the conductor material in degrees C.

Example:

Assume 100 feet of 20-gauge wire has a resistance of 1.015 Ohms at 20°C (room temp). If the temperature of the wire increases by 10°C, what will the resistance of the wire be?
R = Rref [1 + α(T – Tref)]
R = 1.015 [1 + 0.00393 (30 – 20)]
R = 1.015 [1 + 0.00393 (10)]
R = 1.015 [1 + 0.0393]
R = 1.0549 Ohms

The change in resistance (ΔR) can be expressed by a simple change to the original formula:

$$\Delta R = R_{ref} [\alpha(T - T_{ref})] \quad (6)$$

Note: I am not currently adjusting resistivity for temperature.

The values for alpha at 20 deg C are given in Table 2.

Table 2. Temperature Coefficient of Resistivity for Some Materials

Copper	Element	0.004041
Silver	Element	0.003819
Platinum	Element	0.003729
Gold	Element	0.003715
Zinc	Element	0.003847
Steel*	Alloy	0.003
Nichrome	Alloy	0.00017
Nichrome V	Alloy	0.00013
Manganin	Alloy	+/- 0.000015
Constantan	Alloy	-0.000074

Note that constantan resistivity goes down with increasing temperature at 20 deg C and the change in resistivity versus temperature is small across a wide temperature range.

Magnetic Field Strength

The magnetic field at the center of a single coil of wire with radius, a, is

$$B = u_o I/(2a) \text{ tesla,} \quad (7)$$

where,

$u_o = 4pi \times 10^{-7}$ = vacuum permeability

a = ring radius in meters

I = ring current in amperes.

Note: 1 tesla = 10,000 gauss = 10^4.

In gauss units,

$$B = 4pi \times 10^{-3} I/(2a) \text{ gauss.} \quad (8)$$

The strength of the Earth's magnetic field varies by latitude, ranging from 25–30 microteslas (μT) at the equator to 65–70 μT at the poles. This is roughly equivalent to 0.25–0.65 gauss (G). The field is dipolar, meaning it's oriented vertically downward at the north magnetic pole, vertically upward at the south magnetic pole, and horizontal at the equator.

Thermal Analysis

A thermal circuit for the ring is shown in Figure 8a.

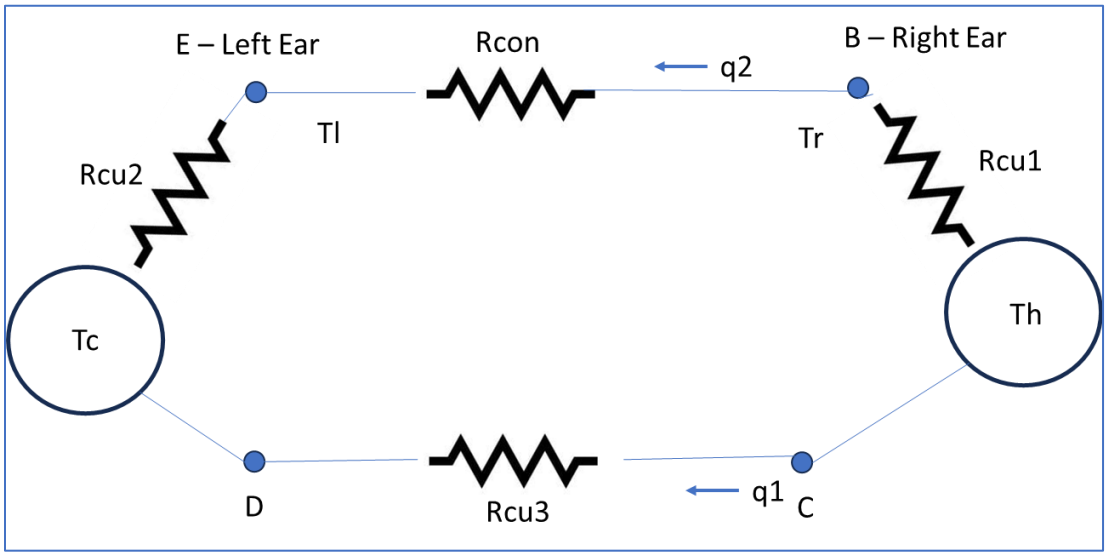

Figure 8a. *Thermal Circuit for a Simple Ring*

This circuit is oversimplified, but can be used to estimate the steady-state heat flow required given fixed-temperature heating and cooling sources. The hot and cool source temperatures are represented by Th and Tc. These sources are assumed to adjust the heat flow (power) required to keep their connection point at the specified temperature. The heat flow from the hot side to the cool side can be estimated from basic thermal equations. Once in steady state, the required heating and cooling power are at least as large as the estimated heat flow. This analysis ignores convection and radiation of heat to simplify the analysis.

Heating and Cooling Power Required

It is desired to calculate the power required to simultaneously heat and cool the ring to some desired steady state temperature difference. It would also be nice to know how long it is expected for the ring to reach a thermal steady state condition. If the cooling and heating power are constant, the ring should reach some thermal steady state. I am an electrical and systems engineer, so thermal engineering is not an area of expertise.

Some thermal references are given in Appendix F. The amount of energy required to heat a mass, m, of metal to a change in temperature, dT, is given by the

$$Er = SH \times m \times dT,$$

where,

Er is energy required to heat the mass by dT,

SH is the specific heat of the material,

M = mass being heated,

dT = increase in temperature.

The specific heat of copper is

$$SHcu = 0.385 \text{ J/g } ^\circ \text{ C}.$$

To initially simplify the analysis, we assume we are heating one half of the ring and cooling the other half with a discrete temperature change at a boundary between hot and cool (can't really happen). As an initial estimate we will assume we cool the ring to some desired cool temperature, Tc. Then calculate the energy required to heat ½ of the ring up to a desired hot temperature, Th. The density of copper is about

$$Density_{cu} = 8.95 \text{ grams/cm}^3.$$

One half of the ring will have mass

$$m1/2 = V1/2 \times Density_{cu},$$

where

V1/2 = ½ of the ring volume = Vring/2.

The energy required is then

Er = SH_{cu} x Vring x $Density_{cu}$ x (Th-Tc)/2.

If the heating is to be performed within a period given by

Theat = time required to heat the ring to desired hot temperature,

Then the power required is

Pr = Er/Theat = SH_{cu} x $Density_{cu}$ x Vring x (Th-Tc)/(Theat x 2). (8a)

This does not include the additional power needed to account for the energy radiated and conducted to the air and to the cool side of the ring. One a steady state temperature is reached, the power required to maintain this temperature is equal to the rate at which energy is lost from the ring through transfer to the cool side and transfer to air.

Rate of heat flow from hot side to cool side

Heat will propagate from the hot side of the ring to the cool side via the copper by a rate given by

$q = k A dT/L$ *(8b)*

where,

q = heat transfer (W, J/s, Btu/hr)

k = Thermal Conductivity of material (W/m K or W/m ^oC, Btu/(hr ^oF ft^2/ft))

L = heat transfer distance (m, ft) (ring distance from hot point to cool point)

A = heat transfer area (m^2, ft^2) (ring cross sectional area)

$dT = t_1 - t_2$ = temperature gradient - difference - over the material (^oC, ^oF)

Note: $U = k / L =$ *Coefficient of Heat Transfer* *(W/(m^2 K), Btu/(ft^2 h ^oF))*

We can write

q = dT/R,

where

R = Thermal Resistance = L/(Ak) = 1/(AU).

The heat transfer will be through both the lower path through the copper, q1 and the upper path through the constantan, q2. The heating and cooling sources are some effective distance from the constantan-copper junction at the ends of the gap. These distances are represented by Lh and Lc for the distances from the heating and cooling sources to the gap, respectively. The distance over the direct copper path from hot-to-cool is given by

$$Ldc = C - G - Lh - Lc,$$

where

C = ring circumference

G = constantan gap length

Lh = gap distance to heating

Lc = gap distance to cooling.

Defining

$$dT = Th-Tc,$$

the heat transfers will be given by

$$q1 = dT/Rcu3$$

and

$$q2 = dT/(Rcu1+Rcu2+Rcon).$$

The total heat transfer is

$$qt = q1 + q2.$$

The temperatures at the thermocouple junctions will be given by

$$Tr = Th - q2\ Rcu1$$

and

$$Tl = Tc + q2\ Rcu2.$$

The thermal resistivity, R, is given by

$$R = L/(Ak),$$

where

L = distance heat travels,

A = cross-sectional area of conductor,

k = thermal conductivity of material.

The above equations will be used in the following sections to estimate the power required for the scale-model ring and the full-size ring. These equations are also used to estimate the temperature at the thermocouple junctions.

Scale Model Design

To prove and demonstrate the current and magnetic fields that would be generated by hot and cool thermocouples connected in a ring configuration, a scale model of the Dotto ring has been designed, built, and tested. It is of interest how much current flows by just heating and cooling the two thermocouple junctions. It is also to be determined if there is an alternating voltage component, as claimed by Dr. Dotto. The ring configuration may produce some thermal and/or electrical resonance that is difficult to analytically predict.

I will describe the design sequence and construction with documentation of design decisions and construction techniques, including lessons learned.

Ring Design

The first step is evaluating potential ring sizes and scale factors from the full-size Dotto ring. The selection criteria were availability of material/parts at a reasonable cost and ease of construction. I selected a ¼ scale model and determined the required values from the ring sizes in Dotto's patent. Table 1 lists the parameters for the Dotto ring and the corresponding scaled-down values. I will call the model "Nadia's Improved Dotto Ring" (NIDR).

A copper ring the size specified by Dotto would be hard to find and make. The full-size copper ring would weigh about 124 lbs. The best quality and cost copper plate I could find was C110 99.99% pure 0.5" thick copper plate for about $\$2/inch^2$ in large (12x12") plates ($\$5/inch^2$ for smaller plates). The minimum copper cost for a full-scale ring would be 76" x 9"x \$2 = \$1,368, but this would need to be cut, bent to the correct radius, and brazed, welded, or soldered together. With smaller plates, the copper cost would be \$3,420. The cooling and heating power required for a full-scale ring would also be higher, more expensive, and harder to construct. See here for additional info on building a full-scale ring.

Scaling the ring size down by a factor of 4 results in a convenient size that can be made from pure copper sheet (flashing) rolls. The rolls come in a 2-inch width and various thicknesses. I determined that 6 layers of 24-gauge flashing produce about ¼ of the full-size thickness and requires two 5-foot rolls. The copper flashing purity is 99.95% compared with the Dotto spec of 99.99% (not C110 copper, but close enough).

The copper flashing rolls were cut, sized to the right diameter, and bolted together with small copper bolts though holes drilled on the edge of the ring. The outer two layers were cut longer and bent up to form the ring "ears."

Dr. Dotto did not give a specific gap size for the constantan rod(s) or the rod diameter. He said to adjust the gap to get the desired frequency, then braze the correct rod size to the copper ears.

I could not find any large diameter constantan. Constantan wire is typically used for heating elements with a small diameter wire (high resistance intentionally). The largest diameter constantan wire available was 0.7 mm. I decided that securing the wires between the copper ring layers with bolts is better than trying to braze or solder the wires to the copper. This also makes adjusting the gap size easier. I selected a gap size of 2 inches for convenience in fitting wires and measurement devices. A hall-effect current sensor is required around the wires in the gap to measure the ring current.

I also added circular tubes inside the ring top sides to accommodate standard thermocouple sensors. To make the tubes, a drill bit of the correct size is used in place of the thermocouple and then the copper is bent around the drill bit using a vice.

Table 3 summarizes and compares the scale model parameters with the full-size Dotto ring parameters. In some cases, I use calculated values instead of Dotto's values if they cannot be correct or are inconsistent with the other values. I add a question mark if the value is not specified by Dotto and I am assuming a reasonable value.

***Table 3**. Comparison of Full-Size and Scale Model Parameters*

Parameter	Full Size	Scale Model	Scale Factor
Diameter (inches)	27	6.75	4
Width (inches)	9	2	4.5
Thickness (inches)	0.5	0.129	3.9
Circumference – gap (inches/m)	76.8/1.95	19.2/0.49	4
Copper Ring Volume (in^3/cm^3)	345.6/5663.4	5.0/81.2	69
Ring Weight of Copper (lbs.)	112	1.4	80
Gap size (inches)	8?	2	4?
Number of constantan wires/rods	1	20	0.05
Constantan wire/rod diameter (inches/mm)	4/101.6	0.02756/0.7	7.25
Copper Purity (%)	99.99	99.95	1.00
Copper Resistance (uOhms)	11.4	51.8	0.22
Copper Voltage (mV)	8.8	0.055	160
Constantan Resistance (uOhms)	11.4	3250	0.004
Constantan Voltage (mV)	8.8	3.4	2,6
Total Resistance (uOhms)	22.8	3301.8	0.007
Net Thermocouple Voltage (mV)	17.6	3.51	5
Hot Side Temperature (deg F)	700	213	3.3
Cool Side Temperature (deg F)	120?	67.8	1.8?
Hot-Cool Temperature Difference (deg F)	580?	145.2	4
Current (A)	771	1.06	727
Max magnetic Field at Ring Center (gauss)		0.088	
Resonant Frequency (MHz)	0.1 to 1.9		
Bandwidth (kHz)	10 to 100		
Heating Capacity (kW)	3 to 6	0.23	13 to 26
Heating Area on Ring (in^2)	200	2.75	72.7
Active Cooling Capacity (BTU/hr./ kW)	10,000/2.93	181/0.053	55.2
Active Cooling Area on Ring (in^2)	200?	2.25	88.9
Active Cooling Heatsink Area ($in^{2)}$)	200?	157.5	
Active Cooling Air Flow Rate (CFM)		80	
Passive Cooling Heatsink Area (in^2)	N/A	315	
Passive Cooling Air Flow Rate (CFM)	N/A	80	

Ring Base

With the ring size determined, the next step is constructing a wood base. I use a walnut base with a convenient size of 6.75” x 5.75” x 1”. The base is sanded and finished with Swedish wood oil. The ring is attached to the base using 4 brass wood screws.

Heating Subsystem

With the ring, gap, and base constructed, the next step is designing how the hot side of the ring is heated. I have a Hakko soldering station that can generate a tip temperature of between 120 and 899 deg F. The tip temperature can be monitored, adjusted, and calibrated. The soldering station iron is only 65 watts, but it is convenient. I created a hole in the copper to accommodate the soldering iron tip. I then drilled a hole through one layer of copper and a soldering iron tip to enable securing the tip to the ring with a copper pin. To add additional heating capacity, I placed a small thermoelectric cooler/heat pump device with the device hot side on the inside of the ring. The thermoelectric heat pump can provide about 113 watts of heating. So, the total model heating power is 113+65 = 178 watts. This is a factor of 33.7 less than the 6 kW specified for the full-size ring, so we don't expect it to get as hot; although the end of Dotto's patent says 3 kW is enough, not 6 kW. If a 10,000 BTU/hr. (0.83-ton) cooling source is used for the full-size ring (3 kW), then the heating power applied needs to be less than 3 kW, plus how much heat is conducted and radiated to the air.

The combined Hakko and 6-amp-max TEC reached a 213 deg F temperature. Unfortunately, the Hakko soldering iron broke the TEC heater below it. After this, I replaced the Hakko heat source with another TEC configured as a heater. This new heating design only reaches a max of 189 deg F. I plan to add some higher-power TECs to increase the temp back above 200 deg F. TEC devices with 10-amp and 15-amp max currents are readily available and I have ordered some of both. These devices do not typically run at their max currents. The 6-amp-max TECs have been drawing about 4 to 5 amps (48 to 60 watts). The max operating environment is listed as 181 deg F and the maximum operating temperature is listed as 248 deg F for the 6-amp TEC devices.

The hot temperature is monitored and the heat is turned off if the temperature exceeds some maximum set temperature. This temperature should be set to less than the maximum operating temperature for the TEC (before it melts down).

I also added a ceramic-fiber-based heat shield to contain the heat near the heat source. This is to help maximize the temperature and to prevent breaking the nearby heat controller. The insulation also isolates the hot and cool sides of the TEC. This is required to prevent the TEC from thermally short-circuiting itself. It is not desired for the heat pumped from the cool side to immediately flow from the hot side back to the cool side.

I broke one controller before I realized it was too close to the hot ring. The ceramic fiber insulation is coated with polyurethane to make it more durable and prevent little pieces of it everywhere. This is also done for the Styrofoam used as the cooling insulation.

Cooling Subsystem

Cooling something to less than the ambient temperature is more difficult than heating. I decided to use both active and passive cooling devices to provide the required ring cooling. The larger the difference in temperature between the hot and cool sides of the ring at the gap, the larger the thermocouple voltage and resulting ring current will be.

A readily-available and inexpensive thermoelectric cooler (TEC)/heat pump device has been selected for both the cooling and heating subsystems. The device can come with a heat sink that can be attached to the hot side to help dissipate the combined heat pumped from the cool side plus the heat consumed by the device. However, the heatsink it comes with has nowhere near enough cooling capacity to cool the device with a reasonable airflow. The device can provide about 53 watts of cooling (188 BTU/hr.) while using 60 watts of power (5 amps at 12 volts). This active cooling can help reduce the cool-side temperature below ambient, but is insufficient to dissipate the heat being transferred through the ring from the hot side (178 watts of heating). To reduce the cooling size capacity required, passive heat sinks are added between the heat pump/cooling device and the hot side of the ring. Heat sinks with fans are placed on both the inside and outside of the ring, just before the active cooling device. Heat will also be transferred from the hot to cool side through the constantan connection, but the thermal conductivity of constantan is less than copper.

I had 2 old broken Pentium-based PCs that have large heat sinks for CPU cooling that I repurposed for both the active and passive cooling. I needed to use a tap & die set and much hole-drilling to mount the heat sinks and fans to the ring. The active cooling heatsink is also spring mounted. A copper plate is inserted between the heatsink and the cooling chip to increase cooling efficiency. Thermal conducting paste connects the plate to both the heatsink and the TEC. Custom copper brackets mount the fans, heat sinks, meters, and temperature-controlled switches.

It turns out that, with high-capacity active cooling, I probably didn't need the additional passive cooling unless the ring is operated for a long time.

Temperature and Fan Control and Voltage/Current Monitoring

Inexpensive and small digital readout meters/controllers are used to monitor the temperature of the ring sides and heat sinks. See figure R1 here for a photo.

There are two combined digital voltage/current meters. One for the source voltage at the ring and the ring current and one for the raw output power supply voltage and current. A third higher-precision voltmeter is mounted at the very top to measure the gap voltage. This higher-precision voltmeter has a resolution of 0.1 mVolts. The source voltage/current meter is mounted below the gap voltage meter. Below this meter is a dual temperature sensor digital readout. The blue reading is for the cool side of the ring

near the active cooling and thermocouple joint. The red reading is for the hot side near the other thermocouple joint and heat sources.

Below the main hot/cool temperature meter are 4 meters showing the measured temperatures in red. These measured temperatures are used to control (on vs off) the heating sources, cooling sources, and heatsink fans. Fans are turned on if the heat sink temperature exceeds a preset value. The active cooling and heat pump heating are controlled by four digital temperature controller devices. Two controllers (top) are used for the active heating/cooling and two controllers (bottom) are used for the heat sink fan control. The blue bottom numbers are the temperature control set points. The measured primary ring hot and cool temperatures on the controllers (top 2 controllers in red) are from almost the same location as the sensors for the main temperature meter. They ideally should be the same, but are not. The controller temperatures tend to be lower than the main meter. I think the time smoothing is different and they lag a temperature change. The bottom 2 measured temperatures (in red) are the heat sink temperatures. The primary active heat sink temperature is on the left and the passive heat sink temperature is on the right.

All the meters and controllers are 12-volt and have a standard size for automotive use, 1.75" x 1".

Except the input power meter, the other meters are mounted in front of the ring using custom copper mounts secured with copper bolts. The meters are mounted near what they monitor or control. The copper meter mounts are connected to the copper active cooling plate to add to the cooling capacity.

Power Subsubsystem

The model ring components use up to about 9 amps at 12 volts (108 watts). A 240-watt (20 amp) power supply (ac-to-dc converter) is used. The power supply is mounted to the base with custom copper mounting brackets.

A small electrical component box is used to house the electrical connections to the power supply, the on/off switch, and the power voltage/current meter. The power control box is mounted to the lower-left of the base. Note that due to the odd color choice for the meter wires and my available wire colors, the box output -12v wire is red and the +12v wire is blue (opposite of convention for DC voltage).

A 16-amp, 12-position terminal strip with screw connections is mounted on the base behind the ring to distribute the 12-volt power to all the components that need it. Terminals A are +12v and B are -12v. The terminal assigned positions are:

1. Inside Small Fan
2. Active Cooling Fan Controller
3. Active Cooling TEC Controller
4. Hot/Cool Temperature Monitor

5. Hall Current/Voltage Meter
6. Heating TECs Controller
7. Hall Current/Voltage Meter Voltage Input (+12v only)
8. Outside TEC Heater (+12v only)
9. Inside TEC Heater (+12v only)
10. Spare
11. Precision Voltmeter (+12v only)
12. Passive Cooling Fan Control

Design Photos

Here are some photos documenting the scale-model ring development.

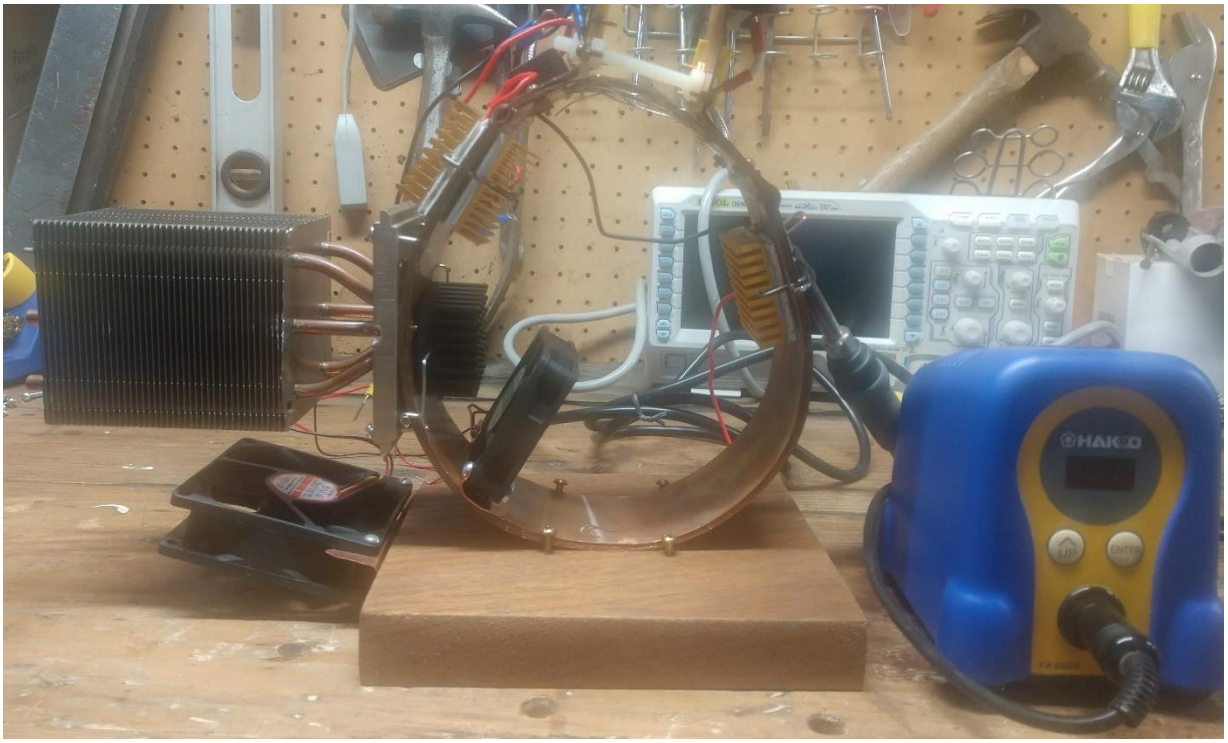

Figure D1. *Initial Early Ring Design Where You Can Still See the Ring*.

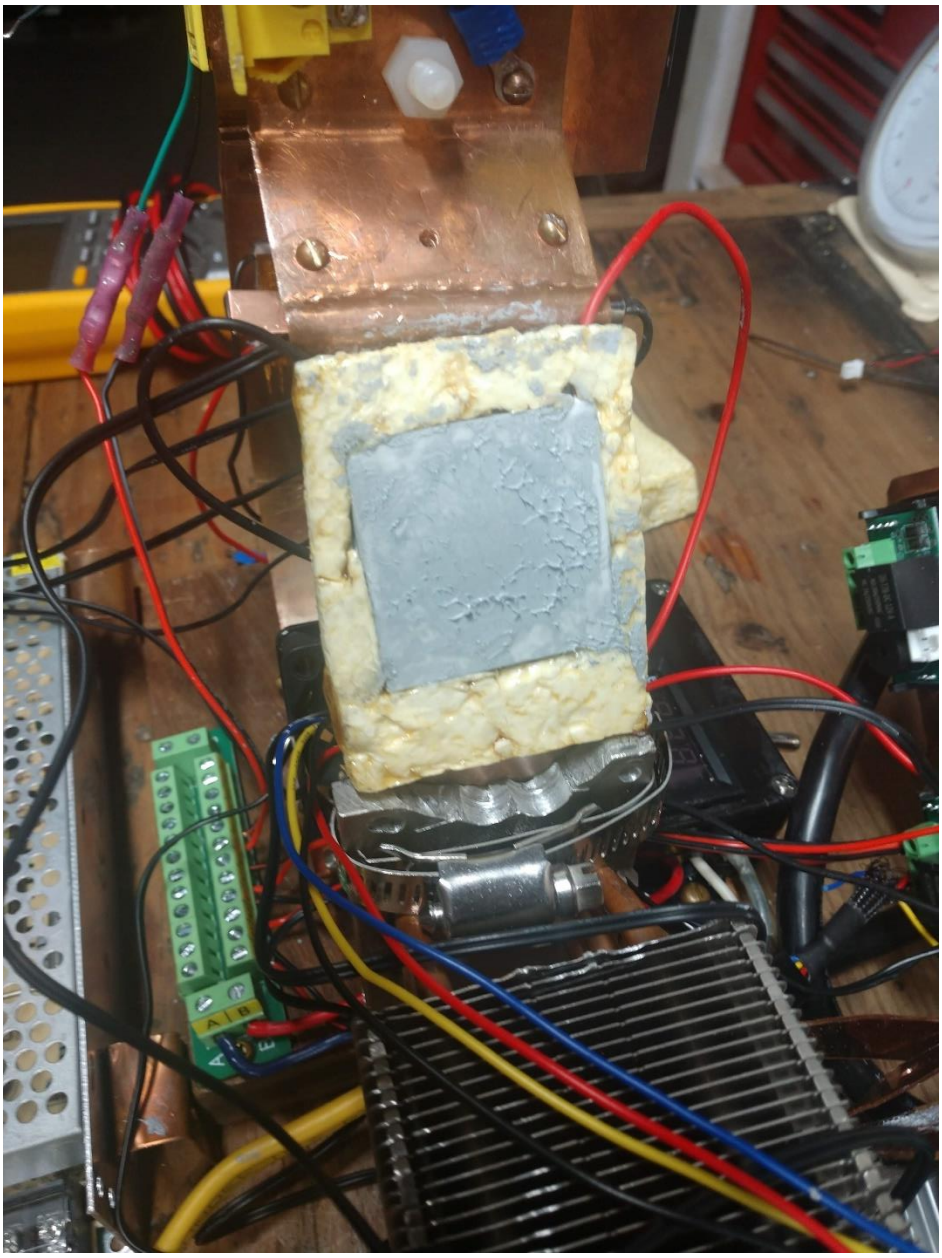

Figure D2. *Thermal paste (gray) connects all thermal components. TECs are isolated with insulation. This photo shows the cooling TEC isolated by a custom Styrofoam insulator.*

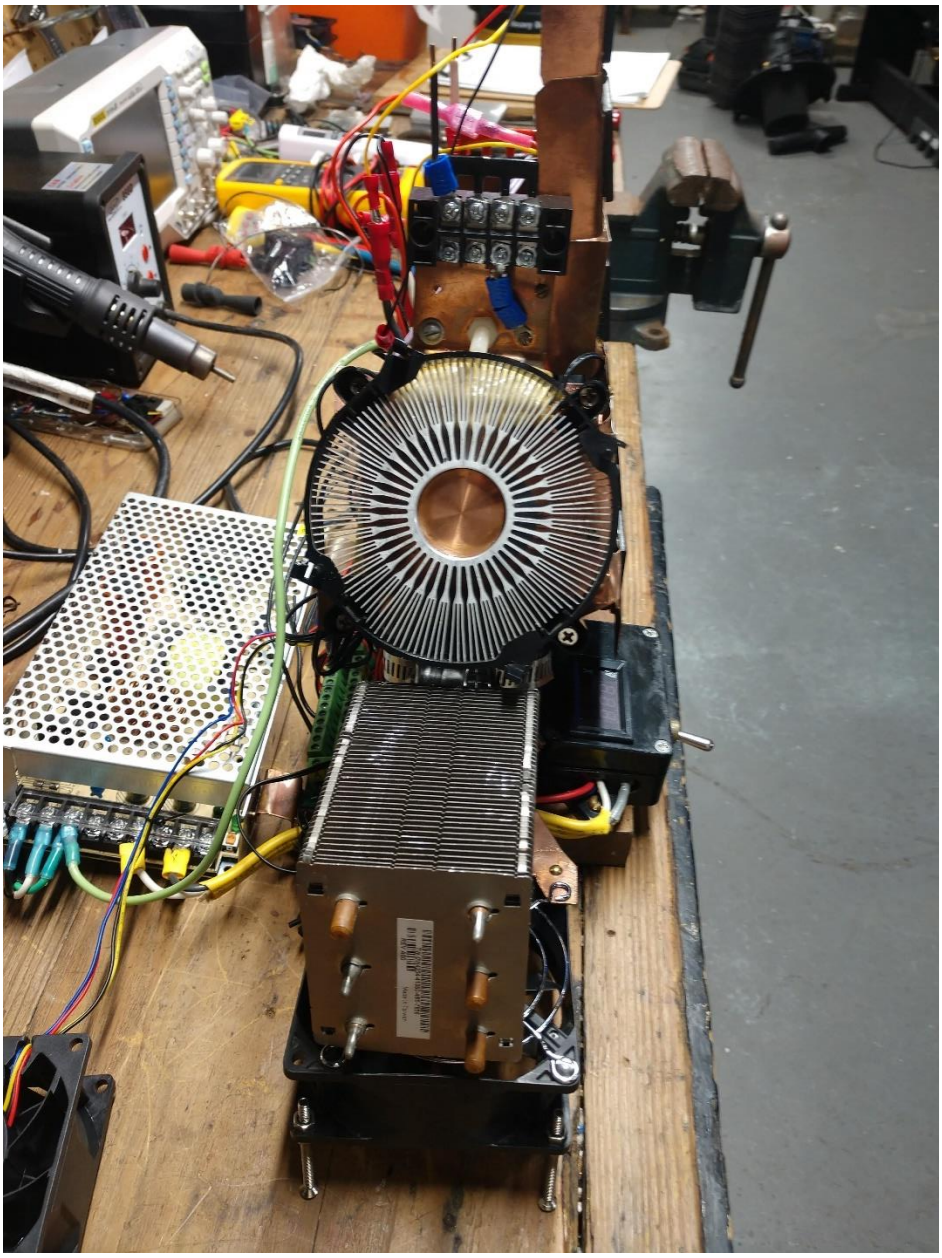

Figure D3*. Upgraded cooling subsystem includes a circular heat sink attached to the TEC with a cooling plate. Passive heatsinks are mounted below the primary heatsink and inside the ring (the primary cooling fan is removed from the heatsink here to show it).* ***Note:*** *Due to Nadia's concern for my safety, I added a grounding wire (light green) from the power supply ground to the ring. A ground-fault circuit breaker is used to power the supply so if any copper is energized to a dangerous voltage and touched, the circuit breaker will trip. Also, fortunately (or not) I was not transported to any other dimensions or dangerously levitated.*

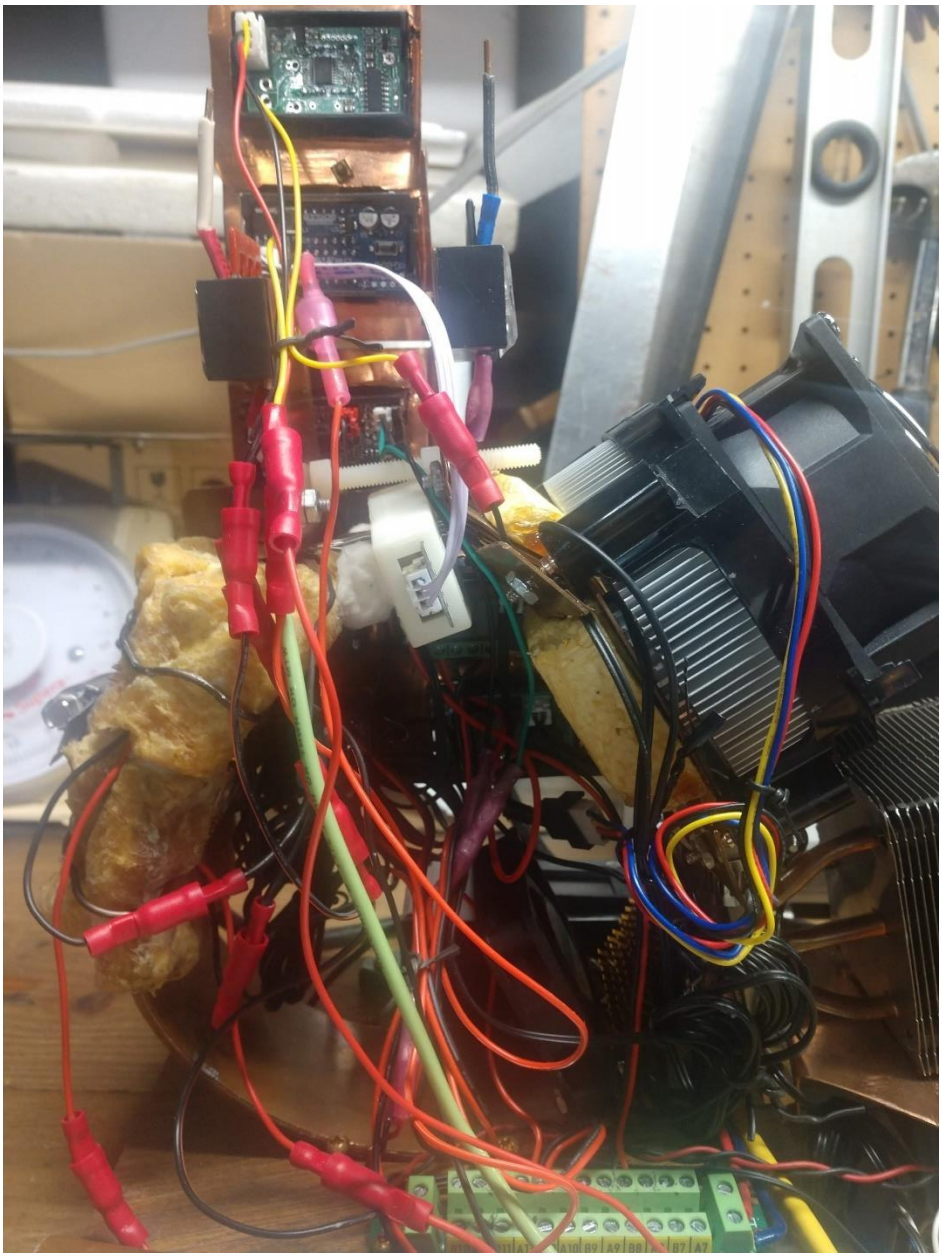

Figure D4*. Back View of Ring. Heating and cooling subsystems hide most of the ring.*

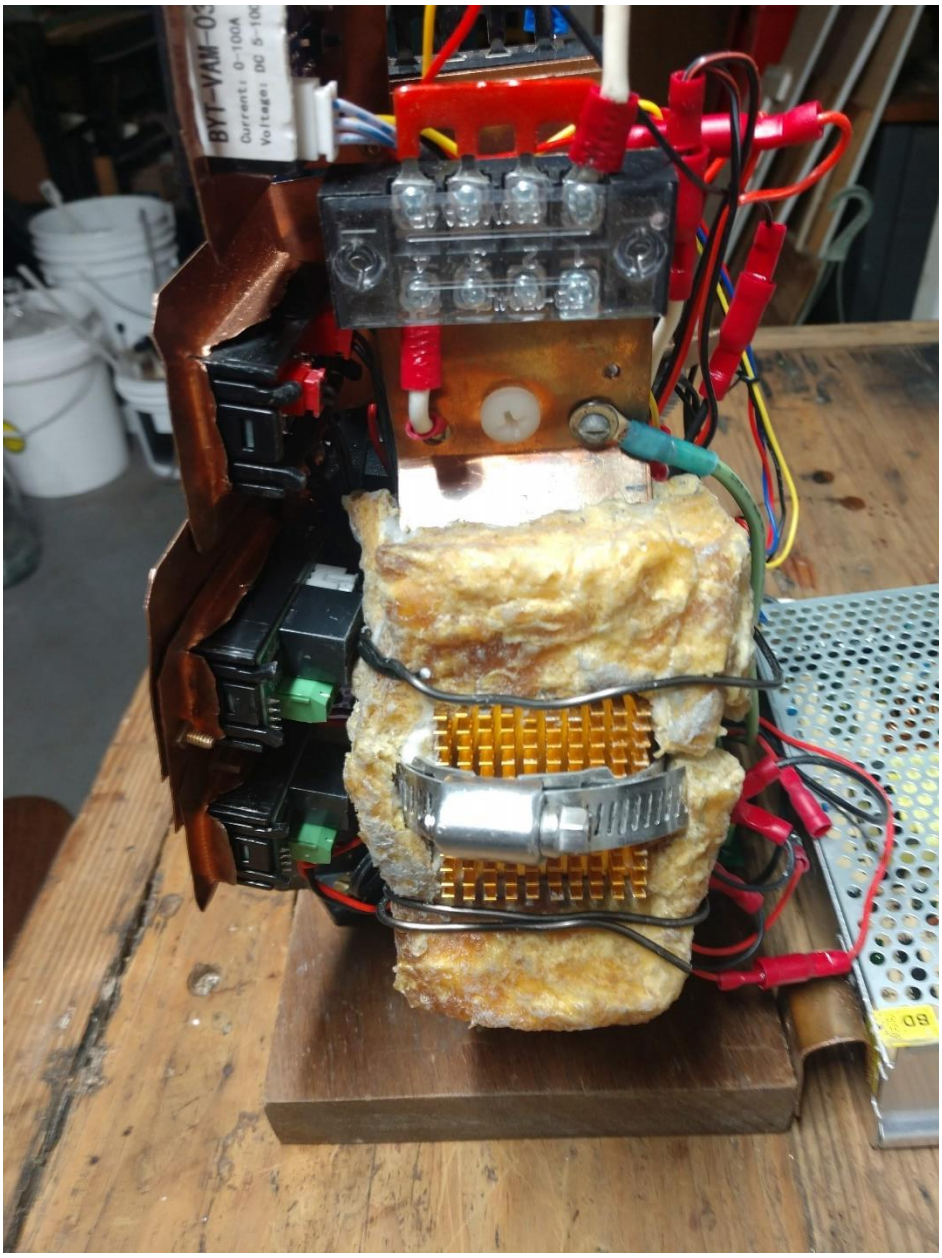

***Figure D6**. Outside of heating subsystem with 2 TEC heaters and ceramic insulation*

Figure D7*. Front of ring after reaching max temperature (two 6-amp heating TECs)*

Scale Model Electrical Performance Predictions

Our scale model's important ring parameters:

Constantan gap: 5.08 cm (2 inches)

Circumference of copper (-gap): 48.8 cm

Width: 5.08 cm

Thickness: 0.28 cm

Copper volume: 69.4 cm^3

Hot side temp (Th): 213 deg F

Cool side temp (Tc): 67.8 deg F

The following sections show predictions for voltage, resistance, current, and magnetic field. The important results are highlighted in light blue.

Thermocouple Voltage

Since both hot and cool side thermocouples are the same type and configuration, the voltage difference between the hot and cool thermocouples is what matters. The voltage as a function of temperature can be looked up on a chart for the thermocouple type or approximated by a linear equation of voltage vs temperature. Using the Table 1 chart for a type-T thermocouple and a 213 deg F (101 deg C) temperature, the hot thermocouple junction voltage is

Vh = 4.3 mV.

The cool side junction temperature at steady state is about 67.8 deg (19.9 deg C) producing a "cool" side thermocouple voltage of

Vc = 0.79 mV.

The net voltage for the two junctions is then

Vnet = 4.3-0.79 = 3.51 mV (9)

Ring Resistance

Copper

The resistance of a metal ring or wire depends on the metal properties (resistivity/temperature), the cross-sectional area, and the length. The resistance is equal to the resistivity times the length divided by the area.

Using 1.72x10-6 ohm-cm resistivity of annealed copper:

Copper Resistance Rcu = 1.72×10^{-6} ohm-cm*42.8cm/0.28cm/5.08cm = 51.8×10^{-6} Ohms,

or

$$Rcu = 51.8 \text{ uOhms} \quad (\text{uOhms} = \times 10^{-6}) \qquad (10)$$

It is hard to measure resistance this small with an ohm meter. The lowest resistance I can measure with my expensive Fluke meter is about 0.2 ohms (200 mOhms or 200,000 uOhms!).

Note that this resistance calculation is approximate and does not account for heating of the ring or a temperature gradient across the ring. Both these can increase the copper resistance.

Constantan

The largest diameter constantan wire I could find has a diameter of 0.7 mm (0.0007 m). Due to relatively high resistivity, this wire is usually used as a heating element with a small diameter to get a high resistance/heating for a given current. This is like Nichrome (also called chromel) wire that has an even higher resistivity. I used to use nichrome wire to ignite my model rocket engines. The corresponding cross sectional area of a single wire is pi*r^2, or $(3.1415926)*(0.0007/2)^2 = 3.85 \times 10^{-7}$ m^2.

The resistivity of constantan is 5.00×10^{-7} Ω·m. The expected resistance of a single 5 cm length of 0.7 m diameter constantan wire is then

Rcon1 = $(5 \times 10^{-7})(0.05)/(3.85 \times 10^{-7}) = 65$ mOhms.

Rcon can be reduced, if desired, to increase the ring current by 1) Adding additional wires in parallel, and/or 2) shortening the wire length. For multiple wires, the resistance will be reduced by a factor of about the number of wires. With a 0.05 m gap length, it would take about 528 wires to get down to the same resistance as the copper ring.

There are about 20 constantan wires in parallel across the NIDR gap, so the combined resistance of the 20 parallel wires is about

$$Rcon = 65/20 = 3.25 \text{ mOhms}. \qquad (11)$$

(Note: 1/Rtotal = 1/R1 +1/R2 + 1/R3 + … . So for N equal resistance wires: 1/Rtotal = N/R and Rtotal = R/N).

The resulting total series ring resistance is

$$Rtot = 0.0518 + 3.25 = 3.3018 \text{ mOhms} \qquad (12)$$

Ring Current

The current flowing through the ring will be:

Ring Current = I = (hot junction thermocouple voltage – cool junction thermocouple voltage)/(Rcon+Rcu)

or

I = Vnet/Rtot = 3.51 mV/3.3018 mOhms = 1.06 A. (13)

For a higher current: 1) decrease copper ring resistance, 2) decrease gap constantan wire resistance, and/or increase gap voltage (temperature delta cool-to-hot junctions).

Magnetic Field Strength

A metal ring with

Ring radius = 0.076 m

will have a magnetic field strength at the ring center of

$B = (4pi \times 10^{-7})(1.06)/(2*0.076) = 87.6 \times 10^{-7}$ teslas (T)

or

B = 8.8uT = 0.088 gauss. (14)

The scale model Dotto ring has a magnetic field at the center of about 1/5 the earth's magnetic field.

Power Required to Heat and Cool

The power required to ½ heat the ring from the cool temperature to the hot temperature is

$Prmin = Sh_{cu} \times Density_{cu} \times Volring \times (Th-Tc)/(Theat \times 2)$

Assuming Theat = 60 seconds and using

$Sh_{cu} = 0.385$ J/g ° C,

$Density_{cu} = 8.95$ g/cm^3,

Volring = 69.4 cm^3

Th-Tc = dT = 145 deg F = 62.8 deg C

yields

Prmin = 146 J/s = 125 W.

This does not include the additional power needed to account for the energy radiated and conducted to the air and to the cool side of the ring. Once a steady state temperature is reached, the power required is equal to the rate at which energy is lost from the ring through transfer to the cool side and transfer to the air.

The heat transfer rate is

$$q = k A \, dT/L \qquad (8b)$$

where for the direct copper path,

k = thermal conductivity of copper = 401 W/m^{o}C

L = heat transfer distance = 0.39 m (ring distance from hot point to cool point)

A = heat transfer area = 0.0001664 m^2 = 1.664 cm^2 (ring cross sectional area)

dT = 62.8 deg C = temperature difference from hot to cool.

The resulting heat transfer rate for the direct copper path is

q1 = 10.7 W.

The constantan path has thermal resistance,

Rq2 = Rcu1 + Rcu2 + Rcon = L1/Ak + L2/Ak + Lcon/Aconk, = path q2 resistance

where,

L1 = hot-to-gap distance = 0.0508 m

L2 = cool-to-gap distance = 0.0508 m

Lcon = constantan gap distance = 0.0508 m

Acon = 77 x 10^{-7} m^2.

This results in

Rq2 = 1.52 + 16.4 = 17.92.

The q2 constantan-path heat transfer rate is

q2 = dT/Rq2 = 62.8/17.92 = 3.5 W.

The total heat transfer rate is then

qt = q1 + q2 = 14.2 W.

The scale model has 2 cooling and 2 heat sources at different locations on the ring. The effective location of the heat source is not as close as the primary cooling source or the sources of the full-scale ring. A prediction of the temperature drop from the heating source to the gap junction is given by

Tr = Th – q2 Rcu1.

The temperature drop from the source to the gap is estimated as

Th-Tr = q2 Rcu1 = (17.92)(0.76) = 13.6 deg C (56.5 deg F).

If the temperature sensor is 1 inch from the heat source, the temperature drops over that distance by 6.8 deg C or 44.2 deg F. This means the heating TEC shut off temperature should be about 45 deg cooler than the maximum TEC operating temperature.

Full-Size Dotto Ring Electrical Performance Predictions

The important Dotto ring parameters given or assumed are:

Constantan gap: 20 cm (7.9 inches) (assumed)

Circumference of copper (-gap): 195 cm (76.8 inches (27-inch diameter, 8-inch gap))

Width: 22.9 cm (9 inches)

Thickness: 1.27 cm (0.5 inches)

Copper volume: 5671 cm^3

Hot side temp (Th): 700 deg F

Cool side temp (Tc): 120 deg F (assumed)

Ring Voltage

The ring has two voltage generations sources: 1) copper-to-constantan thermocouple junctions and 2) temperature difference between ends of the copper ring (Seebeck effect).

Approximate max. hot-side ring temperature: 700 deg F (371 deg C) (+273.15 for K), 644.15 K. It may be less at gap thermocouple junction because heat source is probably not applied right at the gap.

At 700 deg F, a single type-T thermocouple will generate about 19.1 mV (from Table 1). Note that 700 deg F is about the maximum operating temperature for a type T thermocouple.

Assuming the cool side can be kept at 120 deg F (48.9 deg C), the cool side voltage will be 2 mV. The 120 deg F cool side temperature assumes getting a gap delta temperature 4 times that achieved by our ¼ scale model. Mr Dotto does not specify a cool-side temperature. If it is colder, then the voltage would be a little higher.

The net gap voltage will then be

$$Vnet1 = 17.1\ mV. \qquad (15)$$

2) Seebeck effect due to difference in temperature at ends of copper ring. Seebeck coefficient relative to platinum:

copper: 6.5 uVolt/K at 0 deg C.

constantan: -35uV/K

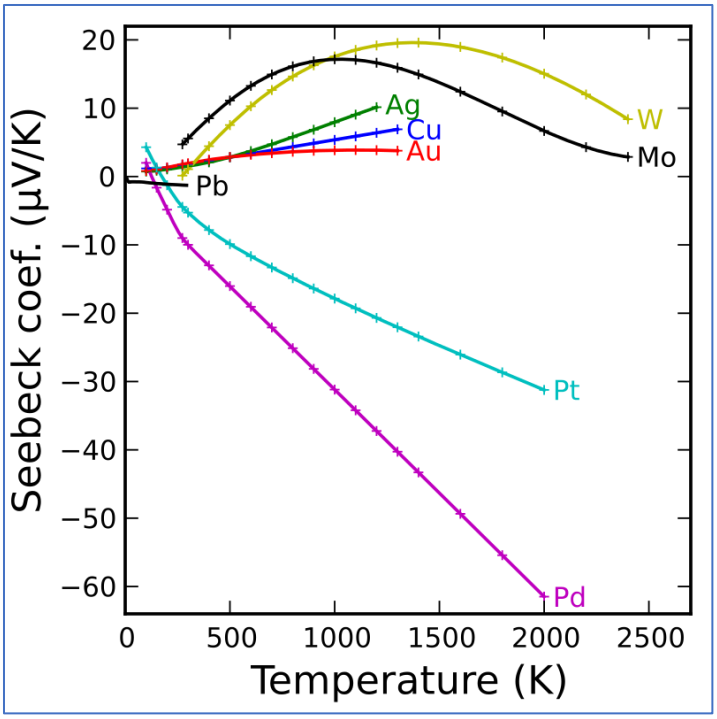

Figure 9. *Copper has a Seebeck Coefficient of about 1.5uV/K.*

Delta T is about 371-49.8 = 321.2 K. Voltage due to this difference will be 1.5uV/K x 321.2 K = 48 uV = 0.48 mV.

So total voltage due to temperature is 17.1 mV + 0.48 mV or

Vnet = 17.58 mV. (16)

Most of the gap voltage is due to the thermocouples.

Dotto says 25 to 45 mV across the gap (seems too high, max achievable should be about 21 mV). For max temp in Table 1, 400 deg C (752 deg F), the type-T thermocouple the voltage is 20.9 mV. Type-T thermocouples do not work well above 700 deg F. The Dotto paper text mentions that a semiconductor pellet is between constantan rod and copper, but this is not shown or described in the patent. A semiconductor would prevent heat transfer, but would also reduce electrical current. Semiconductors are used in TEC devices.

In his patent, Dotto claims to have measured "0.156 millivolts between the ears" and that this would produce 30,000 A with a 5.27 uOhm ring resistance. This cannot be correct. Either the voltage is 0.156 volts (156 millivolts) to produce 30,000 A or the current is 0.156 millivolts/5.27 uOhms = 30 A. Neither one makes much sense.

The voltage measured between the ears during operation would be the voltage across the copper portion of the ring, Vcu = I*Rcu.

Ring Resistance

Copper

The resistance of a metal ring or wire depends on the metal properties (resistivity and temperature), the cross-sectional area, and the length. The copper ring dimensions for an assumed 8-inch (20 cm) gap are (length x thickness x width) 195 x 1.27 x 22.9 cm. The resistance is equal to the resistivity times the length divided by the area.

Using 1.7×10^{-6} ohm-cm resistivity of annealed copper (Dotto value, approximately correct):

$$Rcu = 1.7 \times 10^{-6} \text{ohm-cm} * 195 \text{ cm} / 1.27 \text{ cm} / 22.9 \text{ cm} = 11.4 \times 10^{-6} \text{ Ohms}$$

or

$$Rcu = 11.4 \text{ uOhms.} \quad (17)$$

The Dotto patent says that the ring resistance is 5.27 uOhms. Not sure how he gets this low of a resistance when the copper ring resistance is about 2x higher. If we define the ring resistance, Rring, as the resistance of the copper and constantan in parallel (what you might measure with an ohm meter connected to the ears), then

$$1/Rring = 1/Rcu + 1/Rcon$$

He would have to have a constantan resistance equal to the copper ring resistance to get this value, which is not his nominal resistance of pi times higher than Rcu for the Peltier effect (described in Dotto paper, not patent – patent is dated 2 years after the paper).

Constantan

The resistivity of constantan specified by Dotto is 49 uOhm-cm, which is about right. Since Dr. Dotto did not specify the gap length or constantan rod size, I will assume a gap about 4x my scale model gap or 20 cm (about 8 inches). Dr. Dotto did say the constantan rod resistance for the Peltier effect would be the copper resistance times pi (in paper, not patent). Dotto paper says this is a constraint on rod minimum length to get the Peltier effect. Peltier effect is opposite of Seebeck effect where current through the junction of two different materials produces a temperature difference. Seebeck effect results in a temperature difference producing a current. Dotto says

$$Rcon = \text{pi} \times Rcu = 3.14159 \times 11.4 \text{ uOhms}$$

or

$$Rcon = 35.8 \text{ uOhms.} \quad (18)$$

If the ring resistance is defined as the copper and constantan resistances in parallel, the resistance would be

$$Rring = 1/(0.0279 + 0.0877) = 8.6 \text{ uOhms.}$$

(Not sure how Dotto gets 5.27 uOhms, may be an inaccurate measurement or different Rcon). Since the Peltier effect does not seem required for ring operation, the constantan resistance might have been selected to be equal to the copper resistance,

Rcon = Rcu = 11.4 uOhms.

In this case, the value of parallel ring resistance would be

Rring = 1/(2 x 0.0877) = 5.7 uOhms.

This is close to the claimed Dotto ring resistance of 5.27 uOhms. Therefore, I will use Rcon=11.4 uOhms in calculating the ring current.

Since in normal operation, the current is flowing around the ring through both the constantan and copper in series, the appropriate resistance for calculating the current is

Rtot = Rcon + Rcu = 11.4 + 11.4 = 22.8 uOhms. (19)

We can estimate the constantan rod diameter needed to get the specified resistance for the assumed length of 20 cm. The rod cross sectional area will be

Rarea = pi x r^2.

The rod resistance will be

Rcon = (49uOhm-cm)*Rlen cm/Rarea cm^2,

or

pi*r^2 = (49 x 20/Rcon)

or

r = sqrt((49x20/11.4)/pi).

Solving for r = Rrod (for Rcu = Rcon) gives

Rrod = 5.2 cm (2.03 inches). (20)

This would mean a 4-inch diameter rod, which is large, but less than the 9-inch width of the copper ring. This would leave 2.5 inches on both sides of the rod. Dr. Dotto may have had a smaller rod – I don't know.

Ring Current

The current flowing through the ring will be:

I = Ring current = (hot junction thermocouple voltage – cool junction thermocouple voltage)/(Rcon+Rcu),

or

I = V/R = $17.58x10^{-3}/22.8x10^{-6}$ = 771 A. (21)

The Dotto patent and paper are all over the place regarding the ring current value. Values are given from 3 to 30,000 A. I believe none of the specific values given in the paper or the patent are correct.

Magnetic Field Strength

The magnetic field strength at the center of a ring can be calculated using the formula

$B=\mu_0 I/2r$, where:

- B: is the magnetic field strength (teslas)
- μ_0: is the magnetic permeability of free space, $\mu_0=4\pi\times10^{-7}$ T m A^{-1}
- I: is the current in the wire
- r: is the radius of the coil

The predicted magnetic field at the Dotto ring center (r = 0.34 m) for a 370 A current is then

$$B = 6837.6 \times 10^{-7} \text{ T} = 6.8376 \text{ gauss.} \qquad (22)$$

Dotto claims 160 gauss at center, but also claims current up to 30,000 A. He claims the magnetic field at ring edge is higher, 240 gauss, but this can't be correct because the highest field strength for a ring with current flowing is at the center. Once again, none of the specific magnetic field values in the Dotto paper or patent are correct, for multiple reasons, including incorrect current values.

Note: 1 tesla = 10,000 gauss

Power Required to Heat and Cool

The power required to ½ heat the ring from the cool temperature to the hot temperature is

$$Prmin = Sh_{cu} \times Density_{cu} \times Volring \times (Th-Tc)/(Theat \times 2)$$

Assuming Theat = 240 seconds (4 minutes) and using

Sh_{cu} = 0.385 J/g ° C,

$Density_{cu}$ = 8.95 g/cm^3,

Volring = 5671 cm^3

Th-Tc = dT = 580 deg F = 304.4 deg C

yields

Prmin = 12,400 J/s = 12.4 kW.

This means it will take at least 8 minutes to heat ½ the ring from the cool to the hot temperature if the heating power is 6kW. This does not include the additional power needed to account for the energy radiated and transferred (by convection) to the air and conducted to the cool side of the ring. Once a steady state temperature is reached, the power required is equal to the rate at which energy is lost from the ring through transfer to the cool side and transfer to the air.

For the full-scale model, I will assume the distance from the heating and cooling points to the gap is about 11 in from the gap. This is ½ of the 200 in^2 heat and cool areas divided by the ring width of 9 in (center of the heating and cooling points). This is about

L1 = L2 = 28 cm = 0.28m.

The copper direct path length is then about

L3 = 139 cm = 1.39 m.

The heat transfer rate is

$$q = k\,A\,dT/L \qquad (8b)$$

where for the direct copper path,

k = thermal conductivity of copper = 401 W/m^oC

L3 = heat transfer distance = 1.39 m (ring distance from hot point to cool point)

A = heat transfer area = 29.1 cm^2 = 0.00291 m^2 (ring cross sectional area)

dT = 304.4 deg C = temperature difference from hot to cool.

The resulting heat transfer rate for the direct copper path is

q1 = 255 W.

The constantan path has thermal resistance,

Rq2 = Rcu1 + Rcu2 + Rcon = L1/Ak + L2/Ak + Lcon/Aconk, = path q2 resistance

where,

Lcon = constantan gap distance = 0.2 m

Acon = 0.0085 m^2.

This results in

Rq2 = 0.48 + 0.06 = 0.54.

The q2 constantan-path heat transfer rate is

q2 = dT/Rq2 = 304.4/0.54 = 564 W.

The total heat transfer rate is then

qt = q1 + q2 = 819 W.

Results

The electrical results using the ¼-scale ring model and how they compare with predictions are summarized in this section. For details on the scale-model design, see the design section here. Example measurements with a single TEC heat source and the combined TEC and Hakko soldering station set at a temperature of 750 deg F are shown in Table R1. Unfortunately, I didn't take a video of the combined TEC and Hakko Station before the Hakko station burned out the heating TEC; causing me to replace the Hakko with a 2nd TEC heater. The TEC heater is not as effective as the Hakko, so the 2-TEC-heater-design does not get as hot as when the Hakko and a single TEC are used. The max temperature with the Hakko and TEC heating is 213 deg F. The max temp with two TEC heaters is 189 deg F. The max temperature with a single TEC is about 133 deg F. The max temperature with just the Hakko is also 178 deg F. My goal for the temperature is above ¼ of the maximum full-scale Dotto ring temperature of 800 deg F. This goal is >200 deg F.

A photo of the NIDR when both the Hakko and TEC were used and close to the max temperature is shown in Figure R1. Note that the upper voltmeter is not accurate enough to measure the millivolt-level gap voltage (later added a higher precision voltmeter). This meter was later used to measure the source voltage (about 12v). A higher-precision voltmeter has been added to constantly measure the gap voltage. The primary measurements of interest shown in Figure R1 are the gap current (top meter in red) and the ring hot and cool temperatures (red and blue in the 2nd from top meter). The lower 4 meters show the measured temperatures in red used to control the heating and cooling sources and heatsink fans. The numbers in blue on these lower displays are the temperature set points being used for device control. The measured hot and cool temperatures on the controllers (top 2 controllers in red) are from almost the same location as the sensors for the main temperature meter. They ideally should be the same but are not (66.3 vs 68.0 cool and 193 vs 205 hot). The controller temperatures tend to be lower than the main meter. They appear to be more smoothed in time (lag a temperature change) and seem slightly less accurate. The bottom 2 measured temperatures in red are the heat sink temperatures. The primary active heat sink temperature is on the left and the passive heat sink temperature is on the right. If the small red LED light on the right of the controller is on, the controlled device is on.

The ring current and gap voltage increase with the measured hot temperature, as expected. The predicted voltage and current are slightly higher than measured. The predicted current is 1.06 amps and the measured current is 0.85 amps with a measured temperature of 213 deg F. The 0.85 current estimate has been manually recorded because the meter was fluctuating between 0.8 and 0.9.

The measured copper ring resistance is higher than predicted and the measured constantan gap resistance is lower than predicted. See Table R1 for the values. Most of the difference between the predictions and measurements is thought to be due to the higher-than-predicted copper resistance. I don't have a full explanation for the higher resistance yet. Part of the reason is that I have not compensated for the increase in resistance with temperature and/or with a temperature gradient. Placing the constantan wires between the ends of the copper layers may have also increased the copper ring resistance.

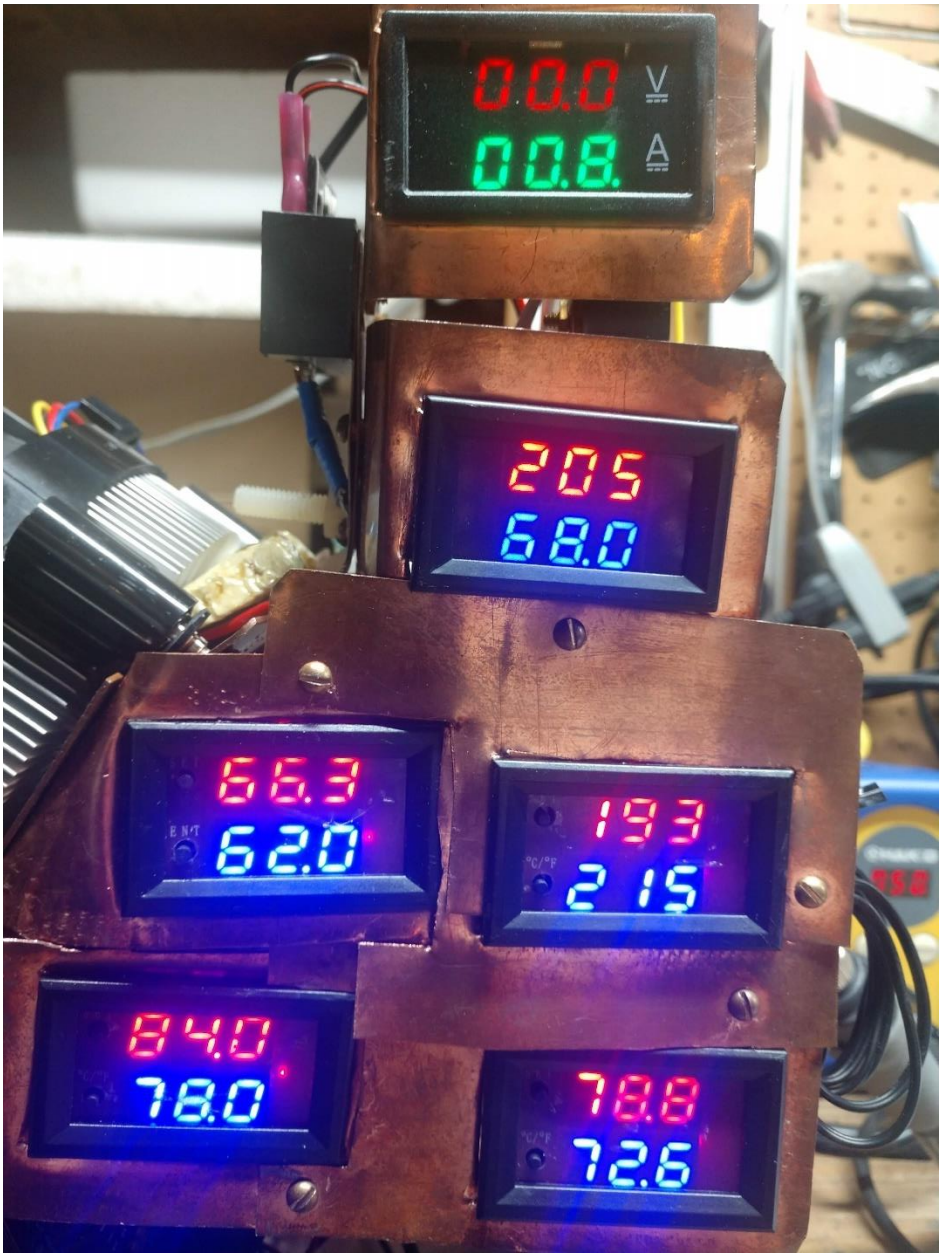

Figure R1*. Current and Temperature Measurements with Both the Hakko and TEC Heat Sources Near the Maximum Temperature*

***Table R1**. Scale Model Ring Measurements (18 July 2024)*

	Single TEC Heat Source	**TEC and Hakko**	**Predicted (213 deg)**
Measured Current (A)	0.4	0.85	1.06
Max Hot Ring Temp. (deg F)	129	213	
Cool Ring Temp. (deg F)	65.6 to 66.2	67.8	
Delta Temp. Achieved (deg F)	62.8 to 63.4	145.2	
Cool Controller Measured (deg F)	63.6 to 64.4	66.3	
Cool Controller Setting	62.0	62.0	
Primary Cooling Heat Sink Temp (deg F)	83.4 to 84.2	84.0	
Primary Cooling Fan Control Setting (deg F)	78.0	78.0	
Hot Ring Control Temp (deg F)	127.0 to 130.0	198.0	
Hot Ring TEC Control Setting (deg F)	215	215	
Secondary Heat Sink Temp (deg F)	75.5 to 77.7	78.8	
Secondary Heat Sink Fan Control Setting	72.6	72.6	
Power Source Volage (running) Volts	11.9	11.9	
Power Source Current (A)	6.55	8.02	
Measured Ring Voltage Across Constantan (mV)	0.55	1.1	
Measured Ring Voltage Across Copper (mV)	0.1	0.2	
Total Voltage (mV)	0.65	1.3	3.5
Ring Constantan Resistance (mOhms)	1.57	1.29	3.25
Ring Copper Resistance (uOhms)	250	235	51.8
Total R (mOhms)	1.82	1.525	3.30

The Table R1 values give an approximate measurement of the copper ring and constantan wire resistances. Note that the mV-level voltages were measured with an expensive Fluke multimeter. The measured resistance is equal to the measured voltage divided by the measured current. Assuming the measured voltage and current are reasonably accurate, the constantan wire resistance is measured as approximately 1.3 mOhms (milli ohms; milli=10^{-3}). The copper ring resistance is measured as about 235 uOhms (micro ohms; u=10^{-6}).

The predicted delta voltage for the ring thermocouples is the voltage differences for the hot side minus the cool side:

Net Type T Thermocouple for (213 deg F (100.6 deg C) hot to 67.4 deg F (19.7 deg C) cool): 4.3 -0.77 = 3.5 mV

A link to a video of ring operation with the 2-TEC heat source (each 6-amp max) is provided below. The major thing to watch is the top 3 meters that show as the hot side gets hotter and the cool side gets cooler, the gap voltage and current get higher. The ring takes a long time to reach a steady state maximum temperature. The video is 15

minutes long. The steady state condition occurs after about 10 minutes when the temperature is hot enough that the heat leaving the ring equals the heat entering.

Link to video with 3 TECs, 1 cooling, 2 heating

Figure R2. *Photo at End of Above Video Showing Steady State Condition*

A preliminary analysis of the alternating component of the ring voltage has been performed using a digital oscilloscope. There is a low-level alternating (AC) component, but it is not clear what is causing it. It could result from one or more of the ring electrical components. The measured voltages are so low that some of the measured AC component is due to electromagnetic energy present that couples with the ring. As Dr. Dotto mentioned, the ring can operate as a type of antenna.

A video that includes the scope output is included below. The video starts showing the constantan gap voltage with the ring off. This gap voltage is then shown with the ring on. In the middle of the video, I change the voltage source from the gap to across the copper ring. If you can read it, the scope shows the voltage scale and the measured frequency of the signal displayed. I plan to do further analysis if a higher temperature and voltage can be achieved with higher-power heat sources.

Link to video with digital scope output from voltage across gap and across copper.

Figure R3*. Scope Ring Gap Voltage Output with Ring Power Off (57.8kHz, 30mVolts peak-to-peak). See the video for output when the ring is operating.*

Summary and Discussion

I have reviewed Dr. Dotto's paper and patent and will give my opinion about incorrect or inaccurate information. My credentials making me qualified to review for accuracy related to electromagnetic, physics, and engineering are in Appendix K. I can't evaluate performance as a medical device. If it does have a medical benefit, it is probably not for the reasons claimed by Dr. Dotto. Much has been learned about human biology and cancer since Dr. Dotto performed this work in the early 70's. Dr. Dotto has a very active imagination. He tends to write things that are his theory about how things work as if they are facts.

There is a lot of talk about facts and alternate facts these days. "Alternate facts" is my favorite oxymoron. I am skeptical by nature. I don't accept things as facts unless I am sure and convinced; and I am not easily convinced. At my job, I had a reputation of always being correct. This also means I don't like to speculate. I have seen and found many mistakes and incorrect information in published material. Even worse, anything can be claimed on the internet and it seems most people will believe whatever they want and then claim it as a fact.

It has been reported (see here) that there have been and are still many similar medical electrical stimulation devices (ESDs) that falsely claim to cure or treat illness. It can be difficult to know if such a device has merit or not. There are a range of possible situations for a given device:

1. Complete fraud – device maker knows the device does not really work, but preys on sick people (despicable). It appears this is usually prevented by charging them with fraud. The FDA is also responsible for regulating and banning devices, but rarely bans them. The FDA has only banned 3 devices so far and only one prior to 2016. See here. Note that while the Dotto ring is not currently banned, the ring and Dotto's patented wand might be banned because the above 3 bans include a new 2024-proposed ban (reinstatement) on Electrical Stimulation Devices (ESDs). According to the proposal, this ban is only for devices intended for self-injury.
2. Means well, but may be harmful – device maker believes the device helps, but does not follow an accepted scientific process to develop and test. Because there are so many effective treatments now, this technology can harm people if they rely on it and do not get better treatment.
3. Scientifically developed – Follows accepted medical and legal rules to develop and test the technology.

I will not speculate on where the Dotto ring falls on the above scale. You should review the information in this report and decide for yourself.

In chronological order, here are what I am accepting as facts regarding the Dotto ring:

1) A NY Times article dated 12/29/1970 reports that the Ohio medical board was enforcing a ban and ordered Dotto to stop using his ring device to treat and diagnose human patients. A millionaire patient claimed he was successfully using the device to treat his leukemia and sued to stop the ban on the device. The patient died in 1974 at age 52.
2) Dr. Dotto wrote an article dated 2/8/1972 describing his ring device and his theory on how it works. This article is mostly speculation and has many untrue claims and some inconsistencies (see below for examples). He reports he had been testing the ring device for several years. He quoted from what he said was his 2nd patent application (I assume he was only counting medical patents): "second Dotto patent application # 42,301, filed June 1, 1970: "Milk taken from the right breast of a nursing mother is maintained separate from the milk taken from the left breast. On high-G centrifuge, viruses are separated from proteins and fats. Immunization will start with oral or injection methods, by using RNA type viruses from the right breast and repeated two months later with DNA type viruses from the left breast. In the human breast, there are all the variety of viruses necessary for the immunization."" I was unable to find a record of this patent application. It appears that it was never approved. I note it here to help establish the timeline of Dotto's medical work to treat and prevent cancer.
3) Dr. Dotto holds 43 US patents from 1961 to 1974. Listed here. The first 41 are mostly for automotive technology. Patent #42 dated 1/15/74 is for an electrostatic wand used as a medical device to treat pain. The last patent, dated 8/10/74, is for how to construct a thermionic couple (Dotto ring) used to treat cancer and prevent or reverse aging.

It is interesting that Dotto's article and patent were written (or published) years after the reported ban on his ring in 1970. Note that it is standard for patents to be written before a device is built or tested. This is intentional to ensure getting patent protection as early as possible. It is not necessary for a device to be built and tested to be patented; you can patent an idea and preliminary design. The ring he described in the patent is not necessarily the same as what he was testing in 1970.

In part due to the lack of accurate and correct detail in these documents, I suspect Dotto's prototype ring being tested in 1970 was not identical to that described in the 1972 article and the 1974 patent. The ring described in these documents would be difficult to test on human subjects. Putting a person inside a moving copper ring 9" wide, only 27" in diameter, and heated with 3-6 kW to 600-800 deg F on one side would be a dangerous burn risk. Note that this is twice the typical temperature inside a conventional oven. It would be possible to thermally insulate the ring to prevent this risk, but this is never mentioned. The device tested in 1970 might have been insulated or had lower power and temperature. Perhaps exposure to high temperature is part of

the envisioned treatment. It is also odd that there is not more credible information on the experimental Dotto ring (pictures, design detail, experiment results). There is just one article by an unspecified author that says it was published in an unspecified location. You can't get any less credible. Any tests performed need to be carefully designed and executed. For example, injecting healthy mice with cancer cells is NOT an accurate test of a device's anti-cancer potential. A healthy mouse's immune system can kill the cancer cells on its own.

I assume Dotto's theory and ring design evolved between 1970 and 1974. I note some changes and/or inconsistencies:

1) The 1972 report says a 1.8 MHz center frequency (he called cycles, really cycles/s or Hz) with 100 kHz bandwidth are required and to get these requires a semiconductor pellet (rectifier) between the cold junctions. The 1974 patent does not mention the semiconductor pellet, but describes the adjustment of the gap to produce a 100 kHz (0.1 MHz) center frequency with a 10 kHz bandwidth. The patent says to adjust the constantan rod length until the fluctuating signal is achieved and then braze the rod directly to the copper.

2) The beginning of the patent specifies 6kW of heating, but the example realization at the end uses 3kW of heating.

There are too many unsubstantiated and incorrect statements in these documents to point them all out. I will discuss a few of the major electromagnetic ones below.

Dotto "Scientific" Paper Electromagnetic Issues (1972)

1. Description of "Thermomagnetic Field" – Dr. Dotto claims that there are 4 different types of magnetic forces: 1) Permanent Magnet, 2) Electromagnet, 3) Electrostatic Attraction, and 4) Thermomagnetic Field. Number 3, Electrostatic Attraction, is not a magnetic force, and 4) Thermomagnetic Field is something Dotto is just making up. The magnetic forces of a permanent magnet and electromagnet are both due to magnetic fields created by motion of electrons. Dotto is defining a "Thermomagnetic Field" as the magnetic field that is created by electron motion caused by a thermoelectric effect, as in a thermocouple. This electromagnetic field is no different than a field generated by an electromagnet or wire coil with the same electrical current. Generating the magnetic field using a thermocouple is an extremely inefficient way of generating such a field. An identical magnetic field could be directly produced by applying the proper voltage to the ring.
2. Dotto claims that according to "Dotto Law:" "The thermomagnetic field is responsible for the general gravitation system: heat (sun) attracts cool (planet) and vice versa." While we may not fully understand gravity yet, this is not how it works.
3. Dotto's descriptions of the Thomson, Peltier, and Seebeck thermal effects are wrong. For more accurate descriptions, please see the references or the appendix here.

4. Despite Dotto's incorrect explanation about how they work, thermocouple operation is well-known. The Dotto ring copper-to-constantan connection forms a type-T thermocouple. Dotto goes on to say that "the voltage is maintained at a minimum of 25 to 45 millivolts." This can't be correct because the highest voltage achievable with a type-T thermocouple is about 21 millivolts. He then claims that "the 45 millivolts can produce 9000 amps of current by (ohm's law) with the resistance being 5 uOhms" ($u=10^{-6}$). Since the current is flowing around the ring through the copper and constantan in series, the resistance determining the voltage will be the sum of the copper and constantan resistances. The copper and constantan resistances can easily be calculated by their dimensions and resistivity. The copper part of the ring will have a resistance of about 11.4 uOhms. Therefore, the series resistance of the copper and constantan can't be less than 11.4 uOhms (can't be the claimed 5 uOhms. The patent says 5.27 uOhms.)
5. Dotto claims that the magnetic field at the edge of the ring is higher than at the center. It is known that this is backwards, the magnetic field at the center is highest.

Dotto Ring Patent Electrical Issues (1974)

1. The patent says: "Potential differences between the ears 57 have been recorded in the order of 0.156 millivolts, and the electrical resistance of the ring is in the order of 5.27×10^{-6} ohms. According to Ohm's Law, these conditions would indicate a current in the order of 30,000 amperes." See above #3 for why the ring resistance to use in Ohm's law can't be 5.27×10^{-6} ohms. It is possible this resistance would be measured if an ohmmeter were connected to the ears, but that is not the series resistance of the constantan and copper; and just the copper resistance alone would be higher. Also, the voltage would have to be 0.156 **Volts**, not millivolts, to produce 30,000 amps. A voltage of 0.156 millivolts would only produce about 30 amps. A voltage of 0.156 millivolts is low and 0.156 Volts is way too high for a type-T thermocouple. Perhaps you will say some Dotto magic was happening.

A few minor complaints: 1) units are sometimes incorrect – a cycle is not a frequency or bandwidth unit, this should be cycles per second (hertz, hz); cooling power is BTU/hr, not BTU (but just BTU is often written when BTU/hr is meant); I think he means alnico as the magnet alloy, not alnickel.

On the positive side:

If you are constrained to create a strong "thermomagnetic" field by using thermocouples, the Dotto ring design is a reasonably good one. The copper and constantan materials of a type-T thermocouple are the best for generating a large current around a closed ring. Only the type-E thermocouple has higher efficiency, but the relatively high resistance of type-E thermocouples would limit the ring current to

lower values. The large size and associated low resistance of the Dotto copper ring is required to produce a strong current from a thermocouple that can only produce a small voltage.

I think the ring structure could produce some resonant alternating (AC) frequency component to the generated magnetic field. However, I have not tested or tried to predict this yet. Any low-amplitude measured AC component could also be due to external electromagnetic energy (such as radio waves) coupling with the ring. I have noticed an AC component to the measured voltage on the scale-model ring, but have not determined the source.

Scale Model Ring Summary

To test the electrical characteristics and ability to predict them, I designed and built a ¼-scale model Dotto ring. This took about 3 weeks and about $290 worth of material.

The ¼-scale ring has higher resistance and less current than the full Dotto ring. I also have limited power and cooling sources within a reasonable cost and quick construction constraints (much more than 4x less). I was able to heat on side of the ring to about 213 deg F while cooling the other side to about 67.6 deg F. This temperature difference of 145.4 deg F across the thermocouple produces a total voltage of 1.6 mV and a current around the ring of 0.85 amps. The measured current of 0.85 amps agrees reasonably well with the predicted current of about 1 amp. Therefore, my predictions of the full-scale Dotto ring's electrical properties are probably more accurate than those given by Dr. Dotto.

Lessons Learned

I learned a lot about thermocouples and thermoelectric technology. I originally wanted to find out how much current a short-circuited thermocouple could produce. Some specific lessons are:

1. The thermocouple short circuit current limit depends on the size of the thermocouple wires (internal resistance). Thermocouples designed for temperature measurement have very small wires and are not designed to produce significant current (ideally close to zero).
2. It is more difficult to heat and cool an object to a specific temperature than I expected. The copper ring is a particular challenge because you are trying to both heat and cool it at the same time.
3. Be careful when drilling into thin sheet copper because when the drill bit breaks through, it tends to bind. This can make the copper sheet a sharp rotating blade that can produce a serious cut.
4. Don't mount electrical devices touching or close to a hot copper ring. Also, don't heat an electrical device above its operating temperature. This includes heating a nice digital thermometer above its rated temperature range (I really liked that

thermometer. Even though it has a lifetime warranty on accuracy, I think I voided that by what I did).

5. Don't try to connect the electrical wires after the controller is mounted. Connect them (with long-enough wires) and then mount them.
6. Only apply expensive thermal paste as late in the construction as possible. The paste wants to stick to your hands better than to anything else.
7. Don't bother trying to solder to the copper ring with just a soldering iron. The ring can't be heated enough to make a secure connection. You will just waste solder. You would need to use a torch or other similar device.

Alternative Designs and Future Plans

I'm not sure I can shed more light on the Dotto ring technology. I would like to get a temperature above my original goal of 200 deg F and ideally above the 213 deg F that I achieved so far. This would make it easier to evaluate the source(s) of the AC voltage. I may replace the heating TECs with higher power devices and see if they can produce a higher temperature without burning up. I ordered some 10-amp and 15-amp devices to try. Unfortunately, my ring design does not make it easy to replace the TECs.

Next, I plan to move on from Dotto technology and return to my previous boss's suggestion of developing improved solar cell power technology. He wanted me to evaluate feasibility of one of his ideas for a potentially breakthrough solar device. I have a few ideas of my own. This will be much more challenging than constructing the scale-model Dotto ring.

Alternate Designs

Full Scale Ring

A full-scale ring could be developed by scaling up the ¼ scale model. However, I scaled down the power for the cooling and heating subsystems by much more than a factor of ¼. The scale model cooling capacity is scaled down by about 55 instead of 4. The heating power is scaled down by about 17. In addition, scaling up to the full ring size requires scaling up in 3 dimensions (thickness, diameter, and width). This means the total copper volume is scaled up by a factor of $4^3 = 64$.

Ring Design – The ring could be made from copper sheet (flashing), as for the scale model, or copper plate (0.25" or 0.5" thick). It would be very difficult (for me) to bend copper plate to the correct radius. If flashing is used, the length of a single layer needs to be 76.8 inches or 6.4 feet. A 10-ft roll of 2", 24-gauge flashing costs $32. To get the proper 0.5" thickness, this requires 24 layers. The cost (8" vs 9" width) would be between about (24 x 6.4)/10 x 4 x $32 = $1,968 and 24 x 4 x $32 = $3,072. Building with the lower price requires piecing together (somehow) parts of rolls that are <6.4 feet. Another option is 6" wide, 24-gauge flashing in a 20-ft roll would make three 6"-layers per roll. You would need to use two and get a 12" width (vs spec of 9") or cut ½ of

the layers in half and join the 6" and 3" pieces (would be a pain to do neatly). This sheeting costs $124 per 20 ft. If you cut them and join to get the 9" width, the cost would be (24+12)/3 x $124 = $1,488.

Power, Heating, and Cooling Subsystems – Heating the ring to about 700 deg F would require a different heating component than the TEC devices because the TECs can only heat up to between 200 and 250 deg F. Some direct electrical resistance heater could be used (constantan wires, for example). Higher capacity cooling TECs could be used for cooling, but would require more heatsinks and fans. Assuming they each provide about 135 watts of cooling, about 23 TECs would be needed – cost = 23 x $5 = $115. The electrical power would be scaled up to the >6kW, 3kW for heating and 3kW for cooling. If you used the same 240-watt power supply ($360-watt supplies are also available for about $28 each, 18 needed), about 26 of them would be required (13 for cooling and 13 for heating)– cost = 26 x $20 = $520. The cost of heaters would depend on what is used. There are many options for electric heaters.

Smaller Scale Model

You could also scale down by more than ¼ to get a very inexpensive and easy-to-build design. The ring could be replaced by a thick copper wire. This would not be able to achieve much current due to the increased resistance. This would be just a shorted thermocouple.

Scale Model Components

In case you want to build your own, the components used by my ¼ scale model ring are summarized in Table 4 below.

Table 4. *Scale Model Ring Components, Cost, and Links*

Description	#	Unit Cost ($)	Total Cost	Comments and Links
Wood Base	1			
Screws (Brass wood, round head #, length	6			
Copper Flashing,24 Gauge, 2" width, 5 ft	2	19.13	38.26	https://www.amazon.com/dp/B0CG34ZYLV?ref=ppx_yo2ov_dt_b_product_details&th=1
Copper Flashing,26 Gauge, 2" width, 5 ft	1	12.99	12.99	https://www.amazon.com/dp/B0CG32LYCT?ref=ppx_yo2ov_dt_b_product_details&th=1
Copper Sheet, 18 Gauge (1mm),8"x8" for Fan Brackets and Cooling Plate	1	14.99	14.99	https://www.amazon.com/dp/B0BRD6JR84?ref=ppx_yo2ov_dt_b_product_details&th=1
Brass or Copper Bolts and Nuts (#, size TBD)				
Constantan Wire,0.7mm dia., 20 meters	1	11.70	11.70	https://www.amazon.com/dp/B0879B7V6T?psc=1&ref=ppx_yo2ov_dt_b_product_details
Thermoelectric Heating/Cooling Modules, pair of TEC1-12706 and heatsinks	2	9.58	19.16	https://www.amazon.com/dp/B0C4XGW261?psc=1&ref=ppx_yo2ov_dt_b_product_details
Nylon Screw & Nut, M6x60mm	1	0.60 (11.89/20)	0.60	https://www.amazon.com/dp/B0B527YQ5H?ref=ppx_yo2ov_dt_b_product_details&th=1

Ceramic Thermal Insulation, 12x12x1”	1	12.89	12.89	https://www.amazon.com/gp/product/B0BTNHN4BF/ref=ppx_yo_dt_b_asin_title_o04_s00?ie=UTF8&th=1
Styrofoam Insulation (cool side)	1			
Small Cooling Fan, 60mm x 15mm 12V	1	7.49 (14.98/2)	7.49	https://www.amazon.com/dp/B0BZKY4GF2?ref=ppx_yo2ov_dt_b_product_details&th=1
Cooling Fan Sockets	1	3.99	3.99	https://www.amazon.com/dp/B07FNQC63R?ref=ppx_yo2ov_dt_b_product_details&th=1
High Performance Fan, 80mm x 38mm 12V	2	15.99	31.98	https://www.amazon.com/dp/B0BXSG19ZP?ref=ppx_yo2ov_dt_b_product_details&th=1
Thermal Paste, Arctic MX-6, 8g	1	9.01	9.01	https://www.amazon.com/dp/B09VDLH5M6?psc=1&ref=ppx_yo2ov_dt_b_product_details
Metal Strip Clamp (hose clamp), 13 ft	1	7.99	7.99	https://www.amazon.com/dp/B0D2J1JB65?ref=ppx_yo2ov_dt_b_product_details&th=1
Pentium Circular Heatsink (active cooling)	1	14.95	14.95	https://www.amazon.com/dp/B00HYO2V34/?coliid=I1KXT9E0UHY7OE&colid=1ITQ8GJ0LW76W&psc=1&ref_=list_c_wl_lv_ov_lig_dp_it
Pentium Tower Heatsink (passive cooling)	1	24.50	24.50	https://www.amazon.com/dp/B08P5SR4S2/?coliid=I26GBTJSIWDC7I&colid=1ITQ8GJ0LW76W&psc=1&ref_=list_c_wl_lv_ov_lig_dp_it
Terminal Block, 16A 12x2 position	1	10.99	10.99	https://www.amazon.com/dp/B08TBXQ7H6?psc=1&ref=ppx_yo2ov_dt_b_product_details
Power Cord, 9 ft, 16/3 13 A	1	8.01	8.01	https://www.amazon.com/dp/B07BQB7FH5/ref=sspa_dk_detail_0?pd_rd_i=B07BQB7FH5&pd_rd_w=WJ8O4&content-id=amzn1.sym.386c274b-4bfe-4421-9052-a1a56db557ab&pf_rd_p=386c274b-4bfe-4421-9052-a1a56db557ab&pf_rd_r=D31DSYJSCAVJXDDKGFAS&pd_rd_wg=VO7I2&pd_rd_r=80aaf039-443b-4a4f-a6ac-ddf6884a6570&s=electronics&sp_csd=d2lkZ2V0TmFtZT1zcF9kZXRhaWxfdGhlbWF0aWM&th=1
Electrical Box, Small	1	4.00 (7.99/2)	4.00	https://www.amazon.com/dp/B0BRW7CV1P?ref=ppx_yo2ov_dt_b_product_details&th=1
Power Supply, 12V, 20 A	1	19.99	19.99	https://www.amazon.com/dp/B01E6S0JS4?ref=ppx_yo2ov_dt_b_product_details&th=1
Power Switch, Rocker, SPST	1	2.20 (10.99/5)	2.20	https://www.amazon.com/Nilight-Rocker-Toggle-Switch-Waterproof/dp/B078KBC5VH/ref=sr_1_16?dib=eyJ2IjoiMSJ9.ZJZ72jkRgliQk9rf8MjS5S6unTye9bPXs4WTQGlkz5nB5c7Cf2N7PQoq6z65IynmSIyDrQ75KVhv-DdqWBXQdMSxuj31OPTVUGSl4uou4ss9TnECAqKW21yR8xjzEJnc1cwYhUFIF2w_5jcKqRs7PI-6YFSjymAXDfxS9ulCatuq0Or4v4z9bgI22s9ugQi9tXado3PIY5Rv9IKLtwqQMGEMNRpIZ1xCLIJftnNgJUM.pQdnxWvPhRVMeqnIFloBtnA_zNhwJx1QjLmLdbMSJB0&dib_tag=se&keywords=Power%2Bswitch%2Brocker%2Btoggle&qid=1721750248&sr=8-16&th=1

Digital Voltage/Current Meter	1	4.50 (8.99/2)	4.50	https://www.amazon.com/gp/product/B0CQC6781P/ref=ppx_od_dt_b_asin_title_s00?ie=UTF8&psc=1
Digital Thermometer, Dual LED	1	14.99	14.99	https://www.amazon.com/gp/product/B0928QY786/ref=ppx_od_dt_b_asin_title_s00?ie=UTF8&psc=1
Digital Temperature Controller, 2-pack	2	9.99	19.98	https://www.amazon.com/dp/B08W2BYG2L?ref=ppx_yo2ov_dt_b_product_details&th=1
Volt/Ammeter with Hall Effect Current Sensor	1	21.59	21.59	https://www.amazon.com/dp/B0BFJ5NV5L?psc=1&ref=ppx_yo2ov_dt_b_product_details
High Precision Digital Voltmeter	1	14.99	14.99	https://www.amazon.com/gp/product/B08N45HMCJ/ref=ppx_yo_dt_b_asin_title_003_s00?ie=UTF8&psc=1
Copper Wire and Connectors, Misc.				
Ceramic Fiber Insulation, 24x12x1" (hot side)	1	12.89	12.89	https://www.amazon.com/dp/B0BTNHN4BF?ref=ppx_yo2ov_dt_b_product_details&th=1
TOTAL			344.63	($287.03 if you exclude $57.60 worth of items I got from scrap)

Useful Tools

Figure R2 shows some tools used to create and analyze the model ring.

Figure R2*. Useful Tools for Ring Construction and Analysis (The Hakko soldering station is not shown because it was part of the initial ring design).*

Device Specifications and Reference

TEC1-12706 Thermoelectric Cooler

Peltier 12V Semiconductor Refrigeration TEC1-12706 Peltier Module TEC

Product Description

CXTech thermoelectric cooler (TEC) modules offer efficient cooling, heating, and precise temperature control for various applications. TEC widely used in household appliances and medical beauty equipment, including ice cream machines, mobile phone radiators, car refrigerators, eye massagers, hair extractors, facial massagers, and hair dryers, etc.

Specification

External dimensions:	40*40*3.75mm
Internal resistance:	2.1~2.4Ω (ambient temperature 23±1°C, 1kHZ Ac test)
Large temperature difference:	ΔTmax (Qc = 0) 67 ° C or more.
Working current:	Imax=4-6A (when rated at 12V)
Rated voltage:	12V (Vmax: 15V starting current 5.8A)
Cooling power:	Qcmax = 50-60W (53 in chart below)
Working environment:	Temperature range -55 °C ~ 83 °C (-67 to 181 deg F)
Service	OEM/ODM

QC	100% test the product before the shipment

Note:* For custom sizes or specific requirements, please contact us directly.

Description:

This Peltier thermoelectric cooler creates a temperature differential on each side. One side gets hot and the other side gets cool. Therefore, they can be used to either warm something up or cool something down, depending on which side you use. You can also take advantage of a temperature differential to generate electricity. The thermal tape listed below works very well to attach heat sink to the hot side.

Note: It is imperative that a heat sink is used on the hot side of the module. Running the module without a heat sink (2 seconds) can cause damage to this part. Be careful of the hot side when you attempt to touch it!
The side with "TEC1-12706" text is the hot side, the other side with no text is the cooler side. NOTE: I received some devices with the text on the cool side. A better way of determining the hot side (than the side with writing): place the device on a flat surface with the wires down and the black wire on the right – the top side is hot.

Specifications:

- Operating Voltage: 12 V
- Power: 60 W
- Module Dimension: 40 x 40 x 3.4 mm
- Vcc: Red Wire
- GND: Black Wire
- Max Operating Temp: 120°C (248 deg F)
- Min Operating Temp: -40°C
- Wire Length: 300 mm
- Weight: 23.8 g

About this item

- Model: TEC1-12706 Size: 40mm x 40mm x 3.6mm.
- Refrigeration power: Qcmax 50-60 W.
- Storage Conditions: -40℃ ~ 60 ℃. (to 140 deg F)
- Working Current: 4.3-4.6 A (rated 12 V); Imax: 6 A.

Model	Imax(A)	△Tmax(°C)	Vmax(Qc=0w)	Qcmax(△T=0℃)
TEC1-00702	2	62	0.85	1
TEC1-12704	4	66	15.40	35.56
TEC1-12705	5	66	15.40	44.45
TEC1-12706	6	66	15.40	53.34
TEC1-12707	7	66	15.40	62.23
TEC1-12708	8	66	15.40	71.12
TEC1-12709	9	66	15.40	80.01
TEC1-127010	10	66	15.40	88.9
TEC1-127011	11	66	15.40	97.79
TEC1-127012	12	66	15.40	106.68
TEC1-127013	13	66	15.40	115.57
TEC1-127014	14	66	15.40	124.46
TEC1-12715	15	66	15.40	133.35

Note: there are many more module options, above is just a partial list

20 A Power Supply

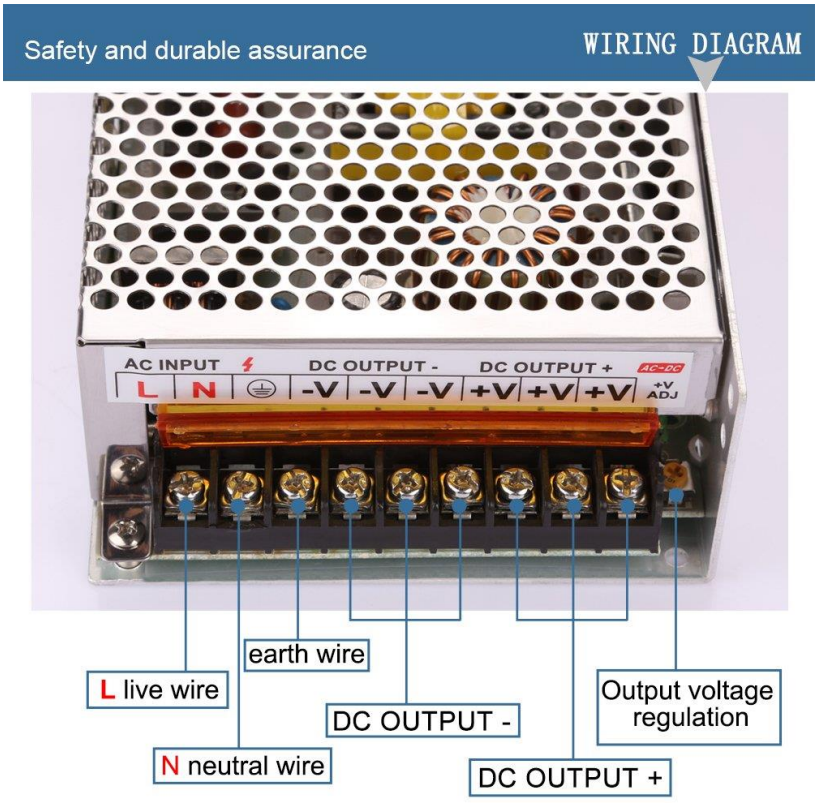

Brand	LEDMO
Power Source	AC
Mounting Type	Surface Mount
Current Rating	20 Amps
Maximum Frequency	60 Hz

About this item

- High quality Switch Power Supply, widely used in Industrial automation, LED display, etc. With anti-jamming to ensures the long-life LED lamps and reduce the LED luminous decay
- Universal AC input / Full range. The input voltage: AC 100V/240V, the output current: 20A
- Smart device surge protection for Shortage, Overload, Over Voltage
- Dual input voltage: AC 110V/220V. There is a switch, choose the proper voltage before use
- widely used in LED lighting, Home Appliance, Instrumentation, Office Automation, Telecom, Process and Engineering Industries etc.

Voltage/Hall-Effect Current Sensor

- Dual display: Display Voltage and (+ -) Current at the same time; Power supply: DC 5~100V; Voltage test range: 0~300V; Current test range: ±0~100A

Bayite DC 5-100V 100A Digital Volt Amp Meter is a 2-in-1 meter for real-time current and voltage monitoring. The display is large, easy to read, and accurate. Package even includes an extension cable (6.5 feet) for the Hall effect sensor, providing more versatile installations.

Main Specifications:

- Power Supply: DC 5-100V
- Current Measurement Range: + -100A
- Voltage Measurement Range: 0-300V
- Measuring Accuracy: + -1%
- Working current: 7-15mA
- Overall Dimensions: 48mm*29mm*18mm
- Cutout size: 45.5mm*26.0mm
- Sensor hole diameter: 3/4 inch (19mm)
- Operating temperature: -4°F - 140°F (-20°C - 60°C)
- Reverse Polarity Protection：Yes

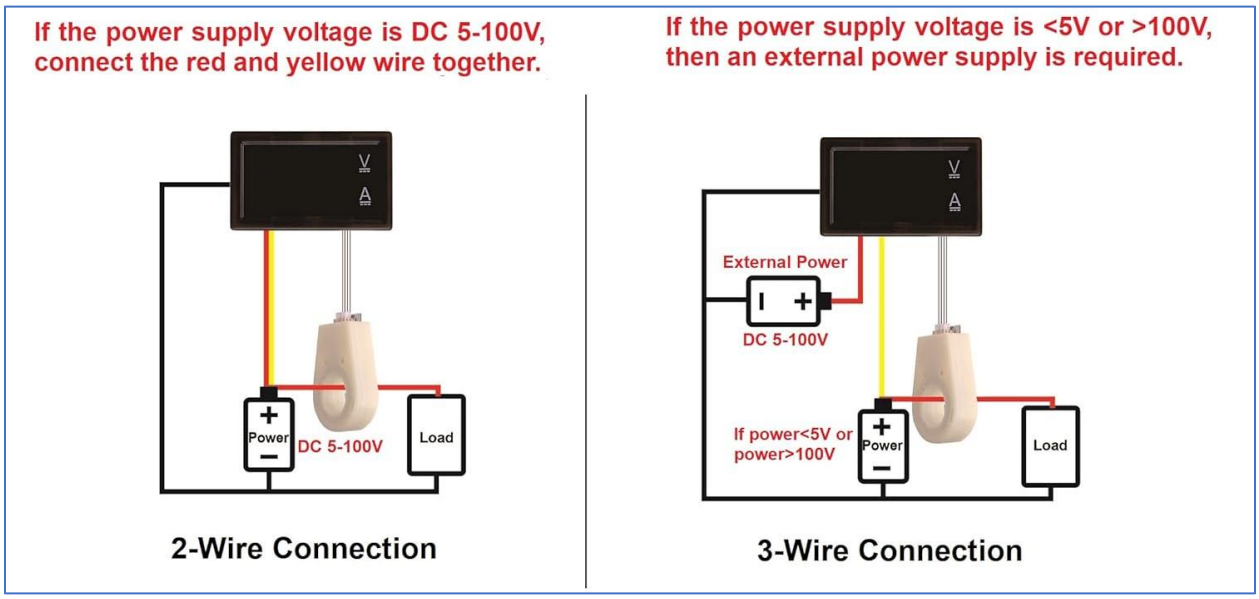

Voltage and Current Meter

Brand: **Exqutoo**	Working Voltage of Meter: **DC 4 - 30V**	Power Source: **Battery Powered, electric**
Material: **Metal, Plastic**	Working Current of Meter: **≤20mA**	Working temperature: **-10°C-65°C**
Display Color: **Red & Blue**	Voltage Measuring Range: **DC 0 - 100V**	Refresh rate: **about 300mS / once**
Style: **2 in 1 Volt Amp Meter**	Current Measuring Range: **DC 0 - 10A**	Dimensions (L*W*H): **48 x 29 x 22 mm**

Share the Power Source

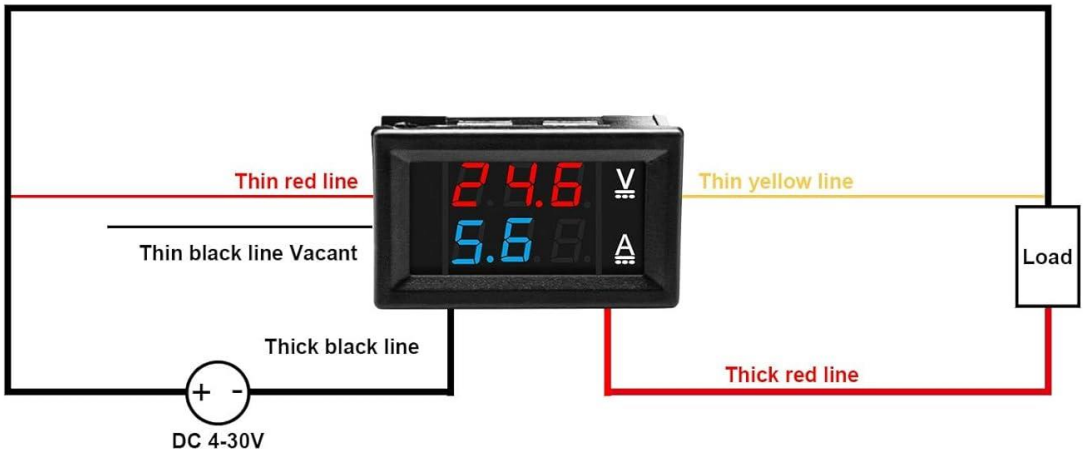

Independent Power Supply

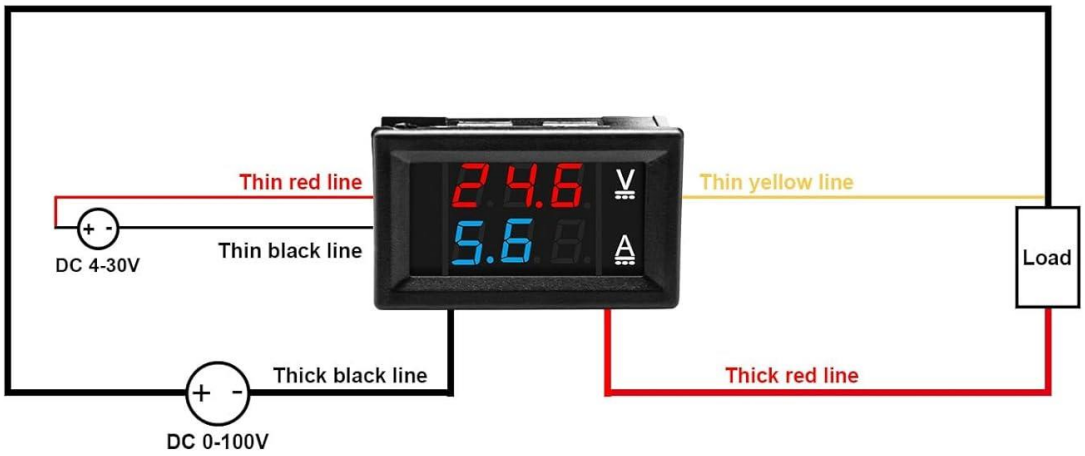

Temperature Controller

Parameter adjustment operation instructions

All button operations are divided into "long press" and "short press"

Long press: Press the button for about 3 seconds to release.
Short press: Press the button for 1 second to release.
Long Press: Enter the next menu, or increase or decrease the number value.
Short Press: Switch between menu items at the same level.
No button operation within 5 seconds: flashing and saving will automatically return to the previous menu.

Setting method

In normal mode, press the button for 3 seconds to enter the setting mode, and C1 is displayed.
At this time, release the button, then press the button briefly, and the loop display: C1 C2 CF CA.

C1: stands for temperature 1 fine adjustment correction setting.
C2: stands for temperature 2 fine adjustment correction setting.
CF: stands for switching between Celsius and Fahrenheit.
CA: It represents two-way temperature recovery factory settings.

When C1 is displayed, long press the button to enter the temperature 1 fine-tuning correction setting
At this point, release the button, and then "long press the button", the value will increase upward,
after releasing the button, "long press the button" again, the value will decrease downward,
and repeatedly adjust to the corresponding temperature value
Wait for the screen to flash to save the settings and return to the previous menu

When C2 is displayed, long press the button to enter temperature 2 fine-tuning correction settings
At this point, release the button, and then "long press the button", the value will increase upward,
after releasing the button, "long press the button" again, the value will decrease downward,
and repeatedly adjust to the corresponding temperature value
Wait for the screen to flash to save the settings and return to the previous menu

Celsius, Fahrenheit switching:

When CF is displayed, long press the button to switch between Celsius and Fahrenheit
At this point, release the button, and then "short press the button", the cycle displays: C/F
C:represents the display in degrees Celsius
F:stands for Fahrenheit
Displays "C" by default
When switching to the corresponding parameter, release the button, wait for the screen to flash,
save and return to the previous menu

Two-way temperature reset to factory settings:

When CA is displayed, long press the button to enter the two-way temperature reset to factory settings
At this point, release the button, and then "short press the button", the cycle displays: NO/YES
NO: not to restore factory settings
YES: restore factory settings
Displays "NO" by default
When switching to the corresponding parameter, release the button, wait for the screen to flash,
save and return to the previous menu

Temperature Control and Load the 12V Cases Wiring Way

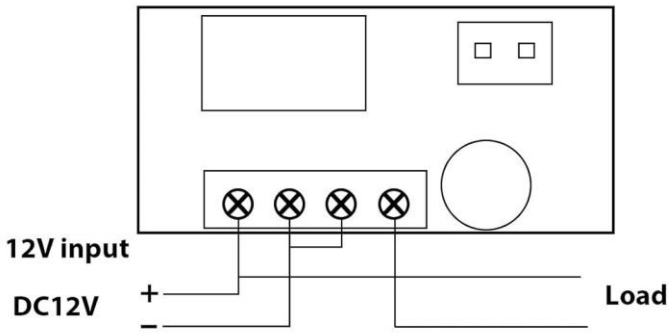

Load and Temperature Control Different Power Wiring Diagram

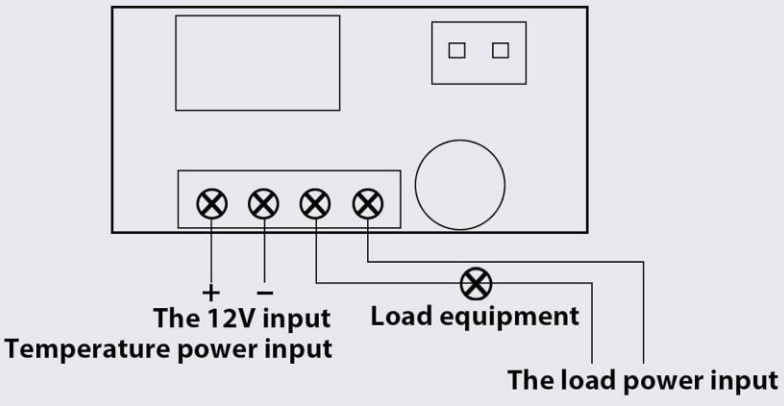

- What will receive: you will get 2 pieces of direct-current 12V 200 mA temperature controllers, the measurement temperature is from -50 to 110℃(-58 to 230℉), the control and backlash precision: 0.1 Celsius, the refresh rate: 0.5 s, the module size: 48 x 29 x 32 mm/ 1.89 x 1.14 x 1.26 inch, the probe length: 1.5 inches, the cable probe length: 1 ft
- Dual color LED display: this digital thermostat control module of dual color LED display, which show the measured temperature (red) and set temperature (blue) at the same time, which can be applied for cooling/ heating mode, you can test indoor or outdoor temperature
- Waterproof design: the NTC (10K 0.5%) probe is waterproof, and you can control the temperature at will, can also control heating or cooling according to different needs
- Reliable to use: the electronic temperature control switch module has been tested for consistency and reliability, and its control accuracy is 0.1 degrees Celsius, backlash precision is 0.1 degrees Celsius with high temperature protection

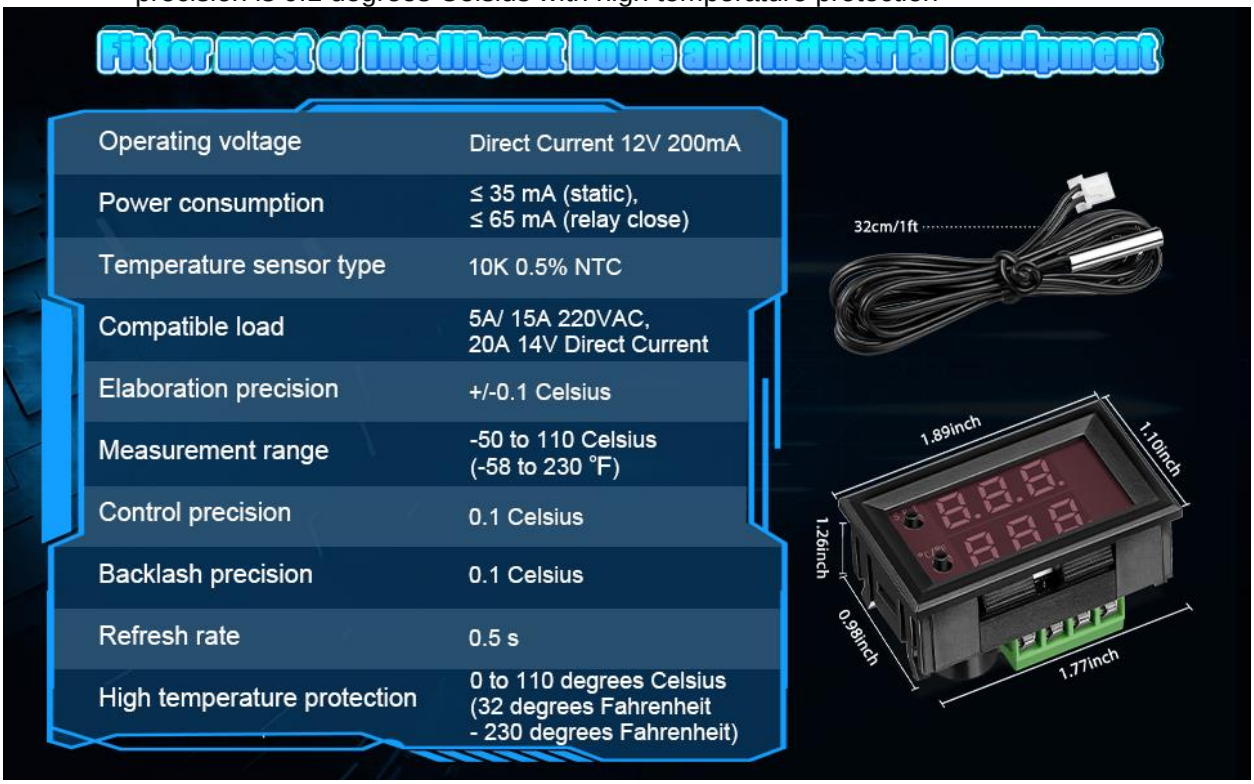

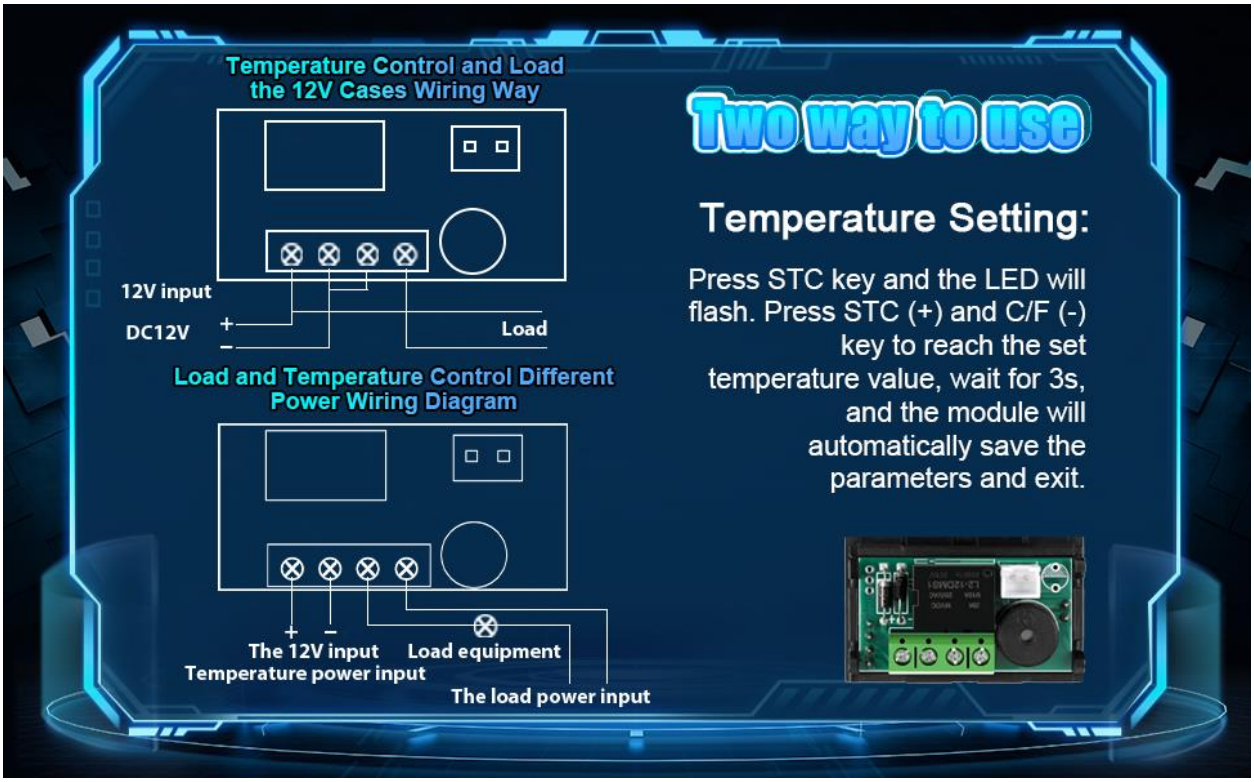
Temperature Control and Load
the 12V Cases Wiring Way
12V input
DC12V
+
−
Load
Load and Temperature Control Different
Power Wiring Diagram
+
−
The 12V input
Temperature power input
Load equipment
The load power input
Two way to use
Temperature Setting:
Press STC key and the LED will flash. Press STC (+) and C/F (-) key to reach the set temperature value, wait for 3s, and the module will automatically save the parameters and exit.

KTF0091 Temperature Controller Operating Manual

1. Overview

- A mini temperature controller.
- With clear LED display for better readability.
- Wide temperature measuring range.
- Heating or cooling control.
- All parameters setting can be saved after short circuit.
- Built-in alarm
- high Control precision 0.1 centigrade
- Can be used for domestic freezer, water tanks, refrigerator, industrial chiller, steamer, industrial equipment and other temperature-controlled system.

2. Specifications

- Power Supply: DC 12V
- Temperature control range: -50~110°C
- Difference Set Value: 0.1~30°C
- Resolution Ratio: 0.1°C(-9.9-99.9); 1°C(other range)
- Measurement accuracy: ±0.1°C
- Control accuracy: 0.1°C
- Refresh rate: 0.5S
- Measuring inputs: NTC(10K0.5%) Waterproof sensor
- Output: Relay Contact Capacity 10A/220V or 20A/110V
- Environmental requirements: -10-60°C , humidity 20% -85%RH
- Size: 48mm(L)*29mm(W)*32mm(Depth)
- Hole size: 46(L)*26.5(W)mm
- Power consumption: Static current: ≤35MA,attract current: ≤65MA

3. Wiring Diagram

Connection 1:Independent power supply for load

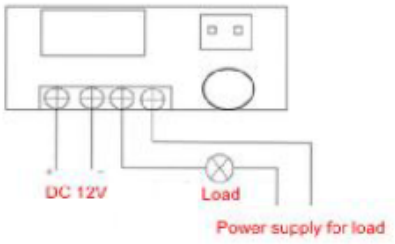

Connection 2:Same power supply for load

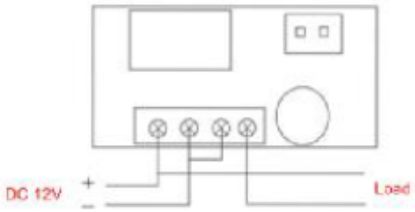

4. Key Instruction

Set Key:Confirm the setting value, Entry, Exit and Set parameter ,Increase Value,
°C/°F:Switch Celsius and Fahrenheit, decrease value
Red Led:Current Temp value
Blue Led:Setting Temp value

5. Key Operation Instruction

- In normal working status, press set key once. The blue led flash.Press Set or **°C/°F** to increase or decrease the setting temperature value. Waiting for 3seconds to save it and back to normal display screen.
- In normal working status, press set key for 5s to enter set mode.press Set or **°C/°F** to switch from P0-P8.
- If you want to adjust P0, when it display P0, press Set and **°C/°F** at the same time,and the P0 figure will flash, Then press Set or **°C/°F** to adjust. Then press Set and **°C/°F** at the same time to save. The setting way of P1-P8 is the same as P0.

6. Operation Instruction

- In normal working status, screen displays the current measuring value and setting value.
- When P0 set to be C, it turns to be cooling mode. If the measuring temperature ≥ TS (temperature set value) + DS (difference set value), the output relay is connected.The load start working. If the measuring temperature ≤ TS, the cool indicator lamp turns off, the output relay is disconnected, and the load stop working.
- When P0 set to be H, it turns to be heating mode. If the measuring temperature ≤ TS (temperature set value) - DS (difference set value), the output relay is connected.The load start working. If the measuring temperature ≥ TS, the cool indicator lamp turns off, the output relay is disconnected, and the load stop working.

7. Parameters

Code	explain	Setting Range	Factory Setting
P0	Heating/Cooling	H/C	C
P1	Return Difference	0.1-30	2.0
P2	Set Limit Max.	+110	110
P3	Set Limit to the Min.	-50	-50
P4	Temperature Correction	-15~15	0
P5	Delay Start	0-10	0
P6	High Temperature Alarm	-50~110	OFF
P7	°C/°F	CS/FH	CS
P8	Factory Reset	ON-OFF	OFF

High-Precision Voltmeter

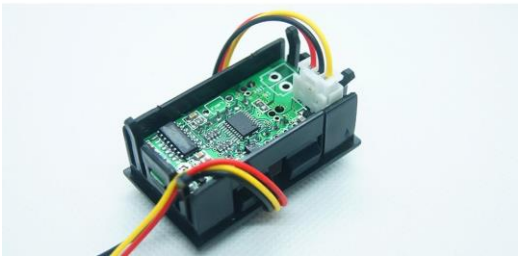

- ☛Voltmeter Digital Voltage Meter: This product is fully functional; you can display the battery voltage; Measurement range: DC: 0.000-33.000V
- ☛ Refresh rate: 5 times per second; Measurement accuracy: ±0.3‰
- ☛Digital Voltmeter Display: High brightness LED display, easy and clear to read
- ☛Easy to Use: Mini size and easy to install, work great for checking voltage and battery power
- ☛Dimensions: 48mm*29mm*22mm; Opening size: 45mm*26mm

Appendix A. References

The Dotto paper and patent are not an accurate source of modern scientific information. The following reference list is provided as better sources related to Dotto ring technology. The references are split between scientific categories and between "Public" and "Private." Public sources are easily found on the internet. Note they are not necessarily accurate and may be copyrighted. The private sources are copyrighted and you should pay for them if you copy and use them. They may be available on the internet from an illegal source. Private sources are more reliable than information found publicly on the internet. It is best to cross check information using multiple sources. Even if found on multiple sources, information may be incorrect because sources may be correlated (from the same wrong source).

Aging

Public

1. Kirkwood, The Origins of Human Ageing, 1997, 8pp
2. Li et al., Aging and age-related diseases: from mechanisms to therapeutic strategies, 2021, 23pp
3. Holliday, The Multiple and Irreversible Causes of Aging, 2024, 5pp
4. AFAR, Theories of Aging, 2016, 9pp
5. Lopez-Otın et al., The Hallmarks of Aging, 2013, 24pp
6. Sgarbieri, Healthy human aging: intrinsic and environmental factors, 2017, 23pp
7. Martynov, Factors and Causes of Aging, 2003, 20pp
8. Park and Yeo, Aging, 2013, 6pp
9. Lopez-Otın et al., Hallmarks of aging: An expanding universe, 2023, 36pp
10. -, Aging: The Biology of Senescence, 57pp
11. Troen, The Biology of Aging, 2021, 21pp
12. Alessio, Physiology of Human Aging, 2001, 31pp
13. Pignolo, The Biology of Aging: An Overview, 2010, 74pp
14. Sobhon et al., Oxidative stress and inflammation: the root causes of aging, 2022, 30pp
15. House of Lords, Ageing, Science, Technology, and Healthy Living, 2021, 132pp
16. Boniewska-Bernacka and Pańczyszyn, SELECTED THEORIES OF AGEING, 2016, 4pp
17. McHugh and Gil, Senescence and aging: Causes, consequences, and Therapeutic Avenues, 2018, 13pp

General Biology

Public

1. -, An Introduction to Biology, 33pp
2. O'Grady et al., Principles of Biology – An Introduction to Biological Concepts, 2021, 448pp
3. OpenStax College, Concepts of Biology, 2013, 638pp
4. -, The Science of Biology, 1226pp
5. Clark et al., Biology 2e, 2020, 1447pp
6. Wheat and Fitzpatrick, Advanced Biology, 1929, 578pp
7. Kratz and Siegfried, Biology for Dummies, 2010, 338pp

Biochemistry & Biophysics

Public

1. Hames & Hooper, Biochemistry, 2005, 449pp
2. Nelson & Cox, Lehninger Principles of Biochemistry, 4e, 1120pp
3. Gilber, Basic Concepts in Biochemistry – A Student's Survival Guide, 2000, 311pp
4. Devlin, Biochemistry, 2010, 2526pp
5. Kopchak et al., Structural Biochemistry, 2021, 85pp
6. Ahern, Biochemistry and Molecular Biology - How Life Works, 2019, 414pp
7. Berg et al., Biochemistry, 5e, 1515pp
8. Nelson, Biological Physics: Energy, Information, Life, 2002, 532pp
9. Casey, BIOPHYSICS Concepts and Mechanisms, 1962, 360pp
10. Kervalishvili, APPLIED BIOPHYSICS, 2021, 281pp
11. Rosana, Biophysics - An Introduction, 2020, 306pp
12. Jackson, Molecular and Cellular Biophysics, 2006, 524pp
13. Voet et al., Fundamentals of Biochemistry Ch 10 Membrane Transport Charts, 2006, 28pp
14. Gajera et al., Fundamentals of Biochemistry – A Textbook, 2008 ,557pp
15. Tuszynski & Kurzynski, Introduction to Molecular Biophysics, 2003, 540pp
16. Adugna et al., Medical Biochemistry, 2004, 264pp
17. -, Biophysics, 56pp
18. Wilson & Walker, Principles and Techniques of Biochemistry and Molecular Biology, 1986, 761pp
19. Meisenberg & Simmons, Principles of Medical Biochemistry, 2017, 635pp
20. Vasudevan et al., Textbook of Biochemistry for Medical Students, 2011, 672pp
21. Schwarz, Theoretical Biophysics, 2021, 237pp
22. Bialek, Biophysics: Searching for Principles, 2011, 310pp

Private

1. Voet et al., Fundamentals of Biochemistry– Life at the Molecular Level, 2016, 1179pp
2. Nelson et al., Lehninger - Principles of Biochemistry, 2021, 4381pp
3. Abali et al., Lippincott Illustrated Reviews: Biochemistry, 2022, 1624pp
4. Hofmann & Clokie, Wilson and Walker's Principles and Techniques of Biochemistry and Molecular Biology, 2018, 960pp

Cell Biology

Public

1. -, CELL CYCLE AND CELL DIVISION, 2024, 11pp
2. -, Cell Division Stages of Mitosis, 4pp
3. -, Cell Division, 8pp
4. -, Cell Cycle: Mitosis Quiz, 2pp
5. -, Cell Cycle and Cell Division, 26pp
6. Brust-Mascher et al., Cell Division, 2014, 8pp
7. Morgan, The Cell Cycle: Principles of Control, 2007, 315pp
8. -, Cell Cycle and Cell Division, 20pp
9. -, The Process of Cell Division Charts, 20pp
10. -, Cell Cycle, 20pp
11. -, Chromosomes, the Cell Cycle, and Cell Division Charts, 2005, 55pp
12. -, Cell Division: Mitosis and Meiosis, 2pp
13. -, Cell Division, Genetics, and Molecular Biology, 158pp
14. -, The Cell Cycle Charts, 2016, 95pp
15. Berridge, Cell Cycle and Proliferation, 2014, 45pp
16. Dikmenli, Misconceptions of cell division held by student teachers in biology: A drawing analysis, 2010, 13pp
17. -, Cell Division. Mitosis and meiosis, 5pp
18. -, Anatomy of the Cell and Cell Division, 14pp
19. Travers & Muskhelishvili, DNA structure and function, 2015, 18pp
20. Brust-Mascher & Mogilner, Cell Division, 2003, 8pp
21. Mattick & Amaral, RNA - The Epicenter of Genetic Information, 2023, 400pp
22. Wong, Cells: Molecules and Mechanisms, 2024, 284pp
23. Bathe & Grodzinsky, Fields Forces and Flows in Biological Systems, 2015, 37pp

DNA

Public

1. Keller & Linko, Challenges and Perspectives of DNA Nanostructures in Biomedicine, 2020, 16pp
2. Bonilla et al., RAD51 Gene Family Structure and Function, 2020, 22pp
3. Edogbanya et al., Evolution, structure and emerging roles of C1ORF112 in DNA replication, DNA damage responses, and cancer, 2021, 12pp
4. Spiegel et al., The Structure and Function of DNA G-Quadruplexes, 2020, 14pp
5. Nasir & Al Ahmad, Cells Electrical Characterization: Dielectric Properties, Mixture, and Modeling Theories, 2020, 17pp
6. Juan et al., The Chemistry of Reactive Oxygen Species (ROS) Revisited: Outlining Their Role in Biological Macromolecules (DNA, Lipids and Proteins) and Induced Pathologies, 2021, 21pp
7. Naaman et al., Chiral Induced Spin Selectivity and Its Implications for Biological Functions, 2021, 16pp
8. Yang et al., Effect of static magnetic field on DNA synthesis: The interplay between DNA chirality and magnetic field left-right asymmetry, 2020, 10pp
9. Maffeo et al., Close Encounters with DNA, 2014, 74pp
10. Paul & Montoya, CRISPR-Cas12a: Functional overview and applications, 2020, 10pp
11. Kwon & Bakhoum, The Cytosolic DNA-Sensing cGAS–STING Pathway in Cancer, 2019, 14pp
12. Fantini et al., What Is life? Rethinking Biology in Light of Fundamental Parameters, 2024, 21pp
13. Kim, Molecular Link between DNA Damage Response and Microtubule Dynamics, 2022, 15pp
14. Cuella-Martin et al., Functional interrogation of DNA damage response variants with base editing screens, 2021, 37pp
15. Huang & Zhou, DNA damage response signaling pathways and targets for radiotherapy sensitization in cancer, 2020, 27pp
16. Giglia-Mari et al., DNA Damage Response, 2011, 19pp
17. Carusillo & Mussolino, DNA Damage: From Threat to Treatment, 2020, 20pp
18. Oh et al., Dynamics Studies of DNA with Non-canonical Structure Using NMR Spectroscopy, 2020, 22pp
19. Robinson et al., DNA G-quadruplex structures: more than simple roadblocks to transcription?, 2021, 13pp
20. Xu et al., Structural basis of DNA replication origin recognition by human Orc6 protein binding with DNA, 2020, 16pp
21. Neidle, Beyond the double helix: DNA structural diversity and the PDB, 2021, 12pp
22. Baum, DNA – The Molecule of Life! Charts, 20pp

23. Banerjee, Basics of DNA Structure & Function Charts, 67pp
24. -, DNA Structure, 44pp
25. -, DNA, RNA, GENES AND CHROMOSOMES, 2021, 4pp
26. Shell, DNA, RNA, replication, translation, and transcription, 2010, 12pp
27. -, DNA: The Genetic Material, 36pp
28. Lipfert et al., Understanding Nucleic Acid–Ion Interactions, 2014, 35pp
29. -, Genetics, DNA, and Heredity Charts, 34pp
30. Reif, Introduction to DNA Charts, 113pp
31. Vierstraete, The Central Dogma of Molecular Biology, 2000, 23pp
32. -, Molecular Basis of Inheritance, 2024, 31pp
33. -, The Structures of DNA and RNA, 2002, 32pp
34. Watson, The Double Helix, 1967, 83pp
35. Travers & Muskhelishvili, DNA structure and function, 2015, 18pp
36. Shi et al., Analytical study of the dynamics in the double-chain model of DNA, 2023, 9pp
37. Mishra et al., Length-Dependent Electron Spin Polarization in Oligopeptides and DNA, 2020, 7pp
38. The ENCODE Project Consortium – Moore et al., Expanded encyclopaedias of DNA elements in the human and mouse genomes, 2020, 27pp
39. Yang et al., Epigenetic regulation in the tumor microenvironment: molecular mechanisms and therapeutic targets, 2023, 26pp
40. Gu et al., Novel insights into extrachromosomal DNA: redefining the onco-drivers of tumor progression, 2020, 10pp
41. Fransson, Charge Redistribution and Spin Polarization Driven by Correlation Induced Electron Exchange in Chiral Molecules, 2021, 7pp
42. Mattei et al., DNA methylation: a historical perspective, 2022, 32pp
43. -, Molecular Biology of the Cell (Samples), 22pp
44. Guerra Liberal et al., Most DNA repair defects do not modify the relationship between relative biological effectiveness and linear energy transfer in CRISPR-edited cells, 1023, 10pp
45. Taiana et al., LncRNA NEAT1 in Paraspeckles: A Structural Scaffold for Cellular DNA Damage Response Systems?, 2020, 17pp
46. Pavan et al., On Broken Ne(c)ks and Broken DNA: The Role of Human NEKs in the DNA Damage Response, 2021, 25pp
47. Chevizovich et al., A review on nonlinear DNA physics, 2020, 23pp
48. Poetsch, The genomics of oxidative DNA damage, repair, and resulting mutagenesis, 2020, 13pp
49. Duboué-Dijon et al., A practical guide to biologically relevant molecular simulations with charge scaling for electronic polarization, 2020, 16pp
50. Bernhofer et al., PredictProtein - Predicting Protein Structure and Function for 29 Years, 2021, 6pp
51. Wang et al., Rapid recruitment of p53 to DNA damage sites directs DNA repair choice and integrity, 2022, 12pp
52. Sang et al., A rewiring model of intratumoral interaction networks, 2019, 7pp

53. Thakur et al., Sequence, Chromatin and Evolution of Satellite DNA, 2021, 28pp
54. Wang et al., Slowing down DNA translocation through solidstate nanopores by edge-field leakage, 2021, 10pp
55. Yuan et al., The influencing factors and functions of DNA G-quadruplexes, 2020, 9pp
56. Tucker et al., Development of Force Field Parameters for the Simulation of Single and Double-Stranded DNA Molecules and DNA–Protein Complexes, 2022, 16pp

Microbiology (not directly related to Dotto Technology, included for completeness & because Lisa is a Microbiologist)

Public

1. Hogg, Essential Microbiology, 2005, 481pp
2. Bruslind, General Microbiology, 2019, 176pp
3. Kayser et al., Medical Microbiology, 2005, 725pp
4. Tadesse & Alem, Medical Bacteriology,2006, 444pp
5. Parija, *Microbiology and Immunology*, 2012, 682pp
6. Parker et al., Microbiology, 2017, 1314pp
7. Parker et al., Microbiology, 2021, 1265pp
8. Trivedi et al., Text Book of Microbiology, 2010, 457pp

Private

1. Tortora et al., Microbiology – An Introduction, 2019, 965pp
2. Pelczar et al., Microbiology, 1986, 957pp
3. Willey et al., Prescott's Microbiology, 2014, 1139pp

MIT Public Biology, Biological Chemistry, Genetics, and Quantum Physics Courses

Biology: https://ocw.mit.edu/courses/7-016-introductory-biology-fall-2018/

Biological Chemistry I: https://ocw.mit.edu/courses/5-07sc-biological-chemistry-i-fall-2013/

Genetics: https://ocw.mit.edu/courses/7-03-genetics-fall-2004

Heat Energy: Direct Solar/Thermal to Electrical Energy Conversion Technologies

Quantum Physics I: https://ocw.mit.edu/courses/8-04-quantum-physics-i-spring-2013/

Quantum Physics II: https://ocw.mit.edu/courses/8-05-quantum-physics-ii-fall-2013/

Quantum Physics III: https://ocw.mit.edu/courses/8-06-quantum-physics-iii-spring-2018/

Molecular Biology

Public

1. -, Molecular Biology of The Cell - An Introduction Charts, 33pp
2. APHL, Molecular Biology 101 Charts, 2013, 57
3. Bhosale, Molecular Biology Charts, 69pp
4. Serrano, An Introductory Course on Molecular Biology, 2023, 30pp
5. -, BIOCHEMISTRY, GENETICS & MOLECULAR BIOLOGY 2017 CATALOG
6. Ahern, Biochemistry and Molecular Biology How Life Works, 2019, 414pp
7. -, Cell and Molecular Biology, 2017, 209pp
8. -, Botany - LABORATORY COURSE-II, 2021, 231pp
9. -, CELL BIOLOGY, MOLECULAR BIOLOGY AND BIOTECHNOLOGY, 2021, 418pp
10. Mann, Lowman & Gaddis, Molecular Biology and Genetics, 2019, 51pp
11. Malinka, Intro to Molecular Biology Charts, 21pp
12. Böhmer et al., Introduction to medical and molecular biology, 2010, 95pp
13. Adem, MOLECULAR BIOLOGY AND APPLIED GENETICS For Medical Laboratory Technician Students, 2006, 529pp
14. -, BASICS ON MOLECULAR BIOLOGY Charts, 52pp
15. Allison, Fundamental Molecular Biology, 2007, 748pp
16. -, Molecular Biology of the Cell Journal Index, 53pp
17. Tompa, Basics of Molecular Biology, 2009, 9pp
18. Schleif, Genetics and Molecular Biology, 1993, 715pp
19. -, Introduction to Cell & Molecular Biology Techniques: Immunofluorescence, 2014, 38pp
20. APHL, Molecular Biology 101 Charts, 57pp
21. Weaver, Molecular Biology, 2012, 914pp
22. -, Molecular Biology of the Cell - Visualizing Cells Ch. 9, 37pp

Private

1. Cooper, The Cell – A Molecular Approach, 2019, 813pp
2. Iwasa & Marshall, Karp's Cell and Molecular Biology, 2020, 2105pp

Genetics

Public

1. -, Help Me Understand Genetics, 227p

2. -, Biological Genetics and Evolution Charts, 43pp
3. -, Working with Molecular Genetics – Fundamental Properties of Genes, 41pp
4. -, Genetics and human behaviour: the ethical context, 2002, 258pp
5. -, Handbook - Help Me Understand Genetics, 2011, 147pp
6. -, Introduction to Genetics, 2024, 242pp
7. -, Key concepts in genetics, 2008, 74pp
8. Singh, Open Genetics, 2019, 513pp
9. Robinson, Genetics for Dummies, 2010, 387pp
10. Minks, Medical Genetics and Genetic Counseling Charts, 2017, 81pp
11. Schleif, Genetics and Molecular Biology,1993, 715pp
12. Singh et al., The Genetics of Aging: A Vertebrate Perspective, 2019, 21pp

Private

1. Griffiths, INTRODUCTION TO Genetic Analysis, 2020, 2937pp
2. Jorde et al., Medical Genetics, 2016, 371pp
3. Klug et al., Concepts of Genetics, 2019, 867pp
4. Kratz & Spock, Genetics for Dummies, 2024, 419pp
5. Lewis, Human Genetics – Concepts and Applications, 2024, 1877pp
6. Pierce, Genetics - A Conceptual Approach, 2020, 3609pp
7. Primrose & Twyman, Principles of Gene Manipulation and Genomics, 2006, 667pp
8. Gardner & Snustad, PRINCIPLES OF GENETICS, 1981, 710pp
9. Turnpenny et al., Emery's Elements of Medical Genetics and Genomics, 2022, 1483pp
10. Watson et al., MOLECULAR BIOLOGY of the GENE, 2014, 911pp

Cancer

https://pubmed.ncbi.nlm.nih.gov/

https://www.cancercomplexity.synapse.org/Explore/Publications

https://www.youtube.com/watch?v=QymKG8mXm6g Cancer Biology 101

Public

1. Hejmadi, Introduction to Cancer Biology, 2010, 48pp
2. Saini et al., CANCER CAUSES AND TREATMENTS, 2020, 15pp
3. Gilbert, Cancer Overview, 2011, 12pp
4. Ruddon, Cancer Biology, 2007, 545pp
5. Flores, Cancer Biology, 2009, 86pp
6. Saravana, FUNDAMENTALS OF CANCER BIOLOGY, 2023, 81pp
7. King & Robbins, Cancer Biology, 2006, 311pp
8. -, Cancer Biology, 330pp
9. -, Cancer Biology: Molecular and Genetic Basis, 2019, 20pp

10. -, The Cancer Process, 2018, 67pp
11. Knowles & Selby, Introduction to the Cellular and Molecular Biology of Cancer, 2005, 552pp
12. Cassidy et al., Oxford Handbook of Oncology, 2015, 897pp
13. Eggert, Biology of Cancer - Introduction, 2009, 14pp
14. Piña-Sanchez et al., Cancer Biology, Epidemiology, and Treatment in the 21st Century: Current Status and Future Challenges From a Biomedical Perspective, 2021, 21pp
15. -, The Biology of Cancer Charts, 85pp
16. Prensner & Chinnaiyan, The Emergence of lncRNAs in Cancer Biology, 2011, 23pp
17. Crespi & Summers, Evolutionary biology of cancer, 2005, 8pp
18. Heiden & DeBerardinis, Understanding the Intersections between Metabolism and Cancer Biology, 2017, 13pp
19. Roos et al., DNA damage and the balance between survival and death in cancer biology, 2016, 14pp
20. DeVita et al., Cancer Principles & Practice of Oncology, 2015, 2281pp
21. Smalley et al., Life isn't flat: Taking cancer biology to the next dimension, 2006, 7pp
22. Wu et al., Natural killer cells in cancer biology and therapy, 2020, 26pp
23. Widschwendter et al., DNA Hypomethylation and Ovarian Cancer Biology, 2004, 9pp
24. Karstedt et al., Exploring the TRAILs less travelled: TRAIL in Cancer Biology and Therapy, 2016, 39pp
25. Sehgal et al., Mutually exclusive teams-like patterns of gene regulation characterize phenotypic heterogeneity along the noradrenergic-mesenchymal axis in neuroblastoma, 2024, 13pp
26. Gong et al., The role of necroptosis in cancer biology and therapy, 2019, 17pp
27. Pearce & Läubli, Sialic acids in cancer biology and immunity, 2016, 34pp
28. Khan & La Thangue, HDAC inhibitors in cancer biology: emerging mechanisms and clinical applications 2012, 10pp
29. Iozzo & Sanderson, Proteoglycans in cancer biology, tumor microenvironment and angiogenesis, 2011, 19pp
30. Mantovani et al., The chemokine system in cancer biology and therapy, 2009, 13pp
31. Nissen et al., Collagens and Cancer associated fibroblasts in the reactive stroma and its relation to Cancer biology, 2019, 12pp
32. Miyoshi et al., Biological Function of Fucosylation in Cancer Biology, 2008, 6pp
33. -, Clinics in Chest Medicine, Multiple Articles
34. Hornberg et al., Cancer: A Systems Biology Disease, 2006, 10pp
35. Lim et al., Inflammatory breast cancer biology: the tumor microenvironment is key, 2018, 16pp

36. Metzcar et al., A Review of Cell-Based Computational Modeling in Cancer Biology, 2019, 13pp
37. Katti et al., CRISPR in cancer biology and therapy, 2022, 89pp
38. Pardal et al., APPLYING THE PRINCIPLES OF STEM-CELL BIOLOGY TO CANCER, 2003, 9pp
39. Sun et al., Effect of exosomal miRNA on cancer biology and clinical applications, 2018, 19pp
40. Hosseinzadeh et al., The androgen receptor interacts with GATA3 to transcriptionally regulate a luminal epithelial cell phenotype in breast cancer, 2024, 28pp
41. Blobe et al., Regulation of protein kinase C and role in cancer biology, 1994, 21pp
42. Shamji et al., Integration of Growth Factor and Nutrient Signaling: Implications for Cancer Biology, 2003, 10pp
43. McDonald et al., Integrin-linked kinase – essential roles in physiology and cancer biology, 2008, 12pp
44. Richon, Cancer biology: mechanism of antitumour action of vorinostat (suberoylanilide hydroxamic acid), a novel histone deacetylase inhibitor, 2006, 5pp
45. Wang et al., Genetics and biology of prostate cancer, 2024, 37pp
46. Modrich & Lahue, MISMATCH REPAIR IN REPLICATION FIDELITY, GENETIC RECOMBINATION, AND CANCER BIOLOGY, 1996, 33pp
47. Cooper et al., Molecular biology of lung cancer, 33pp
48. Leemans et al., The molecular biology of head and neck cancer, 2011, 9pp
49. Ruivo et al., The Biology of Cancer Exosomes: Insights and New Perspectives, 2011, 9pp
50. Suhail et al., Systems Biology of Cancer Metastasis, 2019, 19pp
51. Eroles et al., Molecular biology in breast cancer: Intrinsic subtypes and signaling pathways, 2012, 10pp
52. Peruzzi et al., The IGF-I receptor in cancer biology, 2003, 6pp
53. Pitot, The Molecular Biology of Carcinogenesis, 1993, 9pp
54. Afratis et al., Glycosaminoglycans: key players in cancer cell biology and treatment, 2012, 21pp
55. Tsai & Baylin, Cancer epigenetics: linking basic biology to clinical medicine, 2011, 16pp
56. Sayad et al., CD83 Receptor Unveiled as a Therapeutic Target in Metastatic Breast Cancer through Single-Cell RNA-Seq, 2024, 11pp
57. Azim Jr & Ann H Partridge, Biology of breast cancer in young women, 2014, 9pp
58. Ellis et al., Vascular Endothelial Growth Factor in Human Colon Cancer: Biology and Therapeutic Implications, 2000, 5pp
59. Li & Davie, The role of Sp1 and Sp3 in normal and cancer cell biology, 2010, 10pp

60. Biffi & Tuveson, DIVERSITY AND BIOLOGY OF CANCERASSOCIATED FIBROBLASTS, 2020, 31pp
61. Fadaka et al., Biology of glucose metabolization in cancer cells, 2017, 7pp
62. Aunan et al., The Biology of Aging and Cancer: A Brief Overview of Shared and Divergent Molecular Hallmarks, 2017, 15pp
63. DeBerardinis et al., The Biology of Cancer: Metabolic Reprogramming Fuels Cell Growth and Proliferation, 2008, 10pp
64. Saravana, FUNDAMENTALS OF CANCER BIOLOGY, 2023, 81pp
65. Jain et al., Wireless electrical–molecular quantum signalling for cancer cell apoptosis, 2023, 18pp
66. Hartig et al., iCVD Polymer Thin Film Bio-Interface-Performance for Fibroblasts, Cancer-Cells, and Viruses Connected to Their Functional Groups and In Silico Studies, 2023, 11pp
67. Nath et al., The amino acid transporter SLC7A11 expression in breast cancer, 2023, 15pp
68. Stanger & Wahl, Cancer as a Disease of Development Gone Awry, 2024, 25pp
69. Andrzejczak & Karabon, BTLA biology in cancer: from bench discoveries to clinical potentials, 2024, 25pp
70. Cancer Biology 101 – Video Class on Cancer

Private

1. Fust, The GALE ENCYCLOPEDIA of Cancer A GUIDE TO CANCER AND ITS TREATMENTS, 2015, 2083pp

Tumor Treating Fields (TTFields)

Public

1. Giladi et al., Alternating Electric Fields (Tumor-Treating Fields Therapy) Can Improve Chemotherapy Treatment Efficacy in Non-Small Cell Lung Cancer Both In Vitro and In Vivo, 2014, 7pp
2. Pohling et al., Current status of the preclinical evaluation of alternating electric fields as a form of cancer therapy, 2023, 14pp
3. Wang et al., Tumor-treating fields (TTFields)-based cocktail therapy: a novel blueprint for glioblastoma treatment, 2021, 18pp
4. Guo et al., Tumor-Treating Fields in Glioblastomas: Past, Present, and Future, 2022, 23pp
5. Vergote et al., Tumor Treating Fields (TTFields) Therapy Concomitant with Taxanes for Cancer Treatment, 2023, 19pp
6. Wu et al., Evaluation of a tumor electric field treatment system in a rat
7. model of glioma,2020, 10pp
8. Carrieri et al., Tumor Treating Fields: At the Crossroads Between Physics and Biology for Cancer Treatment, 2020, 7pp

9. Shams & Patel, Anti-cancer mechanisms of action of therapeutic alternating electric fields (tumor treating fields [TTFields]), 2022, 16pp
10. Mun et al., Tumor-Treating Fields: A Fourth Modality in Cancer Treatment, 2018, 10pp

General Chemistry

Public

1. Ball, Beginning Chemistry, 2012, 964pp
2. -, Chemistry, 2015, 1393pp
3. -, CRC Handbook of Chemistry and Physics, 2014, 2666pp
4. Saylor, General Chemistry Principles, Patterns, and Actions, 2365pp
5. Ebbing & Gammon, General Chemistry, 2007, 6991pp
6. Myers et al., Holt Chemistry, 2004, 928pp
7. ACS, Periodic Table Poster

Organic Chemistry

Public

1. Soderberg, Organic Chemistry with a Biological Emphasis, 2016, 457pp
2. CAREY & SUNDBERG, Advanced Organic Chemistry, 2007, 1212pp
3. Neuman, Organic Chemistry (Draft – incomplete)
4. McMurry, Fundamentals of Organic Chemistry, 2011, 667pp
5. Smith & March, MARCH'S ADVANCED ORGANIC CHEMISTRY REACTIONS, MECHANISMS, AND STRUCTURE, 2007, 2374pp
6. Carey, Organic Chemistry, 2000, 1275pp
7. -, An Introduction to the Study of Organic Chemistry, 1227pp
8. McMurry, Organic Chemistry, 2016, 1518pp
9. Solomons et al., Organic Chemistry, 2016, 1293pp
10. Liu, Organic Chemistry I, 379pp
11. McMurry, Organic Chemistry: A Tenth Edition, 2023, 467pp
12. Richard F. Daley & Sally J. Daley, Organic Chemistry, 2005, 414pp

Electromagnetic Fields

Public

1. -, ELECTROMAGNETIC THEORY (Summary of equations and gate questions), 2018, 151pp
2. Marhauser, Lecture: Maxwell's Equations, 2018, 31pp
3. -, Magnetic Field and Magnetic Forces Charts, 28pp
4. Staelin, Electromagnetics and Applications, 2011, 443pp
5. -, Electromagnetism and Relativity, 39pp

6. Papachristou, INTRODUCTION TO ELECTROMAGNETIC THEORY AND THE PHYSICS OF CONDUCTING SOLIDS, 2020, 231pp
7. Ellingson, Electromagnetics, 2018, 470pp
8. Tong, Electromagnetism, 2015, 126pp
9. -, Electromagnetic Theory Summary, 56pp
10. Ahmad, Electromagnetic Field Theory, 2020, 229pp
11. Thide, Electromagnetic Field Theory, 2006, 221pp
12. Chew, Lectures on Electromagnetic Field Theory, 2019, 440pp
13. -, Maxwell's Equations and Electromagnetic Waves, 51pp
14. Romeo et al., Radiofrequency Electromagnetic Field Exposure and Apoptosis: A Scoping Review of In Vitro Studies on Mammalian Cells, 2022, 25pp
15. Kong, Electromagnetic Wave Theory, 2008, 1032pp
16. Baird, Electromagnetic Theory Lecture Notes, 25pp
17. Gherardini et al., Searching for the Perfect Wave: The Effect of Radiofrequency Electromagnetic Fields on Cells, 2014,22pp
18. Zahn, ELECTROMAGNETIC FIELD THEORY: a problem solving approach, 2003, 285pp
19. -, Electromagnetic Theory, 111pp
20. Morin, Electromagnetic Waves (Ch. 8), 33pp
21. Wang, Electromagnetic Wave Theory Charts, 79pp
22. -, ELECTRICAL PROPERTIES OF METALS AND SEMICONDUCTORS, 46pp
23. Stratton, Electromagnetic Theory, 1941, 648pp
24. Aksoy, Advanced Electromagnetic Theory Lecture Notes, 2020, 19pp
25. Heavyside, Electromagnetic Theory, Vol. I, 1925, 496pp
26. Maziarz et al., How electromagnetic fields can influence adult stem cells: positive and negative impacts, 2016, 12pp
27. Miyakoshi, Cellular and Molecular Responses to Radio-Frequency Electromagnetic Fields, 2013, 9pp
28. -, GUIDELINES FOR LIMITING EXPOSURE TO ELECTROMAGNETIC FIELDS (100 kHz to 300 GHz), 2020, 42pp

Magnetism

Public

1. Jeans, THE MATHEMATICAL THEORY OF ELECTRICITY AND MAGNETISM, 1911, 659pp
2. -, THE PHYSICS OF MAGNETISM, 16pp
3. Yamauchi, Fundamentals of Magnetism, 2008, 46pp
4. McDonald, Band Theory of Magnetism in Metals, 2015, 11pp
5. Blundell, Concepts in Magnetism, 2021, 24pp
6. Purcell & Morin, ELECTRICITY AND MAGNETISM, 2013, 200pp (sample)
7. Coey & Mazaleyrat, History of magnetism, 2023, 42pp
8. Lacroix et al., Introduction to Frustrated Magnetism, 2011, 707pp

9. -, Magnets and Magnetism Charts, 20pp
10. -, MAGNETISM AND MATTER, 2024, 18pp
11. Coey, Magnetism and Magnetic Materials, 2009, 633pp
12. Mondal, Theory of Magnetism: A Quantum Approach, 46pp
13. Mohn, Magnetism in the Solid State: An Introduction, 2006, 230pp
14. Coldea, Magnetism in Condensed Matter Physics Handout 1, 2016, 34pp
15. Keeling, Quantum Magnetism, 89pp
16. Calderón, Emergence of quantum phases in novel materials: Magnetism Charts, 190pp
17. Tsirlin, Theory of Magnetism Lecture notes, 2020, 88pp
18. Majumdar, Basics of Magnetism Charts, 2014, 108pp
19. -, Magnetic Field of a Circular Coil, 10pp
20. Schiller, light, charges and brains, 2021, 456pp
21. Shneidman, ELECTRICITY & MAGNETISM, 2020, 58pp
22. Wang, Magnetism Charts, 28pp
23. -, Magnets and electromagnetism, 2021, 15pp
24. Coey, Magnetism and Superconductivity Charts, 2023, 254pp
25. Jascur, QUANTUM THEORY OF MAGNETISM, 2013, 65pp
26. Kusminskiy, Quantum Magnetism, Spin Waves, and Light, 2018, 87pp
27. -, Domain Theory of Ferro Magnetism, 4pp
28. Pop, Magnetism on the atom Charts, 76pp
29. Lewis, Fundamentals of Magnetism & Magnetic Materials Charts, 2015, 115pp
30. Williams, The Electron Theory of Magnetism, 1912, 71pp
31. Timm, Theory of Magnetism, 2010, 94pp

Private

1. Coey & Parkin, Handbook of Magnetism and Magnetic Materials, 2021, 1714pp
2. Purcell & Morin, Electricity and Magnetism, 2013, 863pp

General Physics

Public

1. -, College Physics Vol. 1 of 3, 2013, 464pp
2. -, GRAVITATIONAL FIELD THEORY, 50pp
3. Walker, FUNDAMENTALS OF PHYSICS, 2014, 1450pp
4. Brown, Introductory Physics I and II, 2013, 1304pp
5. -, ENGINEERING PHYSICS-II, 54pp
6. Peatross & Ware, Physics of Light and Optics, 2024, 346pp
7. Tipler & Llewellyn, MODERN PHYSICS, 2008, 758pp
8. Ling et al., University Physics, 2018, 2410pp

Atomic Physics and the Standard Model

Public

1. Gaillard, The Standard Model of Particle Physics, 1998, 26pp
2. Foot, Atomic Physics, 2005, 346pp
3. Mann, An Introduction to Particle Physics and the Standard Model, 2021, 602pp
4. Ewart, Atomic Physics, 68pp
5. Ewart, Atomic Physics Charts, 141pp
6. Ramsey-Musolf, Beyond the Standard Model: the Particle Physics Frontier, 2014, 71pp
7. Viswanathan, Introductory Atomic Physics and Quantum Mechanics, 94pp
8. Haken & Wolf, The Physics of Atoms and Quanta, 2004, 526pp
9. Griffiths, Introduction to Elementary Particles, 2008, 470pp
10. Bransden & Joachain, Physics of atoms and molecules, 1983, 694pp
11. Hall, Standard Model of Particle Physics Charts, 2019, 102pp
12. Friedrich, Theoretical Atomic Physics, 2017, 658pp
13. Wiese, The Standard Model of Atomic Physics, 2021, 331pp
14. Donoghue et al., DYNAMICS OF THE STANDARD MODEL, 2015, 594pp
15. Johnson, Lectures on Atomic Physics, 2006, 262pp
16. -, Atoms, Molecules, and Lasers, 1974, 726pp
17. Lukin, Modern Atomic and Optical Physics II, 2016, 293pp
18. Tong, Particle Physics, 238pp
19. Gopalakrishna, The Standard Model and Beyond, 2015, 102pp

Gravity and Relativity

Public

1. Abdeldayem, Complex Field Theory and Gravity's New Perspective, 2022, 5pp
2. Nasrolahpour, Everything about gravity, 2020, 16pp
3. Butto, New Theory to Understand the Mechanism of Gravitation, 2020, 11p
4. Veringa, New Basic Theory of Gravity, 2016, 27pp
5. Esposito-Farese, Tests of Alternative Theories of Gravity, 2005, 20pp
6. -, Gravity, 45pp
7. -, Einstein's Theory of Gravity, 9pp
8. Wald, Space, Time, and Gravity: The Theory of the Big Bang and Black Holes, 1992, 166pp
9. -, GRAVITATIONAL FIELD THEORY, 50pp
10. Fujii & Maeda, The Scalar-Tensor Theory of Gravity, 2003, 25pp
11. Pal, The Classical Theory of Gravitation, 2022, 5pp
12. Hartle, Gravity – An Introduction to Einstein's General Relativity, 2003, 589pp
13. Oppenheim, A Postquantum Theory of Classical Gravity?, 2023, 37pp
14. Kokkotas, Einstein's Theory of Gravity, 2019, 42pp

15. -, The General Theory of Relativity, 32pp
16. Ionescu, Synopsis of Main Theories of Gravity, 2022, 5pp
17. Ha, Severe Challenges in Gravity Theories, 2011, 12pp
18. Ha, An Underlying Theory for Gravity, 4pp
19. Velez & Romano, Constraining gravity theories with the gravitational stability mass, 2020, 12pp
20. Carroll, Spacetime and Geometry: An Introduction to General Relativity, 2004, 526pp
21. Ortin, Gravity and Strings, 2004, 705pp
22. Smigel, Comments on Theories of Relativity, 2018, 11pp

Quantum Theory

Public

1. Mbagwu et al., Article on Basics of Quantum Theory, 2020, 9pp
2. Kleppner & Jackiw, One Hundred Years of Quantum Physics, 2000, 7pp
3. Dirac, Principles of Quantum Mechanics, 1947, 322pp
4. Viswanathan, Introductory Atomic Physics and Quantum Mechanics – Book 1, 94pp
5. Esposito et al., Advanced Concepts in Quantum Mechanics, 2015, 391pp
6. Eisberg, QUANTUM PHYSICS of Atoms, Molecules, Solids, Nuclei, and Particles, 1985, 866pp
7. Scheck, Quantum Physics, 2013, 746pp
8. Griffiths, Introduction to Quantum Mechanics, 1995, 409pp
9. van Dommelen, Quantum Mechanics for Engineers, 2011, 1603pp
10. Landau & Lifshitz, Quantum Mechanics: Non-Relativistic Theory, 1965, 632pp
11. McMahon, Quantum Mechanics Demystified, 2006, 407pp
12. Styer, The Physics of Quantum Mechanics, 2024, 554pp
13. Negi, Principles of Quantum Mechanics Charts, 44pp
14. Binney & Skinner, The Physics of Quantum Mechanics, 2013, 310pp
15. Tong, Quantum Mechanics, 133pp
16. Schulten, Notes on Quantum Mechanics, 2000, 397pp
17. Chew, Quantum Mechanics Made Simple: Lecture Notes, 2016, 280pp
18. Fitzpatrick, Quantum Mechanics, 222pp
19. Greensite, Lecture Notes on Quantum Mechanics, 2003, 391pp
20. -, Summary of Important Ideas in Quantum Physics, 5pp
21. Holzner, Quantum Physics for Dummies, 2009, 340pp
22. Ross, I Don't Understand Quantum Physics, 2018, 105pp
23. Carroll, Quantum Physics for Beginners, 2020, 107pp
24. Schroeder, Notes on Quantum Mechanics, 2022, 264pp
25. Bellac, Quantum Physics, 2006, 607pp
26. Schwabl, Quantum Physics, 2007, 425pp

27. Tamvakis, Problems and Solutions in Quantum Mechanics, 2005, 344pp
28. Pratt, Lecture Notes on Quantum Mechanics, 2022, 282pp

Private

1. Griffiths & Schroeter, Introduction to Quantum Mechanics, 2018, 644pp
2. Eisberg, QUANTUM PHYSICS of Atoms, Molecules, Solids, Nuclei, and Particles, 1985, 864pp
3. Gasiorowicz, Quantum Physics, 2003, 348pp
4. Liboff, Introductory Quantum Mechanics, 2003, 902pp
5. Shankar, Principles of Quantum Mechanics, 1994, 698pp
6. Sakurai & Napolitano, Modern Quantum Mechanics, 2021, 568pp

Solid State Physics

Public

1. Ashcroft and Mermin, Solid State Physics, 1976, 848pp
2. Grosso, Solid State Physics, 2014, 873pp
3. Hilke, Solid State Physics Lecture notes, 2006, 34pp
4. Ibach & Luth, Solid-State Physics: An Introduction to Principles of Materials Science, 2009, 153pp
5. Kittel, Introduction to Solid State Physics, 2005, 703pp

Private

1. Pillai, Solid State Physics, 2005, 848pp
2. Simon, The Oxford Solid State Basics, 2013, 305pp

Thermal, Thermoelectric, and System Dynamics

Public

1. -, Thermoelectric effects, 7pp
2. Sari et al., Performance Analysis of Electric Coolers TEC1-12706 and TEC1-12715 with Heatsinks at Semi-conductor Cooler Boxes, 2022, 12pp
3. Zhang, Optimizing thermocouple's ZT through design innovation, 2021, 16pp
4. Hust & Lankford, THERMAL CONDUCTIVITY OF ALUMINUM, COPPER, IRON, AND TUNGSTEN FOR TEMPERATURES FROM 1 K TO THE MELTING POINT, 1984, 266pp
5. -, Metals and Semiconductors Charts, 26pp
6. -, Basics of Thermal Resistance and Heat Dissipation, 2021, 6pp
7. Ho, Modeling Thermal Systems, 57pp
8. Mosley & Siegers, Use of Circuit Models in Thermal Calculations, 5pp
9. -, Simple Heat Flow Modeling and Sample Temperature Calculations, 19pp

10. -, Transient thermal measurements and thermal equivalent circuit models, 2020, 11pp
11. Lombard, Thermal Analysis of Electrical Equipment - A review and comparison of different methods, 2017, 11pp
12. Bahrami, Steady Heat Conduction, 14pp
13. -, Thermal Analysis, 19pp
14. Ramirez-Laboreo et al., 2014, 7pp
15. -, TEC1-12706 Thermoelectric Cooler Data Sheet
16. -, TEC1-12715 Thermoelectric Cooler Data Sheet
17. Bramley & Clark, A Quantitative Model for the Thermocouple Effect Using Statistical and Quantum Mechanics, 6pp
18. -, Introduction to Thermocouples, 3pp
19. -, Thermocouple Theory, 6pp

Private

1. Shearer et al., Introduction to System Dynamics, 1971, 420pp
2. Eremia & Shahidehpour, HANDBOOK OF ELECTRICAL POWER SYSTEM DYNAMICS - Modeling, Stability, and Control, 2013, 968pp
3. Palm, System Dynamics, 2021, 791pp
4. Close et al., Modeling and Analysis of Dynamic Systems, 2002, 593pp

Appendix B. Thermoelectric Effects Overview

Note: In general Wikipedia and any other web site not ending in .edu are not very good sources of accurate data (but better than something like Dotto's paper). Be careful what you take as facts. Published and peer-reviewed information is more reliable, but still sometimes has wrong information. See Appendix A for more reliable sources.

Wikipedia: The **thermoelectric effect** is the direct conversion of temperature differences to electric voltage and vice versa via a thermocouple. A thermoelectric device creates a voltage when there is a different temperature on each side. Conversely, when a voltage is applied to it, heat is transferred from one side to the other, creating a temperature difference. At the atomic scale, an applied temperature gradient causes charge carriers in the material to diffuse from the hot side to the cold side.

This effect can be used to generate electricity, measure temperature or change the temperature of objects. Because the direction of heating and cooling is affected by the applied voltage, thermoelectric devices can be used as temperature controllers.

The term "thermoelectric effect" encompasses three separately identified effects: the **Seebeck effect**, **Peltier effect**, and **Thomson effect**. The Seebeck and Peltier effects are different manifestations of the same physical process; textbooks may refer to this process as the **Peltier–Seebeck effect** (the separation derives from the independent discoveries by French physicist Jean Charles Athanase Peltier and Baltic German physicist Thomas Johann Seebeck). The Thomson effect is an extension of the Peltier–Seebeck model and is credited to Lord Kelvin.

Joule heating, the heat that is generated whenever a current is passed through a conductive material, is not generally termed a thermoelectric effect. The Peltier–Seebeck and Thomson effects are thermodynamically reversible, whereas Joule heating is not.

Seebeck effect

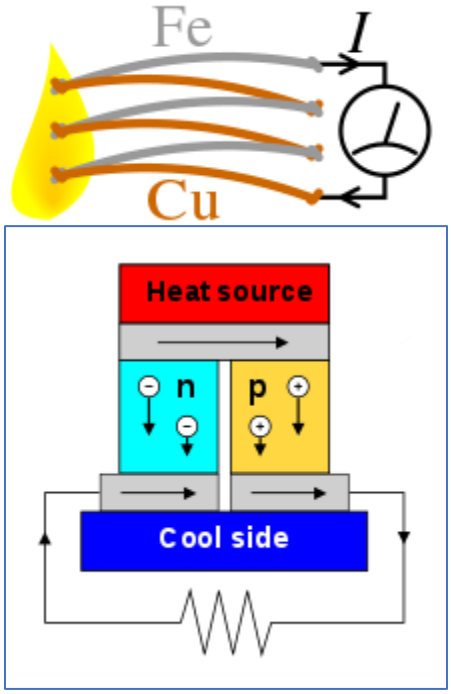

A thermoelectric circuit composed of materials of different Seebeck coefficients (p-doped and n-doped semiconductors), configured as a thermoelectric generator.

If the load resistor at the bottom is replaced with a voltmeter, the circuit then functions as a temperature-sensing thermocouple.

The **Seebeck effect** (German pronunciation: [ˈzeːbɛk]) is the electromotive force (emf) that develops across two points of an electrically conducting material when there is a temperature difference between them. The emf is called the Seebeck emf (or thermo/thermal/thermoelectric emf). The ratio between the emf and temperature difference is the Seebeck coefficient. A thermocouple measures the difference in potential across a hot and cold end for two dissimilar materials. This potential difference is proportional to the temperature difference between the hot and cold ends. First discovered in 1794 by Italian scientist Alessandro Volta, it is named after the Baltic German physicist Thomas Johann Seebeck, who in 1821 independently rediscovered it.

Seebeck observed what he called "thermomagnetic effect" wherein a magnetic compass needle would be deflected by a closed loop formed by two different metals joined in two places, with an applied temperature difference between the joints. Danish physicist Hans Christian Ørsted noted that the temperature difference was in fact driving an electric current, with the generation of magnetic field being an indirect consequence, and so coined the more accurate term "thermoelectricity".

The Seebeck effect is a classic example of an electromotive force (EMF) and leads to measurable currents or voltages in the same way as any other EMF. The Seebeck coefficient is also known as thermopower, a property of the local material.

The Seebeck coefficients generally vary as function of temperature and depend strongly on the composition of the conductor. For ordinary materials at room temperature, the Seebeck coefficient may range in value from −100 μV/K to +1,000 μV/K (see Seebeck coefficient article for more information).

Applications

In practice, thermoelectric effects are essentially unobservable for a localized hot or cold spot in a single homogeneous conducting material, since the overall emfs from the increasing and decreasing temperature gradients will perfectly cancel out. Attaching an electrode to the hotspot to measure the locally shifted voltage will only partly succeed: it means another temperature gradient will appear inside of the electrode, and so the overall emf will depend on the difference in Seebeck coefficients between the electrode and the conductor it is attached to.

Thermocouples involve two wires, each of a different material, that are electrically joined in a region of unknown temperature. The loose ends are measured in an open-circuit state (without any current). The voltage measured at the loose ends of the wires is directly dependent on the unknown temperature, and yet totally independent of other details such as the exact geometry of the wires. This direct relationship allows the thermocouple arrangement to be used as a straightforward uncalibrated thermometer, provided knowledge of the difference in -vs- curves of the two materials, and of the reference temperature at the measured loose wire ends.

Thermopiles are formed from many thermocouples in series, zig-zagging back and forth between hot and cold. This multiplies the voltage output.

Thermoelectric generators are like a thermocouple/thermopile but instead draw some current from the generated voltage to extract power from heat differentials. They are optimized differently from thermocouples, using high quality thermoelectric materials in a thermopile arrangement, to maximize the extracted power. Though not particularly efficient, these generators have the advantage of not having any moving parts.

Peltier effect

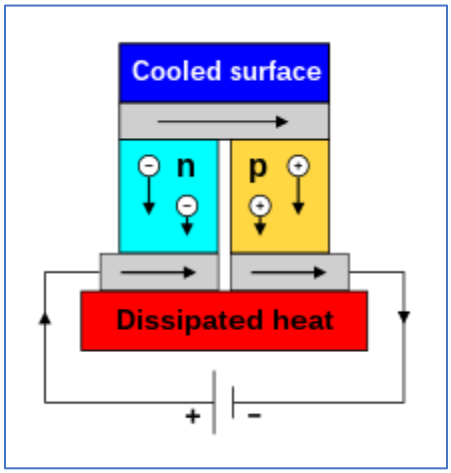

The Seebeck circuit configured as a thermoelectric cooler

When an electric current is passed through a circuit of a thermocouple, heat is generated at one junction and absorbed at the other junction. This is known as the **Peltier effect**: the presence of heating or cooling at an electrified junction of two different conductors. The effect is named after French physicist Jean Charles Athanase Peltier, who discovered it in 1834. When a current is made to flow through a junction between two conductors, A and B, heat may be generated or removed at the junction. The total heat generated is not determined by the Peltier effect alone, as it may also be influenced by Joule heating and thermal-gradient effects (see below).

The Peltier coefficients represent how much heat is carried per unit charge. The Peltier effect can be considered as the back-action counterpart to the Seebeck effect (analogous to the back-EMF in magnetic induction): if a simple thermoelectric circuit is closed, then the Seebeck effect will drive a current, which in turn (by the Peltier effect) will always transfer heat from the hot to the cold junction. The close relationship between Peltier and Seebeck effects can be seen in the direct connection between their coefficients.

A typical Peltier heat pump involves multiple junctions in series, through which a current is driven. Some of the junctions lose heat due to the Peltier effect, while others gain heat. Thermoelectric heat pumps exploit this phenomenon, as do thermoelectric cooling devices found in refrigerators.

Applications

The Peltier effect can be used to create a heat pump. Notably, the Peltier thermoelectric cooler is a refrigerator that is compact and has no circulating fluid or moving parts. Such refrigerators are useful in applications where their advantages outweigh the disadvantage of their very low efficiency.

Other heat pump applications such as dehumidifiers may also use Peltier heat pumps.

Thermoelectric coolers are trivially reversible, in that they can be used as heaters by simply reversing the current. Unlike ordinary resistive electrical heating (Joule heating) that varies with the square of current, the thermoelectric heating effect is linear in current (at least for small currents) but requires a cold sink to replenish with heat energy. This rapid reversing heating and cooling effect is used by many modern thermal cyclers, laboratory devices used to amplify DNA by the polymerase chain reaction (PCR). PCR requires the cyclic heating and cooling of samples to specified temperatures. The inclusion of many thermocouples in a small space enables many samples to be amplified in parallel.

Thomson effect

In different materials, the Seebeck coefficient is not constant in temperature, and so a spatial gradient in temperature can result in a gradient in the Seebeck coefficient. If a current is driven through this gradient, then a continuous version of the Peltier effect will occur. This **Thomson effect** was predicted and later observed in 1851 by Lord Kelvin (William Thomson). It describes the heating or cooling of a current-carrying conductor with a temperature gradient. If a current density is passed through a homogeneous conductor, the Thomson effect predicts a heat production rate per unit volume.

The Thomson effect is a manifestation of the direction of flow of electrical carriers with respect to a temperature gradient within a conductor. These absorb energy (heat) flowing in a direction opposite to a thermal gradient, increasing their potential energy, and, when flowing in the same direction as a thermal gradient, they liberate heat, decreasing their potential energy. The Thomson coefficient is related to the Seebeck coefficient.

Full thermoelectric equations

Often, more than one of the above effects is involved in the operation of a real thermoelectric device. The Seebeck effect, Peltier effect, and Thomson effect can be gathered together in a consistent and rigorous way, described here; this also includes the effects of Joule heating and ordinary heat conduction. As stated above, the Seebeck effect generates an electromotive force, leading to the current equation**.**

If the material is not in a steady state, a complete description needs to include dynamic effects such as relating to electrical capacitance, inductance and heat capacity.

The thermoelectric effects lie beyond the scope of equilibrium thermodynamics. They necessarily involve continuing flows of energy. At least, they involve three bodies or thermodynamic subsystems, arranged in a particular way, along with a special arrangement of the surroundings. The three bodies are the two different metals and their junction region. The junction region is an inhomogeneous body, assumed to be stable, not suffering amalgamation by diffusion of matter. The surroundings are arranged to maintain two temperature reservoirs and two electric reservoirs.

For an imagined, but not actually possible, thermodynamic equilibrium, heat transfer from the hot reservoir to the cold reservoir would need to be prevented by a specifically matching voltage difference maintained by the electric reservoirs, and the electric current would need to be zero. For a steady state, there must be at least some heat transfer or some non-zero electric current. The two modes of energy transfer, as heat and by electric current, can be distinguished when there are three distinct bodies and a distinct arrangement of surroundings.

But in the case of continuous variation in the media, heat transfer and thermodynamic work cannot be uniquely distinguished. This is more complicated than the often-considered thermodynamic processes, in which just two respectively homogeneous subsystems are connected.

Thermoelectric generator

A **thermoelectric generator** (**TEG**), also called a **Seebeck generator**, is a solid state device that converts heat (driven by temperature differences) directly into electrical energy through a phenomenon called the *Seebeck effect* (a form of thermoelectric effect). Thermoelectric generators function like heat engines, but are less bulky and have no moving parts. However, TEGs are typically more expensive and less

efficient.[2] When the same principle is used in reverse to create a heat gradient from an electric current, it is called a thermoelectric (or Peltier) cooler.

Thermoelectric generators could be used in power plants and factories to convert waste heat into additional electrical power and in automobiles as automotive thermoelectric generators (ATGs) to increase fuel efficiency. Radioisotope thermoelectric generators use radioisotopes to generate the required temperature difference to power space probes. Thermoelectric generators can also be used alongside solar panels.

History

In 1821, Thomas Johann Seebeck discovered that a thermal gradient formed between two different conductors can produce electricity. At the heart of the thermoelectric effect is the fact that a temperature gradient in a conducting material results in heat flow; this results in the diffusion of charge carriers. The flow of charge carriers between the hot and cold regions in turn creates a voltage difference. In 1834, Jean Charles Athanase Peltier discovered the reverse effect, that running an electric current through the junction of two dissimilar conductors could, depending on the direction of the current, cause it to act as a heater or cooler.

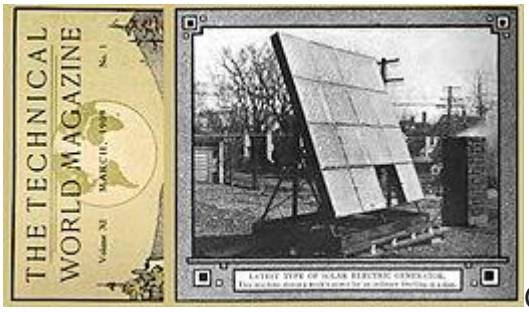

George Cove's solar panel pictured in *The Technical World Magazine* in March 1909.

George Cove had been supposed to invented a photovoltaic panel as a concentrated photovoltaic but it was actually a concentrated thermoelectric generator with thermocouples in 1909.

Efficiency

The typical efficiency of TEGs is around 5–8%, although it can be higher. Older devices used bimetallic junctions and were bulky. More recent devices use highly doped semiconductors made from bismuth telluride (Bi_2Te_3), lead telluride (PbTe), calcium manganese oxide ($Ca_2Mn_3O_8$), or combinations thereof, depending on application temperature. These are solid-state devices and unlike dynamos have no moving parts, with the occasional exception of a fan or pump to improve heat transfer. If the hot region is around 1273K and the ZT values of 3 - 4 are implemented, the efficiency is approximately 33-37%; allowing TEG's to compete with certain heat engine efficiencies.

As of 2021, there are materials (some containing widely available and inexpensive arsenic and tin) reaching a ZT value > 3; monolayer (ZT = 3.36 on the armchair axis); n-type doped (ZT = 3.23); p-type doped (ZT = 3.46); p-type doped (ZT = 3.5).

Construction

Thermoelectric power generators consist of three major components: thermoelectric materials, thermoelectric modules, and thermoelectric systems that interface with the heat source.

Thermoelectric materials

Thermoelectric materials show the thermoelectric effect in a strong or convenient form.

The *thermoelectric effect* refers to phenomena by which either a temperature difference creates an electric potential or an electric current creates a temperature difference. These phenomena are known more specifically as the Seebeck effect (creating a voltage from temperature difference), Peltier effect (driving heat flow with an electric current), and Thomson effect (reversible heating or cooling within a conductor when there is both an electric current and a temperature gradient). While all materials have a nonzero thermoelectric effect, in most materials it is too small to be useful. However, low-cost materials that have a sufficiently strong thermoelectric effect (and other required properties) are also considered for applications including power generation and refrigeration. The most used thermoelectric material is based on bismuth telluride.

Thermoelectric materials are used in thermoelectric systems for cooling or heating in niche applications, and are being studied as a way to regenerate electricity from waste heat. Research in the field is still driven by materials development, primarily in optimizing transport and thermoelectric properties.

Thermoelectric figure of merit

The usefulness of a material in thermoelectric systems is determined by the device efficiency. This is determined by the material's electrical conductivity (σ), thermal conductivity (κ), and Seebeck coefficient (S), which change with temperature (T).

Power factor

Often the thermoelectric **power factor** is reported for a thermoelectric material, given by

$$\text{Power factor} = \sigma S^2 \left[W/m/K^2\right]$$

where S is the Seebeck coefficient, and σ is the electrical conductivity.

Although it is often claimed that TE devices with materials with a higher power factor can 'generate' more energy (move more heat or extract more energy from that temperature difference) this is only true for a thermoelectric device with fixed geometry and unlimited heat source and cooling.

Aspects of materials choice

For good efficiency, materials with high electrical conductivity, low thermal conductivity and high Seebeck coefficient are needed.

The band structure of semiconductors offers better thermoelectric effects than the band structure of metals.

The Fermi energy is below the conduction band causing the state density to be asymmetric around the Fermi energy. Therefore, the average electron energy of the conduction band is higher than the

Fermi energy, making the system conducive for charge motion into a lower energy state. By contrast, the Fermi energy lies in the conduction band in metals. This makes the state density symmetric about the Fermi energy so that the average conduction electron energy is close to the Fermi energy, reducing the forces pushing for charge transport. Therefore, semiconductors are ideal thermoelectric materials.

Conductivity

In the efficiency equations above, thermal conductivity and electrical conductivity compete.

The thermal conductivity κ in crystalline solids has mainly two components:

$$\kappa = \kappa_{electron} + \kappa_{phonon}$$

According to the Wiedemann–Franz law, the higher the electrical conductivity, the higher $\kappa_{electron}$ becomes. Thus, in metals the ratio of thermal to electrical conductivity is about fixed, as the electron part dominates. In semiconductors, the phonon part is important and cannot be neglected. It reduces the efficiency. For good efficiency a low ratio of $\kappa_{phonon} / \kappa_{electron}$ is desired.

Therefore, it is necessary to minimize κ_{phonon} and keep the electrical conductivity high. Thus, semiconductors should be highly doped.

G. A. Slack proposed that in order to optimize the figure of merit, phonons, which are responsible for thermal conductivity must experience the material as a glass (experiencing a high degree of phonon scattering—lowering thermal conductivity) while electrons must experience it as a crystal (experiencing very little scattering—maintaining electrical conductivity): this concept is called phonon glass electron crystal. The figure of merit can be improved through the independent adjustment of these properties.

Quality factor (detailed theory on semiconductors)

Materials of interest

Strategies to improve thermoelectric performances include both advanced bulk materials and the use of low-dimensional systems. Such approaches to reduce lattice thermal conductivity fall under three general material types: (1) Alloys: create point defects, vacancies, or rattling structures (heavy-ion species with large vibrational amplitudes contained within partially filled structural sites) to scatter phonons within the unit cell crystal; (2) Complex crystals: separate the phonon glass from the electron crystal using approaches similar to those for superconductors (the region responsible for electron transport should be an electron crystal of a high-mobility semiconductor, while the phonon glass should ideally house disordered structures and dopants without disrupting the electron crystal, analogous to the charge reservoir in high-T_c superconductors); (3) Multiphase nanocomposites: scatter phonons at the interfaces of nanostructured materials,[21] be they mixed composites or thin film superlattices.

Materials under consideration for thermoelectric device applications include:

Bismuth chalcogenides and their nanostructures

Materials such as BiTe and BiSe comprise some of the best performing room temperature thermoelectrics with a temperature-independent figure-of-merit, ZT, between 0.8 and 1.0. Nanostructuring these materials to produce a layered superlattice structure of alternating BiTe and SbTe layers produces a device within which there is good electrical conductivity but perpendicular to which thermal conductivity is poor. The result is an enhanced ZT (approximately 2.4 at room temperature for p-type). Note that this high value of ZT has not been independently confirmed due to the complicated demands on the growth of such superlattices and device fabrication; however the material ZT values are consistent

with the performance of hot-spot coolers made out of these materials and validated at Intel Labs.

Bismuth telluride and its solid solutions are good thermoelectric materials at room temperature and therefore suitable for refrigeration applications around 300 K. The Czochralski method has been used to grow single crystalline bismuth telluride compounds. These compounds are usually obtained with directional solidification from melt or powder metallurgy processes. Materials produced with these methods have lower efficiency than single crystalline ones due to the random orientation of crystal grains, but their mechanical properties are superior and the sensitivity to structural defects and impurities is lower due to high optimal carrier concentration.

The required carrier concentration is obtained by choosing a nonstoichiometric composition, which is achieved by introducing excess bismuth or tellurium atoms to primary melt or by dopant impurities. Some possible dopants are halogens and group IV and V atoms. Due to the small bandgap (0.16 eV) Bi_2Te_3 is partially degenerate and the corresponding Fermi-level should be close to the conduction band minimum at room temperature. The size of the band-gap means that Bi_2Te_3 has high intrinsic carrier concentration. Therefore, minority carrier conduction cannot be neglected for small stoichiometric deviations. Use of telluride compounds is limited by the toxicity and rarity of tellurium.

Silicon-germanium alloys

Bulk Si exhibits a low ZT of ~0.01 because of its high thermal conductivity. However, ZT can be as high as 0.6 in silicon nanowires, which retain the high electrical conductivity of doped Si, but reduce the thermal conductivity due to elevated scattering of phonons on their extensive surfaces and low cross-section.

Combining Si and Ge also allows to retain a high electrical conductivity of both components and reduce the thermal conductivity. The reduction originates from additional scattering due to very different lattice (phonon) properties of Si and Ge. As a result, Silicon-germanium alloys are currently the best thermoelectric materials around 1000 °C and are therefore used in some radioisotope thermoelectric generators (RTG) (notably the MHW-RTG and GPHS-RTG) and some other high-temperature applications, such as waste heat recovery. Usability of silicon-germanium alloys is limited by their high price and moderate ZT values (~0.7); however, ZT can be increased to 1–2 in SiGe nanostructures owing to the reduction in thermal conductivity.

Sodium cobaltate

Experiments on crystals of sodium cobaltate, using X-ray and neutron scattering experiments carried out at the European Synchrotron Radiation Facility (ESRF) and the Institut Laue-Langevin (ILL) in Grenoble were able to suppress thermal conductivity by a factor of six compared to vacancy-free sodium cobaltate. The experiments agreed with corresponding density functional calculations. The technique involved large anharmonic displacements of NaCoO contained within the crystals.

Nanomaterials and superlattices

In addition to nanostructured BiTe/SbTe superlattice thin films, other nanostructured materials, including silicon nanowires,[69] nanotubes and quantum dots show potential in improving thermoelectric properties.

PbTe/PbSeTe quantum dot superlattice

Another example of a superlattice involves a PbTe/PbSeTe quantum dot superlattices provides an enhanced ZT (approximately 1.5 at room temperature) that was higher than the bulk ZT value for either PbTe or PbSeTe (approximately 0.5).

Nanocrystal stability and thermal conductivity

Not all nanocrystalline materials are stable, because the crystal size can grow at high temperatures, ruining the materials' desired characteristics.

Nanocrystalline materials have many interfaces between crystals, which Physics of SASER scatter phonons so the thermal conductivity is reduced. Phonons are confined to the grain, if their mean free path is larger than the material grain size.

Nanocrystalline transition metal silicides

Nanocrystalline transition metal silicides are a promising material group for thermoelectric applications, because they fulfill several criteria that are demanded from the commercial applications point of view. In some nanocrystalline transition metal silicides the power factor is higher than in the corresponding polycrystalline material but the lack of reliable data on thermal conductivity prevents the evaluation of their thermoelectric efficiency.

Nanostructured skutterudites

Skutterudites, a cobalt arsenide mineral with variable amounts of nickel and iron, can be produced artificially, and are candidates for better thermoelectric materials.

One advantage of nanostructured skutterudites over normal skutterudites is their reduced thermal conductivity, caused by grain boundary scattering. ZT values of ~0.65 and > 0.4 have been achieved with $CoSb_3$ based samples; the former values were 2.0 for Ni and 0.75 for Te-doped material at 680 K and latter for Au-composite at T > 700 K.

Even greater performance improvements can be achieved by using composites and by controlling the grain size, the compaction conditions of polycrystalline samples and the carrier concentration.

Graphene

Graphene is known for its high electrical conductivity and Seebeck coefficient at room temperature. However, from thermoelectric perspective, its thermal conductivity is notably high, which in turn limits its ZT. Several approaches were suggested to reduce the thermal conductivity of graphene without altering much its electrical conductivity. These include, but not limited to, the following:

- Doping with carbon isotopes to form isotopic heterojunction such as that of ^{12}C and ^{13}C. Those isotopes possess different phonon frequency mismatch, which leads to the scattering of the heat carriers (phonons). This approach has been shown to affect neither the power factor nor the electrical conductivity.
- Wrinkles and cracks in the graphene structure were shown to contribute to the reduction in the thermal conductivity. Reported values of thermal conductivity of suspended graphene of size 3.8 μm show a wide spread from 1500 to 5000 W/(m·K). A recent study attributed that to the microstructural defects present in graphene, such as wrinkles and cracks, which can drop the thermal conductivity by 27%. These defects help scatter phonons.
- Introduction of defects with techniques such as oxygen plasma treatment. A more systemic way of introducing defects in graphene structure is done through O_2 plasma treatment. Ultimately, the graphene sample will contain prescribed-holes spaced and numbered according to the plasma intensity. People were able to improve ZT of graphene from 1 to a value of 2.6 when the defect density is raised from 0.04 to 2.5 (this number is an index of defect density and usually understood when compared to the corresponding value of the un-treated graphene, 0.04 in our case). Nevertheless, this technique would lower the

electrical conductivity as well, which can be kept unchanged if the plasma processing parameters are optimized.

- Functionalization of graphene by oxygen. The thermal behavior of graphene oxide has not been investigated extensively as compared to its counterpart; graphene. However, it was shown theoretically by Density Functional Theory (DFT) model that adding oxygen into the lattice of graphene reduces a lot its thermal conductivity due to phonon scattering effect. Scattering of phonons result from both acoustic mismatch and reduced symmetry in graphene structure after doping with oxygen. The reduction of thermal conductivity can easily exceed 50% with this approach.

Superlattices and roughness

Superlattices – nano structured thermocouples, are considered a good candidate for better thermoelectric device manufacturing, with materials that can be used in manufacturing this structure.

Their production is expensive for general-use due to fabrication processes based on expensive thin-film growth methods. However, since the amount of thin-film materials required for device fabrication with superlattices, is so much less than thin-film materials in bulk thermoelectric materials (almost by a factor of 1/10,000) the long-term cost advantage is indeed favorable.

This is particularly true given the limited availability of tellurium causing competing solar applications for thermoelectric coupling systems to rise.

Superlattice structures also allow the independent manipulation of transport parameters by adjusting the structure itself, enabling research for better understanding of the thermoelectric phenomena in nanoscale, and studying the phonon-blocking electron-transmitting structures – explaining the changes in electric field and conductivity due to the material's nano-structure.

Many strategies exist to decrease the superlattice thermal conductivity that are based on engineering of phonon transport. The thermal conductivity along the film plane and wire axis can be reduced by creating diffuse interface scattering and by reducing the interface separation distance, both which are caused by interface roughness.

Interface roughness can naturally occur or may be artificially induced. In nature, roughness is caused by the mixing of atoms of foreign elements. Artificial roughness can be created using various structure types, such as quantum dot interfaces and thin-films on step-covered substrates.

Tin selenide

In 2014, researchers at Northwestern University discovered that tin selenide (SnSe) has a ZT of 2.6 along the b axis of the unit cell. This was the highest value reported to date. This was attributed to an extremely low thermal conductivity found in the SnSe lattice. Specifically, SnSe demonstrated a lattice thermal conductivity of 0.23 $W \cdot m^{-1} \cdot K^{-1}$, much lower than previously reported values of 0.5 $W \cdot m^{-1} \cdot K^{-1}$ and greater. This material also exhibited a ZT of 2.3±0.3 along the c-axis and 0.8±0.2 along the a-axis. These results were obtained at a temperature of 923 K (650 °C).

Anderson localization

Anderson localization is a quantum mechanical phenomenom where charge carriers in a random potential are trapped in place (i.e. they are in localized states as opposed to being in scattering states if they could move freely). This localization prevents the charge carriers from moving, which inhibits their contribution to the thermal conductivity of a material, but because it also lowers the electrical conductivity, it was thought to reduce ZT and be detrimental for thermoelectric materials. In 2019, it was proposed that by localizing only the minority charge carriers in a doped semiconductor (i.e. holes in an n-doped semiconductor or electrons in a p-doped semiconductor), Anderson localization could increase ZT. The heat conductivity associated with movement of the minority charge carriers would be reduced while electrical conductivity of the majority charge carrier would be unaffected.

In 2020, researchers at Kyung Hee University demonstrated the use of Anderson localization in an n-type semiconductor to improve the thermoelectric properties of a material. They embedded nanoparticles of silver telluride (Ag_2Te) in a lead telluride (PbTe) matrix. Ag_2Te undergoes a phase transition around 407 K. Below this temperature, both holes and electrons are localized at the Ag_2Te nanoparticles, while after the transtion, holes are still localized, but electrons can move freely in the material. The researchers were able to increase ZT from 1.5 to above 2.0 using this method.

More Thermoelectric Information

Thermoelectric materials generate power directly from the heat by converting temperature differences into electric voltage. These materials must have both high electrical conductivity (σ) and low thermal conductivity (κ) to be good thermoelectric materials. Having low thermal conductivity ensures that when one side is made hot, the other side stays cold, which helps to generate a large voltage while in a temperature gradient. The measure of the magnitude of electrons flow in response to a temperature difference across that material is given by the Seebeck coefficient (S). The efficiency of a given material to produce a thermoelectric power is simply estimated by its "figure of merit" $zT = S^2\sigma T/\kappa$.

For many years, the main three semiconductors known to have both low thermal conductivity and high power factor were bismuth telluride (BiTe), lead telluride (PbTe), and silicon germanium (SiGe). Some of these materials have somewhat rare elements which make them expensive.

Today, the thermal conductivity of semiconductors can be lowered without affecting their high electrical properties using nanotechnology. This can be achieved by creating nanoscale features such as particles, wires or interfaces in bulk semiconductor materials. However, the manufacturing processes of nano-materials are still challenging.

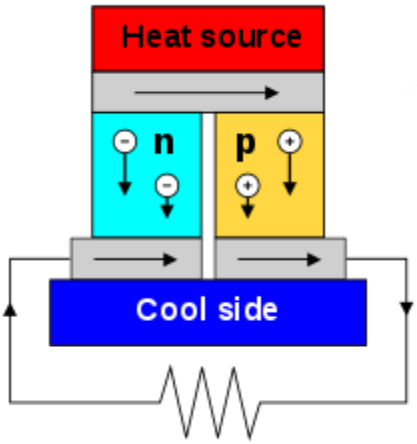

A thermoelectric circuit composed of materials of different Seebeck coefficient (p-doped and n-doped semiconductors), configured as a thermoelectric generator.

Thermoelectric advantages

Thermoelectric generators are all-solid-state devices that do not require any fluids for fuel or cooling, making them non-orientation dependent allowing for use in zero-gravity or deep-sea applications. The solid-state design allows for operation in severe environments. Thermoelectric generators have no moving parts which produce a more reliable device that does not require maintenance for long periods. The durability and environmental stability have made thermoelectrics a favorite for NASA's deep space

explorers among other applications. One of the key advantages of thermoelectric generators outside of such specialized applications is that they can potentially be integrated into existing technologies to boost efficiency and reduce environmental impact by producing usable power from waste heat.

Thermoelectric module

A thermoelectric module is a circuit containing thermoelectric materials which generate electricity from heat directly. A thermoelectric module consists of two dissimilar thermoelectric materials joined at their ends: an n-type (with negative charge carriers), and a p-type (with positive charge carriers) semiconductor. Direct electric current will flow in the circuit when there is a temperature difference between the ends of the materials.

In application, thermoelectric modules in power generation work in very tough mechanical and thermal conditions. Because they operate in a very high-temperature gradient, the modules are subject to large thermally induced stresses and strains for long periods. They also are subject to mechanical fatigue caused by many thermal cycles.

Thus, the junctions and materials must be selected so that they survive these tough mechanical and thermal conditions. Also, the module must be designed such that the two thermoelectric materials are thermally in parallel, but electrically in series. The efficiency of a thermoelectric module is greatly affected by the geometry of its design.

Thermoelectric design

Thermoelectric generators are made of several thermopiles, each consisting of many thermocouples made of a connected n-type and p-type material. The arrangement of the thermocouples is typically in three main designs: planar, vertical, and mixed. Planar design involves thermocouples put onto a substrate horizontally between the heat source and cool side, resulting in the ability to create longer and thinner thermocouples, thereby increasing the thermal resistance and temperature gradient and eventually increasing voltage output. Vertical design has thermocouples arranged vertically between the hot and cool plates, leading to high integration of thermocouples as well as a high output voltage, making this design the most widely-used design commercially. The mixed design has the thermocouples arranged laterally on the substrate while the heat flow is vertical between plates. Microcavities under the hot contacts of the device allow for a temperature gradient, which allows for the substrate's thermal conductivity to affect the gradient and efficiency of the device.

For microelectromechanical systems, TEGs can be designed on the scale of handheld devices to use body heat in the form of thin films. Flexible TEGs for wearable electronics are able to be made with novel polymers through additive manufacturing or thermal spraying processes. Cylindrical TEGs for using heat from vehicle exhaust pipes can also be made using circular thermocouples arranged in a cylinder. Many designs for TEGs can be made for the different devices they are applied to.

Thermoelectric systems

Using thermoelectric modules, a thermoelectric system generates power by taking in heat from a source such as a hot exhaust flue. To operate, the system needs a large temperature gradient, which is not easy in real-world applications. The cold side must be cooled by air or water. Heat exchangers are used on both sides of the modules to supply this heating and cooling.

There are many challenges in designing a reliable TEG system that operates at high temperatures. Achieving high efficiency in the system requires extensive engineering design to balance between the heat flow through the modules and maximizing the temperature gradient across them. To do this, designing heat exchanger technologies in the system is one of the most important aspects of TEG engineering. In addition, the system requires to minimize the thermal losses due to the interfaces between materials at several places. Another challenging constraint is avoiding large pressure drops between the heating and cooling sources.

If AC power is required (such as for powering equipment designed to run from AC mains power), the DC power from the TE modules must be passed through an inverter, which lowers efficiency and adds to the cost and complexity of the system.

Materials for TEG

Only a few known materials to date are identified as thermoelectric materials. Most thermoelectric materials today have a zT, the figure of merit, value of around 1, such as in bismuth telluride (Bi_2Te_3) at room temperature and lead telluride (PbTe) at 500–700 K. However, to be competitive with other power generation systems, TEG materials should have a zT of 2–3. Most research in thermoelectric materials has focused on increasing the Seebeck coefficient (S) and reducing the thermal conductivity, especially by manipulating the nanostructure of the thermoelectric materials. Because both the thermal and electrical conductivity correlate with the charge carriers, new means must be introduced to conciliate the contradiction between high electrical conductivity and low thermal conductivity, as is needed.

When selecting materials for thermoelectric generation, several other factors need to be considered. During operation, ideally, the thermoelectric generator has a large temperature gradient across it. Thermal expansion will then introduce stress in the device which may cause fracture of the thermoelectric legs or separation from the coupling material. The mechanical properties of the materials must be considered and the coefficient of thermal expansion of the n and p-type material must be matched reasonably well. In segmented thermoelectric generators, the material's compatibility must also be considered to avoid incompatibility of relative current, defined as the ratio of electrical current to diffusion heat current, between segment layers.

When the compatibility factor from one segment to the next differs by more than a factor of about two, the device will not operate efficiently. The material parameters determining s (as well as zT) are temperature-dependent, so the compatibility factor may change from the hot side to the cold side of the device, even in one segment. This behavior is

referred to as self-compatibility and may become important in devices designed for wide-temperature application.

In general, thermoelectric materials can be categorized into conventional and new materials:

Conventional materials

Many TEG materials are employed in commercial applications today. These materials can be divided into three groups based on the temperature range of operation:

1. Low temperature materials (up to around 450 K): Alloys based on bismuth (Bi) in combinations with antimony (Sb), tellurium (Te) or selenium (Se).
2. Intermediate temperature (up to 850 K): such as materials based on alloys of lead (Pb)
3. Highest temperatures material (up to 1300 K): materials fabricated from silicon-germanium (SiGe) alloys.

Although these materials remain the cornerstone for commercial and practical applications in thermoelectric power generation, significant advances have been made in synthesizing new materials and fabricating material structures with improved thermoelectric performance. Recent research has focused on improving the material's figure-of-merit (zT), and hence the conversion efficiency, by reducing the lattice thermal conductivity.

Practical limitations

Besides low efficiency and relatively high cost, practical problems exist in using thermoelectric devices in certain types of applications resulting from a relatively high electrical output resistance, which increases self-heating, and a relatively low thermal conductivity, which makes them unsuitable for applications where heat removal is critical, as with heat removal from an electrical device such as microprocessors.

- **High generator output resistance:** To get voltage output levels in the range required by digital electrical devices, a common approach is to place many thermoelectric elements in series within a generator module. The element's voltages increase, but so does their output resistance. The maximum power transfer theorem dictates that maximum power is delivered to a load when the source and load resistances are identically matched. For low impedance loads near zero ohms, as the generator resistance rises the power delivered to the load decreases. To lower the output resistance, some commercial devices place more individual elements in parallel and fewer in series and employ a boost regulator to raise the voltage to the voltage needed by the load.
- **Low thermal conductivity:** Because a very high thermal conductivity is required to transport thermal energy away from a heat source such as a digital microprocessor, the low thermal conductivity of thermoelectric generators makes them unsuitable to recover the heat.
- **Cold-side heat removal with air:** In air-cooled thermoelectric applications, such as when harvesting thermal energy from a motor vehicle's crankcase, the large amount of thermal energy that must be dissipated into ambient air presents a significant challenge. As a thermoelectric generator's cool side

temperature rises, the device's differential working temperature decreases. As the temperature rises, the device's electrical resistance increases causing greater parasitic generator self-heating. In motor vehicle applications a supplementary radiator is sometimes used for improved heat removal, though the use of an electric water pump to circulate a coolant adds parasitic loss to total generator output power. Water cooling the thermoelectric generator's cold side, as when generating thermoelectric power from the hot crankcase of an inboard boat motor, would not suffer from this disadvantage. Water is a far easier coolant to use effectively in contrast to air.

Appendix C. Thermocouple References

Most Efficient Thermocouple

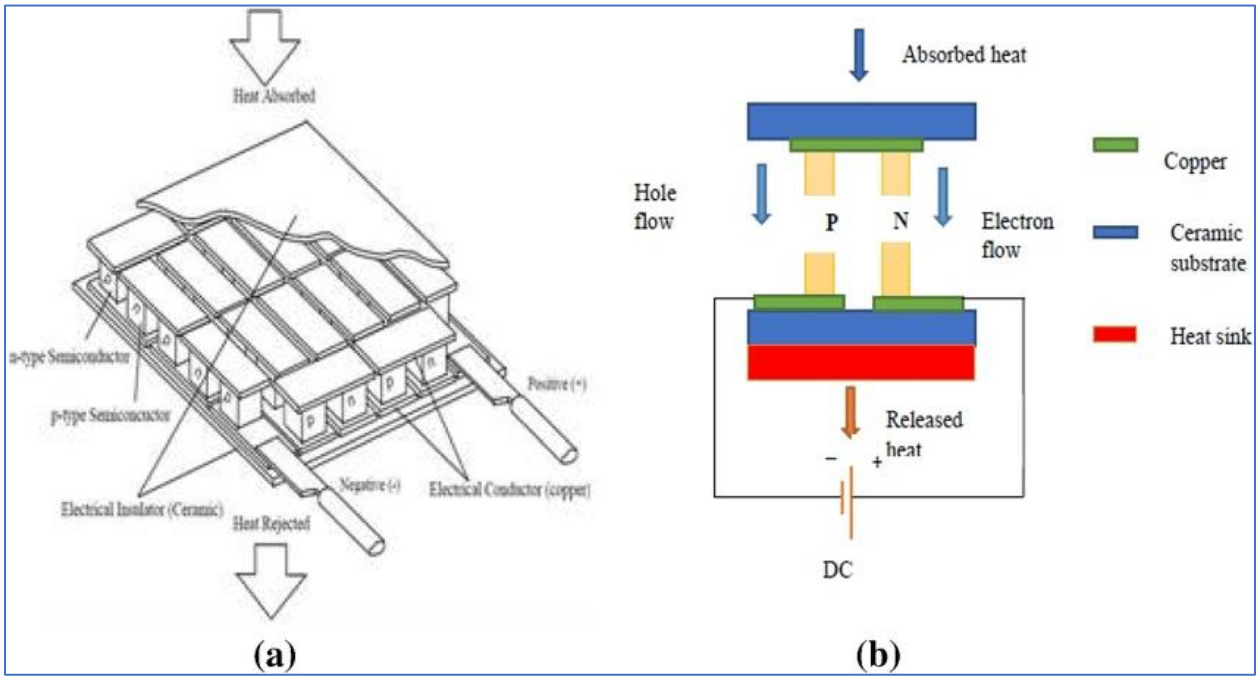

Thermocouple Types

Thermocouples are available in different combinations of metals or calibrations. The most common are the “Base Metal” thermocouples known as Types J, K, T, E and N. There are also high temperature calibrations - also known as Noble Metal thermocouples - Types R, S, C and GB

Difference in Thermocouple Types

Each calibration has a different temperature range and environment, although the maximum temperature varies with the diameter of the wire used in the thermocouple. Although thermocouple calibration dictates the temperature range, the maximum range is also limited by the diameter of the thermocouple wire. That is, a very thin thermocouple may not reach the full temperature range.

Common Thermocouple Temperature Ranges

Calibration	Temperature Range	Standard Limits Of Error	Special Limits Of Error
J	0° to 750°C (32° to 1382°F)	Greater of 2.2°C or 0.75%	Greater of 1.1°C or 0.4%
K	-200° to 1250°C (-328° to 2282°F)	Greater of 2.2°C or 0.75%	Greater of 1.1°C or 0.4%
E	-200° to 900°C (-328° to 1652°F)	Greater of 1.7°C or 0.5%	Greater of 1.0°C or 0.4%
T	-250° to 350°C (-418° to 662°F)	Greater of 1.0°C or 0.75%	Greater of 0.5°C or 0.4%

What are the accuracies and temperature ranges of the various thermocouples?

It is important to remember that both accuracy and range depend on such things as the thermocouple alloys, the temperature being measured, the construction of the sensor, the material of the sheath, the media being measured, the state of the media (liquid, solid, or gas) and the diameter of either the thermocouple wire (if it is exposed) or the sheath diameter (if the thermocouple wire is not exposed but is sheathed).

Thermocouple Reference Tables

Thermocouples produce a voltage output that can be correlated to the temperature that the thermocouple is measuring. The documents in the table below provide the thermoelectric voltage and corresponding temperature for a given thermocouple type. Most of the documents also provide the thermocouple temperature range, limits of error and environmental considerations.

Thermocouple Type B(° C)	Thermocouple Type B(° F)	Thermocouple Type C(° C)	Thermocouple Type C(° F)
Thermocouple Type E(° C)	Thermocouple Type E(° F)	Thermocouple Type J(° C)	Thermocouple Type J(° F)
Thermocouple Type K(° C)	Thermocouple Type K(° F)	Thermocouple Type N(° C)	Thermocouple Type N(° F)
Thermocouple Type R(° C)	Thermocouple Type R(° F)	Thermocouple Type S(° C)	Thermocouple Type S(° F)
Thermocouple Type T(° C)	Thermocouple Type T(° F)		

Why do thermocouples have different colors?

Click on this link to check the thermocouple color code chart

Why are Type K thermocouples so popular?

Type K thermocouples are so popular because of their wide temperature range and durability. The conductor materials used in Type K thermocouples are more chemically inert than Type T (copper) and Type J (Iron). While the output of Type K thermocouples is slightly lower than Types T, J and E, it is higher than its closest competitor (Type N) and has been in use longer. If you want to learn more about what a K-type thermocouple is, read our full guide.

How do I choose between different types?

Each thermocouple type has a designated color-code defined in either ANSI/ASTM E230 or IEC60584. The type can be identified by color as follows:

Calibration	ANSI/ASTM E230	IEC 60584
Type K:	Yellow (+)/ Red (-)	Green (+)/ White (-)
Type J:	White (+)/ Red (-)	Black (+)/ White (-)
Type T:	Blue (+) / Red (-)	Brown (+) / White (-)
Type E:	Purple (+)/ Red (-)	Purple (+) / White (-)
Type N:	Orange (+)/ Red (-)	Rose (+) / White (-)
Type R:	Black (+)/ Red (-)	Orange (+) / White (-)
Type S:	Black (+)/ Red (-)	Orange (+) / White (-)
Type B:	Black (+)/ Red (-)	Orange (+) / White (-)
Type C:	None established	None established

Also, some materials are strongly to slightly magnetic:

Type J Positive (strongly Magnetic), Type K Positive (slightly magnetic).

To determine polarity, connect the thermocouple to a voltmeter capable of measuring millivolts or microvolts and looking for increasing output when the tip is heated slightly.

How do I choose between different types?

Choosing the right type of thermocouple is a matter of matching the thermocouple to your measurement requirement. Here are some areas to take into consideration:

- **Temperature Range:** The different thermocouple types have different temperature ranges. For example, Type T with its Copper leg has a max temperature of 370C or 700F. Type K on the other hand can be used up to 1260C or 2300F.
- **Conductor Size:** The diameter of the thermocouple wires also needs to be taken into consideration when long duration measurements are needed. For example, Type T thermocouples are rated to 370C/700F, however if your thermocouple has #14AWG wires (.064" Diameter) they are rated for 370C/700F. If your thermocouple has #30AWG wires, that drops to 150C/300F.
- **Accuracy:** Type T thermocouples have the tightest accuracy of all the base metal thermocouples at ±1C or ±0.75% whichever is greater. This is followed by Type E (±1.7C or 0.5%) and Types J, K and N (±2.2C or 0.75%) for standard limits of error (per ANSI/ASTM E230).

Other important considerations are the sheath materials (if immersion probe style), insulation material (if wire or surface sensor) and sensor geometry.

Types of Thermocouple (https://www.thermocoupleinfo.com/thermocouple-types.htm)

NiChrome Foil Source: https://www.aliexpress.us/item/3256807068822193.html?src=google&gatewayAdapt=glo2usa

NiChrome Wire Sources: https://www.amazon.com/Nichrome-Resistant-General-Purpose-Support/dp/B0CD5N2WDV/?_encoding=UTF8&ref_=pd_wlh&pd_rd_w=VjoFL&content-id=amzn1.sym.8204b485-11a7-46e5-99d6-924574f6f1b2&pf_rd_p=8204b485-11a7-46e5-99d6-924574f6f1b2&pf_rd_r=SHJ555VYFQ4ZFCHF8E5Y&pd_rd_wg=23SiC&pd_rd_r=c06988a6-8643-45c6-b318-7fa36ba27f04&th=1

https://www.amazon.com/Nichrome-80-Gauge-Resistance-Wire/dp/B07CHTY1VV/ref=pd_bxgy_d_sccl_1/141-4854192-9569021?pd_rd_w=xBtj7&content-id=amzn1.sym.c51e3ad7-b551-4b1a-b43c-3cf69addb649&pf_rd_p=c51e3ad7-b551-4b1a-b43c-3cf69addb649&pf_rd_r=F8D5X318EJR2D8ERCFXF&pd_rd_wg=xu7hS&pd_rd_r=120944cb-d425-4416-8f2e-dce8bfdbe884&pd_rd_i=B07CHTY1VV&psc=1

https://www.amazon.com/CYPHE-Nickel-Chromium-Diameter-0-08MM-0-45MM-Resistance/dp/B0CNZ2THXS?th=1

Type E Thermocouple (Nickel-Chromium(Chromel)/Constantan): The Type E has a stronger signal & higher accuracy than the Type K or Type J at moderate temperature ranges of 1,000F and lower. The type E is also more stable than the type K, which adds to its accuracy.

Type E Temperature Range:

- Thermocouple grade wire, -454 to 1600F (-270 to 870C)

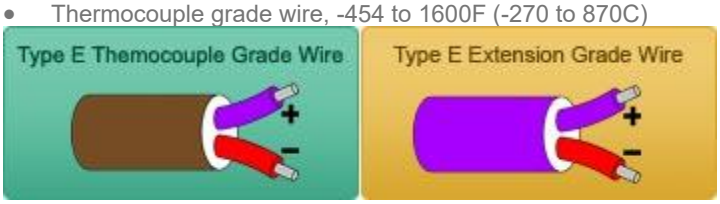

- Extension wire, 32 to 392F (0 to 200C)

Type E Accuracy (whichever is greater):

- Standard: +/- 1.7C or +/- 0.5%
- Special Limits of Error: +/- 1.0C or 0.4%

Consideration for bare wire type E thermocouple applications:

- In oxiding or inert atmospheres the operating range is roughly –418F to 1,652F (–250C to 900C).

Type E Thermocouple Reference Table

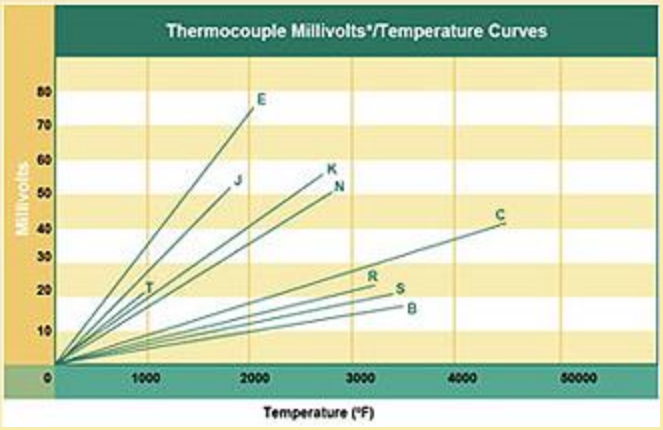

Click for PDF

Type J Thermocouple: The type J is also very common. It has a smaller temperature range and a shorter lifespan at higher temperatures than the Type K. It is equivalent to the Type K in terms of expense and reliability.

Type J Temperature Range:

- Thermocouple grade wire, -346 to 1,400F (-210 to 760C)
- Extension wire, 32 to 392F (0 to 200C)

Type J Accuracy (whichever is greater):

- Standard: +/- 2.2C or +/- .75%
- Special Limits of Error: +/- 1.1C or 0.4%

Consideration for bare wire type J thermocouple applications:

- The Type J Is Well Suited To Oxidizing Atmospheres

Type J Thermocouple Reference Table

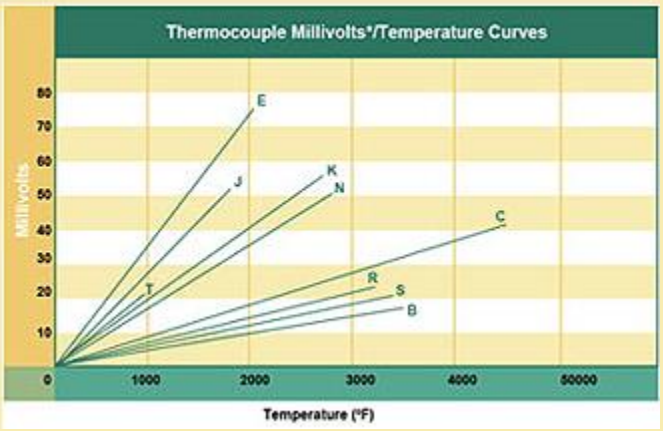

Click for PDF

Type K Thermocouple (Nickel-Chromium / Nickel-Alumel): The type K is the most common type of thermocouple. It's inexpensive, accurate, reliable, and has a wide temperature range. The type K is commonly found in nuclear applications because of its relative radiation hardness. Maximum continuous temperature is around 1,100C.

Type K Temperature Range:

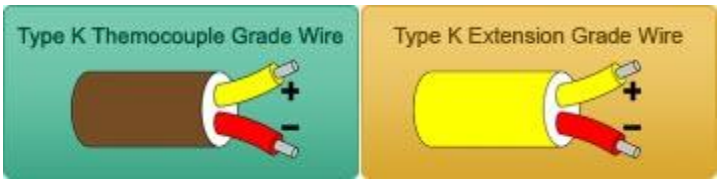

- Thermocouple grade wire, –454 to 2,300F (–270 to 1260C)
- Extension wire, 32 to 392F (0 to 200C)

Type K Accuracy (whichever is greater):

- Standard: +/- 2.2C or +/- .75%
- Special Limits of Error: +/- 1.1C or 0.4%

Consideration for bare wire type K thermocouple applications:

- The Type K Is Well Suited To Oxidizing Atmospheres

Type K Thermocouple Reference Table

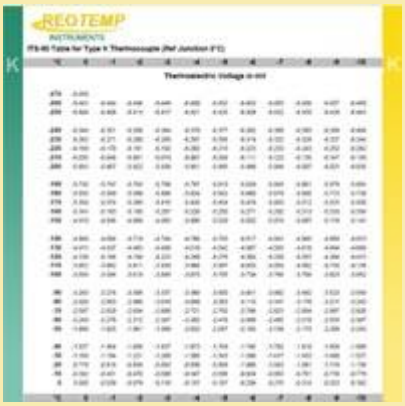

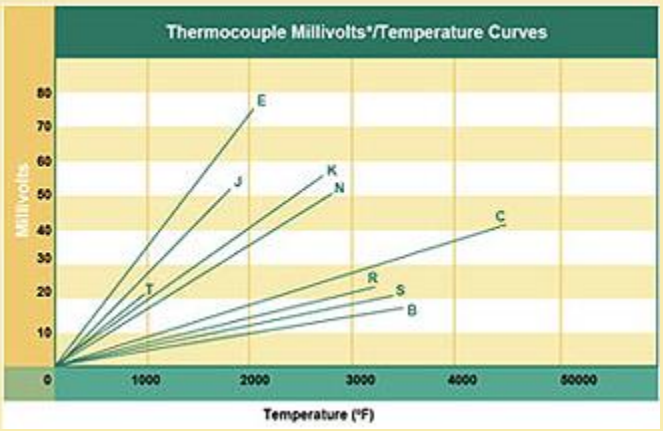

Click for PDF

Type T Thermocouple (Copper/Constantan): The Type T is a very stable thermocouple and is often used in extremely low temperature applications such as cryogenics or ultra low freezers. It is found in other laboratory environments as well. The type T has excellent repeatability between –380F to 392F (–200C to 200C)..

Type T Temperature Range:

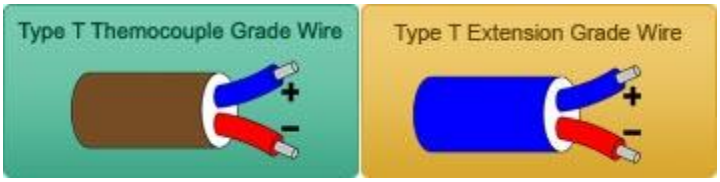

- Thermocouple grade wire, -454 to 700F (-270 to 370C)
- Extension wire, 32 to 392F (0 to 200C)

Type T Accuracy (whichever is greater):

- Standard: +/- 1.0C or +/- .75%
- Special Limits of Error: +/- 0.5C or 0.4%

Consideration for bare wire type T thermocouple applications:

- The Type T Is Well Suited To Oxidizing Atmospheres

Type T Thermocouple Reference Table

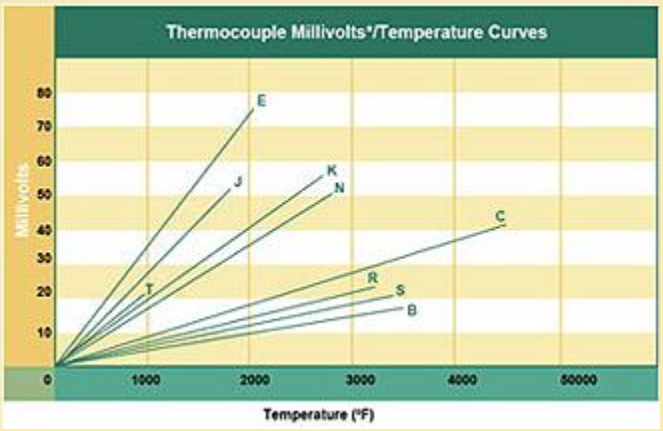

Click for PDF

Type N Thermocouple (Nicrosil / Nisil): The Type N shares the same accuracy and temperature limits as the Type K. The type N is slightly more expensive. The type N has better repeatability between 572F to 932F (300C to 500C) compared to the type K.

Type N Temperature Range:

- Maximum continuous operating temperature: up to 2,300F (1,260C)

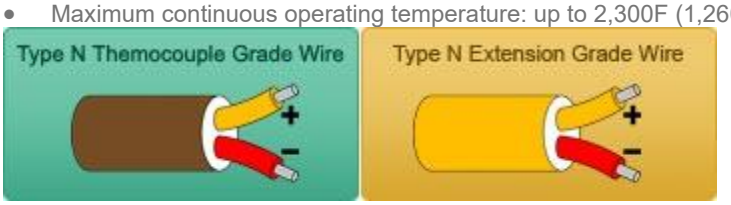

- Short term use: 2,336F (1,280C)
- Thermocouple grade wire, -454 to 2300F (-270 to 1,260C)
- Extension wire, 32 to 392F (0 to 200C)

Type N Accuracy (whichever is greater):

- Standard: +/- 2.2C or +/- .75%
- Special Limits of Error: +/- 1.1C or 0.4%

Consideration for bare wire type E thermocouple applications:

- The type N holds up better to oxidation at high temperatures when compared to the type K.

Type N Thermocouple Reference Table

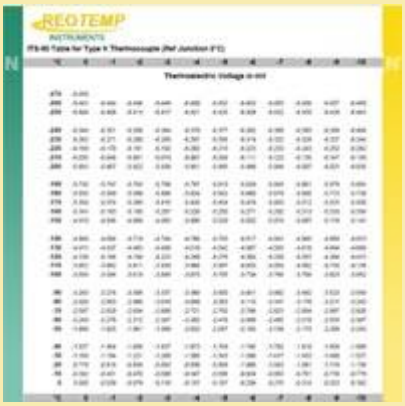

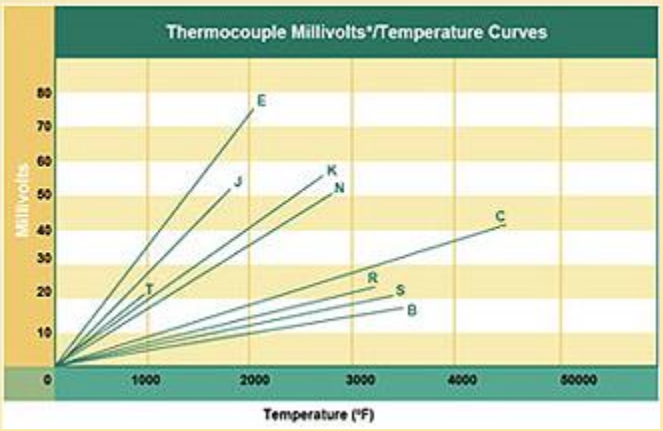

Click for PDF

Type B Thermocouple (Platinum Rhodium – 30% / Platinum Rhodium – 6%): The Type B thermocouple is used in extremely high temperature applications. It has the highest temperature limit of all the thermocouples listed above. It maintains a high level of accuracy and stability at very high temperatures. The type B has a lower output than the other noble metals (type R & type S) at temperatures below 1,112F (600C).

Type B Temperature Range:

- Thermocouple grade wire, 32 to 3100F (0 to 1700C)
- Extension wire, 32 to 212F (0 to 100C)

Accuracy (whichever is greater):

- Standard: +/- 0.5%
- Special Limits of Error: +/- 0.25%

Type B Thermocouple Reference Table

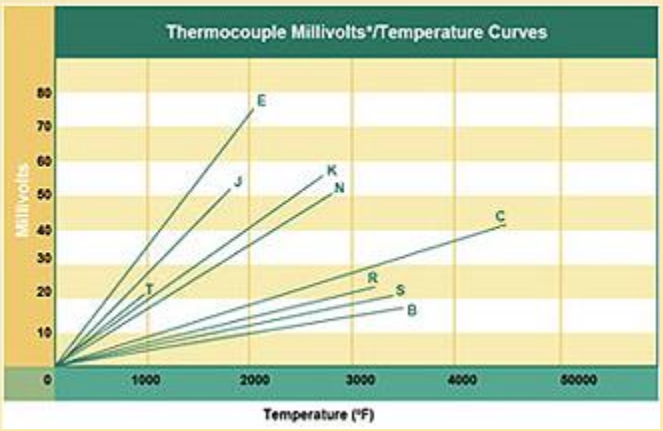

Click for PDF

Type R Thermocouple (Platinum Rhodium -13% / Platinum): The Type R is used in very high temperature applications. It has a higher percentage of Rhodium than the Type S, which makes it more expensive. The Type R is very similar to the Type S in terms of performance. It is sometimes used in lower temperature applications because of its high accuracy and stability. Type R has a slightly higher output and improved stability over the type S.

Type R Temperature Range:

- Thermocouple grade wire, -58 to 2700F (-50 to 1480C)
- Extension wire, 32 to 392F (0 to 200C)

Accuracy (whichever is greater):

- Standard: +/- 1.5C or +/- .25%
- Special Limits of Error: +/- 0.6C or 0.1%

Type R Thermocouple Reference Table

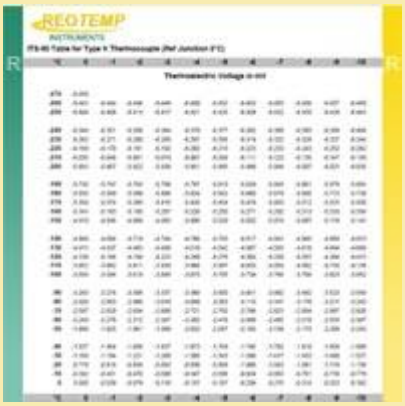

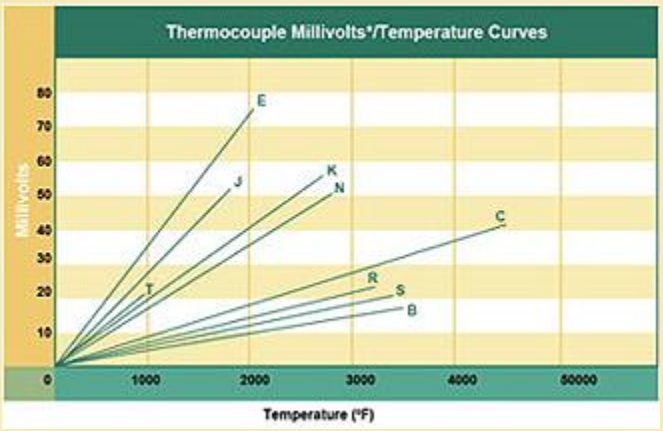

Click for PDF

Type S Thermocouple (Platinum Rhodium - 10% / Platinum): The Type S is used in very high temperature applications. It is commonly found in the BioTech and Pharmaceutical industries. It is sometimes used in lower temperature applications because of its high accuracy and stability. The type S is often used with a ceramic protection tube.

Type S Temperature Range:

- Maximum continuous operating temperature: up to 2,912F (1600C)
- Short term use: up to 3,092F (1,700C)
- Thermocouple grade wire, -58 to 2700F (-50 to 1480C)
- Extension wire, 32 to 392F (0 to 200C)

Accuracy (whichever is greater):

- Standard: +/- 1.5C or +/- .25%
- Special Limits of Error: +/- 0.6C or 0.1%

Consideration for bare wire type J thermocouple applications:

- The Type S can be used in inert and oxidizing atmospheres up to 2,912F (1600C) continuously and up 3,092F (1,700C) for short term use.

Type S Thermocouple Reference Table

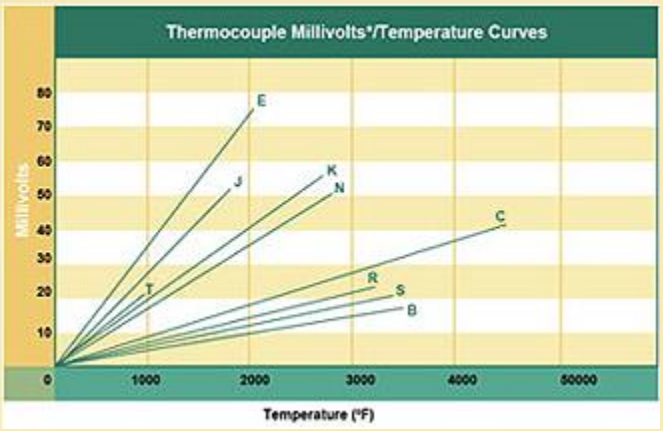

Click for PDF

GUIDE TO THERMOCOUPLES – TYPES AND USES & RANGES

By Neal Messier and Nicole Chotain Industry Update August 31, 2022

All types of thermocouples are temperature sensors consisting of two dissimilar metals acting as electric conductors. Temperature measurement is based on a phenomenon where the reference is subtracted from the high temperature of the measuring junction. The measuring end is called the hot junction, while the reference is the cold junction.
Thermocouples are the conventional temperature measuring tool in the manufacturing industry because they are accurate, withstand extreme temperatures, inexpensive and durable.

Temp-Pro's Initial Calibration Tolerances to Thermocouple

Thermocouple Type			C°			F°		
WIRE ALLOYS	COLOR CODE	ANSI TYPE SYMBOL	TEMPERATURE RANGE	STANDARD LIMITS	SPECIAL LIMITS	TEMPERTURE RANGE	STANDARD LIMITS	SPECIAL LIMITS
Copper (+) vs. Constantan (-)	Blue Red	T	-200° to -65° -65° to +130° +130° to +350°	±1.5% ±1° ±0.75%	±0.8% ±0.5° ±0.4%	-330° to -85° -85° to +270° +270° to +660°	±1.5% ±1.8° ±0.75%	±0.8% ±0.9° ±0.4%
*Iron (+) vs. Constantan (-)	White Red	J	0° to +285° +285° to +750°	±2.2° ±0.75%	±1.1° ±0.4%	+32° to +545° +545° to +1400°	±4° ±0.75%	±2° ±0.4%
Chromel* (+) vs. Constantan (-)	Yellow Red	E	-200° to -170° -170° to +250° +250° to +340° +340° to +900°	±1% ±1.7° ±1.7° ±0.5%	±1° ±1° ±0.4% ±0.4%	-330° to -270° -270° to +480° +480° to +640° +640° to +1600°	±1% ±3° ±3° ±0.5%	±1.8° ±1.8° ±0.4% ±0.4%
Chromel* (+) vs. "Alumel" (-)	Yellow Red	K	-200° to -110° -110° to 0° 0° to +285° +285° to +1250°	±2% ±2.2° ±2.2° ±0.75%	±1.1° ±0.4%	-330° to -165° -165° to +32° +32° to +545° +545° to +2300°	±2% ±4° ±4° ±0.75%	±2° ±0.4%
Nicrosil (+) vs. Nisil (-)		N	0° to 285° +285° to +1250°	±2.2° ±0.75%	±1.1° ±0.4%	+32° to +545° +545° to +2300°	±4° ±0.75%	±2° ±0.4%
Platinum - 10% Rhodium (+) vs. Platinum (-)		S	0° to +600° +600° to +1450°	±1.5° ±0.25%	±0.6° ±0.1%	+32° to +1110° +1110° to +2650°	±2.7° ±0.25%	±1.1° ±0.1%
Platinum - 13% Rhodium (+) vs. Platinum		R	0° to +600° +600° to +1450°	±1.5° ±0.25%	±0.6° ±0.1%	+32° to +1110° +1110° to +2650°	±2.7° ±0.25%	±1.1° ±0.1%
Platinum - 30% Rhodium (+) vs. Platinum - 6% Rhodium (-)		B	+870° to +1700°	±0.5%	±0.25%	+1600° to +3100°	±0.5%	±0.25%
Tungsten (+) vs. Tungsten -26% Rhenium (-)		WR	+400° to 2300°	±1%		+800° to +4200°	±1%	
Tungsten - 3% Rhenium (+) vs. Tungsten - 25% Rhenium (-)		W3	+400° to 2300°	±1%		+800° to +4200°	±1%	
Tungsten - 5% Rhenium (+) vs. Tungsten - 26% Rhenium (-)		W5	+400° to +2300°	±1%		+800° to +4200°	±1%	

* Magnetic
** Trademark, Hoskins Manufacturing Co.
† not ANSI type symbol
NOTE: Percent limits apply directly to temperature in degrees Celsius, but for degrees Fahrenheit equivalents are applied to the number of degrees Fahrenheit above or below the ice point (+32 degrees Fahrenheit).

[i.e., Limit (degrees F) = (Temperature (degrees F) - 32 (degrees F)) * Percentage]

TYPES OF THERMOCOUPLES

The manufacturing industry is particular with the tools used, and the thermocouple is no different. Thermocouple use dissimilar metal based on the industry, thermocouple temperature ranges and conductor sensitivity. There are eight thermocouple types; B, E, J, K, N, R, S and T.

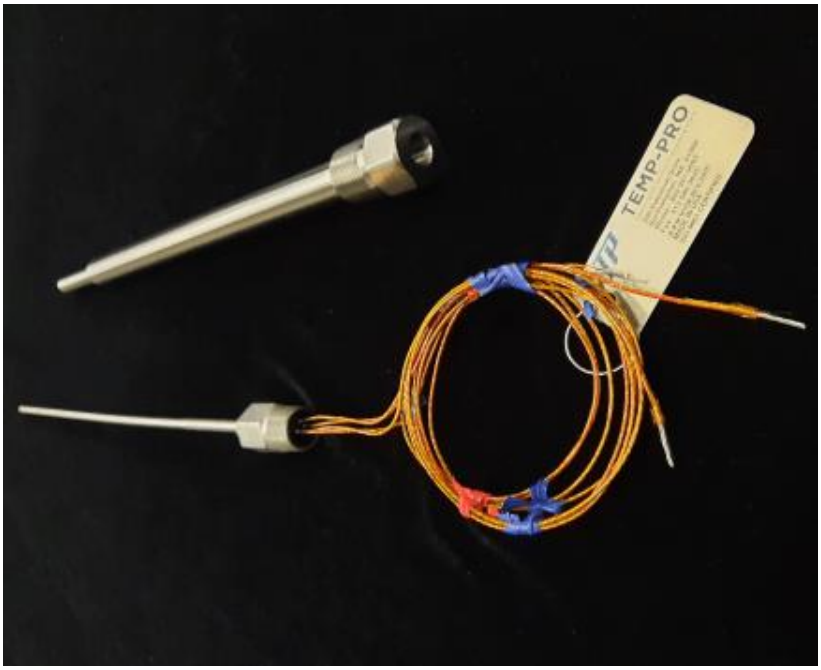

B-TYPE THERMOCOUPLE

B-type thermocouples combine the Platinum (30% Rhodium) and Platinum (6% Rhodium) alloys. These thermocouples are best suited for high-temperature activities and processes and have temperature ranges of 1370-1700℃ or 2500-3100℉. Cold junctions are not required in B-type thermocouples because they produce the same electrical output at 0℃ and 42℃. Their incredible heat resistance makes them perfect for inert and harsh conditions, such as glass production and cement manufacturing.

R-TYPE THERMOCOUPLE

R-type thermocouples made from platinum (10% Rhodium) and Platinum alloys can be used for activities whose working temperatures fall between 870-1450℃ or 1600-2640℉. Despite its accuracy, R-type thermocouples become reactive at temperatures above the thousand-degree Celsius mark and can be easily contaminated. Therefore, their accuracy and stability are better utilized for low-temperature activities like sulfur recovery units. R-Type thermocouples are ideal for high-temperature applications in industries such as glass production & petrochemical processing.

S-TYPE THERMOCOUPLE

Although the S-type performs similarly to the R-type, it is nowhere near as stable. This means that S-types must be protected from metallic and non-metallic vapors. Platinum only became the standard to measure temperature ranges between 630-1064°C as the freezing points of antimony, silver and gold are not so distinct during this span. S-types are Platinum (10% Rhodium) and Platinum and are commonplace in the medical industry.

E-TYPE THERMOCOUPLE

Chromel and Constantan are the alloy combination in E-type thermocouples, and they have a characteristic temperature range of 0-870°C or 32-1600°F). E-types' high output, fast response times and non-magnetism make them ideal for use in cryogenics, aviation, and flow chambers. E-types are rated over the K and J-types at temperatures 1000°F and lower because of their stability, accuracy, and stronger signal.

Constantan

1. Constantan is an alloy of 55% Copper and 45% Nickel.
2. The main feature of this alloy is its low temperature coefficient of resistance due to which its resistivity remains constant over a wide range of temperatures. This makes it suitable for making thermocouples with wires made of Iron, Copper, or Chromel (alloy of 90% Nickel and 10% Chromium by weight) which is used to measure temperature. This property also makes it suitable for use as standard resistances.
3. It has a high specific heat resistance which makes it a good insulator and high ductility which means that it can be easily stretched out into wires. These properties make it the ideal alloy for electric motor starter resistance wires and heavy-duty industrial rheostats.

So, Constantan is an alloy of 55% Copper and 45% Nickel. Its high ductility, high specific heat resistance and low temperature coefficient of resistance make it ideal for a wide range of applications.

Constantan, also known in various contexts as Eureka, Advance, and Ferry, refers to a copper-nickel alloy commonly used for its stable electrical resistance across a wide range of temperatures. It usually consists of 55% copper and 45% nickel. Its main feature is the low thermal variation of its resistivity, which is constant over a wide range of temperatures. Other alloys with similarly low temperature coefficients are known, such as manganin (Cu [86%] / Mn [12%] / Ni [2%]).

History

In 1887, Edward Weston discovered that metals can have a negative temperature coefficient of resistance, inventing what he called his "Alloy No. 2." It was produced in Germany where it was renamed "Konstantan".

Constantan alloy

Of all alloys used in modern strain gauges, constantan is the oldest, and still the most widely used. This situation reflects the fact that constantan has the best overall combination of properties needed for many strain gauge applications. This alloy has, for example, an adequately high strain sensitivity, or gauge factor, which is relatively insensitive to strain level and temperature.
Its resistivity (5.00×10^{-7} Ω·m)[2] is high enough to achieve suitable resistance values in even very small grids, and its temperature coefficient of resistance is fairly low. In addition, constantan is characterized by a good fatigue life and relatively high elongation capability. However, constantan tends to exhibit a continuous drift at temperatures above 65 °C (149 °F);[5] and this characteristic should be taken into account when zero stability of the strain gauge is critical over a period of hours or days. Constantan is also used for electrical resistance heating and thermocouples.

A-alloy

Very importantly, constantan can be processed for self-temperature compensation to match a wide range of test material coefficients of thermal expansion. A-alloy is supplied in self-temperature-compensation (S-T-C) numbers 00, 03, 05, 06, 09, 13, 15, 18, 30, 40, and 50, for use on test materials with corresponding thermal expansion coefficients, expressed in parts per million by length (or μm/m) per degrees Fahrenheit.

P alloy

For the measurement of very large strains, 5% (50,000 microstrain) or above, annealed constantan (P alloy) is the grid material normally selected. Constantan in this form is very ductile; and, in gauge lengths of 0.125 inches (3.2 mm) and longer, can be strained to >20%. It should be borne in mind, however, that under high cyclic strains the P alloy will exhibit some permanent resistivity change with each cycle, and cause a corresponding zero shift in the strain gauge. Because of this characteristic and the tendency for premature grid failure with repeated straining, P alloy is not ordinarily recommended for cyclic strain applications. P alloy is available with S-T-C numbers of 08 and 40 for use on metals and plastics, respectively.

Physical properties

Property	Value
Electrical resistivity at room temperature[2]	5.00×10^{-7} Ω·m
Temperature coefficient at 20 °C[7]	8 ppm·K^{-1}

Temperature coefficient −55 to 105 °C[2]	±40 ppm·K^{-1}
Curie point[8]	35 K
Density[2]	8.9 × 10^{3} kg/m^{3}
Melting point	1221–1300 °C
Specific heat capacity	390 J/(kg·K)
Thermal conductivity at 23 °C	19.5 W/(m·K)
Linear coefficient of thermal expansion at 25 to 105 °C[2]	14.9×10^{-6} K^{-1}
Tensile strength[2]	455–860 MPa
Elongation at fracture	<45%
Elastic modulus	162 GPa

Temperature measurement

Constantan is also used to form thermocouples with wires made of iron, copper, or chromel. It has an extraordinarily strong negative Seebeck coefficient above 0 degrees Celsius, leading to a good temperature sensitivity.

Chromel

Chromel is an alloy made of approximately 90% nickel and 10% chromium by weight that is used to make the positive conductors of ANSI Type E (chromel-constantan) and K (chromel-alumel) thermocouples. It can be used at temperatures up to 1,100 °C (2,010 °F) in oxidizing atmospheres. Chromel is a registered trademark of Concept Alloys, Inc.

Characteristics and properties of chromel (Ni, 90%; Cr, 10% by weight)

Characteristic	Value
Temperature coefficient	0.00032 K^{-1}
Electrical resistivity	0.706 μΩ m
Mechanical	
Elongation at break	<44%
Izod impact strength	108 J m^{-1}
Modulus of elasticity	186 GPa
Tensile strength	620–780 MPa
Physical	
Density	8.5 g cm^{-3}
Melting point	1420 °C
Thermal	
Coefficient of thermal expansion	12.8×10^{-6} K^{-1} at 20–1000 °C
Maximum use temperature in air	1100 °C
Thermal conductivity	19 W m^{-1} K^{-1} at 23 °C

Chromel A

Chromel A is an alloy containing approximately 80% nickel and 20% chromium (by weight), with low-level quantities of Si (1%), Fe (0.5%), and Ni. It is used for its excellent resistance to high-temperature corrosion and oxidation. It is also commonly called Nichrome 80-20, and is used for electric heating elements.

Chromel C

Chromel C is an alloy containing 60% nickel, 16% chromium and 24% iron. It is also commonly called Nichrome 60 and is used for heating elements, resistance windings, and hot wire cutters.

Chromel-R

Chromel R has a composition of Cr 20%, Ni 80%.

Chromel-R was also produced as a woven fabric of chromel wires. It was developed by Litton Industries for use by NASA in the Gemini and Apollo programs.

The Gemini G4C spacesuit did not use Chromel-R as standard. However the Gemini 9 mission was to test the use of the Astronaut Maneuvering Unit, a free-flying 'rocket pack'. To protect against the hot exhaust of its hydrogen peroxide engine, Gene Cernan's suit was given additional protection with an over-trouser layer of Chromel-R. The spacewalk during this flight gave a number of problems, with Cernan overheating and finding the suit difficult to move in it, with "all the flexibility of a rusty suit of armor".The Chromel-R layer was an integral part of the spacesuit, although the confined Gemini capsule did not require much movement until the spacewalk. Once pressurized, the suit became difficult to move in.

Smaller patches of Chromel-R formed an outer layer of the Apollo spacesuit where abrasion resistance was needed. These patches can be seen as silver-grey areas over the white Beta cloth of the main suit. Using patches, rather than an entire garment, avoided the flexibility problems with Gemini. The upper areas of the overshoes, the gloves and patches beneath the life support backpack were of Chromel-R. Gold-plated open-weave Chromel-R mesh has also been used as the reflecting surface for compact-folding parabolic antenna on spacecraft.

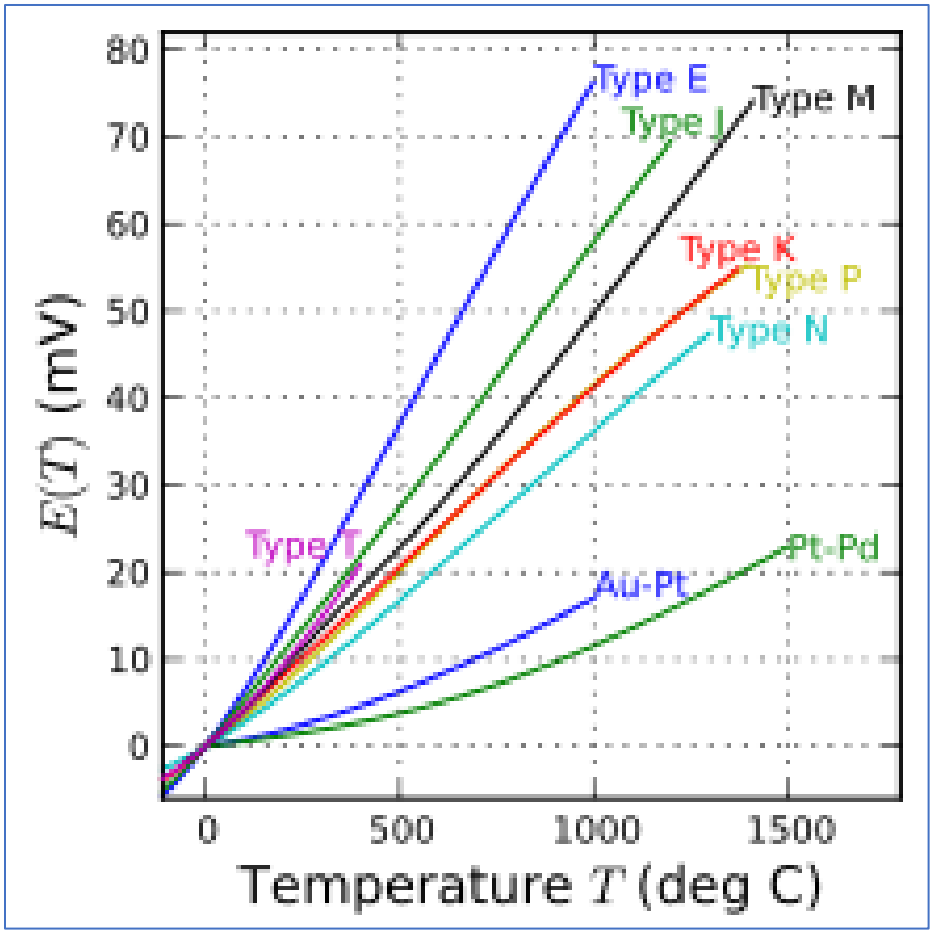

Characteristic functions for nickel alloy thermocouples that reach intermediate temperatures, as covered by nickel-alloy thermocouple types E, J, K, M, N, T. Also shown are the noble-metal alloy type P and the pure noble-metal combinations gold–platinum and platinum–palladium.

Type E

Type E (chromel–constantan) has a high output (68 μV/°C), which makes it well suited to cryogenic use. Additionally, it is non-magnetic. Wide range is −270 °C to +740 °C and narrow range is −110 °C to +140 °C.

Type J

Type J (iron–constantan) has a more restricted range (−40 °C to +1200 °C) than type K but higher sensitivity of about 50 μV/°C. The Curie point of the iron (770 °C) causes a smooth change in the characteristic, which determines the upper temperature limit. Note, the European/German Type L is a variant of the type J, with a different specification for the EMF output (reference DIN 43712:1985-01).

Type K

Type K (chromel–alumel) is the most common general-purpose thermocouple with a sensitivity of approximately 41 μV/°C.[1] It is inexpensive, and a wide variety of probes are available in its −200 °C to +1350 °C (−330 °F to +2460 °F) range. Type K was specified at a time when metallurgy was less advanced than it is today, and consequently characteristics may vary considerably between samples. One of the constituent metals, nickel, is magnetic; a characteristic of thermocouples made with magnetic material is that they undergo a deviation in output when the material reaches its Curie point, which occurs for type K thermocouples at around 185 °C.

They operate very well in oxidizing atmospheres. If, however, a mostly reducing atmosphere (such as hydrogen with a small amount of oxygen) comes into contact with the wires, the chromium in the chromel alloy oxidizes. This reduces the emf output, and the thermocouple reads low. This phenomenon is known as *green rot*, due to the color of the affected alloy. Although not always distinctively green, the chromel wire will develop a mottled silvery skin and become magnetic. An easy way to check for this problem is to see whether the two wires are magnetic (normally, chromel is non-magnetic).

Hydrogen in the atmosphere is the usual cause of green rot. At high temperatures, it can diffuse through solid metals or an intact metal thermowell. Even a sheath of magnesium oxide insulating the thermocouple will not keep the hydrogen out.

Green rot does not occur in atmospheres sufficiently rich in oxygen, or oxygen-free. A sealed thermowell can be filled with inert gas, or an oxygen scavenger (e.g. a sacrificial titanium wire) can be added. Alternatively, additional oxygen can be introduced into the thermowell. Another option is using a different thermocouple type for the low-oxygen atmospheres where green rot can occur; a type N thermocouple is a suitable alternative.

J-TYPE THERMOCOUPLE

The temperature range of J-types is 0-760℃ or 32-1400℉, and they can tolerate heat for up to 1000℃ (2552℉). They degrade rapidly in oxidizing atmospheres above 550°C. Their maximum continuous operating temperature is around 750°C though they can withstand short duration excursions to 1000°C. They are made from Iron and Constantan and are the least expensive thermocouple option in manufacturing. However, they are susceptible to rust, and using them below ambient temperatures shortens their lifespan further.
They are generally not used below ambient temperature due to condensation forming on the wires leading to rusting of the iron. It has a smaller temperature range and a shorter lifespan at higher temperatures than the Type K. Best suited for the plastics industry & general industrial offering cost-effectiveness and reliability.

N-TYPE THERMOCOUPLE

N-types sport an alloy combo of Nicrosil and Nisil. They are more consistent when measuring between 300℃ and 500℃ (572 to 932℉) but are less stable because the thermocouple wires oxidize quickly. With an accuracy and price point that rivals the K-type, the N-type is considered a better alternative to the R and S-types. Perfect for the aerospace and power generation industries, offering superior performance and stability in high-temperature environments especially where thermocouple longevity and resistance to oxidation are required.

K-TYPE THERMOCOUPLE

K-type thermocouples are formed by the Chromel and Alumel combination of metals, with preferred working conditions between 0-1260°C or 32-2300°F. Type K thermocouples are the most widely used thermocouples in the Oil & Gas, and refining industries due to their wide range and low cost. The type K is also commonly used in nuclear applications because of its relative radiation hardness.
While K-types may be accurate, they need recalibration when used for temperatures around and above 750°C. Noble metal types are an alternative if corrosive resistance is the primary concern.
They are occasionally referred to as Chromel-Alumel thermocouples. The type K is the most common type of thermocouple. It's inexpensive, accurate, reliable, and has a wide temperature range.
The most versatile and widely used thermocouple, ideal for the oil & gas and food processing industries providing both durability and accuracy across various applications.

T-TYPE THERMOCOUPLE

T-type thermocouples are very stable and work best between -59°C to 370°C or -75 to +700°F, making them the best bet for use in low-temp lab processes like cryogenics and ultra-low freezers. The T-type is consistent with measurements between -200°C and 200°C and is decomposition-resistant. They are made from Copper and Constantan.

CHOOSING THE RIGHT THERMOCOUPLE

Thermocouples can measure different ranges and might be more accurate within a certain range. It is important to make sure that your application use is within the range before purchasing. The temperature range of the temperature sensor is provided on the datasheet.

Selecting the thermocouple type is not the only consideration. Factors such as sheath materials, time at temperature and degree of accuracy are also critical. Ensuring sufficient immersion length, the sensor should extend into the process a minimum length equal to one-third the inside diameter of the pipe, with the optimal location at the center of the pipe diameter. Design considerations include how the temperature sensor will be connected to the application and how the temperature is going to be measured as these will both affect the choice.

Appendix D. Thermoelectric Power Generation

Bismuth Telluride-based thermoelectric modules are designed primarily for cooling or combined cooling and heating applications where electrical power creates a temperature difference across the module. By using the modules “in reverse,” however, whereby a temperature differential is applied across the faces of the module, it is possible to generate electrical power. Although power output and generation efficiency are very low, useful power often may be obtained where a source of heat is available.

A thermoelectric module used for power generation has certain similarities to a conventional thermocouple. Let us look at a single thermoelectric couple with an applied temperature difference as shown in Figure (D-1)

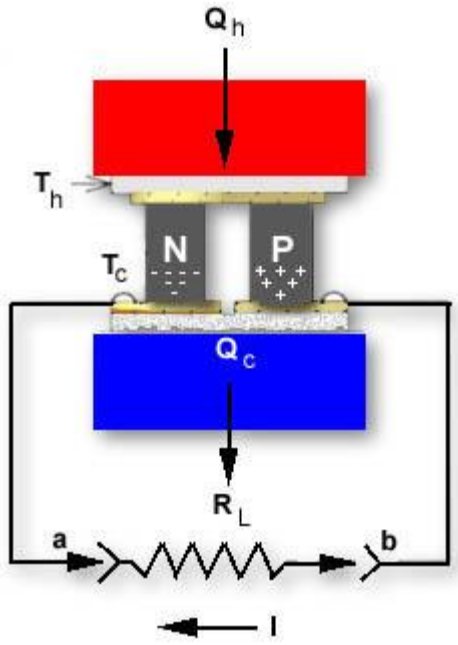

Figure (D-1)

Single Thermoelectric Couple where Th > Tc

With no load (RL not connected), the open circuit voltage as measured between points a and b is:

$$V = S \times DT$$

where:
V = the output voltage from the couple (generator) in volts
S = the average Seebeck coefficient in volts/°K
DT = the temperature difference across the couple in K where DT = Th-Tc
When a load is connected to the thermoelectric couple the output voltage (V) drops as a result of internal generator resistance. The current through the load is:

$$I = \frac{S \times DT}{R_c + R_L}$$

where:

I = the generator output current in amperes
R_c = the average internal resistance of the thermoelectric couple in ohms
R_L = the load resistance in ohms
The total heat input to the couple (Q_h) is:

$$Q_h = (S \times T_h \times I) - (0.5 \times I^2 \times R_c) + (K_c \times DT)$$

Where:
Q_h = the heat input in watts
K_c = the thermal conductance of the couple in watts/°K
T_h = the hot side of the couple in °K
The efficiency of the generator (E_g) is:

$$E_g = \frac{V \times I}{Q_h}$$

We have thus far discussed an individual thermoelectric couple, but since a complete module consists of several couples, it is necessary to rewrite our equation for an actual module, as follows:

$$V_o = S_M \times DT = I \times (R_M + R_L)$$

where:
V_o = the generators output in volts
S_M = the module's average Seebeck coefficient in volts/°K
R_M = the module's average resistance in ohms

It must be remembered that module Seebeck coefficient, resistance and thermal conductance properties are temperature dependent and their values must be calculated as described in Section 11, paragraphs 11.2 through 11.2.4. The values of S_M, R_M, and K_M must be selected at the average module temperature T_{avg}
Where:

$$T_{avg} = \frac{T_h + T_c}{2}$$

The power output (P_o) from the module in watts is:

$$P_o = R_L \times$$

It is possible, but unlikely, that the precise conditions will exist within a given generator application whereby one module will provide the exact output power desired. As a result, most thermoelectric generators contain several individual modules which may be electrically connected in either series, parallel, or series/parallel arrangement. A typical generator configuration is illustrated in Figure (13.2). This generator has a NT total number of modules with NS number of modules connected in series and NP number of modules connected in parallel. The total number of modules in the system is:

$$NT = NS \times NP$$

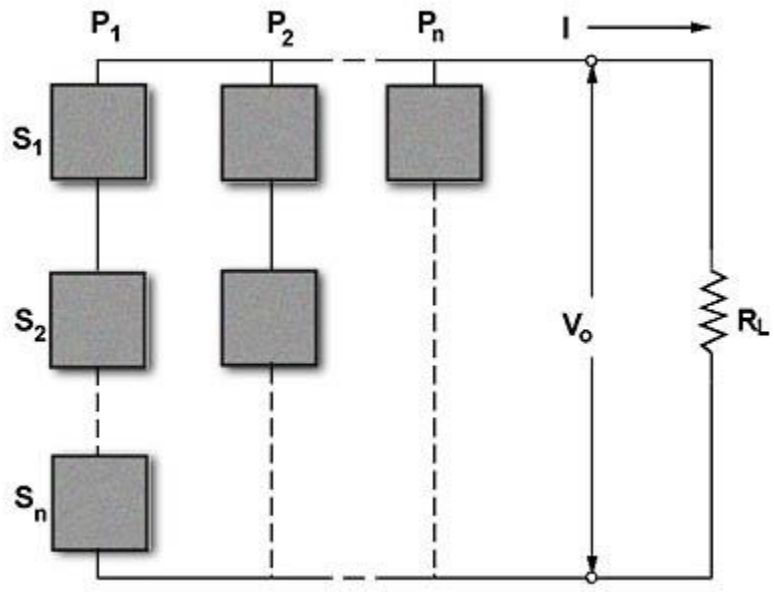

Figure (D-2)

Typical Thermoelectric Generator with a Series-Parallel Arrangement of Modules

The current (I) in amperes passing through the load resistance R_L is:

$$I = \frac{NS \times S_M \times DT}{\frac{NS \times R_M}{NP} + R_L}$$

The output voltage (V_o) from the generator in volts is:

TBD

The Output Power (P_o) from the generator in watts is:

$$\mathbf{P_o = V_o \times I} = \frac{NT \times (S_M \times DT)^2}{4 \times R_M}$$

.

The total heat input (Qh) to the generator in watts is:

TBD

The efficiency (E_g) of the generator is:

$$E_g = \frac{P_o}{Qh} \times 100\%$$

Maximum efficiency occurs when the internal resistance of the generator (R_{GEN}) equals the load resistance (R_L). The generator resistance is:

$$R_{GEN} = \frac{NS \times R_M}{NP}.$$

DESIGN EXAMPLE: To illustrate the typical design process let us analyze a requirement for a 12-volt, 1.5 ampere thermoelectric power generator. The generator is needed to power telemetry electronics at a remotely located oil pipeline where the hot, continuously flowing oil produces a 130 C pipe casing temperature. Flowing water (having a temperature of 10°C) also is available at the remote site, and it has been determined that an efficient water-cooled heat sink can maintain the TE generator cold-side at a temperature of +30 C. We will use the equations from Section 11 to obtain the values of SM, RM and KM for our calculations.

To begin the design process, we will review the system parameters and make some preliminary calculations.

Given:
T_h = + 130°C = 403.2°K
T_c = + 30°C = 303.2°K
V_o = 12 volts
I = 1.5 amperes
Therefor:
$T_{av} = (T_h+T_c)/2 = (403.2+303.2)/2 = 353.2°K$
$R_L = V_o/I = 12 / 1.5 = 8.0$ ohms
$P_o = V_o \times I = 12 \times 1.5 = 18$ watts
$DT = T_h-T_c = 403.2 – 303.2 = 100°K$
It is usually desirable to select a relatively “high power” thermoelectric module for generator applications to minimize the total system cost. For this reason, we will choose a 127 couple, 6-ampere module to be used in our design.

Calculating SM, RM, and KM for our selected 127-couple, 6-ampere module, the following values are obtained at Tav = 353.2°K:

S_M = 0.05544 volts/°K
R_M = 3.0994 ohms
K_M = 0.6632 watts/°K

The required power for the load has been calculated as 18 watts. It is now necessary to determine the minimum number of modules needed to meet this load requirement. The maximum output power from one module is:

$$P_{max} = \frac{(S_M \times DT)^2}{4 \times R_M} = \frac{(0.05544 \times 100)^2}{4 \times 3.0994} = 2.479 \text{ watts}$$

The minimum number of modules needed is:

$$NT_{min} = \frac{P_o}{P_{max}} = \frac{18}{2.479} = 7.3 \approx 8$$

Because maximum generator efficiency occurs when $R_{GEN} = R_L$, it is desirable for most applications to select the series/parallel module configuration that will best approximate this resistance balance. One possible exception to the equalizing R_{GEN} with R_L is in the situation where a relatively low current

(in the milliampere range) and moderate voltage is required. In this case, the connection of all modules electrically in series may give the best results. Be aware, however that the maximum output voltage from the generator will be obtained from a straight series-connected group of modules only when the resistance of the load is significantly higher than the internal resistance of the generator.

As a starting point in the evaluation of any thermoelectric power generator, it is often helpful to first examine the straight series-connected configuration. The resistance of a series string of eight modules is:

$$R_{GEN} = \frac{NS \times R_M}{NP} = \frac{8 \times 3.0994}{1} = 24.8 \text{ ohms}$$

It can be seen that the 24.8-ohm generator resistance is considerably higher than the 8.0-ohm load resistance, thereby indicating that a straight series module connection probably is not the best arrangement. For the all-series condition where NS = 8 and NP = 1, the output voltage is:

With a group of eight modules, the next most logical connection configuration is two parallel strings of four modules, i.e., NS = 4 and NP = 2. Generator resistance for this configuration is thus:

$$R_{GEN} = \frac{NS \times R_M}{NP} = \frac{4 \times 3.0994}{2} = 6.2 \text{ ohms}$$

While 6.2-ohm R_{GEN} value does not exactly match the 8.0-ohm load resistance, this value normally would be considered as being within the satisfactory range. In any event, this is the closest resistance match that can be obtained with the selected module type. The voltage for this arrangement (12.49 volts) is calculated as follows:

We can now see that Vo is quite close to the desired value and it is apparent that we have obtained the optimum series/parallel configuration. If “fine tuning” of Vo is required, it will be necessary to accomplish this either by some form of electronic voltage regulation or by externally altering the applied temperature differential (DT). In certain instances, it will be found that the output voltage is significantly out of range despite trying all possible series/parallel combinations. In this event it may be necessary to use an alternate thermoelectric module having a different current rating and/or number of couples.

It is now possible to complete our design analysis by determining power levels and efficiency. Since we have established Vo, output power (Po) can be simply calculated:

$$P_o = \frac{(V_o)^2}{RL} = \frac{(12.49)^2}{8.0} = 19.5 \text{ watts}$$

The total heat input (Qh) to the generator is:

$$Q_h = (S \times T_h \times I) - (0.5 \times I^2 \times R_c) + (K_c \times DT)$$

where:
Q_h = the heat input in watts
K_c = the thermal conductance of the couple in watts/°K
T_h = the hot side of the couple in °K

The generator efficiency (Eg) is:

$$E_g = \frac{P_o}{Q_h} \times 100\% = \frac{19.5}{657.5} \times 100\% = 2.97\%$$

The heat transferred to the cold-side heat sink (Qc) is:

$$Q_c = Q_h - P_o = 657.7 - 19.5 = 638.2 \text{ watts}$$

The maximum allowable thermal resistance (Qs) of the cold-side heat sink is:

$$(Qs) = \frac{T_{rise}}{Q_c} = \frac{30°C - 10°C}{638.2} = 0.031 \text{ °C/watt}$$

For any thermoelectric generator design, it is always desirable to maximize the applied temperature differential to minimize the total number of modules in the system. This situation can be clearly seen in Figure (13.3). Module requirements for a typical 12-volt, 1-ampere power generator are plotted at several fixed values of Th based on the use of 127-couple 6-ampere TE modules. From this graph, it is evident that a very large number of modules is needed when the cold side temperature (Tc) is high and the temperature differential, therefore, is small. Performance of the cold-side heat sink is of the utmost importance and its thermal resistance must be extremely low. In many cases, cold-side heat sink design will prove to be the most challenging engineering problem.

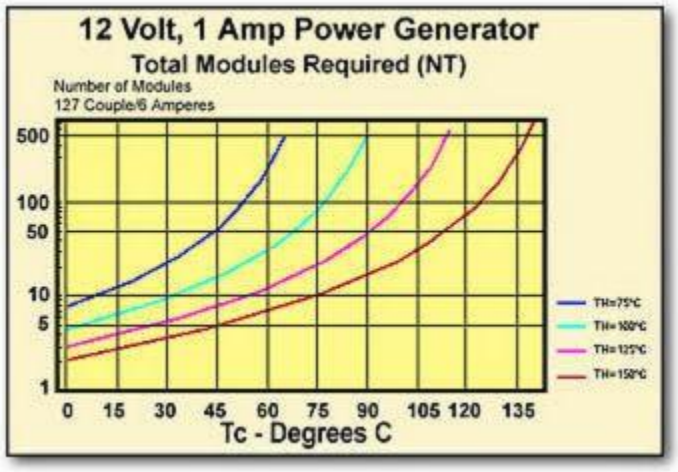

Figure (D-3)

The Total Number of 127-Couple, 6-Amp Modules Required for a 12-volt, 1 Ampere Thermoelectric Power Generator

USE OF THERMOELECTRIC MODULES IN A CALORIMETER: A lesser, yet viable, application for thermoelectric modules operating in the power generation mode is in the construction of calorimeters. The conventional calorimeter uses common thermocouples for heat measurement based solely on the Seebeck effect. Using a multi-couple thermoelectric cooling module, it is possible to fabricate a calorimeter having a sensitivity (output voltage per unit of heat flux density) as much as 10 to 200 times the sensitivity of a standard copper-constantan thermocouple. When used in a calorimeter application, the thermoelectric module is often referred to as a thermopile. The

open-circuit output voltage (V) of a single thermoelectric couple, as described in paragraph 13.2 and illustrated in Figure (13.1), is:

$$V = S \times DT$$

where:
V = the output voltage from the couple in volts
S = the average Seebeck coefficient in volts/°K
DT = the temperature difference across the couple in °K where DT=Th-Tc
For an actual TE module having several couples and a Seebeck coefficient of SM, the output voltage (Vo) is:

$$V_o = S_M \times DT$$

The heat flow through the TE or “thermopile” is:

$$Q = K_M \times DT = \frac{K_M \times V_o}{S_M}$$

where:
Q = the heat flow in watts
KM = the thermal conductance of the module in watts/°K
The total cross-sectional area (AM) of all elements in the module is:

$A_M = A \times N$

Where:
AM = total area of all module elements in cm^2
A = cross-sectional area of one element in cm^2
N = total number of elements in the module

The heat flux density (q) in watts/cm^2 is:

$$q = \frac{K_M \times DT}{A_M} = \frac{K_M \times V_o}{S_M \times A_M}$$

Most standard thermoelectric cooling modules may be used in a calorimeter application but improved sensitivity may be realized by modifying the length-to-area (L/A) aspect ratio of the TE elements. A relatively large L/A ratio resulting in a tall and “skinny” element will produce the best calorimeter sensitivity. To illustrate this situation let us consider the following:

The sensitivity of a module as a calorimeter (Sc) is:

$$S_c = \frac{V_o}{q} = \frac{S_M \times A_M}{K_M}$$

It has been seen that sensitivity (Sc) is directly proportional to the Seebeck coefficient (SM) and total cross-sectional element area (AM) and inversely proportional to the thermal conductance (KM). By rewriting the above equation in respect to thermal conductivity (k) instead of thermal conductance (KM) we have:

$$S_c = \frac{S_M \times A_M}{k \times N \times A/L}$$

Since N x A = AM, the expression can be restated as:

$$S_c = \frac{S_M \times L}{k}$$

From this equation, it is evident that calorimeter sensitivity is directly related to the length (L) dimension of an element and it is desirable, therefore, to select a thermoelectric module having the largest possible element aspect ratio. Be aware that there are practical limits on element geometry due to the fragility of crystalline Bismuth telluride material. Working within these limits, however, it is possible to fabricate custom modules that are particularly suited for calorimeter use.

Appendix E. Metal Properties

Periodic Table

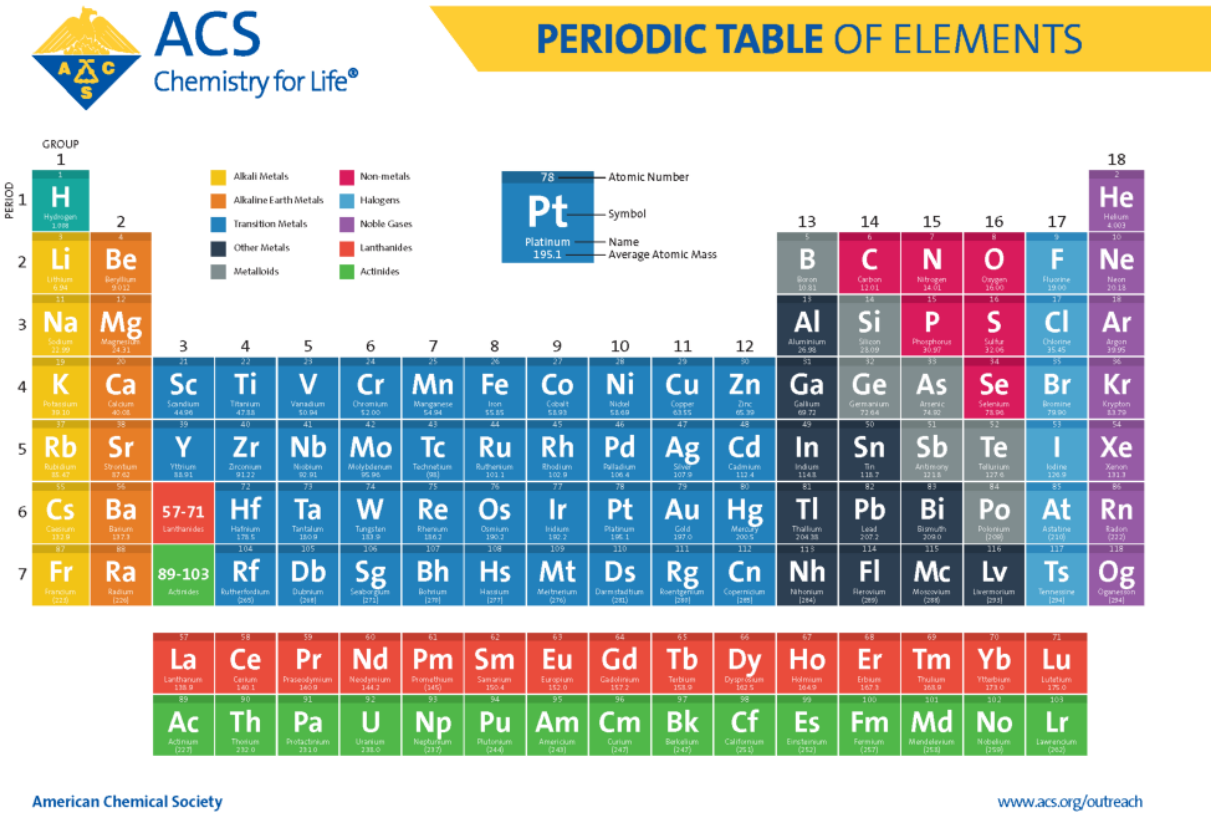

In solid-state physics, the **electronic band structure** (or simply **band structure**) of a solid describes the range of energy levels that electrons may have within it, as well as the ranges of energy that they may not have (called *band gaps* or *forbidden bands*).

Band theory derives these bands and band gaps by examining the allowed quantum mechanical wave functions for an electron in a large, periodic lattice of atoms or molecules. Band theory has been successfully used to explain many physical properties of solids, such as electrical resistivity and optical absorption, and forms the foundation of the understanding of all solid-state devices (transistors, solar cells, etc.).

Copper Types and Designations

Copper UNS No.[A]	Previous Designation	Type of Copper
C10100[B]	OFE	Oxygen-free electronic
C10200[B]	OF	Oxygen-free without residual deoxidants
C10300	OFXLP	Oxygen-free extra low phosphorus
C10400, C10500, C10700	OFS	Oxygen-free, silver bearing
C10800	OFLP	Oxygen-free low phosphorus
C10910	...	Low oxygen
C11000[B, C]	ETP, TP[C]	Electrolytic tough pitch,[C] Tough pitch[C]
C11300, C11400, C11600[B]	STP	Silver bearing tough pitch
C12000	DLP	Phosphorized, low residual phosphorus
C12200[B]	DHP	Phosphorized, high residual phosphorus
C12300	DHPS	Phosphorized, silver bearing
C14200	DPA	Phosphorus deoxidized, arsenical
C14420	...	Tin bearing tellurium copper
C14530	...	Tin tellurium bearing copper

Copper Wire Sizes

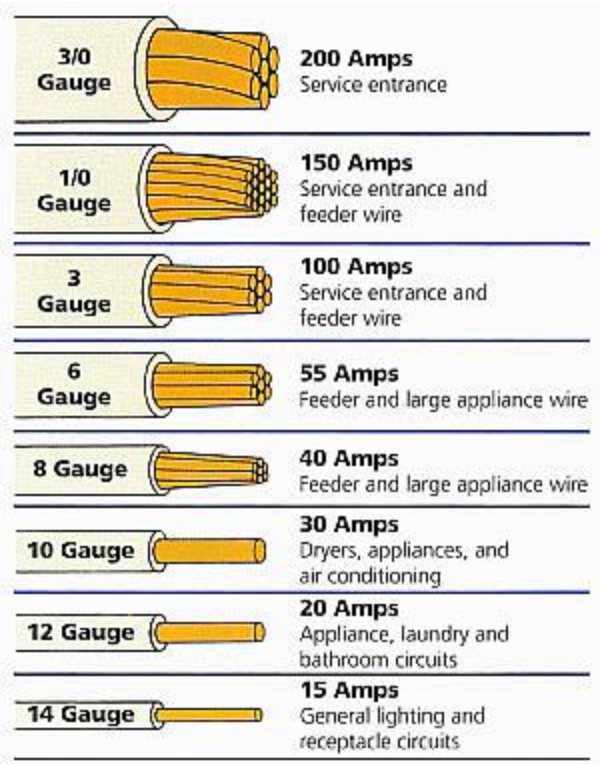

American wire gauges (AWG) are a standard set of sizes for wire conductors — the smaller the wire gauge, the larger the diameter in inches or millimeters, and vice versa. Refer to this American wire gauge conversion chart to help determine the correct wire size to order.

Gauge No.	Inches	Millimeters
7/0	0.651300	16.54
6/0	0.580049	14.73
5/0	0.516549	13.12
4/0	0.460000	11.68
3/0	0.409642	10.40
2/0	0.364797	9.266
1/0	0.324861	8.251
1	0.289297	7.348
2	0.257626	6.544
3	0.229423	5.827
4	0.204307	5.189
5	0.181941	4.621
6	0.162023	4.115
7	0.144285	3.665
8	0.128490	3.264
9	0.114424	2.906
10	0.101897	2.588

11	0.090742	2.305
12	0.080808	2.053
13	0.071962	1.828
14	0.064084	1.628
15	0.057068	1.450
16	0.050821	1.291
17	0.045257	1.150
18	0.040303	1.024
19	0.035891	0.9116
20	0.031961	0.8118
21	0.028462	0.7229
22	0.025347	0.6438
23	0.022572	0.5733
24	0.020101	0.5106
25	0.017900	0.4547
26	0.015941	0.4049
27	0.014196	0.3606
28	0.012641	0.3211
29	0.011258	0.2860
30	0.010025	0.2546
31	0.008928	0.2268
32	0.007950	0.2019
33	0.007080	0.1798
34	0.006305	0.1601
35	0.005615	0.1426
36	0.005000	0.1270
37	0.004453	0.1131
38	0.003965	0.1007
39	0.003531	0.08969
40	0.003145	0.07988
41	0.002800	0.07112
42	0.002494	0.06335
43	0.002221	0.05641
44	0.001978	0.05024
45	0.001761	0.04473
46	0.001568	0.03983
47	0.001397	0.03548
48	0.001244	0.03160
49	0.001108	0.02814
50	0.000986	0.02504
51	0.000878	0.02230
52	0.000782	0.01986
53	0.000697	0.01770
54	0.000620	0.01575
55	0.000552	0.01402
56	0.000492	0.01250

57	0.000438	0.01113
58	0.000390	0.00991
59	0.000347	0.00881
60	0.000309	0.00785

Specific Heat

Substance	Specific Heat or Heat Capacity
Water (liquid)	4.184 J/g ° C (1.000 cal/ g ° C)
Aluminum (solid)	0.900 J/g ° C (0.215 cal/ g ° C)
Copper (solid)	0.385 J/g ° C (0.092 cal/ g ° C)
Constantan(solid)	0.393 J/g ° C
Iron (solid)	0.442 J/g ° C (0.106 cal/ g ° C)
Water (solid) also called ice	2.089 J/g ° C (0.499 cal/ g ° C)

Sample Problem: How much energy is required to raise a cup of water (250 grams) 50 ° C?

Use the equation

$$E = m \times SH \times \Delta T$$

Where m is mass in grams, SH is the specific heat and ΔT is the change in temperature.

$$E = 250 grams \times 4.184 \frac{J}{g^{\circ}C} \times 50^{\circ}C = 52{,}300 J = 52.3 kJ$$

Note: A watt is the SI unit of power, equivalent to one joule per second, corresponding to the power in an electric circuit in which the potential difference is one volt and the current is one ampere.

Thermal Conductivity

The thermal conductivity of pure copper is 401 W/(m·K) (watts per meter kelvin). The thermal conductivity of constantan is 19.5 W/(m·K)

Density

At room temperature, the density of copper is 8.96 g/cm^3. The density of constantan is 8.885 g/cm^3. One gram = 0.00220462 pounds.

Appendix F. Heat Conduction and Conductivity

As you walk barefoot across the living room carpet in a cold house and then step onto the kitchen tile floor, your feet feel colder on the tile. This result is intriguing, since the carpet and tile floor are both at the same temperature. The different sensation is explained by the different rates of heat transfer: The heat loss is faster for skin in contact with the tiles than with the carpet, so the sensation of cold is more intense.

Some materials conduct thermal energy faster than others. Figure 1.20 shows a material that conducts heat slowly—it is a good thermal insulator, or poor heat conductor—used to reduce heat flow into and out of a house.

A molecular picture of heat conduction will help justify the equation that describes it. Figure 1.21 shows molecules in two bodies at different temperatures, T_hTh and T_cTc, for "hot" and "cold." The average kinetic energy of a molecule in the hot body is higher than in the colder body. If two molecules collide, energy transfers from the high-energy to the low-energy molecule. In a metal, the picture would also include free valence electrons colliding with each other and with atoms, likewise transferring energy. The cumulative effect of all collisions is a net flux of heat from the hotter body to the colder body. Thus, the rate of heat transfer increases with increasing temperature difference $\Delta T = T_h - T_c$ΔT=Th−Tc. If the temperatures are the same, the net heat transfer rate is zero. Because the number of collisions increases with the increasing area, heat conduction is proportional to the cross-sectional area—a second factor in the equation.

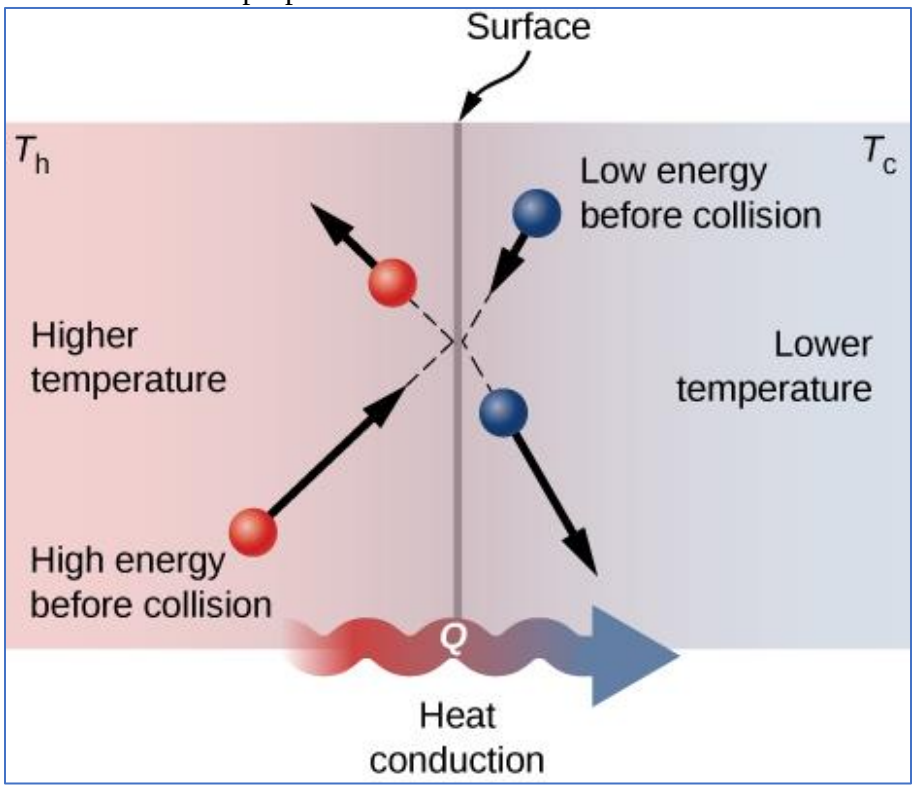

Figure 1.21 *Molecules in two bodies at different temperatures have different average kinetic energies. Collisions occurring at the contact surface tend to transfer energy*

from high-temperature regions to low-temperature regions. In this illustration, a molecule in the lower-temperature region (right side) has low energy before collision, but its energy increases after colliding with a high-energy molecule at the contact surface. In contrast, a molecule in the higher-temperature region (left side) has high energy before collision, but its energy decreases after colliding with a low-energy molecule at the contact surface.

A third quantity that affects the conduction rate is the thickness of the material through which heat transfers. Figure 1.22 shows a slab of material with a higher temperature on the left than on the right. Heat transfers from the left to the right by a series of molecular collisions. The greater the distance between hot and cold, the more time the material takes to transfer the same amount of heat.

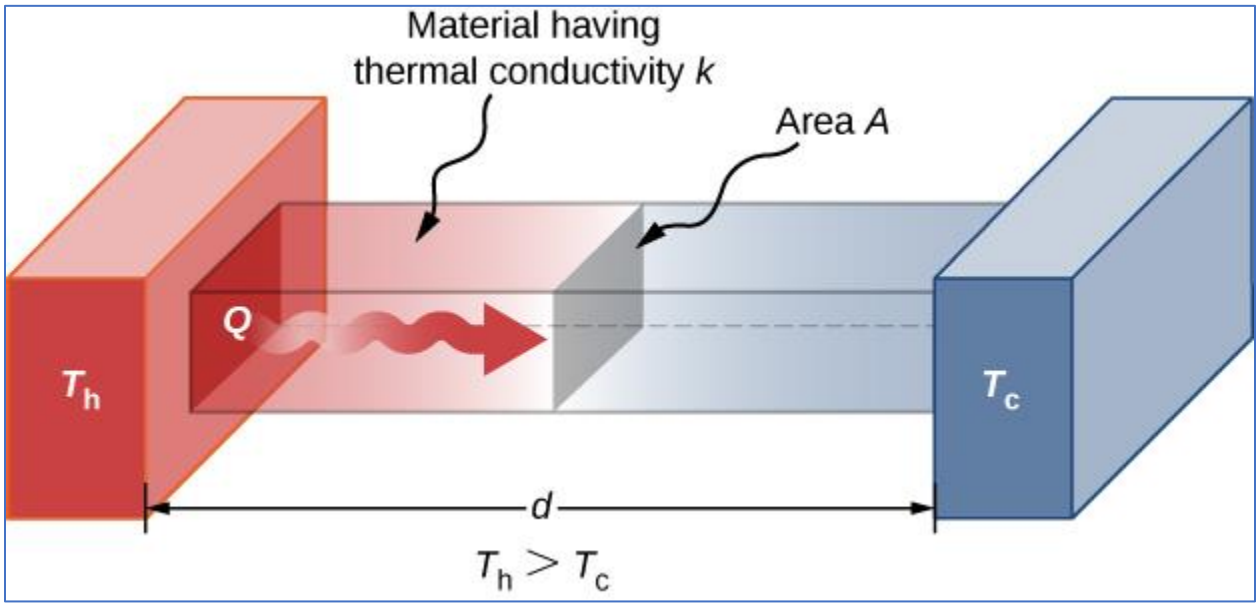

Figure 1.22 *Heat conduction occurs through any material, represented here by a rectangular bar, whether window glass or walrus blubber.*

All four of these quantities appear in a simple equation deduced from and confirmed by experiments. The **rate of conductive heat transfer** through a slab of material, such as the one in Figure 1.22, is given by

$$P=\frac{dQ}{dt}=\frac{kA(T_h-T_c)}{d} \quad (1.9)$$

where P is the power or rate of heat transfer in watts or in kilocalories per second, A and d are its surface area and thickness, as shown in Figure 1.22, $T_h - T_c$ is the temperature difference across the slab, and k is the **thermal conductivity** of the material. Table 1.5 gives representative values of thermal conductivity.

More generally, we can write

$$P=-kA\frac{dT}{dx},$$

where x is the coordinate in the direction of heat flow. Since in Figure 1.22, the power and area are constant, dT/dx is constant, and the temperature decreases linearly from T_hTh to T_cTc.

Table 1.5 Thermal Conductivities of Common Substances. Values are given for temperatures near 0∘C0∘C.

Substance	Thermal Conductivity k (W/m·∘CW/m·∘C)
Diamond	2000
Silver	420
Copper	390
Gold	318
Aluminum	220
Steel iron	80
Steel (stainless)	14
Ice	2.2
Glass (average)	0.84
Concrete Brick	0.84
Water	0.6
Fatty tissue (without blood)	0.2
Asbestos	0.16
Plasterboard	0.16
Wood	0.08–0.16
Snow (dry)	0.10

Cork	0.042
Glass wool	0.042
Wool	0.04
Down feathers	0.025
Air	0.023
Polystyrene foam	0.010

Example 1.10

Calculating Heat Transfer through Conduction

A polystyrene foam icebox has a total area of $0.950 m^2 0.950 m2$ and walls with an average thickness of 2.50 cm. The box contains ice, water, and canned beverages at $0^\circ C 0 \circ C$. The inside of the box is kept cold by melting ice. How much ice melts in one day if the icebox is kept in the trunk of a car at $35.0^\circ C 35.0 \circ C$?

Strategy

This question involves both heat for a phase change (melting of ice) and the transfer of heat by conduction. To find the amount of ice melted, we must find the net heat transferred. This value can be obtained by calculating the rate of heat transfer by conduction and multiplying by time.

Solution

First we identify the knowns.

$k = 0.010 W/m \cdot^\circ C k = 0.010 W/m \cdot \circ C$ for polystyrene foam; $A = 0.950 m^2 A = 0.950 m2$; $d = 2.50 cm = 0.0250 m d = 2.50 cm = 0.0250 m$; $T_c = 0^\circ C Tc = 0 \circ C$; $T_h = 35.0^\circ C Th = 35.0 \circ C$; $t = 1 day = 24 hours - 86{,}400 s. t = 1 day = 24 hours - 86{,}400 s.$

Then we identify the unknowns. We need to solve for the mass of the ice, m. We also need to solve for the net heat transferred to melt the ice, Q. The rate of heat transfer by conduction is given by

$$P = \frac{dQ}{dt} = \frac{kA(T_h - T_c)}{d}. P = \frac{dQ}{dt} = \frac{kA(Th - Tc)}{d}.$$

The heat used to melt the ice is $Q = mL_f Q = mLf$. We insert the known values:

$$P = \frac{(0.010 W/m \cdot^\circ C)(0.950 m^2)(35.0^\circ C - 0^\circ C)}{0.0250 m} = 13.3 W. P = \frac{(0.010 W/m \cdot \circ C)(0.950 m2)(35.0 \circ C - 0 \circ C)}{0.0250 m} = 13.3 W.$$

Multiplying the rate of heat transfer by the time we obtain

$$Q = Pt = (13.3 W)(86.400 s) = 1.15 \times 10^6 J. Q = Pt = (13.3 W)(86.400 s) = 1.15 \times 106 J.$$

We set this equal to the heat transferred to melt the ice, $Q = mL_f Q = mLf$, and solve for the mass *m*:

$$m = \frac{Q}{L_f} = \frac{1.15 \times 10^6 J}{334 \times 10^3 J/kg} = 3.44 kg. m = \frac{Q}{Lf} = \frac{1.15 \times 106 J}{334 \times 103 J/kg} = 3.44 kg.$$

Significance
The result of 3.44 kg, or about 7.6 lb, seems about right, based on experience. You might expect to use about a 4 kg (7–10 lb) bag of ice per day. A little extra ice is required if you add any warm food or beverages.

Table 1.5 shows that polystyrene foam is a very poor conductor and thus a good insulator. Other good insulators include fiberglass, wool, and goose down feathers. Like polystyrene foam, these all contain many small pockets of air, taking advantage of air's poor thermal conductivity.

In developing insulation, the smaller the conductivity k and the larger the thickness *d*, the better. Thus, the ratio *d/k*, called the *R factor*, is large for a good insulator. The rate of conductive heat transfer is inversely proportional to *R*. *R* factors are most quoted for household insulation, refrigerators, and the like. Unfortunately, in the United States, *R* is still in non-metric units of $\text{ft}^2 \cdot {}^\circ\text{F} \cdot \text{h/Btu}$ft2·∘F·h/Btu, although the unit usually goes unstated [1 British thermal unit (Btu) is the amount of energy needed to change the temperature of 1.0 lb of water by $1.0 {}^\circ\text{F}$1.0∘F, which is 1055.1 J]. A couple of representative values are an *R* factor of 11 for 3.5-inch-thick fiberglass batts (pieces) of insulation and an *R* factor of 19 for 6.5-inch-thick fiberglass batts (Figure 1.23). In the US, walls are usually insulated with 3.5-inch batts, whereas ceilings are usually insulated with 6.5-inch batts. In cold climates, thicker batts may be used.

Note that in Table 1.5, most of the best thermal conductors—silver, copper, gold, and aluminum—are also the best electrical conductors, because they contain many free electrons that can transport thermal energy. (Diamond, an electrical insulator, conducts heat by atomic vibrations.) Cooking utensils are typically made from good conductors, but the handles of those used on the stove are made from good insulators (bad conductors).

Example 1.11

Two Conductors End to End
A steel rod and an aluminum rod, each of diameter 1.00 cm and length 25.0 cm, are welded end to end. One end of the steel rod is placed in a large tank of boiling water at $100 {}^\circ\text{C}$100∘C, while the far end of the aluminum rod is placed in a large tank of water at $20 {}^\circ\text{C}$20∘C. The rods are insulated so that no heat escapes from their surfaces. What is the temperature at the joint, and what is the rate of heat conduction through this composite rod?

Strategy
The heat that enters the steel rod from the boiling water has no place to go but through the steel rod, then through the aluminum rod, to the cold water. Therefore, we can equate the rate of conduction through the steel to the rate of conduction through the aluminum.

We repeat the calculation with a second method, in which we use the thermal resistance R of the rod, since it simply adds when two rods are joined end to end. (We will use a similar method in the chapter on direct-current circuits.)

Solution

1. Identify the knowns and convert them to SI units.
   The length of each rod is $L_{A1} = L_{\text{steel}} = 0.25 \text{m}$LA1=Lsteel=0.25m, the cross-sectional area of each rod

is $A_{A1}=A_{steel}=7.85\times10^{-5}m^2$AA1=Asteel=7.85×10−5m2, the thermal conductivity of aluminum is $k_{A1}=220W/m\cdot{}^\circ C$kA1=220W/m·◦C, the thermal conductivity of steel is $k_{steel}=80W/m\cdot{}^\circ C$ksteel=80W/m·◦C, the temperature at the hot end is $T=100^\circ C$T=100◦C, and the temperature at the cold end is $T=20^\circ C$T=20◦C.

2. Calculate the heat-conduction rate through the steel rod and the heat-conduction rate through the aluminum rod in terms of the unknown temperature T at the joint:

$P_{steel}=k_{steel}A_{steel}\Delta T_{steel}L_{steel}=(80W/m\cdot{}^\circ C)(7.85\times10^{-5}m^2)(100^\circ C-T)0.25m=(0.0251W/^\circ C)(100^\circ C-T)$;Psteel=ksteelAsteelΔTsteelLsteel=(80W/m·◦C)(7.85×10−5m2)(100◦C−T)0.25m=(0.0251W/◦C)(100◦C−T);

$P_{A1}=k_{Al}A_{A1}\Delta T_{Al}L_{A1}=(220W/m\cdot{}^\circ C)(7.85\times10^{-5}m^2)(T-20^\circ C)0.25m=(0.0691W/^\circ C)(T-20^\circ C)$.PA1=kAlAA1ΔTAlLA1=(220W/m·◦C)(7.85×10−5m2)(T−20◦C)0.25m=(0.0691W/◦C)(T−20◦C).

3. Set the two rates equal and solve for the unknown temperature:

$(0.0691W/^\circ C)(T-20^\circ C)=(0.0251W/^\circ C)(100^\circ C-T)T=41.3^\circ C$.(0.0691W/◦C)(T−20◦C)=(0.0251W/◦C)(100◦C−T)T=41.3◦C.

4. Calculate either rate:

$P_{steel}=(0.0251W/^\circ C)(100^\circ C-41.3^\circ C)=1.47W$.Psteel=(0.0251W/◦C)(100◦C−41.3◦C)=1.47W.

5. If desired, check your answer by calculating the other rate.

Solution

1. Recall that $R=L/k$R=L/k.
   Now $P=A\Delta T/R$P=AΔT/R,or $\Delta T=PR/A$ΔT=PR/A.
2. We know that $\Delta T_{steel}+\Delta T_{Al}=100^\circ C-20^\circ C=80^\circ C$ΔTsteel+ΔTAl=100◦C−20◦C=80◦C. We also know that $P_{steel}=P_{Al}$Psteel=PAl, and we denote that rate of heat flow by *P*. Combine the equations:
   $PR_{steel}A+PR_{Al}A=80^\circ C$.PRsteelA+PRAlA=80◦C.
   Thus, we can simply add *R* factors.
   Now, $P=\frac{80^\circ CA}{(R_{steel}+R_{Al})}$P=80◦CA(Rsteel+RAl).
3. Find the R_sRs from the known quantities:
   $R_{steel}=3.13\times10^{-3}m^2\cdot{}^\circ C/W$Rsteel=3.13×10−3m2·◦C/W
   and
   $R_{Al}=1.14\times10^{-3}m^2\cdot{}^\circ C/W$RAl=1.14×10−3m2·◦C/W
4. Substitute these values in to find $P=1.47W$P=1.47W as before.

5. Determine ΔT for the aluminum rod (or for the steel rod) and use it to find T at the joint.
   $\Delta T_{Al} = PR_{Al}A = (1.47 W)(1.14 \times 10^{-3} m^2 \cdot {}^\circ C/W)7.85 \times 10^{-5} m^2 = 21.3 {}^\circ C, \Delta TAl = PRAlA = (1.47 W)(1.14 \times 10-3m2 \cdot {}^\circ C/W)7.85 \times 10-5m2 = 21.3 {}^\circ C,$
   so $T = 20 {}^\circ C + 21.3 {}^\circ C = 41.3 {}^\circ C T = 20 {}^\circ C + 21.3 {}^\circ C = 41.3 {}^\circ C$, as in Solution 1.
6. If desired, check by determining ΔT for the other rod.

Significance
In practice, adding *R* values is common, as in calculating the *R* value of an insulated wall. In the analogous situation in electronics, the resistance corresponds to *AR* in this problem and is additive even when the areas are unequal, as is common in electronics. Our equation for heat conduction can be used only when the areas are equal; otherwise, we would have a problem in three-dimensional heat flow, which is beyond our scope.

Check Your Understanding 1.7

How does the rate of heat transfer by conduction change when all spatial dimensions are doubled?

Conduction is caused by the random motion of atoms and molecules. As such, it is an ineffective mechanism for heat transport over macroscopic distances and short times. For example, the temperature on Earth would be unbearably cold during the night and extremely hot during the day if heat transport in the atmosphere were only through conduction. Also, car engines would overheat unless there was a more efficient way to remove excess heat from the pistons. The next module discusses the important heat-transfer mechanism in such situations.

Heat Conduction in One Dimension


By Jitender Singh on Dec 21, 2019

In general, the temperature at a point (x) varies with time (t) i.e., it is a function $T(x,t) T(x,t)$. In the steady state, the temperature depends on x but not on time t i.e., $T(x,t) = T(x) T(x,t) = T(x)$. In this state, the heat that reaches any cross-section is transmitted to the next without accumulation. The discussion in this article is limited conduction heat transfer in the steady state.

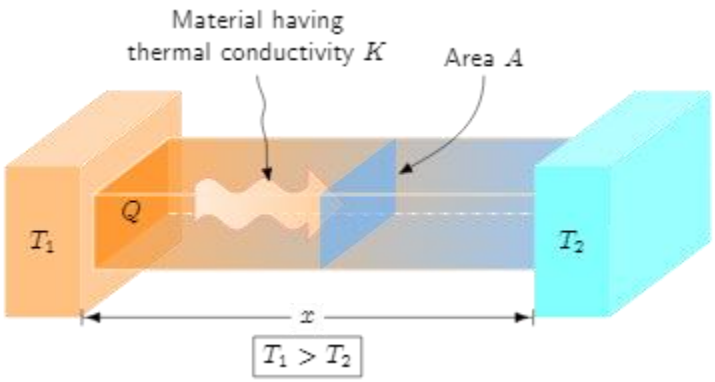

The rate of heat transfer through a rod of length x and cross-section area A whose two ends are maintained at a temperature T_1 and T_2 is given by

$$\frac{dQ}{dt} = \mathbf{K}Ax(T_1 - T_2)$$

where K is the thermal conductivity of the material of the rod.

The SI unit of thermal conductivity is W/(m-K). The dimensional formula of the thermal conductivity is $MLT^{-3}K^{-1}$. Note that heat is transferred from the end at higher temperature T_1 to the end at the lower temperature T_2.

The quantity dQ/dt is also called heat current or the rate of flow of heat. The quantity $(T_1 - T_2)/x$ (and its differential form dT/dx) is called temperature gradient. The thermal resistance of a body is defined as the ratio of temperature difference to the heat current

$$R = \frac{\Delta T}{dQ/dt} = \frac{x}{KA}.$$

In electrical circuits, equivalents of heat current, temperature difference and thermal resistance is electric current, potential difference, and electrical resistance, respectively.

Consider two rods of thermal resistances R_1 and R_2. The effective thermal resistance of a system of two rods connected in series is given by $R_s = R_1 + R_2$ If these rods are of same physical dimensions and of thermal conductivities K_1 and K_2 then effective thermal conductivity of the system is

$$K_s = \frac{K_1 K_2}{K_1 + K_2}.$$

The effective thermal resistance of a system of two rods connected in parallel is given by

$$R_p = \frac{R_1 R_2}{R_1 + R_2}.$$

If rods are parallel and of same physical dimensions but thermal conductivities K_1K1 and K_2K2 then effective thermal conductivity of the system is

$K_p=K_1+K_2$.Kp=K1+K2.

In general, a substance that is a good conductor of heat is also a good conductor of electricity. At a given temperature T, the ratio of thermal conductivity (K) to the electrical conductivity (σ) is constant i.e., K/σT= L (a constant). This is known as Wiedemann-Franz Law.

Thermal conduction

Heat conduction depends on the temperature gradient, cross section, path length, and the properties of materials. The expression is very similar to Ohm's Law for electric conduction. The analog of the voltage difference is the temperature difference, the analog of electric current is the heat flow rate, and the analog of electric resistance is thermal resistance (inverse of thermal conductance).

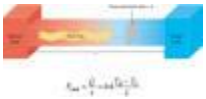

Substance	*k* (W/m·K)
Metals	
Stainless steel	14
Lead	35
Aluminum	235
Copper	401
Silver	428
Gases	
Air (dry)	0.026
Helium	0.15
Hydrogen	0.18
Building Materials	
Polyurethane form	0.024
Rock wool	0.043
Fiberglass	0.048
White pine	0.11
Window glass	1.0

*a*Conductivities change somewhat with temperature. The given values are at room temperature.

Sample problem: Two rods, one lead and the other copper, are connected in series between metal plates held at 2 °C and 106 °C. Both rods have a length of 2 m and a diameter of 10 cm. Neglecting any heat flow through the sides, what is the temperature at the lead-copper junction? What is the rate of heat flow through the rods?
Solution: In this example, the two rods are in series and their thermal "resistances" therefore add as electrical resistances do in series.

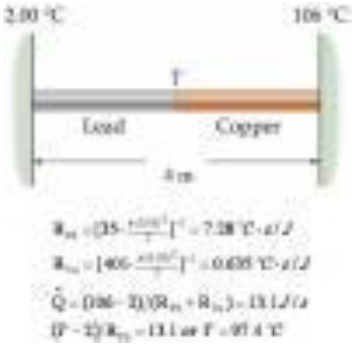

Sample problem: Two rods, one lead and the other copper, are connected between metal plates held at 2 °C and 106 °C. If the rods have a diameter of 10 cm and are 2 m long, what is the rate of heat flow through the rods? Neglect any heat flow through the sides.
Solution: In this example, the rods are in parallel and their thermal "resistances" therefore add as electrical resistances do in parallel.

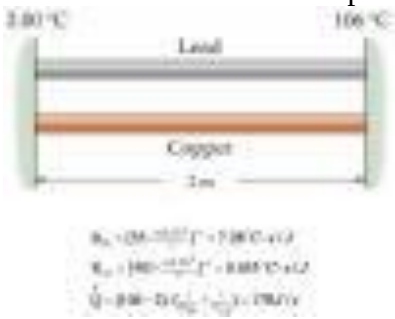

Conductive Heat Transfer

Conductive heat transfer takes place in a solid if there is a temperature gradient.

Conduction as heat transfer takes place if there is a temperature gradient in a solid or stationary fluid medium.

With conduction energy transfers from more energetic to less energetic molecules when neighboring molecules collide. Heat flows in direction of decreasing temperatures since higher temperatures are associated with higher molecular energy.

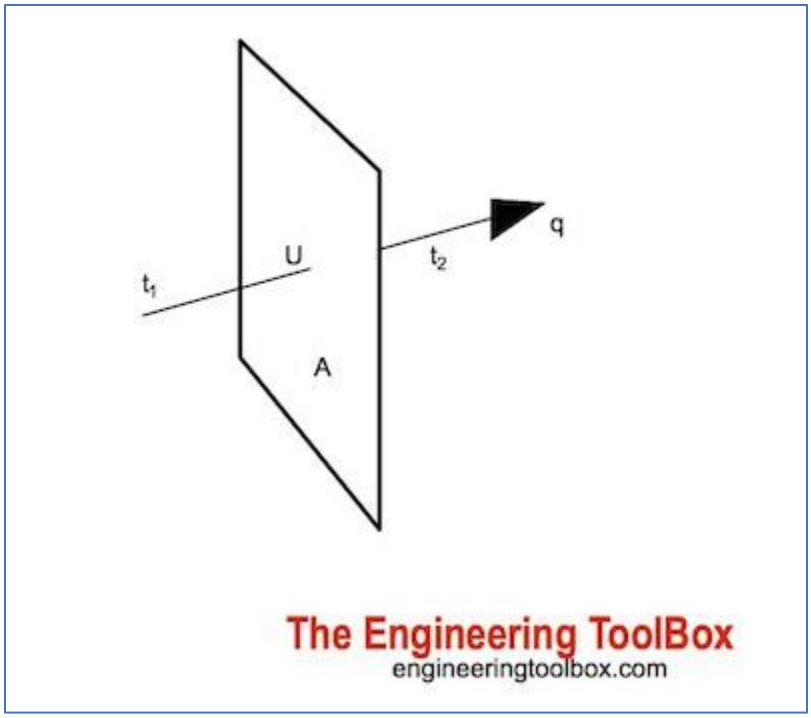

Conductive heat transfer can be expressed with "**Fourier's Law**"

q = (k / s) A dT

= U A dT (1)

where

q = heat transfer (W, J/s, Btu/hr)

k = Thermal Conductivity of material (W/m K or W/m ^oC, Btu/(hr ^oF ft^2/ft))

s = material thickness (m, ft)

A = heat transfer area (m^2, ft^2)

U = k / s

= Coefficient of Heat Transfer (W/(m^2 K), Btu/(ft^2 h ^oF)

dT = t_1 - t_2

= temperature gradient - difference - over the material (^oC, ^oF)

- Calculate Overall Heat Transfer Coefficient - U-value

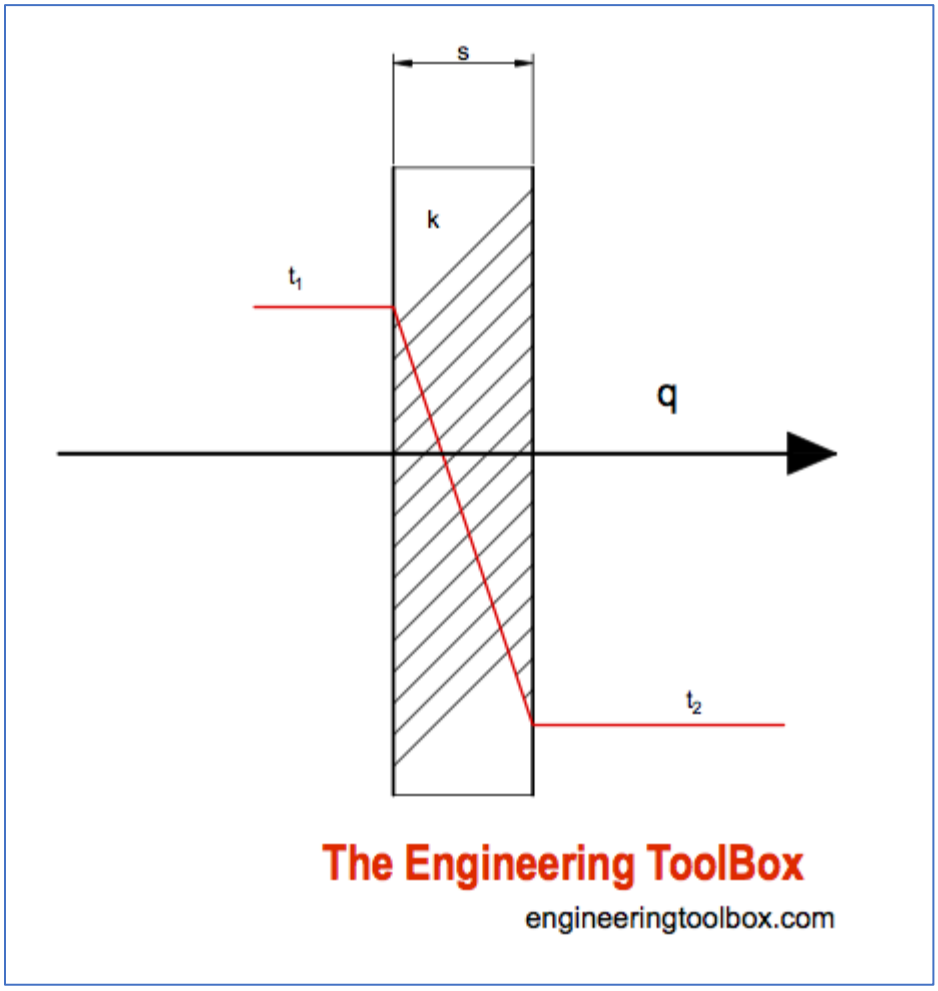

Example - Conductive Heat Transfer

A plane wall is constructed of solid iron with thermal conductivity *70 W/m°C.* Thickness of the wall is *50 mm* and surface length and width is *1 m by 1 m.* The temperature is *150 °C* on one side of the surface and *80 °C* on the other.

The conductive heat transfer through the wall can be calculated

q = [(70 W/m °C) / (0.05 m)] [(1 m) (1 m)] [(150 °C) - (80 °C)]

= 98000 (W)

= 98 (kW)

Conductive Heat Transfer Calculator

This calculator can be used to calculate **conductive** heat transfer through a wall. The calculator is generic and can be used for both metric and imperial units as long as the use of units is consistent.

- Calculate overall heat transfer inclusive convection

k - thermal conductivity (W/(m K), W/(m ^{o}C), Btu/(hr ^{o}F ft^2/ft))

A - area (m^2, ft^2)

t_1 - temperature 1 (^{o}C, ^{o}F)

t_2 - temperature 2 (^{o}C, ^{o}F)

s - material thickness (m, ft)

Conductive Heat Transfer through a Plane Surface or Wall with Layers in Series

The heat conducted through a wall with layers in thermal contact can be calculated as

$$q = dT\ A / ((s_1 / k_1) + (s_2 / k_2) + ... + (s_n / k_n)) \qquad (2)$$

where

$dT = t_1 - t_2$

= *temperature difference between inside and outside wall (^{o}C, ^{o}F)*

Note that heat resistance due to surface convection and radiation is not included in this equation. Convection and radiation in general have major impact on the overall heat transfer coefficients.

Example - Conductive Heat Transfer through a Furnace Wall

A furnace wall of *1 m^2* consist of *1.2 cm* thick stainless steel inner layer covered with *5 cm* outside insulation layer of insulation board. The inside surface temperature of the steel is *800 K* and the outside surface temperature of the insulation board is *350 K*. The

thermal conductivity of the stainless steel is *19 W/(m K)* and the thermal conductivity of the insulation board is *0.7 W/(m K)*.

The conductive heat transport through the layered wall can be calculated as

$q = [(800\ K) - (350\ K)]\ (1\ m^2) / ([(0.012\ m) / (19\ W/(m\ K))] + [(0.05\ m) / (0.7\ W/(m\ K))])$

$= 6245\ (W)$

$= 6.25\ kW$

- Thermal conductivity metals
- Thermal conductiivity Perlite insulation

Thermal Conductivity Units

- *Btu/(h ft² °F/ft)*
- *Btu/(h ft² °F/in)*
- *Btu/(s ft² °F/ft)*
- *Btu in)/(ft² h °F)*
- *MW/(m² K/m)*
- *kW/(m² K/m)*
- *W/(m² K/m)*
- *W/(m² K/cm)*
- *W/(cm² °C/cm)*
- *W/(in² °F/in)*
- *kJ/(h m² K/m)*
- *J/(s m² °C/m)*
- *kcal/(h m² °C/m)*
- *cal/(s cm² °C/cm)*

- *1 W/(m K) = 1 W/(m °C) = 0.85984 kcal/(h m °C) = 0.5779 Btu/(ft h °F) = 0.048 Btu/(in h °F) = 6.935 (Btu in)/(ft² h °F)*

- Thermal Conductivity Units Converter

Thermal conductivity

Thermal conductivity (k, also denoted as λ or κ) is a measure of a material's ability to conduct heat. Heat transfer across materials of high thermal conductivity occurs at a higher rate than across materials of low thermal conductivity. In the International System of Units (SI), thermal conductivity is measured in watts per meter Kelvin (W/(m•K)). In the Imperial System of Measurement (British Imperial, or Imperial units), thermal conductivity is measured in Btu/(hr•ft·F).

Copper has a thermal conductivity of 231 Btu/(hr-ft-F). This is higher than all other metals except silver, a precious metal. Copper has a 60% better thermal conductivity rating than aluminum and has almost 30 times more thermal conductivity than stainless steel.

Thermal conductivity of some common metals

Metal	Thermal conductivity	
	(Btu/(hr-ft-F))	(W/(m•K))
Silver	247.87	429
Copper	231	399
Gold	183	316
Aluminium	136	235
Yellow brass	69.33	120
Cast iron	46.33	80.1
Stainless steel	8.1	14.0

Energy Required to Heat Metal

The amount of energy required to heat metal depends on the type of metal, its mass, and the desired temperature change:

- Specific heat

  Metals generally have low specific heat capacities, around 0.4 J/g°C, which is 10 times less than water. For example, the specific heat of mild steel is 0.122 BTU's per pound per degree Fahrenheit. This means that it takes less energy to heat metal than water.

- Mass

  The amount of energy required to heat metal increases with its mass. For example, to increase the temperature of 1 kg of steel by 20°C, you need 8,400 J.

- Temperature change
  The amount of energy required to heat metal increases with the desired temperature change. For example, to heat 50 lbs of steel by 250°F in 1 hour requires 625 watts, but to reach the same temperature in 15 minutes requires 2,500 watts.

To calculate the wattage required to heat steel, you can use the equation:

(1 BTU = 0.293071 Watt-hr)

Watts = 0.05 x Lbs of Steel x ΔT (in °F) / Heat-Up Time (in hrs)

Heating-melting: how much energy is needed?

How do we quantify the minimum energy needed to heat materials and melt materials? A good rule of thumb is 25 kWh of useful energy to heat each ton of material by each 100°C.

---

(1) Thermodynamics 101. Heating and melting material require energy, inducing particles to vibrate more (specific heat) and ultimately to break the bonds that hold them together as a solid or liquid (latent heat). By definition. 1 Joule can be defined as the **specific heat** energy needed to raise the temperature of 1 gram of air by 1°C (see our note on **energy units and conversions**).

(2) Advanced thermodynamics. If you really want to get into the weeds, and quantify the minimum energy needed to heat, melt, and vaporize different materials,

you will find yourself entering the murky world of quantum physics. For example, the specific heat of different materials can be approximated using the well-known **Dulong-Petit Law**. But different materials' specific heat capacity values are not actually 'constant.' They rise with temperature, as higher-energy particles suddenly gain the ability to spin in novel ways, requiring ever more complex physics, such as the **Einstein photo-electron model**. But we can ignore all of this for now.

(3) Heating a material makes it hotter. We all use this principle every day. For example, the "perfect bath" contains about 100L of water (or 0.1 tons) at 40°C. If it is 15°C outside, then this requires 25°C of heating, at 4.2 J/g°C, or 10MJ of useful energy, aka 2.8 kWh of useful energy. This is the **thermodynamic minimum** useful energy required. Including the losses in a boiler, the unintended heating of pipes and surroundings, a bath probably requires around 4kWh of input energy.

(4) Industrial heat differs in that the volumes are larger and the temperatures are hotter. But a good rule of thumb is that heating each ton of material by each 100°C requires a minimum of around 25kWh of useful energy. The numbers can vary widely, however.

(5) Melting metals is necessary before they can be forged or shaped. Generally, metals have relatively low specific heat capacities, around 0.4 J/g°C. This is literally 10x less than water. It varies by metal. But this shows that for many metals, the energy intensive step may not be melting and working the metal, but smelting it in the first place. For more details, please see our **metals research**.

(6) Silicon stands out for its ridiculously high energy intensity. We think that making solar **PV silicon** requires over 80,000 kWh/ton, and it is one of the most energy intensive materials we have ever looked at. The first step is melting sand at 1,700°C (500 kWh/ton). Then there are multiple steps of re-crystallizing and then re-melting the silicon, as described in our **note here**. Some of these steps grow crystals very slowly, at 10-20 nm per minute, and thus they take 80 – 110 hours, with temperatures in the range of 600-1,100°C.

(7) Water and steam are weird. Finally, we should return to water. Water is weird. Water molecules love sticking together as a liquid. Their latent heat of evaporation is 2,250 J/g, which is 5x more than the next-closest material in our data-file. In other words, it takes 7x more energy to turn 100°C water into steam than it took to bring 20°C water up to 100°C in the first place. This is also the reason that water will "boil" in a saucepan for long enough to make **spaghetti carbonara**, rather than suddenly vanishing into a particularly steamy kitchen. But the upshot is that turbines using water as a working fluid must work very hard to capture all the energy from steam. In turn this underpins **combined cycle gas turbines**, **combined heat and power**, **EGRs**, and even next generation combustion technologies based around **super-critical CO2**, and **next-generation nuclear** using molten sodium or salt.

Appendix G. Electromagnetism Theory Introduction

Wikipedia introduction

In physics, **electromagnetism** is an interaction that occurs between particles with electric charge via electromagnetic fields. The electromagnetic force is one of the four fundamental forces of nature. It is the dominant force in the interactions of atoms and molecules. Electromagnetism can be thought of as a combination of electrostatics and magnetism, which are distinct but closely intertwined phenomena. Electromagnetic forces occur between any two charged particles. Electric forces cause an attraction between particles with opposite charges and repulsion between particles with the same charge, while magnetism is an interaction that occurs between charged particles in relative motion. These two forces are described in terms of electromagnetic fields. Macroscopic charged objects are described in terms of Coulomb's law for electricity and Ampère's force law for magnetism; the Lorentz force describes microscopic charged particles.

The electromagnetic force is responsible for many of the chemical and physical phenomena observed in daily life. The electrostatic attraction between atomic nuclei and their electrons holds atoms together. Electric forces also allow different atoms to combine into molecules, including the macromolecules such as proteins that form the basis of life. Meanwhile, magnetic interactions between the spin and angular momentum magnetic moments of electrons also play a role in chemical reactivity; such relationships are studied in spin chemistry. Electromagnetism also plays several crucial roles in modern technology: electrical energy production, transformation and distribution; light, heat, and sound production and detection; fiber optic and wireless communication; sensors; computation; electrolysis; electroplating; and mechanical motors and actuators.

Electromagnetism has been studied since ancient times. Many ancient civilizations, including the Greeks and the Mayans, created wide-ranging theories to explain lightning, static electricity, and the attraction between magnetized pieces of iron ore. However, it was not until the late 18th century that scientists began to develop a mathematical basis for understanding the nature of electromagnetic interactions. In the 18th and 19th centuries, prominent scientists and mathematicians such as Coulomb, Gauss and Faraday developed namesake laws which helped to explain the formation and interaction of electromagnetic fields. This process culminated in the 1860s with the discovery of Maxwell's equations, a set of four partial differential equations which provide a complete description of classical electromagnetic fields. Maxwell's equations provided a sound mathematical basis for the relationships between electricity and magnetism that scientists had been exploring for centuries, and predicted the existence of self-sustaining electromagnetic waves. Maxwell postulated that such waves make up visible light, which was later shown to be true. Gamma-rays, x-rays, ultraviolet, visible, infrared radiation, microwaves and radio waves were all determined to be electromagnetic radiation differing only in their range of frequencies.

In the modern era, scientists have continued to refine the theorem of electromagnetism to take into account the effects of modern physics, including quantum mechanics and relativity. The theoretical implications of electromagnetism, particularly

the establishment of the speed of light based on properties of the "medium" of propagation (permeability and permittivity), helped inspire Einstein's theory of special relativity in 1905. Meanwhile, the field of quantum electrodynamics (QED) has modified Maxwell's equations to be consistent with the quantized nature of matter. In QED, the changes in the electromagnetic field is expressed in terms of discrete excitations, particles known as photons, the quanta of light.

19th century

Electricity and magnetism were originally considered to be two separate forces. This view changed with the publication of James Clerk Maxwell's 1873 *A Treatise on Electricity and Magnetism*[5] in which the interactions of positive and negative charges were shown to be mediated by one force. There are four main effects resulting from these interactions, all of which have been clearly demonstrated by experiments:

1. Electric charges *attract* or *repel* one another with a force inversely proportional to the square of the distance between them: unlike charges attract, like ones repel.
2. Magnetic poles (or states of polarization at individual points) attract or repel one another in a manner similar to positive and negative charges and always exist as pairs: every north pole is yoked to a south pole.
3. An electric current inside a wire creates a corresponding circumferential magnetic field outside the wire. Its direction (clockwise or counter-clockwise) depends on the direction of the current in the wire.
4. A current is induced in a loop of wire when it is moved toward or away from a magnetic field, or a magnet is moved towards or away from it; the direction of current depends on that of the movement.

A fundamental force

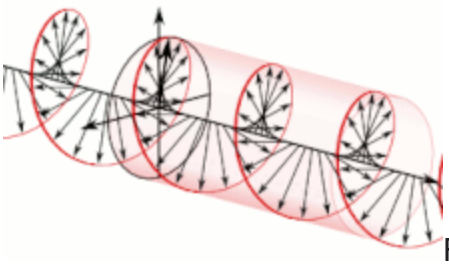

Representation of the electric field vector of a wave of circularly polarized electromagnetic radiation

The electromagnetic force is the second strongest of the four known fundamental forces. It operates with infinite range.[16] All other forces (e.g., friction, contact forces) are derived from these four fundamental forces and they are known as non-fundamental forces.[17] At high energy, the weak force and electromagnetic force are unified as a single interaction called the electroweak interaction.[18]

Roughly speaking, all the forces involved in interactions between atoms can be explained by the electromagnetic force acting between the electrically charged atomic

nuclei and electrons of the atoms. Electromagnetic forces also explain how these particles carry momentum by their movement. This includes the forces we experience in "pushing" or "pulling" ordinary material objects, which result from the intermolecular forces that act between the individual molecules in our bodies and those in the objects. The electromagnetic force is also involved in all forms of chemical phenomena.

A necessary part of understanding the intra-atomic and intermolecular forces is the effective force generated by the momentum of the electrons' movement, such that as electrons move between interacting atoms they carry momentum with them. As a collection of electrons becomes more confined, their minimum momentum necessarily increases due to the Pauli exclusion principle. The behavior of matter at the molecular scale including its density is determined by the balance between the electromagnetic force and the force generated by the exchange of momentum carried by the electrons themselves.

Classical electrodynamics

A theory of electromagnetism, known as classical electromagnetism, was developed by several physicists during the period between 1820 and 1873, when James Clerk Maxwell's treatise was published, which unified previous developments into a single theory, proposing that light was an electromagnetic wave propagating in the *luminiferous ether*. In classical electromagnetism, the behavior of the electromagnetic field is described by a set of equations known as Maxwell's equations, and the electromagnetic force is given by the Lorentz force law.

One of the peculiarities of classical electromagnetism is that it is difficult to reconcile with classical mechanics, but it is compatible with special relativity. According to Maxwell's equations, the speed of light in vacuum is a universal constant that is dependent only on the electrical permittivity and magnetic permeability of free space. This violates Galilean invariance, a long-standing cornerstone of classical mechanics. One way to reconcile the two theories (electromagnetism and classical mechanics) is to assume the existence of a luminiferous aether through which the light propagates. However, subsequent experimental efforts failed to detect the presence of the aether. After important contributions of Hendrik Lorentz and Henri Poincaré, in 1905, Albert Einstein solved the problem with the introduction of special relativity, which replaced classical kinematics with a new theory of kinematics compatible with classical electromagnetism. (For more information, see History of special relativity.)

In addition, relativity theory implies that in moving frames of reference, a magnetic field transforms to a field with a nonzero electric component and conversely, a moving electric field transforms to a nonzero magnetic component, thus firmly showing that the phenomena are two sides of the same coin. Hence the term "electromagnetism". (For more information, see Classical electromagnetism and special relativity and Covariant formulation of classical electromagnetism.)

Today a few problems in electromagnetism remain unsolved. These include: the lack of magnetic monopoles, Abraham–Minkowski controversy, and the mechanism by which some organisms can sense electric and magnetic fields.

Extension to nonlinear phenomena

The Maxwell equations are *linear,* in that a change in the sources (the charges and currents) results in a proportional change of the fields. Nonlinear dynamics can occur when electromagnetic fields couple to matter that follows nonlinear dynamical laws. This is studied, for example, in the subject of magnetohydrodynamics, which combines Maxwell theory with the Navier–Stokes equations.[28] Another branch of electromagnetism dealing with nonlinearity is nonlinear optics.

Quantities and units

Here is a list of common units related to electromagnetism:

- ampere (electric current)
- coulomb (electric charge)
- farad (capacitance)
- henry (inductance)
- ohm (resistance)
- siemens (conductance)
- tesla (magnetic flux density)
- volt (electric potential)
- watt (power)
- weber (magnetic flux)

In the electromagnetic CGS system, electric current is a fundamental quantity defined via Ampère's law and takes the permeability as a dimensionless quantity (relative permeability) whose value in vacuum is unity.[30] As a consequence, the square of the speed of light appears explicitly in some of the equations interrelating quantities in this system.

SI electromagnetism units

- v
- t
- e

Symbol[31]	Name of quantity	Unit name	Symbol	Base units
E	energy	joule	J = C·V = W·s	$kg·m^2·s^{-2}$
Q	electric charge	coulomb	C	A·s
I	electric current	ampere	A = C/s = W/V	A

J	electric current density	ampere per square metre	A/m^2	$A \cdot m^{-2}$
U, ΔV; $\Delta\phi$; $\mathcal{E}$, ξ	potential difference; voltage; electromotive force	volt	V = J/C	$kg \cdot m^2 \cdot s^{-3} \cdot A^{-1}$
R; Z; X	electric resistance; impedance; reactance	ohm	Ω = V/A	$kg \cdot m^2 \cdot s^{-3} \cdot A^{-2}$
ρ	resistivity	ohm metre	Ω·m	$kg \cdot m^3 \cdot s^{-3} \cdot A^{-2}$
P	electric power	watt	W = V·A	$kg \cdot m^2 \cdot s^{-3}$
C	capacitance	farad	F = C/V	$kg^{-1} \cdot m^{-2} \cdot A^2 \cdot s^4$
Φ_E	electric flux	volt metre	V·m	$kg \cdot m^3 \cdot s^{-3} \cdot A^{-1}$
E	electric field strength	volt per metre	V/m = N/C	$kg \cdot m \cdot A^{-1} \cdot s^{-3}$
D	electric displacement field	coulomb per square metre	C/m^2	$A \cdot s \cdot m^{-2}$
ε	permittivity	farad per metre	F/m	$kg^{-1} \cdot m^{-3} \cdot A^2 \cdot s^4$
χ_e	electric susceptibility	(dimensionless)	1	1
p	electric dipole moment	coulomb metre	C·m	A·s·m
G; Y; B	conductance; admittance; susceptance	siemens	$S = \Omega^{-1}$	$kg^{-1} \cdot m^{-2} \cdot s^3 \cdot A^2$
κ, γ, σ	conductivity	siemens per metre	S/m	$kg^{-1} \cdot m^{-3} \cdot s^3 \cdot A^2$
B	magnetic flux density, magnetic induction	tesla	$T = Wb/m^2 = N \cdot A^{-1} \cdot m^{-1}$	$kg \cdot s^{-2} \cdot A^{-1}$
Φ, Φ_M, Φ_B	magnetic flux	weber	Wb = V·s	$kg \cdot m^2 \cdot s^{-2} \cdot A^{-1}$

H	magnetic field strength	ampere per metre	A/m	$A \cdot m^{-1}$
$\mathcal{F}$	magnetomotive force	ampere	A = Wb/H	A
$\mathcal{R}$	magnetic reluctance	inverse henry	H^{-1} = A/Wb	$kg^{-1} \cdot m^{-2} \cdot s^{2} \cdot A^{2}$
$\mathcal{P}$	magnetic permeance	henry	H = Wb/A	$kg \cdot m^{2} \cdot s^{-2} \cdot A^{-2}$
L, M	inductance	henry	H = Wb/A = V·s/A	$kg \cdot m^{2} \cdot s^{-2} \cdot A^{-2}$
μ	permeability	henry per metre	H/m	$kg \cdot m \cdot s^{-2} \cdot A^{-2}$
χ	magnetic susceptibility	(dimensionless)	1	1
m	magnetic dipole moment	ampere square meter	$A \cdot m^{2}$ = $J \cdot T^{-1}$	$A \cdot m^{2}$
σ	mass magnetization	ampere square meter per kilogram	$A \cdot m^{2}/kg$	$A \cdot m^{2} \cdot kg^{-1}$

Formulas for physical laws of electromagnetism (such as Maxwell's equations) need to be adjusted depending on what system of units one uses. This is because there is no one-to-one correspondence between electromagnetic units in SI and those in CGS, as is the case for mechanical units. Furthermore, within CGS, there are several plausible choices of electromagnetic units, leading to different unit "sub-systems", including Gaussian, "ESU", "EMU", and Heaviside–Lorentz. Among these choices, Gaussian units are the most common today, and in fact the phrase "CGS units" is often used to refer specifically to CGS-Gaussian units.

Electromagnetism

Christopher S. Baird

Last reviewed: April 2024

https://doi.org/10.1036/1097-8542.223000

Key Concepts

- Electromagnetism is the physical interaction among electric charges, magnetic moments, and electromagnetic fields.
- An electromagnetic field can be static, slowly changing, or form waves.
- Electromagnetic waves are generally known as light and obey the laws of optics.
- Electromagnetic devices are used ubiquitously in modern society.

The interaction among all electrically charged objects, objects with magnetic moments, and electromagnetic fields. The electromagnetic interaction is one of the four fundamental interactions of the universe. The interaction encompasses all physical phenomena related to electricity, magnetism, electromagnetic fields, light, and atoms. As such, electromagnetism forms the fundamental basis for a wide variety of sciences including solid-state physics, optics, chemistry, and molecular biology. All electromagnetic effects arise from the interaction of electrically charged particles, particles with an intrinsic magnetic moment, and an electromagnetic field.

Fundamental electromagnetic elements

Electric charge

Electric charge is an innate property of all charged fundamental particles and can be either positive or negative. The charged particles that are most common in the universe are negatively charged electrons and positively charged protons. A charged object, such as a statically charged balloon, has an excess or lack of electrons. When charged particles are moving, they are known as electric currents. An example of an electric current is the flow of electrons along an electrical wire.

Intrinsic magnetic moment

In contrast to electric charge, there is no evidence that magnetic charge exists. However, some fundamental particles do have an innate magnetic property known as the intrinsic magnetic dipole moment. A particle with a magnetic moment, such as an electron, can roughly be thought of as a very small bar magnet. A permanent magnet is a collection of particles with aligned magnetic moments.

Electromagnetic field

The electromagnetic field is a physical field created by charged particles and particles with a magnetic moment. The field itself does not carry electric charge or magnetic moment, but it does carry energy and momentum. The field can transfer its energy and momentum to charged particles and particles with magnetic moment. This field can also occasionally create or destroy particles. The electromagnetic field contains two components: an electric field and a magnetic field. Both are inseparable components of one unified field.

The electromagnetic field can take on five general forms:

- Electrostatic fields consist of a static electric field and a negligible magnetic field. An example is the field surrounding a stationary, statically charged balloon.
- Magnetostatic fields consist of a static magnetic field and a negligible electric field. An example is the field surrounding a stationary magnet.
- Electroquasistatic fields consist of a slowly changing electric field and a slowly changing magnetic field, with the electric field dominating. An example is the field inside a simple electric circuit.
- Magnetoquasistatic fields consist of a slowly changing electric field and a slowly changing magnetic field, with the magnetic field dominating. An example is the field inside an electromechanical generator.
- Electromagnetic waves consist of rapidly changing electric and magnetic fields that travel as waves. Electromagnetic waves are emitted any time an electrically charged object or magnet accelerates. These waves are generally referred to as light. All frequencies of light consist of electromagnetic waves, from radio waves on the low-frequency (long wavelengths) end of the electromagnetic spectrum to gamma rays on the high-frequency (short wavelengths) end (Fig. 2).

Fig. 2 The electromagnetic spectrum, arranged by frequency (in hertz) and wavelength (in meters). (Credit: Shutterstock/Fouad A. Saad)

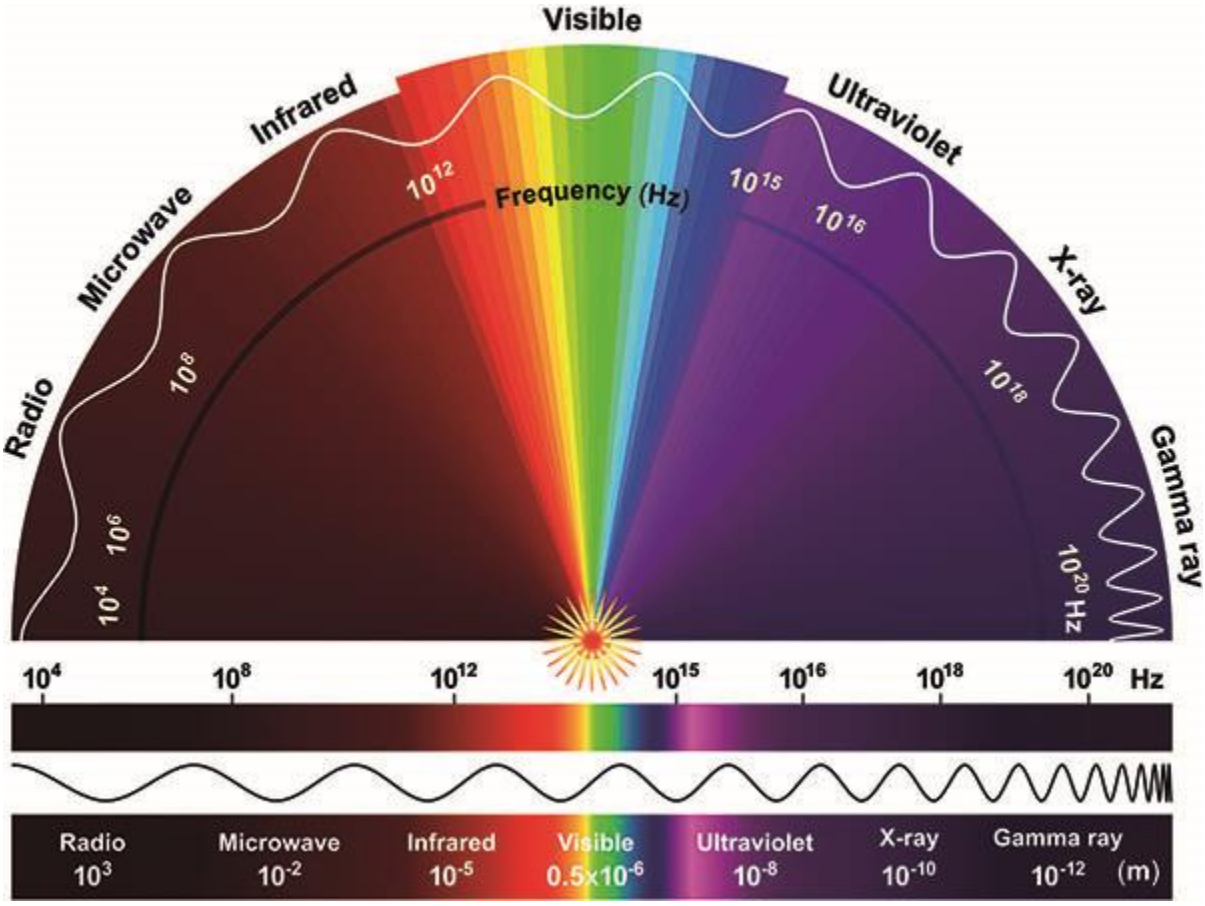

Physical laws of electromagnetism

Behavior of the electromagnetic field

The way electromagnetic fields are created and behave are summarized by four laws known collectively as Maxwell’s equations:

1. An electrically charged particle creates an electric field. This principle, known as Gauss's law, is the operating principle behind simple electric circuits, capacitors, and spark plugs.
2. Magnetically charged particles do not exist and therefore certain types of magnetic fields do not exist. This principle is known as Gauss's law for magnetism.
3. A changing magnetic field creates an electric field. This law is the operating principle behind electric generators, microphones, and transformers. This principle is known as Faraday's law of induction.
4. A moving or spinning electric charge creates a magnetic field. This is the operating principle behind electromagnets and permanent magnets. This principle is known as Ampère’s law. Also, a changing electric field creates a magnetic field. When both principles are combined, it is known as the Ampère-Maxwell law.

As a description of the fields, Maxwell’s equations are complete and self-consistent. Additionally, Maxwell's equations implicitly contain other physical laws, including conservation of charge, conservation of energy, conservation of momentum, conservation of angular momentum, and the electromagnetic wave equation. Furthermore, the electromagnetic wave equation implicitly contains the basic laws of optics. These laws are the operating principles behind optical devices such as lenses, mirrors, and prisms.

The electromagnetic force

While Maxwell's equations describe how electromagnetic fields are generated and behave, the Lorentz force law describes how the fields interact with charged particles. This law states that an electric field exerts a forward or backward force on a charged particle and a magnetic field exerts a sideways force on a moving charged particle. Charged objects, electric currents, and magnets exert forces on each other through the electromagnetic field according to Maxwell's equations and the Lorentz force law. This principle is the operating principle behind chemical bonds, loudspeakers, and electric motors.

Quantum properties

Electric charge, magnetic moment, and the electromagnetic field each come as a collection of discrete, indivisible, quantum packets. The quantum of the electromagnetic field is the photon. The quantum of electric charge is the charge held by a fundamental particle such as an electron or positron. The quantum of intrinsic magnetic moment is the moment carried by a charged fundamental particle with quantum spin such as, again, an electron or positron. The most accurate description of electromagnetism is the quantum version of all of the physical laws mentioned above, which are known collectively as quantum electrodynamics (QED). QED unifies the quantum laws of electromagnetism and the special theory of relativity.

Material effects

In general, charged particles can be either free or bound inside molecules. Materials that act strongly like collections of free charged particles are known as conductors. Important conductors include metals, doped semiconductors, water, and plasma. Materials that act strongly like collections of bound charged particles are known as insulators or dielectrics. Important insulators include plastic, glass, oil, and air.

Similarly, electric currents can be either free or bound inside molecules. Also, intrinsic magnetic moments can be modeled as bound currents because they arise from the quantum spin of charged particles. Materials that act strongly like collections of free currents are known as conductors, as stated previously. Materials that act strongly like collections of bound currents are known as (ferro)magnetic materials. Most magnetic materials are also conductors. Important magnetic materials include iron, steel, and nickel.

Electromagnetic force

The **electromagnetic force**, also called the **Lorentz force**, explains how both moving and stationary charged particles interact. It's called the electromagnetic force because it includes the formerly distinct electric force and the magnetic force; magnetic forces and electric forces are really the same fundamental force.[1] The electromagnetic force is one of the four fundamental forces.

The electric force acts between all charged particles, whether or not they're moving.[1] The magnetic force acts between moving charged particles. This means that every charged particle gives off an electric field, whether or not it's moving. Moving charged particles (like those in electric current) give off magnetic fields. Einstein developed his theory of relativity from the idea that if the observer moves with the charged particles, magnetic fields transform into electric fields and vice versa! One special case of the electromagnetic force, when all the charges are point charges (or can be broken up into point charges), is Coulomb's law.

Because calculating the force from every single individual charge on every other individual charge is ridiculously complicated, physicists have developed tools to simplify these calculations. These simplified calculations turn into the macroscopic, everyday phenomena listed below:

- everyday forces like
    - tension and elasticity
    - friction (how a shoe moves a person forward)
    - normal force (how the shoe doesn't fall through the road that it's sitting on)
    - air drag
- most of chemistry
    - keeping atoms together
    - chemical bonds between atoms to form molecules, like in combustion
    - keeping solids a particular shape
- Sticky things like tape or tar sticking to surfaces
- Magnets sticking artwork to a refrigerator

- The force felt on electrons in a loop of wire when near a changing magnetic field. The electromagnetic force is very closely related to the electromotive force, which is what causes electric current to flow.

Modern physics has unified the electromagnetic and weak forces into the electroweak force. A full understanding of the electromagnetic force and the full implications of electromagnetism takes many years of study. Some good places to go for more information on electromagnetism include hyperphysics.

Below is the Scishow's series on fundamental forces part 4a (electricity) and 4b (magnetism):

https://youtu.be/Yv3EMq2Dgq8

And here is part 2.

https://youtu.be/cy6kba3A8vY

The other videos look at the strong nuclear force, weak nuclear force, and gravity. Check out their youtube channel for more videos like these! (a wonderful resource for curious people).

Appendix H. Aging Science - The Biology of Senescence

Entropy always wins. Each multicellular organism, using energy from the sun, is able to develop and maintain its identity for only so long. Then deterioration prevails over synthesis, and the organism ages. **Aging** can be defined as the time-related deterioration of the physiological functions necessary for survival and fertility. The characteristics of aging—as distinguished from diseases of aging (such as cancer and heart disease)—affect all the individuals of a species.

Many evolutionary biologists (Medawar 1952; Kirkwood 1977) would deny that aging is part of the genetic repertoire of an animal. Rather, they would consider aging to be the default state occurring after the animal has fulfilled the requirements of natural selection. After its offspring are born and raised, the animal can die. Indeed, in many organisms, from moths to salmon, this is exactly what happens. As soon as the eggs are fertilized and laid, the adults die. However, recent studies have indicated that there are genetic components to senescence, and that the genetically determined life span characteristic of a species can be modulated by altering genes or diet.

Maximum Life Span and Life Expectancy

The **maximum life span** is a characteristic of the species. It is the maximum number of years a member of that species has been known to survive. The maximum human life span is estimated to be 121 years (Arking 1998). The life spans of tortoises and lake trout are both unknown, but are estimated to be more than 150 years. The maximum life span of a domestic dog is about 20 years, and that of a laboratory mouse is 4.5 years. If a *Drosophila* fruit fly survives to eclose (in the wild, over 90% die as larvae), it has a maximum life span of 3 months.

However, a person cannot expect to live 121 years, and most mice in the wild do not live to celebrate their first birthday. The **life expectancy**, the amount of time a member of a species can expect to live, is not characteristic of species, but of populations. It is usually defined as the age at which half the population still survives. A baby born in England in the 1780s could expect to live to be 35 years old. In Massachusetts during that same time, the life expectancy was 28 years. This was the normal range of human life expectancy for most of the human race in most times. Even today, the life expectancy in some areas of the world (Cambodia, Togo, Afghanistan, and several other countries) is less than 40 years. In the United States, a child born in 1986 can expect to live 71 years if male and 78 years if female.[*]

Given that in most times and places, humans did not live much past 40 years, our awareness of human aging is relatively new. A 65-year-old person was rare in colonial America, but is a common sight today. Some survival curves for female *Homo sapiens* in the United States are plotted in Figure F-1. In 1900, 50% of American women were dead by age 58. In 1980, 50% of American women were dead by age 81. Thus, the phenomena of senescence and the diseases of aging are much more common today than they were a century ago. In 1900, people did not have the “luxury” of dying from heart attacks or cancers. These diseases generally occur in people over the age of 50 years. Rather, people died (as they are still dying in many parts of the world) from infectious diseases and parasites (Arking 1998). Similarly, until recently, relatively few people exhibited the more general human sensecent phenotype: graying hair, sagging and wrinkling skin, joint stiffness, osteoporosis (loss of bone calcium), loss of muscle fibers and muscular strength, memory loss, eyesight deterioration, and the slowing of sexual

responsiveness. As Shakespeare noted in *As You Like It*, those who did survive to senescence left the world "sans teeth, sans eyes, sans taste, sans everything."

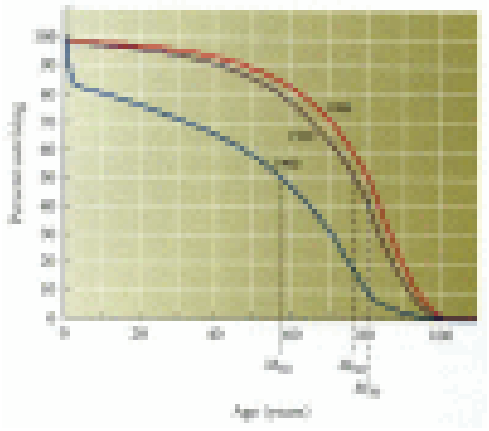

Figure F-1

Survival curves for U.S. females in 1900, 1960, and 1980. M_{50} represents the age at which 50% of the individuals of each population survived. (After Arking 1998.)

Causes of Aging

The general senescent phenotype is characteristic of each species. But what causes it? This question can be asked at many levels. We will be looking primarily at the cellular level of organization. Even here, there is evidence for many different theories, and there is not yet a consensus on what causes aging.

Oxidative damage

One major theory sees our metabolism as the cause of our aging. According to this theory, aging is a by-product of normal metabolism; no mutations are required. About 2–3% of the oxygen atoms taken up by the mitochondria are reduced insufficiently to **reactive oxygen species** (**ROS**). These ROS include the superoxide ion, the hydroxyl radical, and hydrogen peroxide. ROS can oxidize and damage cell membranes, proteins, and nucleic acids. Evidence for this theory includes the observation that *Drosophila* that overexpress enzymes that destroy ROS (catalase, which degrades peroxide, and superoxide dismutase) live 30–40% longer than do controls (Orr and Sohal 1994; Parkes et al. 1998). Moreover, flies with mutations in the *methuselah* gene (named after the Biblical fellow said to have lived 969 years) live 35% longer than wild-type flies. The *methusaleh* mutants have enhanced resistance to paraquat, a poison that works by generating ROS within cells (Lin et al. 1998). These findings not only suggest that aging is under genetic control, but also provide evidence for the role of ROS in the aging process. In *C. elegans*, too, individuals with mutations that increase the synthesis of ROS-degrading enzymes live much longer than wild-type nematodes (Larsen 1993; Vanfleteren and De Vreese 1996).

The evidence for ROS involvement in mammalian aging is not as clear. Mutations in mice that result in the lack of certain ROS-degrading enzymes do not cause premature aging (Ho et al.

1997; Melov et al. 1998). However, there may be more genetic redundancy in mammals than in invertebrates, and other genes may be up-regulated to produce related ROS-degrading enzymes. Migliaccio and colleagues (1999) have observed mutant mice that live one-third longer than their wild-type littermates. These mice lack a particular protein, $p66^{shc}$. They develop normally, but the lack of $p66^{shc}$ apparently gives them cellular resistance to ROS, and thus higher resistance to oxygen-induced stress on membranes and proteins. The $p66^{shc}$ protein may be a component of a signal transduction pathway that leads to apoptosis upon oxygen stress, and it may be involved in mediating the life spans of mammals.

Another type of evidence does suggest that ROS may be important in mammalian aging: aging in mammals can be slowed by caloric restriction (Lee et al. 1999). However, caloric restriction can also have other effects, so it is not certain if it works by preventing ROS synthesis. Also, vitamins E and C are both ROS inhibitors, and vitamin E increases the longevity of flies and nematodes when it is added to their diet (Balin et al. 1993; Kakkar et al. 1996). However, results in mammals are not as easy to interpret, and there is no clear evidence that ROS inhibitors work as well as in invertebrates (Arking 1998).

General wear-and-tear and genetic instability

"Wear-and-tear" theories of aging are among the oldest hypotheses proposed to account for the general scenescent phenotype (Weismann 1891; Szilard 1959). As one gets older, small traumas to the body build up. Point mutations increase in number, and the efficiencies of the enzymes encoded by our genes decrease. Moreover, if a mutation occured in a part of the protein synthetic apparatus, the cell would make a large percentage of faulty proteins (Orgel 1963). If mutations arose in the DNA-synthesizing enzymes, the rate of mutations would be expected to increase markedly, and Murray and Holliday (1981) have documented such faulty DNA polymerases in senescent cells. Likewise, DNA repair may be important in preventing senescence, and species whose members' cells have more efficient DNA repair enzymes live longer (Figure 18.36; Hart and Setlow 1974). Moreover, genetic defects in DNA repair enzymes can produce premature aging syndromes in humans (Yu et al. 1996; Sun et al. 1998).

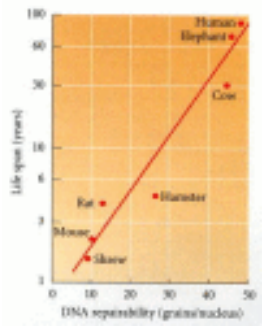

Figure F-2

Correlation between life span and the ability of fibroblasts from various mammalian species to repair DNA. Capacity for repair is represented in autoradiography by the number of grains from radioactive thymidine per cell nucleus. Note that the *y* axis (more...)

Mitochondrial genome damage

The mutation rate in mitochondria is 10–20 times faster than the nuclear DNA mutation rate (Johnson et al. 1999). It is thought that mutations in mitochondria could (1) lead to defects in energy production, (2) lead to the production of ROS by faulty electron transport, and/or (3) induce apoptosis. Age-dependent declines in mitochondrial function are seen in many animals, including humans (Boffoli et al. 1994). A recent report (Michikawa et al. 1999) shows that there are "hot spots" for age-related mutations in the mitochondrial genome, and that mitochondria with these mutations have a higher replication frequency than wild-type mitochondria. Thus, the mutants can outcompete the wild-type mitochondria and eventually dominate the cell and its progeny. Moreover, the mutations may not only allow more ROS to be made, but may make the mitochondrial DNA more susceptible to ROS-mediated damage.

Telomere shortening

Telomeres are repeated DNA sequences at the ends of chromosomes. They are not replicated by DNA polymerase, and they will shorten at each cell division unless maintained by **telomerase**. Telomerase adds the telomere onto the chromosome at each cell division. Most mammalian somatic tissues lack telomerase, so it has been proposed (Salk 1982; Harley et al. 1990) that telomere shortening could be a "clock" that eventually prohibits the cells from dividing any more. When human fibroblasts are cultured, they can divide only a certain number of times, and their telomeres shorten. If these cells are made to express telomerase, they can continue dividing (Bodnar et al. 1998; Vaziri and Benchimol 1998).

However, there is no correlation between telomere length and the life span of an animal (humans have much shorter telomeres than mice), nor is there a correlation between human telomere length and a person's age (Cristofalo et al. 1998). Telomerase-deficient mice do not show profound aging defects, which we would expect if telomerase were the major factor in determining the rate of aging (Rudolph et al. 1999). It has been suggested that telomere-dependent inhibition of cell division might serve primarily as a defense against cancer rather than as a kind of "aging clock."

Genetic aging programs

Several genes have been shown to affect aging. In humans, Hutchinson-Gilford progeria syndrome causes children to age rapidly and to die (usually of heart failure) as early as 12 years. It is caused by a dominant mutant gene, and its symptoms include thin skin with age spots, resorbed bone mass, hair loss, and arteriosclerosis. A similar syndrome is caused by mutations of the *klotho* gene in mice (Kuro-o et al. 1997). The functions of the products of these genes are not known, but they are thought to be involved in suppressing the aging phenotypes. These proteins may be extremely important in determining the timing of senescence.

In *C. elegans*, there appear to be at least two genetic pathways that affect aging. The first pathway involves the decision to remain a larva or to continue growth. After hatching, the *C. elegans* larva proceeds through four instar stages, after which it can become an adult or (if the nematodes are overcrowded or if there is insufficient food) can enter a nonfeeding, metabolically dormant **dauer stage**. It can remain a dauer larva for up to 6 months, rather than becoming an adult that lives only a few weeks. When it comes out of the dauer stage, it will live as long as if it had never been a dauer larva. In the dauer stage, adult development is suppressed, and extra

defenses against ROS are synthesized. If some of the genes involved in this pathway are mutated, adult development is allowed, but the ROS defenses are still made. The resulting adults live twice to four times as long as wild-type adults (Figure F-3; Friedman and Johnson 1988). The second pathway involves the gonads. Germ cells appear to inhibit longevity, while the somatic cells of the gonads act to prolong the life of the nematode (Hsin and Kenyon 1999).

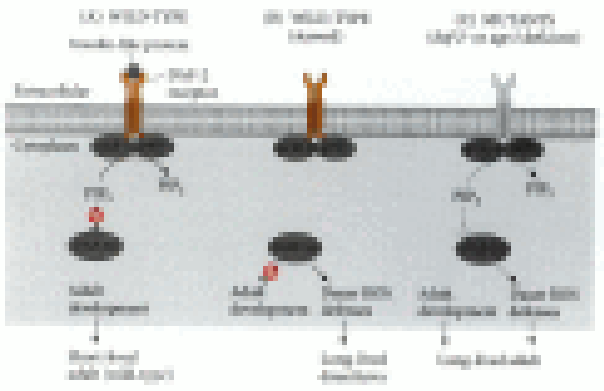

Figure F-3

Proposed mechanism for extending the life span of *C. elegans* through the dauer larva pathway. (A) Wild-type animal in a favorable environment makes a ligand that activates a pathway that inhibits the DAF-16 protein. This allows metamorphosis to the adult (more...)

As human life expectancy increases due to our increased ability to prevent and cure disease, we are still left with a general aging syndrome that is characteristic of our species. Unless attention is paid to the general aging syndrome, we risk ending up like Tithonios, the miserable wretch of Greek mythology to whom the gods awarded eternal life, but not eternal youth.

Snapshot Summary: Metamorphosis, Regeneration, and Aging

1. Amphibian metamorphosis includes both morphological and biochemical changes. Some structures are remodeled, some are replaced, and some new structures are formed.

2. Many changes during amphibian metamorphosis are regionally specific. The tail epidermis dies, the head epidermis does not. An eye will persist even if transplanted into a degenerating tail.

3. The hormones responsible for amphibian metamorphosis are the thyroid hormones thyroxine (T_4) and triiodothyronine (T_3). The coordination of metamorphic changes appears to be due to early changes that occur at low concentrations of the thyroid hormones. This is called the threshold concept. The molecular basis for the autoinduction of thyroid hormones may be the ability of thyroid hormones to induce production of more thyroid hormone receptor protein. Thyroid hormones act predominantly at the transcriptional level.

4. Heterochrony involves changing the relative rate of development in different parts of the animal. In animals with direct development, the tadpole stage has been lost. Some frogs, for instance, form limbs while in the egg.

5. In neoteny, the juvenile (larval) form is slowed down, while the gonads and germ cells mature at their normal rate. In progenesis, the gonads and germ cells mature rapidly, while the rest of the body matures normally. In both instances, the animal can mate while in its larval form.

6. In ametabolous insects, there is direct development. In hemimetabolous insects, there is a nymph stage wherein the immature organism is usually a smaller version of the adult. In holometabolous insects, there is a dramatic metamorphosis from larva to pupa to sexually mature adult.

7. In the period between larval molts, the larva is called an instar. After the last instar stage, the larva undergoes a metamorphic molt to become a pupa. The pupa will undergo an instar molt to become an adult.

8. During the pupal stage, the imaginal discs and histoblasts grow and differentiate to produce the structures of the adult body.

9. The anterior-posterior, dorsal-ventral, and proximal-distal axes are sequentially specified and involve interactions between different compartments in the imaginal discs.

10. Molting is caused by the hormone hydroxyecdysone. In the presence of high titres of juvenile hormone, the molt is an instar molt. In low concentrations of juvenile hormone, the molt produces a pupa; and if no juvenile hormone is present, the molt is an imaginal molt.

11. The ecdysone receptor gene can produce nRNA that can form at least three different proteins. The types of ecdysone receptors in a cell may influence the response of that cell to hydroxyecdysone. The ecdysone receptors bind to DNA to activate or repress transcription.

12. There are three major types of regeneration. In epimorphosis (such as regenerating limbs), tissues dedifferentiate into a blastema, divide, and re-differentiate into the new structure. In morphallaxis (characteristic of hydra), there is a repatterning of existing tissue with little or no growth. In compensatory regeneration (such as in the liver), cells divide but retain their differentiated state.

13. In the regenerating salamander limb, the epidermis forms an apical ectodermal cap. The cells beneath it dedifferentiate to form a blastema. The differentiated cells lose their adhesions and re-enter the cell cycle. This does not happen in mammals.

14. In hydras, there appear to be head activation gradients, head inhibition gradients, foot activation gradients, and foot inhibition gradients. Hydra budding occurs where these gradients are minimal.

15. In mammals, medical researchers are testing whether paracrine factors may permit local regeneration. Bone and neural cells are being returned to embryonic conditions in the hopes that they will regrow. Natural inhibitors of neural regeneration have recently been discovered, and their circumvention may allow spinal cord regeneration.

16. The maximum life span of a species is how long its longest observed member has lived. It is largely characteristic of a given species. Life expectancy is the time at which approximately 50 percent of the members of a given population of a species still survive.

17. There are several levels at which we can study aging, including cellular, biochemical, and genetic studies. Reactive oxygen species (ROS) can damage cell membranes, inactivate proteins, and mutate DNA. Mutations that alter the ability to make or degrade ROS can change the life span of the mutants.

18. Mitochondria may be a target for proteins that regulate aging.

19. Aging is the time-related deterioration of the physiological functions necessary for survival and reproduction. The phenotypic changes of senescence (which affect all members of the species) are not to be confused with diseases of senescence, such as cancer and heart disease (which affect individuals).

Appendix I. Hunza Valley

People in this remote valley live to 100—they follow 5 distinct diet and lifestyle habits for longevity

Published Sat, Feb 17 2024 9:47 AM EST

Samantha Shea, Contributor

A Wakhi woman and her yak in Avgarch Village, one of the oldest settlements of Hunza Valley that's only accessible by foot.

Photo: Samantha Shea

In a little-known mountainous area called Hunza Valley, located far north of Pakistan, people seem to defy all medical odds.

It is primarily home to the Burusho and Wakhi people, who for centuries have survived and thrived in remote villages — with minimal amenities and rudimentary health facilities. Studies have found that the average life expectancy here is around 100 years.

My husband was born and raised here, and is from the Burusho indigenous community. After we got married, I left the U.S. and we settled down in the Central part of the valley.

Here are some intriguing habits that help the people of Hunza live longer:

1. They consume apricot seeds and oil

Apricot trees are one of the most important local crops in the valley. Studies have shown that apricot seeds can help fight cancer and other sources of inflammation in the body, in part due to a compound called amygdalin.

Most people in Hunza have at least one apricot tree, and the seeds are harvested from inside the apricots every summer.

Photo: Samantha Shea

Nearly every traditional Hunzai dish includes apricot oil. Back in the day, it was made by hand, but now locals use machines to extract it from their harvested kernels.

My mother-in-law told me that 50 years ago, it was all anyone used to cook food with, even meat. Dried versions of the fruit also help with altitude sickness, and are boiled into a soup come winter.

My father-in-law organizing dried apricots on his roof

Photo: Samantha Shea

2. They never stop moving

People here are healthy and active throughout their lives, well into old age. It's very common to see folks in their 80s outside, even in the winter. Elderly family members still graze their cows and sheep, collect wood, and do other household tasks.

They also participate in community activities like "rajaki," which involves cleaning out the elevated water canals when spring arrives.

Locals of all ages cycle, skate, and play sports like soccer and cricket every day.

3. They drink glacier water

Hunza is filled with dozens of glaciers, all of which melt throughout the summer.

A shiny, dark-grey liquid, "Hunza water" has long held the interest of scientists. Unlike other water sources, this glacial water is naturally filtered by layers of ice and rock and contains precious minerals.

A view of the Passu Glacier from Patundas, a meadow in Upper Hunza where locals bring their livestock to every summer

Photo: Samantha Shea

Some argue that the water contains quartz (sillica) minerals in colloid form, which are considered to be powerful antioxidants.

What Hunza glacier water looks like straight from the source

Photo: Samantha Shea

The runoff generally lasts from May to October each year, which is when you'll find it served at restaurants and in homes. Locals swear by it, and prefer it to filtered water.

4. They rarely eat processed foods

Almost every piece of meat eaten in Hunza comes from a locally sourced animal that's been recently killed.

People rarely eat processed foods, and you certainly won't find any fast-food spots here. Meals are typically prepared fresh in the home daily, and almost every household grows some kind of vegetable.

Spinach is especially popular, and other favorites like tomatoes and potatoes are grown locally and organically.

5. They have strong community values

Neighborhoods and villages are tight-knit, and the people of Hunza take care of each other, especially the older members of the community.

Retirement homes don't exist here. Elders are highly respected and attended to by their families.

Myself and two strong older women from Chapursan Valley, which is one of the most remote parts of Hunza situated alongside the Wakhan Corridor

Photo: Samantha Shea

With essentially zero crime, it's safe enough for kids to wander about on their own, even at young ages. It's likely one of the last places where you'll see more outdoor play than iPad play.

Having lived here for for the past two years, I can happily say that I've never had the privilege of experiencing a society as collective as this one.

Samantha Shea is a Polish-American travel writer from Connecticut. She lives and works remotely in Hunza Valley, Pakistan, and runs women's tours to the region. Follow her on Instagram and YouTube.

Appendix J. Dotto Ring References

Gianni A. DOTTO

Thermionic Couple
("The Dotto Ring")

The Dotto Ring was a successful treatment for cancer, yet it disappeared from public notice in the 1970s after the FDA suppressed the technology. In one account of the story, it has been claimed that the device also tended to LEVITATE, and this was the real reason the government suppressed the discovery. Dotto states (Section 2 below) that the combined Thompson-Peltier-Seebeck effect is akin to gravity.

The Story of the Dotto Ring [An unidentified article published (where?) in the 1970s; author unknown]

Gianni A. Dotto was born in Venice, son of a prominent engineer who was the designer of two hydro-electric generating plants on both the American and Canadian sides of Niagara Falls. His father was an Italian Marquis and since Gianni is the eldest son, he would have inherited the title had he not become an American citizen. The family is directly descended form Galileo and the Galileo coat of arms has been adopted for use as the Foundation's letterhead.

Before World War II, Gianni had received flight training but Mussolini never did trust the Dotto family so Gianni was drafted into the Italian Army as a paratrooper. When Italy surrendered, Gianni was able to join the American Air Force as a fighter pilot in time to participate in numerous engagements against the German Messerschmidts before the war ended.

After the war, Gianni became the head of the racing division of Alfa-Romero and started race-driving cars of his own design. His racing career ended when his wife, Renata, handed him an ultimatum: "Either give up racing or me". He is a prolific inventor as he is the owner of many Italian patents bearing on the automotive industry and, subsequently, just as many American patents.

He is highly educated, holding the Italian equivalent of an American PhD in nuclear physics from Milan University and the same degree in mechanical engineering from another Italian technical school. Subsequently, he received a degree in electrical engineering from Wayne University of Detroit.

While Gianni was teaching at Milan University, the medical school requested the services of a physicist to collaborate with the doctors on a research project. This started him on a career as a "bio-physicist" --- that is, a physicist that specializes in the area of the science of physics that bears on the human body. This embraces an amazingly wide field, as it has to do with the magnetic fields, polarity, the various vibrations and pulsations generated by the brain and, of course, the effect of the many facets of nuclear fission on the human body.

It was there that Gianni discovered that magnetic fields induced by an electric coil and by permanent magnets had a small effect on the human body, but that a mild magnetic field created by adjacent hot and cold areas was definitely beneficial. In other words, the thermal unbalance created a magnetic field that matched the natural field of the human body. The development of the "Dotto Ring" was Gianni's practicable way of producing a piece of equipment that could impress the beneficial magnetic field on the body. The ring is 27 inches in diameter, made of heavy copper and has an adjacent heated and refrigerated area.

Through the ring he has reproduced in a compact, accessible form the same magnetic environment responsible for the good health and longevity of the Hunza people. Visitors to Hunzaland always attribute this great advantage to their diet, air and water, but Gianni could not accept this belief because there are many valleys in the Himalaya Mountains where the diet, air and water are similar to that of the Hunzas' but the inhabitants of these valleys are devoid of the same health and longevity manifestations as in Hunza. With the principle of the Dotto Ring in mind, a panoramic view of the Hunza valley makes Gianni's theory easy to understand. At the head of the valley there is a huge glacier or ice mass and in the valley itself the temperature becomes quite warm, thus creating the thermal unbalance mentioned previously and which is recreated in the principle of the Dotto Ring. When a Hunza travels across this valley, they receive a beneficial treatment from a mild magnetic field. The similarity of the Dotto Ring to the Hunza valley is interesting to say the least.

Gianni has written what he describes as a "simple explanation of just how the ring works." Simple to a physicist perhaps, but difficult for a layman to understand;

consequently, the following preliminary explanation has been outlined for the purpose of clarification:

The nucleus of each cell contains a material known as the DNA, which is an abbreviation for deoxyribonucleic acid. This substance contains the life or genetic code. The presence and function of the DNA has long been suspected by our doctor-scientists and had been presented as a theory, but it was only about 7 years ago with the development of the electron microscope that the presence of the DNA was confirmed. Now it can be seen, photographed, and sketched. Imagine a tiny ladder twisted together in a coil fashion until the unit forms a double helix. The DNA is pliable and rubbery an is never still as it constantly vibrates in resonance with brain signals and even outside influences. The DNA is polarized, with one end being plus and the other being minus. A healthy DNS reproduces healthy cells and aids the body to naturally overcome and eliminate an invasion of bacteria or toxins. This, of course, adds up to good health. When the body is within the beneficial magnetic field of the Dotto Ring, polarization of the DNA is oriented properly and resonance is synchronized to that of a healthy cell.

Important animal tests required by the medial authorities have been underway for the past three years, culminating in seven official tests that were conducted under rigidly controlled conditions. The tests were conducted by Prof. Gerald Willis (Biology Professor at the University of Dayton) and Dr. Robert Zipf, PhD. Dr. Zipf is owner of a group of biological laboratories and has been Coroner of Montgomery Country (OH) for 20 years. The room in which the tests were conducted was kept under triple lock so that only Prof. Willis had access to the area. Dr. Zipf performed the pathology on the test mice.

Mice (6 per cage and 8 per cage per test) were injected with cancer cells. In three tests, C-27 cancer cells were used and in two other tests, Krib type carcinoma cells were used. The most recent tests were conducted in mice that had induced leukemia.

Results have been very good indeed. The untreated mice died in about 7 days while with few exceptions the treated mice survived. When the treated mice were finally sacrificed, they showed no evidence of cancer. These tests, as well as actual experience using the ring on the human body, prove definitely that there are no side effects.

Gianni Dotto has now had 5 years of experience in the use of his ring. For the past 2 years the ring has been in operation in his Bio-Physics Laboratory (Kettering, OH). Results have been uniformly good.

Following is the scientific paper prepared by Gianni Dotto.

Background of the Theory of the Dotto Ring by Gianni Dotto

Most of the external physical factors which have been implicated in the evolution of life are of an electromagnetic nature. It has now been established that throughout the reviewable geological period the biosphere has been a region of electromagnetic fields and radiations of all the frequencies known to us --- from slow periodic variations to the earth's magnetic field and electric fields to gamma rays.

It is fundamentally possible on the basis of general considerations that any of the ranges of the electromagnetic spectrum could have played some role in the evolution of life and are involved in the vital processes of organisms. This has already been demonstrated for a considerable region of the spectrum; for electromagnetic radiations in the infrared to ultraviolet range (photobiology) and from x-rays (radiobiology).

The situation is different with the vast remaining region of the spectrum, which includes electromagnetic fields (EMFs) of super-high, ultra-high, high, low, and infra-low frequencies. Experimental investigations and theoretical considerations suggest that EMFs can have a significant biological action only when their intensity is fairly high and that such action can be due to only one process: conversion of electromagnetic energy to heat or vice versa.

There is an increasing amount of reliable experimental data which indicates that EMFs can have non-thermal effects and that living organisms of diverse species, from unicellular organisms to man, are extremely sensitive to EMFs.

Finally, it has been found that very weak natural EMFs can have non-thermal effects and that living organisms of diverse species, from unicellular organisms to man, are extremely sensitive to EMFs.

Finally, it has been found that very weak natural EMFs can affect organisms of various species. All this indicates the necessity for a fundamentally new approach to the problem of the biological action of EMFs and for the need to reconsider the question of the possible role of EMFs in the vital activity of organisms (Parin).

It is believed that my work is not the first attempt at such an approach to the problem on the basis of the concept of the informational role of EMFs in the evolution and vital activity of organisms. There are three kinds of "biological activity of EMFs":

(1) The effect of natural environment EMFs on the regulation of vital processes.

(2) The role of internal fields in the organism in the coordination of physiological processes.

(3) The interaction between organisms by means of EMFs.

It is not sufficient to consider only the energetic aspect of the interaction of EMFs with biological systems and a portion of my past investigations have dealt with the informational functions of these fields in living nature.

I have constructed equipment necessary to conduct my cancer research. A substantial data bank of case histories has been accumulated. Not all case histories are well defined, but general results are amazingly good. This is understandable, however, since I am in the process of establishing the first formulation of a new biological problem.

My concept of the information functions of EMFs in living organisms and the hypothesis expresses in this respect will undoubtedly rouse interest in a wide circle of the medical readers.

The objectives of this research project are:

(1) Prove that the human body responds favorably when exposed to EMFs.

(2) Establish what types of EMFs are more effective.

(3) Determine the specific frequency of EMFs for different types of disease.

Working Theory of the Dotto Ring

There are four basic, major but disparate theories explaining the development of cancerous tissue.

(1) Virus (theory supported by scientists of Sloan-Kettering, NY).

(2) Low negative voltage across cancer cell skin (Cone, NASA).

(3) Excess of base pairs per turn on DNA double helix (Dotto).

(4) Alteration of the DNA code due to a certain type of virus (Temin).

The first theory would be correct if we are to accept the hypothesis that all the viruses of the four groups responsible for the manufacture of the nuclei (even if similar in size, shape, and crystal form) are tuned to a different frequency, according to the location in the human body of different groups of cells. In this case, a virus out of position can create the Temin phenomena of mixing up the sequence of the DNA code. If this is the case, the theory that someday immunization against cancer will be as simple as polio immunization is unrealistic. The variety of cancer immunization viruses will be in the numerical magnitude of trillions.

Theory #2 (Cone, NASA) would be acceptable if we consider a cancerous cell a parasite cell, to some extent.

According to Theory #3 (Dotto), the magnetic charge of the genetic code is maintained at the proper level by the electrical property of the double helix, which functions as a common transformer; where voltage of the primary and the secondary winding is proportional to the number of turns of the coils.

If the DNA double helix of a cancer cell has a lesser number of turns than the DNA double helix of a normal cell, then the voltage across the cancer cell must be lower than the voltage across the normal cell; consequently, the number of base pairs per turn will be greater. Greater base pairs per turn of the double helix and eagerness of completing the outer electron orbiting of the atomic structure of the nucleus leads to a greater capacity of reproduction of the DNA.

The second and third theories then are similar in principle but explained from a different observer's viewpoint. One explains the result; the other explains the cause.

Theory #4 (Temin) is a consequence of Theory #1 (Sloan-Kettering, NY) --- however, with an incorrect interpretation of the phenomena. Due to the tremendous variety of viruses classified in 8 distinct groups, 4 RNA types and 4 DNA types, there is no way in which to resolve the immunization capability unless the immunization factor can be obtained with the natural method described in the second Dotto patent application # 42,301, filed June 1, 1970:

"Milk taken from the right breast of a nursing mother is maintained separate from the milk taken from the left breast. On high-G centrifuge, viruses are separated from proteins and fats. Immunization will start with oral or injection methods, by using RNA type viruses from the right breast and repeated two months later with DNA type viruses from the left breast. In the human breast, there are all the variety of viruses necessary for the immunization."

Why, then, the electronic reactor (Dotto Ring Device) and not chemistry to resolve the problem?

To begin with: in the normal process of life of a healthy body, when a new cell is produced, the orbital electron spinning of the new cell assumes a direction opposite to one of the mother cell, in order to maintain the mutual attraction. When the increasing kinetic electron energy of the new cells overcome the energy of the mother cell, the orbital electron spinning of the mother cell is forced to change direction and mutual rejection occurs. In the process, the entire energy of the mother cell collapses (in the same fashion as a transformer core) and its energy is absorbed entirely by the new cells.

However, if the energy potential and derived magnetic field in the human body is diminished or unbalanced, the new cell loses the body support to increasing kinetic energy and the dying cell never changes direction electron spinning. The dying cell then maintains enough residual energy to be attracted by the new born cell and becomes its parasite. The DNA of the new cell now must perform double work; support the new cell and the parasite cell, with the result that the life span of the new DNA will be shortened. The oncoming new DNA must now have enough energy to support the dying cell and the parasite cell. Furthermore, it cannot rely any longer on the body support due to a weak or unbalanced magnetic field. In a desperate attempt

to be liberated of the parasite cell, the DNA sends a message to the enzymes. Most of the time the enzymes are too busy in the assimilation of the processed food of modern civilization with the result that the DNA of the new cell has to support two parasite cells, and so on…

When the combined energy of the parasite cells becomes greater than the energy of the new cell, the new DNA loses control over the RNA in the formation of protein. The RNAs are then formed by the combined genetic code of the DNA of the parasite cells. This will occur when enough or greater genetic code in the summation of parasite cells overcomes the control of the normal DNA. The DNA code so completed may have all the information necessary to sustain life, but in the wrong sequential order; and a new strange life in the life is born. This phenomenon is known as cancer. From the above explanation it is quite obvious that a cell in the dying process must lose its entire energy to be removed by the blood or lymphatic system; otherwise, the body must have enough enzyme supply to destroy the cells before they become parasites.

To prevent and control cancer, several methods can be applied:

(1) Magnetic intensity, homogeneity, and orientation in the human body must always be maintained at the optimum level.

(2) Mineral balance and proper distribution are essential.

That is, the cell needs copper to convert AC impulse from the nervous system to DC energy. This energy is necessary to maintain the DNA in the proper oscillatory frequency.

Aluminum and zinc are necessary to maintain the voltage level.

Iron is necessary to accumulate inductive energy EMF.

The most important elements, magnesium and oxygen, are necessary to insure the total collapsing effect of the iron when the electron orbital spinning in the nucleus reverses.

In modern civilization, where the entire environmental surrounding is bound to destroy humanity, the above conditions are essential for survival. While natural food consumption maintains the proper mineral balance, and may maintain the enzyme proportion in the high level, the most important factor is to supply the body with enough energy to maintain the magnetic field as described above. However, we must clarify that we call the magnetic force any energy capable of attracting or repelling matter. In reality, there are four different types of magnetic force, each one caused by a different physical phenomenon.

(1) *Permanent Magnet* ~ If we try to magnetize a copper bar, we will never succeed because in the copper the outer orbit of the electrons increases the kinetic energy

without shifting electrons from one orbit to another. We will obtain the same effect if we try to magnetize a bar of nickel.

Now let's take a copper-nickel alloy, such as alnickel, and expose it to the EMF of a high inductive coil. The directional spinning of the electrons' orbit in the nickel does not change, but the orbital spinning of the electrons in the copper reverses its direction. Result: any atom of nickel strongly attracts an atom of copper, creating a bipole. The energy summation of all bipoles combined creates one of the strongest permanent magnets on the market --- alnickel V. Every permanent magnet then must be composed of at least two different atoms, one of which is willing to change the orbital spinning direction of the electrons. This type of permanent magnet is not recommended for any therapeutic purpose for the human body.

While in mice tests this type of permanent magnet seems to be very promising (Barnothy, Pressman, etc.), the physical working principle is similar to the H bonds' attraction that holds together the DNA. The tumor in the mouse disappears due to the disassembly of the DNA in the affected cell by the demagnetization effect of the H bonds. At the same time the genetic code of the healthy cell is also altered and the consequences in the following generations could be very undesirable.

(2) *Electromagnet* ~ This type of magnetic field obeys the third Newtonian law of motion (to every action there is always an equal and opposite reaction).

If an iron bar is inserted in the center of an inductive coil, every electron traveling along the coil wire forces one electron in the iron bar to travel in the opposite direction. This type of magnetic field is not recommended for any therapeutic purposes. On the contrary, it has been proved to be detrimental even in mice tests. Electrons flowing along the magnetic coil will shift electrons from one part of the body to another. In this process RNA type viruses of negative polarity will be shifted from diseased cells to healthy cells in the same fashion as electrons. Furthermore, the shifting of electrons deprives the healthy cells of the energy necessary to support life and will produce severe side effects of dizziness that will last for several days thereafter.

(3) *Electrostatic Attraction* ~ When we rub a bar of hard rubber or a bar of amber, one acquires electrons in excess and the other loses electron from the outer shell orbit. Consequently, one will attract particles rich in electrons and the other will attract particles poor of electrons. This type of magnetic attraction is not recommended because one will weaken the energy of the normal cells; the other will increase the negative potential of the skin of the cancer cell, thus facilitating the growth of the cancer.

(4) *Thermomagnetic Field* ~ The thermomagnetic field is the product of the Thompson-Peltier effects combined, known in physics as the Seebeck Effect.

The thermomagnetic field is responsible for the general gravitation system: heat (sun) attracts cool (planet) and vice versa. According to Dotto law:

$F = G\ M'M''/[\text{sq root of}]\ 1-(K'/Pamu/K''/Eamu\ 4/3\ pi)^2 / R^2 / [\text{sq. root of}]1-(K''/K1)^2$

K' = warmest body; K" = coolest body; Pamu = 1.00759; Eamu = 0.00055; G = 6.66 x 10^{-8} cm^3 g^{-1} sec^{-2}

The Newtonian law of attraction $F = G\ (M'M''/R^2)$ can be applied only between two masses having the same temperature.

This type of magnetic field is the only type of energy proven to be beneficial to animals and humans. Since humans have lived in this constant magnetic or gravitational field for millions of years, the body has become very sensitive to any variation.

The Thompson Effect

One end of a copper rod is heated and the other is cooled. If the hot side is heated high enough, it will thermally increase the kinetic energy of the outer orbit electrons to a point where their kinetic energy ($1/2\ mv^2$) will be greater than the work function and allow them to discharge into space. Due to the copper conductivity the electrons, instead of dissipating into the air, will shift in tremendous quantity toward the cools side in straight lines, following the heat propagation velocity. By reaction, excited electrons for the cool side will travel in the opposite direction at the speed of a particle ($1/2\ mv^2$) toward the hot side encircling the copper rod by gyroscopic phenomenon and following Fleming's rule. The product is very low voltage (few millivolts) as a resultant of the electrons traveling in a circular motion. But, as in any electrical circuit, the EMF in the copper rod is governed by Ohm's law (E/R = I) and will be in the range of several thousand amperes.

The Peltier Effect

In a metal alloy bar (such as constantan, 60% Cu, 40% Ni) one end is heated and the other is maintained cold. When the hot end is heated enough, electrons of nickel and copper atoms become excited. The electrons of nickel force the electrons of copper to reverse orbital spinning (as described in part 1). By centripetal force electrons form the cool side shift toward the hot side. The hot side becomes negative in respect to the cold positive side, exactly opposite to the Thompson effect.

Of course, the Thompson and the Peltier effects are temporary; they last only until the proportion between the cool and the hot side reaches the electrons' numerical balance.

Let's now combine the Thompson and Peltier effects together in the thermocouple fashion. In the Thompson effect the electrons move from the hot side toward the cold side. In the Peltier effect the electrons travel from the cold toward the hot side, and back to the hot side of the copper to complete the circuit. The temporary phenomenon of the Thompson-Peltier effect now combined becomes permanent for as long as the

temperatures of the hot and cold junction are maintained unbalanced. In physics this is known as the Seebeck Effect.

Let's now reduce the Peltier Effect rod to the minimum possible length according to the equation:

Con R = Cu R x pi. The electrons, in the reaction phenomenon described in the Thompson Effect, instead of traveling toward the copper hot junction, will be attracted by the centripetal force of the electrons spinning in the Peltier Effect, and the free electrons in the Peltier Effect will be attracted by the hot junction of the Thompson Effect. Furthermore, to obtain a sawtooth effect of a unijunction transistor, a silicon pellet is added between the two cold junctions, and the EMF becomes unidirectional with oscillatory frequency of approximately 1.9 megacycles. In this condition 95% of the EMF traveling in linear velocity motion equal to the heat propagation will be accelerated time and time again by the hot side of the ring, and the resulting kinetic energy in the orbital electrons will be so great that the various electron shells will travel on the same orbital plane. As a result, portions of the atom proton energy will be exposed toward the center of the ring. The phenomena that then occur in the Ring Device are unique in their nature and not replaceable by any artificial means.

In the Ring Device the following phenomena can be detected:

(1) The voltage is maintained at a minimum of 25 to 45 millivolts. This EMF will produce 120 gauss at the ring circumference, and 10 gauss at the center of the ring. This is approximately 5 times the earth's magnetic field. This magnetic field is sufficient to maintain the orientation of the human body, but too weak to jeopardize the orbital spinning in the H bonding of the DNA.

(2) In the electromagnetic field and permanent magnet the electrons travel from the south toward the north pole. If this type of magnetic field is applied to the human body it will have the same deteriorating effect as if the jumper used to start a car is connected to the opposite polarity of the battery. In the ring the EMF travels from the positive pole toward the negative in the same fashion dry batteries are instantly charged by inductive methods.

(3) Like in any electrical circuit, the energy across the ring is regulated by the Ohm law where ($E = .045$ volt / $R = 5 \times 10^{-6}$) $I = 9{,}000$ amp, as explained before.

It is quite obvious that there is enough energy to supply every one of the 6.3 trillion human cells the proper energy needed. The energy from the ring is transferred to the body by an inductive method similar to the one used to instantly charge a dry battery. During the treatment the ring is maintained at constant slow motion of 1-1/2 inch per second. This velocity is sufficient to cause energy transfer from the ring to the body by inductive method, but not fast enough to create any disturbance to the electron orbital spinning in the DNA H bonds. In the process, the parasite cells (cancer cells) are also charged to the energy level of the healthy cells, and like a faulty car battery,

they release the energy and reverse polarity at each end of the inductive effect. Four to five passages of the ring near the tumor are sufficient to deprive the cell energy and to reverse the orbital spinning of the electrons in the phosphate bonds. In this condition, the bases of the DNA repel each other and the DNA dissolves. At the end of the cell life span the tumor disappears. Of course, for the Ring to be effective, the treatment must start when the disease is first detected. Radiations of any nature prior to the ring treatment will accelerate the orbital electron spinning in the DNA H bonds and will jeopardize the benefit of the Ring treatment.

From the above clarification it is quite evident that the Ring Device does not remagnetize, reorient, and homogenize the magnetic field in the body by external magnetization, but by energy transfer in the inductive fashion.

Let's explain with an example. Let's consider an electric generator where the rotor is formed of a plurality of magnetic poles. If the rotor is rotated by external means, the coil winding of the stator absorbs and transfers EMF at the expense of the magnetic pole (electric generator).

If the EMF is supplied to the stator winding, the rotor generates power (electric motor) at the expense of external EMF, while the magnetic pole of the rotor will gain intensity.

The human body is like a rotor with an infinite number of poles, DNA frequency, field orientation, etc. By applying energy from the stator (Dotto Ring) the body will create power, while the magnetic level, DNA H bond and the field orientation gain intensity. The Ring then transfers energy to the body and does not force the body to give up energy by means of external magnetic field. Furthermore, as will be explained later, the electrons at the end of sugar phosphate rod and in the atom of hydrogen (H bonds) present at the ends of the bases (nucleotides) have the electron orbital spinning in different directions. This is to ensure that sugar is bonded only with phosphate, adenine only with thymine, and guanine only with cytosine.

When in the 6 billion bases joined together to form the human DNA, one or two electrons spinning in the phosphate bond are forced to reverse orbital direction by means of a cosmic ray, radiation, high energy photon, microwave beam (radar), permanent magnet, high intensity electromagnet, laser, etc., due to the property of the sugar crystal of rotating the plane of polarized light to the right, the DNA immediately will release the hit base and attract a new one to reestablish the genetic code. But now it is quite possible that the new base connects itself upside down: phosphate with phosphate, sugar with sugar, and adenine or thymine with cytosine or guanine. The elements attract each other because of opposite directional spinning of the electrons in the H bonds and not because of different chemical composition.

The DNA now is completed again but with a wrong sequence in the genetic information. By reestablishing the homogeneity of the magnetic orientation of the

DNA by means of inductive energy, the wrong base is rejected again and the proper one is attracted. In nature plants like peach, apricot, etc., restore the proper DNA sequence by means of glycosides, always present in the fruit pit. Glycosides are solids, generally crystalline, and most have a bitter taste. Their solution shows the property of rotating the plane of polarized light to the left. Under the influence of naturally occurring substances (enzymes) present in trace amounts in neighboring cells, glycosides can be split into one or more sugar and non-sugar portions termed Amygdalin.

Amygdalin shows greater property of rotating the plane of polarized light to the left than the crystalline sugar to the right. Under the influence of ultraviolet light coming from the sun, the plane of polarization is shifted to the left, and the proper orbital electron spinning in the phosphate base is restored.

The DNA readjustment effect is proportional, of course, to the amount of ultraviolet light available to the plant. For humans, the use of inductive energy is more effective and less complicated.

The Thompson-Peltier Effect then, such as produced in the Ring Device, is unique in its form and energy creation and cannot be replaced by any artificial means.

The ring is capable of creating a field feasible for use on the human body as a product of a voltage intensity similar to the voltage measured across a normal cell, but with a current intensity greater than the total amount of energy measured across the entire human body (3-6,000 amps).

The Aging Process

To understand the human aging process, let's now examine the structure and the function of the DNA. Imagine a flexible ladder 1 meter (39" long) composed of 6 billion steps. Each step has the form of two capital T's facing each other. The horizontal line of the "T" has 70% of its length made of sugar and 30% of phosphate.

The vertical line is of a different composition: adenine or guanine, or thymine, or cytosine.

At the vertical ends of the "T" there are atoms of hydrogen (The hydrogen, first element in the atomic chart, is composed of one proton and one electron).

Refer now to the alnickel permanent magnet explanation.

At the end of the phosphate rod the orbital electrons spin clockwise. At the end of the sugar rod the orbital electrons spin counter-clockwise. In the hydrogen atoms, at the end of adenine and thymine, the electrons spin clockwise, and in the hydrogen atoms at the end of guanine and cytosine they spin counter-clockwise. This type of "T" is called base or nucleotide. The DNA is then formed by 12 billion nucleotides facing each other and connected in a straight line to form the double helix. This is the genetic code and every one of the 6.3 trillion cells of the human body has at least one.

To form a new cell the DNA must repeat itself. This is accomplished by splitting the ladder along the middle of the step and reforming two DNAs absolutely identical and in the same sequence. To form two DNAs, another 12 billion nucleotides are necessary.

Inside the cell nucleus there are constantly at least 8 different types of virus, 4 RNA types (negative charge) and 4 DNA types (positive charge). Every pair of viruses (one RNA and one DNA type) attracts each other to form a dipole. They do so first to protect themselves against any external magnetic disturbance, and second to accumulate energy in the following manner:

Inactive viruses are crystalline forms, but in active status, such as inside the cell nucleus, they reveal one RNA or DNA core covered with protein. Of course, even inactive status they still maintain all the properties of a crystal, and as a crystal they are very sensitive to the high sound frequencies.

Under sound frequency up to 5 megacycles the two viruses continuously strain each other and produce energy due to the piezoelectric effect (the same principle is used in the energy conversion of the supersonic generator). In the ultrahigh sound frequency over 5 megacycles, an isolated inactive virus can be excited to alter the transition temperatures or Curie point and disintegrate (Ruben). The human DNA (like a Yogy antenna one meter long) is tuned to any radio emission between 375-385 megacycles)

Furthermore, the DNA is under the constant influence of charged ions traveling through the nervous system and acting as a modulation frequency. The combined action of the two physical phenomena force the DNA to emit a high frequency sound in the range of 1.9-2 megacycles in order to detect, by returning echo, what type of protein is missing in the cell. These sound frequencies are not only necessary to the DNA in scanning the type of RNA to produce, but also to maintain active the virus in bipole form by means of the strain effect.

To control the energy level from the piezoelectric effect, the RNA type virus covers itself with phosphate and the DNA type virus with sugar. In forming this special type of coating the virus, like any living organism, produces waste. These wastes are accumulated in the center of the rod just formed and will be called adenine, guanine, thymine or cytosine according to the type of virus in the bipole. The process to make the coating is accomplished at the expense of the electrical charge accumulated by the piezoelectric effect. At the end of the charge, to remain active the group of viruses removes the coating that now is in the form of a capital "T" and exposes itself to the high frequency sound produced by the DNA and the process starts all over again.

Due to the described phenomena, the DNA has always enough bases available to produce RNA strains and to reproduce itself. Now, let's go back to the flexible ladder composed of 6 billion steps. Suppose we twist this strange ladder so many times to have only a few steps for every turn of the coil so formed (these coils are called base

pair per turn). Since every base has a different polarity according to the code formed by passed generations, the DNA can be compared to the multi-polarity rotor of an alternator. In the alternator, the speed is inversely proportional to the number of poles and the output power is directly proportional to the energy applied. At every electrical impulse flowing through the nervous system the DNA moves back and forth as many degrees as one base is separated from the next one. The more base pairs per turn the less degree the DNA has to move and less energy is required to make it vibrate.

Then there are three controlling factors for the DNA to reproduce itself and create a new cell:

(1) The kinetic energy of the electron in the H bonds.

(2) The number of the base pairs per turn in the double helix.

(3) Energy and the frequency of charged ions traveling along the nervous system; i.e, the DNA of the embryo cell in the mother's womb has 46 base pairs per turn; the kinetic energy of the electrons in the H bond is weak; charged ions coming from the mother's body are strong. Result: the DNA produces one cell per second. After 6 weeks of pregnancy, the DNA in the cell of the embryo has 34 base pairs per turn, the kinetic energy of the electrons in the H bonds increases, the charged ions from the mother are unchanged; the DNA produces one cell every minute, and so on. By the time the fetus is in the 10th lunar month, the single DNA (half from the mother, half from the father) has already reproduced itself more than 6 trillion times.

When the baby is born, the slowing process of reproduction increases. At the age of two, the DNA winds again to have 22 base pairs per turn, 14 at the age of 21, and 10 at the age of 35. From the age of 35 to 55, the 10 base pairs per turn in the DNA do not change. At approximately the age of 55, the base pairs per turn are reduced to 6. By this time, the kinetic energy of the electron in the H bond and the energy of the charged ion become very weak and the DNA stops reproducing itself, and the aging process beings. To slow down the body aging process, three factors must be considered:

(1) Ways of stretching the DNA to increase the base pairs per turn back up to 10, by means of energy in motion up and down along the body as in the Ring Device.

(2) Increase the electron kinetic energy in the H bonds by means of proton pulling force. The proton energy available (as previously explained) toward the center of the ring is high enough to attract (in the vacuum) one electron 20 feet away)

(3) Increase the energy of the charged ions in the nervous system by means of exercise and proper diet.

At this point it is necessary to clarify one important factor that is the basic secret of life creation. Without explaining the working principle of this secret, we will never understand the vital importance of the homogeneity and orientation of the magnetic

field in the human body. All the 6.3 trillion DNAs of the human body are absolutely identical, all are tuned to the same resonance frequency, all have exactly the same genetic code sequence. Yet the 6.3 trillion cells in the human body, where each DNA is enclosed, are all different, and each one of these cells fits exactly the proper place and functionality in the human system. How is this possible?

The human DNA, as mentioned before, is approximately 39 inches (1 meter) long and has 6 billion steps formed by 12 billion base pairs. The entire length of the DNA is necessary to maintain and transmit from generation to generation the entire genetic code. Yet only a portion of the DNA (different in every cell) is used to create a specific cell. How is this accomplished?

Suppose we have a thread one meter long. On this thread we insert 46 nylon light beads 1/2 inch long. Now let's insert this strange chain in the center of an electrostatic tube with bipole orientation. After a few seconds all the nylon beads will be charged with the same electrostatic energy and they will repel each other, leaving an interspace between them. They will repel each other, but not with the same force. The interspace between the beads located near the north side of the electrostatic charge will be shorter; gradually toward the opposite polarity of the tube the interspace will be longer. Now the only part of the thread we see is the one not hidden by the beads. Let's now call the thread DNA and the 46 beads chromosomes. Since the chromosomes act as a shield, the only portion of the DNA that controls a specific cell is the one of the interspace between the chromosomes, which for every cell has a different length according to different magnetic intensity, polarity and orientation in the human body. Each chromosome encloses 1,250 DNA lengths (genes) and each gene is formed of 100,000 base pairs (microgene). Of the total 6 billion steps of the ladder (DNA), only 250 million are really controlling the cell life.

The chromosomes appear immediately after the DNA is formed and they disappear when the cell is completed and just before the DNA is ready to repeat itself, to reappear again only in the new DNA. If the chromosomes of the new DNA, due to the phenomenon previously explained, have the wrong interspace sequence, it is quite possible that the DNA will produce, i.e., in the neck a cell that belongs in the kidney or vice versa. This also can be called a cancer.

Furthermore, like in a musical instrument, the sound produced by the DNA in the scanning system has different harmonics according to the chromosome's interspace.

The virus responsible for the creation of nucleotides in a different group of cells of different harmonics, adjusts the equilibrium potentials of the component charges in the crystal lattice. This pressure effect in the electrical field distribution governs the final crystal structure of the many compounds of the virus. If a group of RNA type of virus with a final crystal structure as a result of harmonics of one group of cells is transferred by means of electromagnetic reaction in a different group of cells, under

the influence of the new harmonics, it will alter the transition temperature (Curie point).

In this transaction it will lose the protein coating and release the core DNA to control the protein creation in the new cell (Ruben). As a result, a new type of cell will be created different from any surrounding cell, and this also will be a cancer cell.

From the above-described phenomenon, well known in physics, the Temin theory that the RNA type virus uses its own RNA core as a template to modify the structure of the genetic code and create the reversal of the DNA is absurd. If the phenomenon exists, it could not be a creation of the present civilization, but has existed from the beginning of time. And there are no records available of claims of apes deriving from humans.

Theories #1 and #4 of the introductory explanation support the principle that some forms of cancer and leukemia are caused by isolated viruses. In this case a physical principle known as the Pyro-Piezoelectric Effect will be with solution of the problem.

If a Rochelle salt crystal is rapidly cooled from 25° to 0° C., the polarization increases so fast that the normal conductivity cannot bring about equilibrium and a transient potential as great as a thousand volts can be produced between two electrodes contacting the crystal (Ruben).

Since in the isolated virus crystal, the RNA or DNA type core acts as an electrode between the two poles, when the voltage potential overcomes the core's DC resistance, the energy discharges across it will be so great as to disintegrate the virus core like a common electric fuse. The same phenomena, of course, is applied to the joint virus (one DNA and one RNA type) existing in the cell nucleus and responsible for the DNA creation. Because of the electrical principle that in an inductance, two joint EMFs opposite and contrary eliminate each other, no voltage will appear across the joint virus.

In an experiment with dying AKR mice (mice carrying leukemia), a constant laboratory temperature of 35° was maintained. The cage containing the mice was placed two times a day for 20 minutes each time in a small refrigerator where temperature was kept at 0° C. After 5 days of treatment the mice were sacrificed and pathological studies revealed no evidence of lymphosarcoma. A piezobaric chamber, where a temperature body change of 25° C can be obtained in less than 1 minute, is under construction to repeat the experiment.

Conclusion

By evenly re-establishing the orientation of the body's magnetic field, the virus groups responsible for the manufacture of the nuclei (necessary for the reproduction of the DNA) are bound to stay only in the specific group of cells tuned to their own resonance frequency with no chance of spreading to other parts of the body.

With the correction of the environmental resonance frequency of a group of cells, a virus out of position will become inactive in the same fashion as a portion of a variable capacitor not facing the stator. In Theory #3 (Dotto), the Ring re-establishes the proper number of base pairs per turn on the DNA double helix due to the phenomenon known as the Wunder Effect.

In a vacuum, a suspended secondary coil inserted in a primary coil of fixed number of turns, adjusts itself to the same primary number of turns when voltage is applied, with capability proportional to the current intensity and inversely proportional to the square of the spring reaction strength of the secondary coil. This principle is widely applied in automatic tuning devices for modern color television. By applying to the human body voltage, EMF and magnetic intensity similar to the value existing in the DNA of normal cells (in the human between the ages of 35 and 55) a voltage of 45 to 75 millivolts maintains a linearity of 10 base pairs per turn in the double helix (Crick-Watson). The DNA of the cancer cell adjusts itself to the proper level of functionality, regardless of cell condition, since absorbed energy will be inversely proportional to the existing cell energy level.

In the case of 6 base pairs per turn in the double helix (humans over 55), when the DNA stops the reproduction capability, the base pairs per turn are triggered back to 10 and remain so as long as the magnetic intensity is reapplied at least once every 14 days. This results in slowing down the aging process.

Another important factor must be clarified: In widely known mice experiments (Presman, Barnothy), a combined action of a constant permanent magnetic field and microwaves in the gigacycle range proved to be very effective in causing tumor regression in mice. This phenomenon is caused by the disturbance action of the microwaves on the normal orbital spinning of electrons in the DNA H bonds. But we must not forget that to the humans we must give the right to live, not merely to survive. However, frequency in the range of 1 to 3 mc and modulation frequency of 80 to 200 kc is known to penetrate deeper into the human body and is capable of breaking the thin skin of the cancer cell without jeopardizing the DNA code of normal cells (Presman).

For this reason, the Ring is pretuned on the Peltier junction to the average frequency of 1.8 mc and modulation frequency of 100 kc to obtain a current fluctuation chopping effect similar to a unijunction transistor. The Ring also is a 350 ohms television antenna, where the lower band resonance is tuned to a VHF (Thompson Effect junction) and the upper band (Peltier junction) is tuned to UHF resonance. The upper frequency then maintains the activity of the normal cell on the correct level, while the penetrating low frequency neutralizes the activity of the cancer cell.

Theory #2, which postulates that cancer cells, to some extent, may be considered as parasitic cells, is proven correct as far as the Ring is concerned. The Ring is an inductive coil. In the motion along the body, the Ring recharges the cells to the proper

desired level. While the normal cells retain the charge, the cancer cells behave like a faulty battery. At the passage of the Ring, the temporary magnetic charge collapses in the same fashion as transformer laminations.

This collapsing effect is detectable by electrodes of an EEG sensitive to electrical brain impulses. By synchronizing a recorder to the Ring velocity, the location of the collapsing tumor can be detected within 5 cm accuracy.

Many years of investigation have proved the Ring to have no detrimental or side effects. On the contrary, it has proved to be very helpful for people who have suffered from exposure to radiation, cobalt, linear accelerators, etc.

For all the reasons stated above, the Ring should be considered primarily as a tool for physicians in disease prevention and disease control, rather than a cure.

Signed,

Dr. Gianni A. Dotto
(8 February, 1972)

Author of below?

http://orgoneproducts.org/blog/anti-aging-device-electromagnetic-radio-frequency-generator/

DOTTO RING - Anti Aging Device- Electromagnetic Radio Frequency generator

The last month has been an Odyssey. The good news the Radio Frequency version of the Dotto Ring is in. I will call it the Heavy Gravity machine for now. The field strength is about 120 Gauss with a frequency of 1.9MHz. This is the frequency that Dotto claims triggers DNA replication. Anyone interested in this device, I urge them to read up on Dotto.

The Reader's Digest is that Gravity=Life. More gravity=More Life or Negative Entropy or Anti-aging. Dotto studied an area in Northern Pakistan called the Hunza valley where the average lifespan was over 120 years old. Most people attribute the longevity of the Hunza's to the food and the water found in that particular area. Dotto discounted this as the reason for the long lifespans. Dotto said the region contained magnetic anomalies not found anywhere else in the world. The Hunza valley has a unique juxtaposition of a mountainous glacier area next to a hot valley. Dotto states that it is the thermal unbalance of the region that creates a magnetic field stronger than the surrounding area.

The original Dotto Ring is a Thermo-couple that creates a hot and cold magnetic field equivalent to 5X the field strength of the Hunza valley. According to the legend, Dotto reversed people's age over 20 years. The premise is that the device created magnetic induction or energy transfer directly into the DNA. The DNA is a spiraling coil like a caduceus, as you age the coil shortens and tightens as a function of conservation of energy.

The DNA bases are proteins that hold magnetic charge like a battery. The proteins convert the magnetic energy into electrical energy to run the processes of the cells. This is known as pre-natal chi by the Chinese. The Chinese system believes you have a limited amount of pre-natal Chi and that once it is exhausted you die.

The RNA is on both ends of a DNA base, as the cells replicate pieces of the RNA are lost. The RNA strands shorten until they are too short to communicate to the DNA to split.

This essentially is also death from a western scientific point of view. In addition, as the DNA coil shortens and tightens electrical impedance increases. Electricity is harder to run through the DNA coil. The replication process slows down as impedance increases. As you age, you notice you do not have as much energy and you need to

sleep more. The feeling that people are growing younger around you and that you are growing older is another function of loss of energy within your genetics. The Bible has stories of people living for close to 1000 years old. We live for approximately 120, why the difference?

GRAVITY… and the use of Nuclear weapons. The garden of Eden was a heavier gravitational environment. Nuclear radiation has degraded our DNA through unhealthy mutations. Essentially genetics is a function of consciousness, higher evolved beings have longer DNA strands. There are functions within the junk DNA, that when rearranged will lead to much extended lifespans. My contention is that this can be achieved in this lifetime with the use of Bridge technologies such as the Heavy Gravity machine.

Now for the test results since I have received the machine on Feb 19th. For now all experiences are anecdotal and not the result of any medical tests. While the device is on after about 10 minutes, it triggers a response from the parasympathetic nervous system. That is relaxation, it nothing else happens it is a great meditation machine. The connective tissue in the body starts to soften and relaxation flows everywhere. Bowels movements are heavy, who needs colonics. The first two treatments my eyes were hurting while the machine was on. I am now noticing a month later, I am not squinting nearly as much. The most remarkable improvement has been my hearing, I can hear out of my right ear as well as my left now. There is surprisingly little wax buildup either even though I am a habitual cellphone user.

Over the last month I have had a tremendous amount of stress, tax troubles, family members dying and possible harassment from my new landlord due to condo conversion, yet I have held together and accomplished more in the last month than at any previous time in my life. This I attribute to the machine. Emotional detox, wow! The machine seems to work on different areas of the body almost like it is alive, quite strange. On two separate occasions, my liver was moving like a heartbeat and the rage that was coming off it was intense. I would say probably limit treatments to 30 minutes per day to start and not the 2 hours or more that I do. I have lost weight from my midsection, this may be due to bowel movements or perhaps there is a switch in the type of hormones being released into my bloodstream. I don’t need as much sleep and definitely have more energy. For now, I am much more emotionally reactive, moving from vulnerable states to angry and vengeful. These moods pass quickly and are akin to the Reichian therapy sessions I use to go through. Organ pulsation is a sign of body armoring dissolving and the person becoming whole.

I am a lot less self-conscious and more spontaneous in the last month, I seem to just do things without thinking. One of the thought forms that I have been focusing on generating on the last few years is unlimited abundance, the irony of the recent problems with my landlord may lead to a buyout of my apartment, an interesting way

to create abundance. What I am beginning to see is that this device creates compression, everything seems to speed up.

From the above website (orgoneproducts.org):

Orgone is the universal Life force, the basic building block of all organic and inorganic matter on the material planet. Coined by Dr. Wilhelm Reich, Orgone has been called by the Great mystics and philosophers; Chi, Prana or simply the Force. Dr. Reich, an Austrian scientist, philosopher and psychoanalyst; developed a technology to tap into the Cosmic Orgone Sea to provide a continuous stream of Life-force energy.

The possible uses for this device are only limited by your imagination. for less than the cost of a Doctor's visit, you could have in your hands, a device that could lead to the end of all disease. Reported to heal Cancer, Aids, not to mention a few more mundane illnesses like Allergies, Asthma, Chronic fatigue and Candida. Why have I not heard Orgone? Money and power pure and simple, the AMA scared of losing it's monopoly on medicine ($$$$), conducted a witchhunt which ultimately led to Dr. Reich's death in jail for this cutting edge technology.

Meditation Video using the Xcalibur Magnetic Field Generator with an Age Reversal Subliminal. The Xcalibur machine is based on the Dotto Ring a suppressed Anti Aging device from the 1980's. Dotto after studying the Hunza valley believed it was the enhanced gravity field of the area that caused the life extension anomalies found in the Hunza tribe. There are reports of individuals living over 150 years..
This machine replicates the Dotto frequencies of 1.9-2.1Mhz with a magnetic field of over 120 gauss. Dotto claimed that his device will extend the telomeres, the aging clock of the cells. We are in the very early stages of testing. This machine will be included in the suite of radionic technologies found at
the Ascensionenergyprogram.com

US Patent # 3,839,771 Method for Constructing a Thermionic Couple

October 8, 1974

Giani A. Dotto

Abstract

A method for constructing a thermionic couple comprising an apparatus in the form of a ring or loop of metal such as copper having high electrical and thermal conductivity. The ring has spaced ends forming a gap joined by a bridge member formed of material having significantly lower electrical and thermal conductivity than the ring. A substantial thermal unbalance is induced between the junctions of the ring and the ring member. The width of the gap and the effective length of the bridge member is adjusted to produce a recurrent thermoelectric balance, resulting in repeated changed in the energy level of the metal atoms of the ring.

Summary

In a typical embodiment of the present invention, an electrically and thermally conductive metal strip has end portions thereof bridged by a member of a material having substantially different thermoelectric properties. Means are provided to establish a substantial temperature difference between the opposite end portions of the metal strip and bridge member, with an appropriate adjustment being made with respect to the point of connection of the bridge to one end portion of the strip, to provide a loop wherein oscillation involving high electrical excursions occurs, resulting in continuing changes in energy levels of the metal atoms in the strip.

Figure 1 is a plan view of one embodiment of the apparatus.

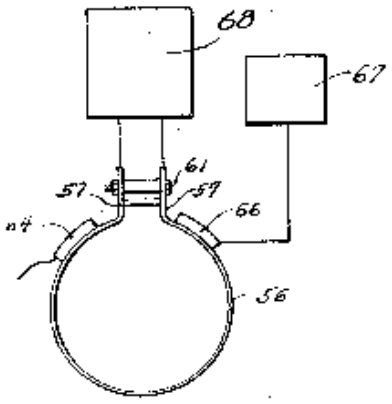

Figure 2 is an enlarged fragmentary section showing detail of the bridge member and opposite ends of the ring of the embodiment in my invention shown in Figure 1.

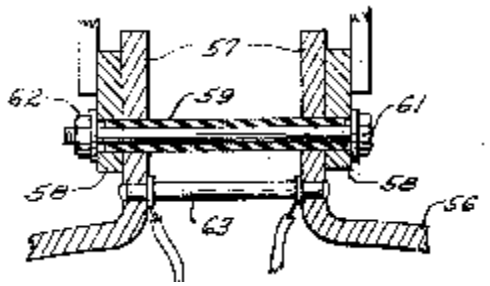

Description of the Preferred Embodiments

Referring now to Figure 1 and Figure 2, a ring or loop 56 is formed with spaced apart ends 57 defining a gap therebetween. In an embodiment of the invention constructed and operated successfully, the ring was formed of a copper bar having a width of 9 inches and a thickness of 1/2 inch, formed into a loop approximately 27 inches in diameter, with a gap between the ears 57. The copper material used was an annealed copper having a purity of 99.99% copper, and an electrical resistance of [1.7 microhm-cm] ohms-circular mil per foot at 20° C. This is the international standard of resistance for annealed copper and is equal to 100% electrical conductivity. The thermal conductivity of this copper is in the order of 1 calorie per second through a thickness of 1 cm and across an area of one square cm at a temperature difference of 1° C.

On the outer sides of the ears 57 there are blocks 58 of insulating material which are both electrically and thermally insulative. Insulating tubes 59 (one shown in Figure 2) extend through the blocks 58 and the ears 57, providing an insulating passage for bolts 61 having suitable threaded fasteners 62 at one or both ends. This provides a means for adjusting the gap between the ears 57 without short-circuiting across the gap either thermally or electrically.

Attached to the ears 57, as by brazing or the like, is a bridge member 63 forming a separate "short circuit" electrical and thermal path between the ears, apart from the continuity of the bar. The bridge member is formed of one or more rods of a metal alloy such as Constantan, which is an alloy of essentially 60% copper and 40% nickel., having a significantly lower electrical and thermal conductivity than the copper bar and hence a significantly higher electrical and thermal resistance than the ring 56. For example, Constantan has an electrical resistivity in the order of 49 microhm-centimeter at 20° C and a thermal conductivity in the order of 0.054 calories per second through a thickness of 1 centimeter across one square centimeter at a temperature of 1° C.

A means for heating one end of the ring 56 is provided in the form of an electrical heater 64 (The number is garbled in Figure 1 – looks like n4, but is 64) connected to a suitable source of electrical power, and in the case of the specific device disclosed, having a capacity of 6000 watts and a heat exchanging area on the order of 200 square inches. A means for cooling the other end of the ring 56 is provided in the form of a refrigerating coil 66 connecting through suitable tubing to a refrigerating unit 67. In the case of the specific device disclosed, the refrigerating unit has a cooling capacity of 10,000 BTU and the cooling coil 24 has a heat exchanging area on the order of 200 square inches.

A two-channel electroencephalograph 68 (Figure 1) has one of its channels connected to the ears 57, to record the potential difference between the junctions of the ears and the bridge member. While operating the heating and cooling means, and observing the output of the oscillograph, the apparatus is initially "tuned" by fastening one end of the bridge member 63 to one of the ears 57, having the other end of the bridge member in contact with the other ear, and adjusting the threaded fasteners of the bolts 61 until the output in the oscillograph is observed to fluctuate in recurrent cyclic fashion. When this condition is achieved, the other end of the bridge member 63 is brazed to the other ear 57 of the ring.

Potential differences between the ears 57 have been recorded in the order of 0.156 millivolts, and the electrical resistance of the ring is in the order of 5.27×10^{-6} ohms. According to Ohm's Law, these conditions would indicate a current in the order of 30,000 amperes, at a frequency which, from observing the oscillograph readings, is in the order of 100 kilocycles per second with a modulation frequency of 10 kilocycles.

It appears that in operation of the device there is a change caused in the energy level of the electrons of the metal (copper) atoms, which is exhibited in a form of electron acceleration around the ring. No electron emission from the ring has been observed, by irradiating the ring with ultraviolet light during operation of the device, whereupon a pale blue-white "halo" appears about the ring or by enclosing the ring in a foggy chamber "curie" method. On the other hand, if a bar of cadmium is positioned in the center of the ring and the bar is heated high enough to thermally excite the kinetic energy of the outer orbit electrons to a point where their kinetic energy ($1/2\ MV^2$) will be greater than the work function and allow discharge into space, the electron will be attracted by the proton energy of the ring. The phenomenon is shown by the deposit of cadmium on the internal service of the copper ring as if cadmium-plated.

It is sometimes desirable to maintain the magnetic field of the ring between 240 and 160 Gauss. The amount of energy is determined by the temperature difference and the amount of resistance in the ring. The high temperatures are obtained by conventional electrical heaters. As an example. A heater having three elements, each one with a 1,000 watt rating, may be used. It is desirable to obtain a temperature of about 600° to

800° F. For the cold side a conventional coil like that of a freezer cabinet can be used, and connected to a refrigeration compressor.

The invention claimed is:

(1) The method of constructing a thermionic couple capable of exhibiting a cyclic thermionic unbalance in operation, comprising the steps of:

forming a ring of material such as copper having a low electrical resistivity in the order of 1.7 microhm-cm (at 20° C) and a relatively high thermal conductivity in the order of one calorie per second through a thickness of 1 cm and across an area of 1 square cm at a temperature difference of 1° C, with the ends of the ring defining a gap therebetween;

forming a bridge member spanning said gap of a material such as Constantan, having a significantly higher electrical resistivity, in the order of 49 microhm-cm (at 20° C) and a significantly lower thermal conductivity in the order of 0.054 calories per second through a thickness of 1 cm across an area of 1 square cm at a temperature difference of 1° C;

causing a substantial temperature difference between the ends of said ring to induce an electrical potential gradient between the ends of said ring;

placing the bridge member in contact with the ends of said ring resistance between the ends of said ring;

measuring the potential difference between the rods of said ring while the temperature difference is induced;

and adjusting the spacing between the ends of said rings and hence adjusting the effective length of the bridge member until the observed potential difference fluctuates in a cyclic manner;

and then securing said bridge member to the ends of said ring.

Gianni A. Dotto (from Sympathetic and Vibratory Physics – Bridging Science and Spirtuality https://svpwiki.com/Gianni-A.-Dotto)

Gianni A. Dotto was born in Venice, son of a prominent engineer who was the designer of two hydro-electric generating plants on both the American and Canadian sides of Niagara Falls.

His father was an Italian Marquis and since Gianni is the eldest son, he would have inherited the title had he not become an American citizen. The family is directly descended from Galileo and the Galileo Coat of Arms has been adopted for use as the Foundation's letterhead.

Before World War II, Gianni had received flight training but Mussolini never did trust the Dotto family so Gianni was drafted into the Italian Army as a paratrooper.

When Italy surrendered, Gianni was able to join the American Air Force as a fighter pilot in time to participate in numerous engagements against the German Messerschmitts before the war ended.

After the war, Gianni became head of the racing division of Alfa-Romeo and started race-driving cars of his own design. His racing career ended when his wife, Renata,

served him with an ultimatum: 'Either give up racing or me.' He is a prolific inventor as he is owner of many Italian patents bearing on the automotive industry and, subsequently, just as many American patents.

He is highly educated, holding the Italian equivalent of an American Ph.D. in nuclear physics from Milan University and the same degree in mechanical engineering from another Italian technical school. Subsequently, he received a degree in electrical engineering from Wayne University in Detroit.

While Gianni was teaching at Milan University, the medical school requested the services of a physicist to collaborate with the doctors on a research project. This started him on a career as a 'Bio-Physicist;' that is, a physicist that specializes in the area of the science of physics that bears on the human body. This embraces an amazingly wide field as it has to do with magnetic fields, polarity, the various vibrations and pulsations generated by the brain and, of course, the effect of the many facets of nuclear fission on the human body.

It was there that Gianni discovered that magnetic fields induced by an electric coil and by permanent magnets had a small effect on the human body, but that a mild magnetic field created by adjacent hot and cold areas was definitely beneficial. In other words, the thermal unbalance created a magnetic field that matched the natural field of the body.

Gianni invented what is called the Dotto Ring. This device was tested in the SLoan-Kettering Hospital where it was found to cause telomeres to actually lengthen. This phenomenon leads one to believe rejuvenation of the body.

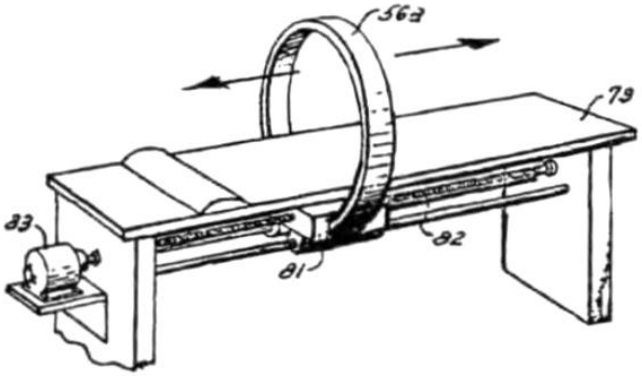

FIG. 7. *L'acceleratore thermionico in configurazione orizzontale.*

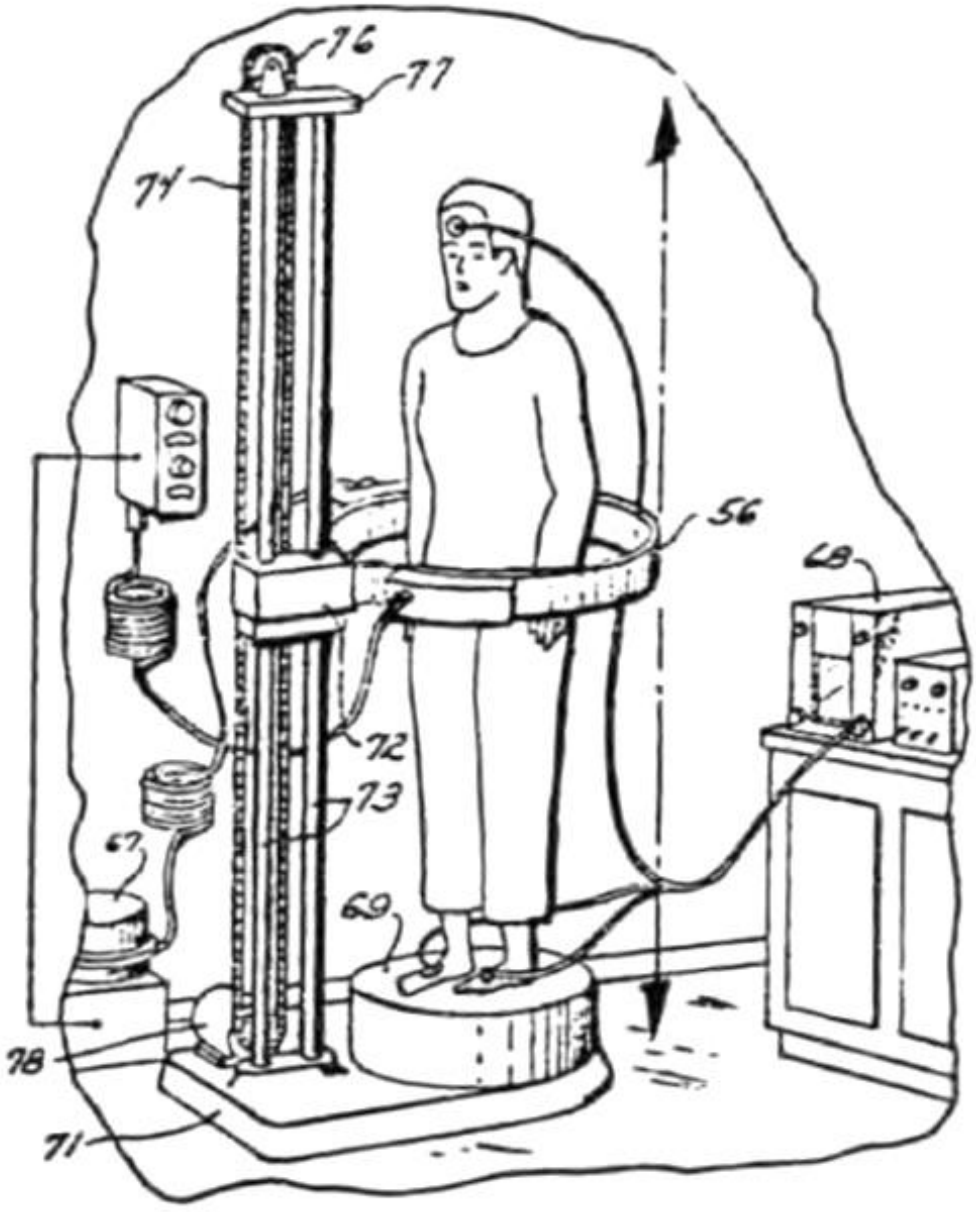
76
77
74
56
68
72
73
67
69
78
71

US Patent # 3,785,383 Electrostatic Wand

by

Gianni A. Dotto

(January 15, 1974)

Abstract --- Electrostatic means radiating electrical energy at selected frequencies of the order of megacycles per second is safely and harmlessly coupled capacitatively to tissue structure of a human being or of an animal with no significant flow of electrons for reducing sensitivity to pain, at least temporarily. The radiating means may comprise an evacuated glass envelop of inert gas and also contain an electrode that is intermittently subjects to an electropositive voltage during certain portions of the cycle to promote positive space charges within the envelope together with a controlled amount of ionization of said atmosphere and the production of selected forms of electromagnetic radiation such as infrared light, ultraviolet light, visible light, an mixtures thereof.

Figures

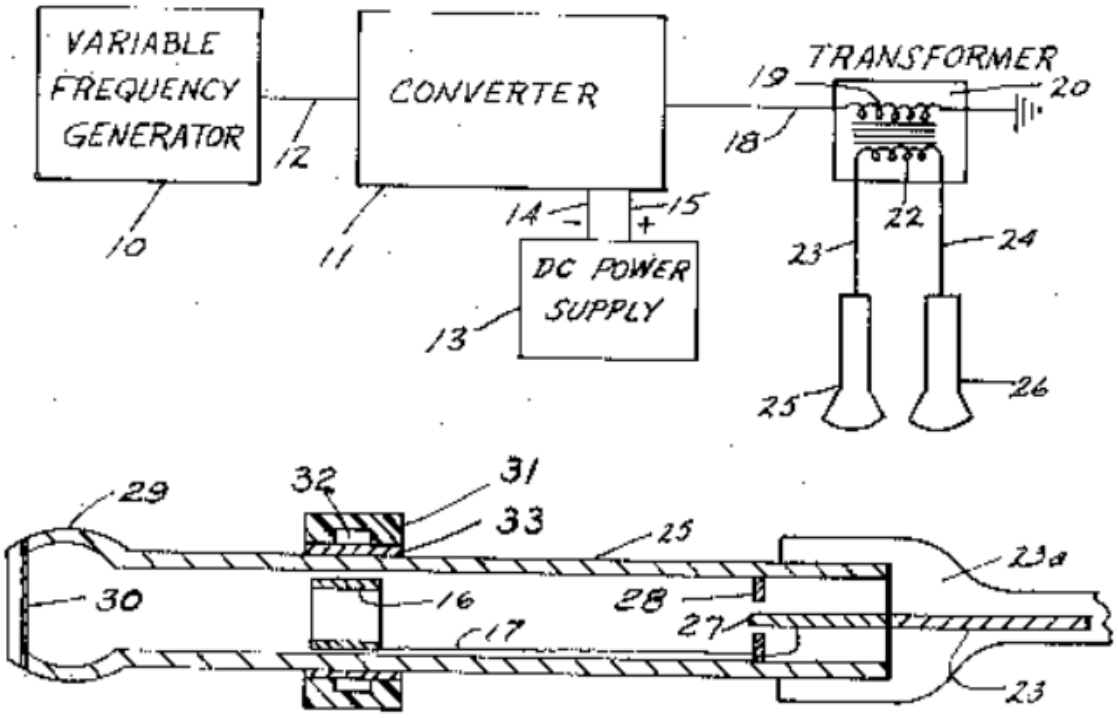

Dr. Dotto's US Patents

43 US-3839771-A METHOD FOR CONSTRUCTING A THERMIONIC COUPLE 1974-10-08 5

42 US-3785383-A ELECTROSTATIC WAND 1974-01-15

41 US-3716098-A AUTOMOTIVE APPARATUS 1973-02-13 14

40 US-3559195-A ALARM SYSTEM DOTTO GIANNI A 1971-01-26 5

39 US-3517259-A LAMP SOCKET INCLUDING AN ELECTRICAL CONTROL CIRCUIT FOR REGULATING LAMP 1970-06-23 7

38 US-3477460-A FLUID LEVEL CONTROL SYSTEM 1969-11-11 4

37 US-3459981-A SHADED POLE SYNCHRONOUS MOTOR 1969-08-05 4

36 US-3453492-A CAPACITOR DISCHARGE IGNITION SYSTEM DOTTO GIANNI A 1969-07-01 6

35 US-3447076-A ELECTRIC SPEEDOMETER INCLUDING A STEPWISE ACTUATED PERMANENT - MAGNET MOTOR 1969-05-27 4

34 US-3447110-A MAGNETIC SNAP ACTION SWITCH 1969-05-27 4

33 US-3437876-A AUTOMOTIVE SEMICONDUCTOR IGNITION CONTROL APPARATUS 1969-04-08 16

32 US-3427485-A SYNCHRONOUS MOTOR 1969-02-11 9

31 US-3419740-A Self-commutated direct current motor with permanent magnet rotor 1968-12-31 4

30 US-3413501-A Electric motors 1968-11-26 4

29 US-3401265-A Current control circuit with silicon controlled rectifiers and a phase shifting circuit 1968-09-10 8

28 US-3401279-A Low speed-high torque motor 1968-09-10 3

27 US-3394296-A Synchronous motor stator circuit employing commutator and rectifier during starting 1968-07-23 6

26 US-3382382-A Two-speed synchronous motor 1968-05-07 14

25 US-3382407-A Ignition system for an internal combustion engine 1968-05-07 14

24 US-3374689-A Worm gear escapement 1968-03-26 9

23 US-3372597-A Timer having an adjustable time interval and a rapid advance 1968-03-12 6

22 US-3349199-A Timer having an adjustable time interval 1967-10-24 5

21 US-3345915-A PDF Snap action fluid escapement for obtaining intermittent rotary motion 1967-10-10 15

20 US-3345998-A Safety check valve 1967-10-10 7

19 US-3322240-A Disc brake for washing machine 1967-05-30 6

18 US-3313895-A Rapid advance and intermittent drive mechanism for a time sequence switch 1967-04-11 6

17 US-3308873-A Venetian blind operation 1967-03-14 5

16 US-3307417-A Worm gear escapement 1967-03-07 11

15 US-3302045-A Vibrator motor with stepped rotary output 1967-01-31 13

14 US-3301233-A Rotary type engine 1967-01-31 18

13 US-3280276-A Sequential timer 1966-10-18 8

12 US-3271541-A Multi-position snap switch 1966-09-06 11

11 US-3267243-A Breaker arm assembly for a contact set 1966-08-16 4

10 US-3243530-A Escapement for producing intermittent rotary motion of predetermined increments 1966-03-29 10

9 US-3225595-A Fluid depth measuring apparatus 1965-12-28 10

8 US-3217841-A Disc brake and actuating means therefor 1965-11-16 8

7 US-3217216-A Rotary capacitor apparatus 1965-11-09 5

6 US-3196695-A Combined u.h.f.-v.h.f. indexing mechanism 1965-07-27 15

5 US-3159245-A Brake apparatus 1964-12-01 7

4 US-3081843-A Improvement in caliper type disk brakes 1963-03-19 5

3 US-3064768-A Automatic brake adjusting mechanism 1962-11-20 7

2 US-3064765-A Automatic brake adjusting mechanism 1962-11-20 4

1 US-3013636-A Brakes 1961-12-19 6

New York Times Article


The New York Times

The Life, Toil and Frustrations of Ladder 120

Student Forfeits 'Luxury' To Offer Help to Neediest

Early Evidence Rules Out Bomb in Jersey Oil Blast

News Summary and Index

The Major Events of the Day

The Other News

Overview of the Day

Millionaire Sues to End Ban on Cancer Device (1970)

COLUMBUS, Ohio, Dec. 29 (UPI)—Robert E. Lehmann, a millionaire sports man suffering from leukemia, filed suit yesterday to halt the Ohio Medical Board from enforcing a ban on a device used to treat victims of cancer.

Mr. Lehmann. owner of the 1970 Kentucky Derby winner Dust Commander, said in his Federal District Court suit that he suffered from leukemia for three years and began using a device invented by Gianni A. Dotto that he said had allayed the disease.

The medical board on Dec. 22 ordered Dr. Dotto to discontinue the "Dotto ring device" in the treatment or diagnosis of cancer in humans.

Note: Robert E. Lehmann's obituary in 1974:

PARIS, Ky., Jan, 19 (AP)—Robert E. Lehmann, owner of the 1970 Kentucky Derby winner, Dust Commander, died at Golden Chance Farm today. He was 52 years old.

Mr. Lehmann, a former Ohio construction executive and a banker in Florida, hunted big game as a hobby. He held a number of safari records, among them one for killing an elephant that had a tusk weighing more than 110 pounds.

Also note: I could find no documentation about a medical ban on the Dotto ring or thermionic couple in either the FDA's or Ohio Medical Board's records. Granted that electronic records were not yet standard in the 1970's. This article is from 2 years before Dotto's paper on the ring and 4 years before the patents. This article raises some questions: What was the result of the lawsuit? Why is there no documentation of the lawsuit or ban?

According to the FDA, who currently regulates medical devices, the FDA did not ban the Dotto ring. Below is from an FDA link, FDA medical-device-bans. I also searched all the FDA's archives.

FDA Medical Device Bans

What is a Medical Device Ban?

A medical device ban is a total prohibition on the current and future sales, distribution, and manufacturing of a medical device.

The FDA has the authority to ban a medical device intended for human use if it finds, on the basis of all available data and information, that the device presents substantial deception to patients or users, or an unreasonable and substantial risk of illness or injury, which cannot be corrected by a change in the labeling. (see Section 516(a) of the Federal Food, Drug and Cosmetic Act; 21 CFR 895.20)

How Often Does the FDA use this Authority to Protect Public Health?

The FDA very rarely acts on this authority. Prior to 2016 the FDA had banned only one other medical device, prosthetic hair fibers. The FDA found there was no public health benefit to this device. This device presented a substantial deception to patients or users about the benefits of the device. The prosthetic hair fibers did not stimulate hair growth nor conceal baldness, but could actually cause serious infections, illness, and injuries from their implantation. We believed that the labeling and advertising materials directly or impliedly misrepresented the device as safe, effective, and causing little or no discomfort, among other misleading claims.

On December 19, 2016, the FDA published a final rule banning powdered gloves based on the unreasonable and substantial risk of illness or injury to individuals exposed to the powdered gloves. The risks to both patients and health care providers when internal body tissue is exposed to the powder include severe airway inflammation and hypersensitivity reactions. Powder particles may also trigger the body's immune response, causing tissue to form around the particles (granulomas) or scar tissue formation (adhesions) which can lead to surgical complications.

For a detailed description of the risks that the FDA identified, please refer to the final rule. There are other surgical and patient examination gloves available that provide the same level of protection, dexterity, and performance without posing the same risks to patients and health care providers.

The final ban is effective for powdered surgeon's gloves, powdered patient examination gloves, and absorbable powder for lubricating a surgeon's glove that are already in commercial distribution and for these devices that are already sold to the ultimate user, such as small medical practices and hospitals, on January 18, 2017.

On March 4, 2020, the FDA published a final rule to ban electrical stimulation devices (ESDs) intended for self-injurious or aggressive behavior because they present an unreasonable and substantial risk of illness or injury that cannot be corrected or eliminated through new or updated device labeling. The 2020 ban was challenged in Federal court and, in effect, annulled (vacated) based on the court's interpretation of the FDA's authorities under the Federal Food, Drug, and Cosmetic Act (FD&C Act). Since that decision, changes to the FD&C Act make clear that the FDA has authority to issue a ban such as the 2020 ban on ESDs for self-injurious or aggressive behavior, which applies to specific intended uses. On March 26, 2024, the FDA plans to issue a new proposed rule to ban these devices.

ESDs administer electrical shocks through electrodes attached to the skin of individuals to interrupt the behavior or attempt to condition them to stop engaging in self-injurious or aggressive behaviors. Some people getting exposed to these devices have intellectual or developmental disabilities that make it difficult to communicate their pain or consent. A number of significant psychological and physical risks are associated with the use of these devices, including depression, anxiety, worsening of self-injury behaviors and symptoms of posttraumatic stress disorder, pain, burns, and tissue damage. In addition, there is a risk of errant shocks from a device malfunction. As these risks cannot be eliminated through new or updated labeling, banning the product is necessary to protect public health. The proposed ban does not apply to ESDs used to create aversions to other conditions or habits, such as smoking. For a detailed description of the risks that the FDA identified, please refer to the proposed rule.

What Process Does the FDA Follow to Ban a Medical Device?

The FDA makes the determination to ban a device by analyzing and weighing the risks and benefits the device poses to individuals. This analysis may include:

- Identifying and studying the device, including assessing adverse events,
- Analyzing the risks and benefits posed by alternative devices and treatments being used in current medical practice,
- Analyzing whether a change in labeling on the device mitigates the risk,

- Evaluating the medical literature,
- Conducting a panel meeting with outside experts,
- Discussing concerns with professional societies, and
- Reviewing information from health care professionals and patients.

The FDA can ban a device without actual proof of illness or injury, and only needs to find that a device has the potential to present the required degree of risk based on all available data and information.

The FDA may initiate proceedings to ban the device if:

- the device presents substantial deception or an unreasonable and substantial risk of illness or injury, and
- such deception or risk cannot be, or has not been, corrected or eliminated by labeling or a change in labeling.

If the FDA decides to initiate proceedings to ban a device, a notice of proposed rulemaking is published in the Federal Register.

List of Medical Device Bans

The list below contains bans that have been proposed or issued.

Device Name	
Proposal to Ban Electrical Stimulation Devices for Self-Injurious or Aggressive Behavior	
Powdered Surgeon's Gloves, Powdered Patient Examination Gloves, and Absorbable Powder for Lubricating a Surgeon's Glove	
Prosthetic Hair Fibers	

What is the Difference between a Proposed and a Final Ban?

Proposed Ban

A proposed ban is the FDA's statement of intent to ban a device.

In a proposed ban, the FDA outlines its assessment of the benefit-risk profile of the device. Specifically, a proposal to ban a device requires a summary of the:

1. Agency's findings regarding substantial deception or the unreasonable and substantial risk of illness or injury;
2. Reasons why the FDA initiated the proceeding;
3. Evaluation of the data and information the FDA obtained under provisions (other than section 516) of the FD&C Act, as well as information submitted by the device manufacturer, distributer, or importer, or any other interested party;
4. Consultation with a panel of experts that classify a device, if conducted (see the Advisory Committee webpage for more information about FDA Panel Meetings);
5. Determination that labeling, or a change in labeling, cannot correct or eliminate the deception or risk;
6. Determination of whether, and the reasons why, the ban should apply to devices already in commercial distribution, sold to ultimate users, or both; and
7. Other data and information the FDA believes are pertinent to the proceeding.

The public can comment during the comment period, which is at least 30 days.

Special Effective Date

In some cases, the FDA can put a special effective date in the proposed ban which puts the ban immediately into place as soon as it is published in the Federal Register.

This procedure may be used when the FDA determines that the potential or actual injury involved is serious enough that the agency believes will endanger the health of individuals who have been, or will be exposed to the device. For a proposed ban with a special effective date, the FDA will finalize the rule by affirming, modifying, or revoking the proposed rule. Even if the proposed ban has a special effective date, the public can comment during the comment period. Interested persons may request an informal hearing to discuss the ban.

Final Ban

A final ban is the FDA's statement of action and tells the public what device the FDA is banning and when that ban will go into effect.

The FDA considers any comments it receives on the proposed ban and determines whether to affirm, modify, or revoke the proposed regulation. If the proposal is affirmed or modified, the FDA will publish a final regulation banning the device. In this case, the device can no longer be legally marketed on or after the date of

publication of the final regulation, except under an approved investigational device exemption. If the proposed regulation is revoked, the FDA will publish a notice to this effect in the Federal Register.

Seattle Times Newspaper Article

Here is a newspaper article in the Seattle Times about similar devices to the Dotto ring, Worldwide Medical Scams. It seems that Dr. Dotto truly believed that his ring could treat cancer, so I am not suggesting that the ring was a similar scam. But it may have unintentionally helped other less noble people to run scams. It is credible to me (based on the current TTFields technology) that the ring might have had some medical benefit, but I can't address if this is true or not. I can find no information on why the Dotto ring was banned. The ban did not prevent it from being patented 4 years later.

How one man's invention is part of a growing worldwide scam that snares the desperately ill

Originally published November 18, 2007 at 12:00 am Updated November 19, 2007 at 9:35 am

1 of 10 | Bill Cunningham, William Nelson's longtime friend, leads a Budapest training session while a volunteer has her health "examined" by placing her hand on the EPFX. She was judged healthy. Nelson claims the device can analyze samples such as... More

What does "FDA registered" mean? Not much The FDA registers manufacturers of energy-medicine devices — not the products. Many manufacturers submit basic...

By Christine Willmsen and Michael J. Berens

In the late 1980s, an out-of-work math instructor in Colorado built an electronic device he claimed could diagnose and destroy disease — everything from allergies to cancer — by firing radio frequencies into the body.

But the U.S. Food and Drug Administration, which regulates medical devices, ordered William Nelson to quit selling his machine and making false claims. Nelson refused, and he was indicted on felony fraud charges. He fled the country, never to return.

That should have been the unremarkable end of another peddler of medical miracles.

Today, Nelson, 56, orchestrates one of America's boldest health-care frauds from a century-old building in Budapest, Hungary. Protected by barred gates, surveillance cameras and guards, he rakes in tens of millions of dollars selling a machine used to exploit the vulnerable and desperately ill.

This device is called the EPFX. In the U.S. alone, Nelson has sold more than 10,000 of them. More have been sold in the Northwest than in any other region, company officials said.

Nelson built his business by recruiting a sales force of physicians, chiropractors, nurses and thousands of unlicensed providers, from homemakers to retirees, drawn by the promise of easy money.

Nelson is just one profiteer, with one device.

A Seattle Times investigation has uncovered a global network of manufacturers who sell unproven devices, and practitioners who prey on unsuspecting patients.

Capitalizing on weak government oversight, they have used these devices — some illegal, others potentially dangerous — to drain patients' bank accounts, misdiagnose diseases, and divert critically ill people from life-saving care.

These victims are casualties in the growing field called "energy medicine" — alternative therapies based on the belief that the body has energy fields that can be manipulated to improve health. Energy devices range from handheld machines the size of television remotes to behemoth machines that weigh hundreds of pounds, with costs ranging from $1,200 to $55,000.

Many manufacturers and operators do follow FDA rules and disclose that treatments are unproven.

But The Times' investigation, based on government records and more than 200 interviews, found thousands who skirt the law. Among its findings:

• FDA officials do not know how many energy-medicine devices exist, where they are used and even whether they are safe. Ten years ago, Congress reduced medical-device oversight. Ever since, most energy-device manufacturers who register with the FDA submit little more than basic contact information.

• Federal and state regulators failed to warn the public about a dangerous energy device, the PAP-IMI, which is linked to patient injuries and death. Nor did they confiscate all of the devices, which pulse the body with strong electromagnetic waves. They had been smuggled into the country as seed germinators. The PAP-IMI remains in use today in at least five states, including Washington.

• Many energy-medicine operators dupe the public by posing as highly trained health-care professionals through the use of deceptive credentials and unaccredited degrees.

Some of the largest and seemingly independent credentialing organizations are in fact controlled by two men who run competing mail-order operations.

FDA spokeswoman Karen Riley said the agency is looking into the EPFX, based on The Times' findings.

Medical charlatans have used energy devices in this country for more than a century.

In the past decade, the machines exploded into the mainstream, fueled by the Internet, which quickly and cheaply reached prospective buyers and patients.

Today, dozens of energy-device manufacturers present flashy Web sites with video testimonials and fake science.

"The message itself has stayed the same for centuries: 'This is the cure that I discovered and it's backed with testimonials from lots of people snatched from the grave by using it,' " said James Whorton, professor of medical history at the University of Washington's School of Medicine.

The National Institutes of Health says research in the area of energy medicine may hold promise, but so far none of the devices, or their treatments, has been scientifically validated.

"Undoubtedly, there's a lot of quackery," Whorton said. "They will tell you what you want to hear. The average person isn't educated or trained to be able to evaluate these therapies critically."

Couple's final hope

In a clinic in Tulsa, Okla., JoAnn Burggraf, 58, sat in an oversized armchair as she was hooked up to an EPFX.

Clinic owner Sigrid Myers, who was trained on the device in Seattle, wrapped black straps containing electrodes around Burggraf's forehead, wrists and ankles. The straps were connected to the shoe-box-sized EPFX, which plugged into a desktop computer.

Myers used the EPFX to scan and analyze Burggraf's body. Burggraf watched as the monitor displayed bright-colored graphics representing parts of her body that Myers said were unhealthy.

Then, Myers recounted, she set the EPFX to "zap mode" and transmitted imperceptible, low-level frequencies through the electrodes and into Burggraf's body.

She and her husband, Jerry Burggraf, owned a successful cleaning and restoration company in Tulsa. He developed leukemia and underwent chemotherapy. In 2004, he began EPFX treatments, hoping to stop the disease.

He died in March 2005 at age 59.

Her husband endured painful side effects from the chemotherapy. After that, she distrusted doctors.

She started EPFX sessions, at $60 an hour, seeking relief from pain in her joints and legs.

“I begged her to go to the hospital,” her son, Bryan Burggraf, 37, said. “Mom told me this device would make her well.”

But her pain grew worse, becoming so intense that she frequently blacked out. In October 2005, Bryan finally convinced his mother that she needed to go to a hospital immediately. She was so weak and sick, with inflamed, open sores on her legs, that she eventually had to be transported by helicopter.

She died within hours of admission. Tests showed that her body had been devastated by undiagnosed leukemia.

Her son said doctors speculated that his parents were exposed to now-banned solvents used in their restoration business.

“I’m outraged that this fraudulent device is still out there,” Burggraf said. “If my mom had gone to the hospital earlier there may have been hope. If nothing else, she would not have died in incredible pain.”

Myers, a massage therapist, has no formal medical training or college degree. But on the wall of her home clinic were half a dozen framed certificates that bestowed her with health-care titles and credentials such as “naturopathic doctor.”

“We’re not supposed to say it, legally, but it can zap away disease,” she told a reporter who visited the clinic. Asked why the EPFX did not cure JoAnn Burggraf, Myers tearfully explained: “I had just a few days of training. I really didn’t know what I was doing.”

Now she says she’s more experienced.

Myers continues to treat patients in her home office with a newer EPFX. She persuaded an elderly patient to buy the machine for her, which cost $12,000. In exchange, Myers said, she didn’t charge the woman for EPFX sessions to treat her heart disease.

That patient died, too.

Performer, pretender

Last year, at an international EPFX conference in Budapest, William Nelson bounded to a stage in front of a cheering crowd of several hundred — operators of the machine or those hoping to buy one. They rose to their feet and applauded.

He explained how he had used the EPFX to cure cancer and AIDS.

“It helps that I’m a genius,” he told them.

But nothing is what it appears with Nelson, including his appearance. On stage, he wore a white dress, heels and heavy makeup.

“Judge the teaching, not the teacher,” he told the crowd in a soothing baritone. Nelson is a polished performer — funny, confident, commanding the tools of a natural-born salesman.

Later, under his stage name Desiré Dubounet, he sang rock songs at his lounge, Club Bohemian Alibi.

This is the Nelson that few patients ever learn about.

From his restored, five-story building in downtown Budapest, Nelson operates the main EPFX business, Eclosion, and lives with his fifth wife and 8-year-old son. He has a personal staff of about a dozen, including a cook, hairdresser, nanny, security guards and chauffeurs.

From his movie production studio, he has created films that portray him as the crusader of alternative medicine and the FDA as the corrupt villain.

He said he has sold 17,000 EPFX devices worldwide. They now cost $19,900 each.

Nelson makes extraordinary claims about his life. He said he worked as a contractor for NASA, helping to save the troubled Apollo 13 mission as a teenager. He boasts that he was an alternate member of the 1968 U.S. Olympic gymnastics team. He says he has eight doctorates, including degrees in medicine and law. See a PDF of his Curriculum Vitae **here.**

None of it checks out. NASA has no record of his employment; he was not an Olympic athlete. And his “degrees” came from unaccredited schools and mail-order businesses.

In truth, at age 33, Nelson was a part-time mathematics instructor at Youngstown State University in Ohio, according to school records.

As an avid “Star Trek” fan and father of an autistic son, Nelson became obsessed with creating a space-age device that melded modern mathematics with alternative therapies to heal the body.

In 1984, he moved his family to Colorado, where he started to sell his homemade medical device, called the Electro-Physio-Feedback-Xrroid System, or the EPFX.

Nelson registered his company with the FDA in 1989 as a maker of biofeedback machines, meaning he could sell them only as stress-relieving tools. By law, he could not claim the devices diagnosed or treated disease.

But Nelson did it anyway. In 1992, the agency ordered him to stop making false claims, then later ordered a recall of the EPFX. But Nelson continued to sell it as a healing machine.

He was indicted on nine counts of felony fraud in 1996 and fled the U.S. See a PDF of Nelson’s court docket **here.**

Eclosion remains registered with the FDA.

Today, Nelson’s sales empire reaches across 32 countries with dozens of distributors, brokers and trainers in the U.S. Top sellers can get hefty commissions, tropical cruises and BMW sedans.

Emma Robinson, a regional manager for the Pacific Northwest, earned one of the BMWs. She said she pulls in about $7,000 a week through sales commissions and by treating patients at her clinic, Quantum Pacific Wellness Center, in Wilderville, Ore.

Nelson and his distributors saturate the Internet with glitzy Web sites packed with animation, music, videos, even operators available to answer questions.

EPFX sales have exploded, fueled by aggressive marketing including such pitchmen as a physician for pop star Britney Spears and a chiropractor for cyclist Lance Armstrong.

As Nelson tells his audiences: Conventional doctors speed patients through appointments with treatments that focus only on symptoms, not on the root causes of ailments. The EPFX treats the whole body, and it does it without surgery or drugs.

Practitioners encourage patients to talk with them about any health problem. EPFX treatments typically last an hour. Afterward, a substantial number of patients will report that they feel better.

Energy-device operators benefit from the placebo effect, a psychological phenomenon in which patients report improvement that cannot be linked scientifically to treatment,

studies show. People feel better through the power of suggestion or because they believe they are expected to feel improvement, experts say.

The EPFX is made up of circuit boards and other computer components that run software full of colorful graphics of the body. During a typical EPFX treatment, a patient may watch as a computer screen displays an animation of the interior of an artery blocked by white blobs, representing cholesterol. Then the blobs shrink and disappear.

Tens of thousands have found Nelson's pitch persuasive. "Traditional doctors don't want you to use the EPFX," he says. "They will tell you it's a fraud. That's because they are scared. I have discovered something that will put them out of business. And they don't want you to have it."

His fervor is shared by Emma Robinson's husband, John, also an EPFX regional sales manager. He says the device can do most anything.

"It's the closest thing to God I know."

Honor-system loophole

In 1997, Congress passed the Food and Drug Administration Modernization Act, which made it cheaper and quicker to bring a device to market.

Consequently, the number of energy-device makers has increased to 462, up 45 percent in the past decade, according to a Times analysis.

The act also exempted many manufacturers of low-risk devices from submitting proof that the machines worked and were safe.

The agency places them on the honor system when it comes to classifying their devices. As a result, a popular strategy for some manufacturers is to list their devices as biofeedback machines. Legally, they can only be used to relieve stress.

But The Times found dozens of biofeedback machines that are marketed to the public with wild claims. Some examples:

• Practitioners using the LIFE System, distributed by Energetic Medicine Research Ltd., offer patients a "full diagnostic and treatment system." They claim the devices can assess the health of organs and "clear health blocks," from allergies to dental problems.

• Hippocampus-Brt Ltd., a Hungarian company registered with the FDA, declares that its Mobile Cell-Com can treat allergies through short "therapy sessions," strengthen the body's immune system and relieve inflammatory ailments.

• California-based Inergetix Inc. sells the Inergetix-CoRe System that can “scan and balance the organs and systems of the body.”

Additionally, health improvements are shown on a computer screen “as they occur.”

Installed in a hospital

Three years ago, EPFX operators scored one of their biggest coups: They managed to get two devices inside a U.S. hospital — St. John’s Hospital, an 866-bed facility in Springfield, Mo.

Nelson markets this as proof that mainstream medicine embraces the EPFX.

On Friday, hospital administrators launched an investigation into how the EPFX machines got approved. They learned about their presence from The Times.

Faith Nelson, a registered nurse who works in the department where the devices are used, is also a regional sales manager for the EPFX, records show. (She is no relation to William Nelson.)

In addition, Susan Blackard, a hospital vice president who oversees that department, conducts training sessions for EPFX operators worldwide, records show.

Blackard, who is also a registered nurse, trained several hundred people at a conference last year in Budapest.

Neither woman returned calls for comment.

St. John’s spokeswoman Cora Scott said the hospital is reviewing the employees’ relationship to Nelson and the EPFX sales network.

The hospital is owned by the Sisters of Mercy Health System. Officials there said the two EPFX devices were used only for stress relief.

One operator cut off, case closed

Washington state regulators first learned about the EPFX in April 2004 when a Puyallup physician filed a complaint that an unlicensed health-care practitioner in Tacoma was using one.

State investigator John Kozar checked out the complaint, interviewing Janet Zibell, who used the EPFX at her spa.

At the same time, Kozar learned that other EPFX operators across the state were using it. In May 2004, Kozar wrote to his superiors: “This device is being used by unlicensed people to treat and diagnose patients with illnesses.”

Zibell told state investigators that she used the EPFX only as a biofeedback machine to help relieve stress, according to state records. In Washington and all states, no license is required to perform biofeedback.

To show investigators how she used the device, Zibell conducted an EPFX session at Department of Health headquarters in Olympia. Zibell connected the EPFX to state investigator Carol Neva. During the demonstration, Zibell said the device detected a parasitic worm in Neva's colon so she "zapped a worm" with the device's electrical frequencies.

That was enough for investigators. Zibell was issued a cease-and-desist order. She agreed not to use the EPFX to diagnose or treat illness. The Health Department stopped there, closing the case. It did not look into the other EPFX operators Kozar warned about, records show.

In Oregon, regulators took a far different approach.

The Oregon Board of Chiropractic Examiners earlier this year barred chiropractors from using the EPFX. "This device is complete hocus-pocus," the board's executive director, Dave McTeague, said. "There is no rational explanation as to how it works."

Karen McBeth's losses

Seattle cancer patient Karen McBeth, 59, had no trouble finding an EPFX operator. A retired employee with state Juvenile Rehabilitation Administration, McBeth had squamous-cell carcinoma that mushroomed into terminal bone cancer. She underwent chemotherapy. By early 2005, she was in so much pain that she could barely walk.

Desperate for a cure, she looked for an alternative and through friends learned of BioScience, a health-care clinic in Port Orchard that offered EPFX treatments. BioScience was run by Robert and Marie Erdmann, and their daughter, Ann Riner. None of them had a state health-care license. McBeth was skeptical at first. But she did some Internet research and learned the device manufacturer was registered with the FDA and that dozens of physicians and chiropractors touted the device.

She began twice-weekly treatments. She was even persuaded to buy a machine for use at home, and spent $17,000 from her retirement savings.

"She was led to believe that treatment would cure her cancer," said her husband, Al Bergstein.

By the summer, she began to doubt whether the device was effective. She died Sept. 3, 2005.

Read McBeth's Seattle Times obituary **here** and a **Web site in her memory.**

Bergstein said the device offered a false hope that consumed his wife and robbed the family of precious remaining time with her.

A retired Microsoft manager, Bergstein looked at the source code in the EPFX's software. It appeared to generate results randomly.

"It's a complete fraud," he said.

Marie Erdmann, 64, who now manages the clinic since the death of her husband last year, defended the EPFX. "It's where medicine will go, but it will take a long time," she predicted.

A cure for everything

The world's largest EPFX distributor, The Quantum Alliance, is headquartered in Calgary, Alberta. It also operates its largest North American training center in Victoria, B.C., not far from Seattle.

Ken Wilkinson, chief executive officer, said the company does not market the EPFX as a diagnostic or healing machine.

However, dozens of such claims are found in the company's brochures and newsletters. For example, one brochure, used by a Washington practitioner this year, claimed that the EPFX can test for toxins, bacteria, viruses, allergens, parasites and disease.

In addition, The Quantum Alliance distributed a training video, narrated by Nelson, that claimed the EPFX can repair injured tissue and accelerate healing.

Wilkinson said the company no longer uses these materials. The EPFX is marketed only as a stress-relief tool, he said.

But a training newsletter, published last month by The Quantum Alliance, provided step-by-step instructions on how to use the EPFX to enlarge lips or cheeks and treat dental problems.

Company President Brian Thompson said the EPFX has "helped thousands of people." He couldn't explain what the device does or how it works. "We just sell them," Thompson said.

Hundreds of other brokers and practitioners sell the device as well, earning up to $2,500 in commissions per sale. Dozens of their Web sites tout testimonials of miraculous healings and declare that the EPFX can provide hundreds of therapies.

One of its strangest features is found on top of the EPFX: a 5-inch silver plate. Nelson claims the device can detect problems in the body by analyzing hair, saliva or blood placed on the plate. The device then fires healing frequencies to patients — even if they're hundreds of miles away.

A taunt to regulators

The EPFX was a big draw at this year's Western Washington Fair in Puyallup. Bart Keough, owner of The Healing Circle Counseling in Eatonville, Pierce County, ran a booth where more than 400 people were treated. They were charged $20 for a half-hour session.

Keough calls himself a "certified biofeedback specialist," a certification he earned from a mail-order training program. He said he has to be careful about how to describe the EPFX to avoid hassles with the FDA.

"We're told not to tell anyone that it heals anything," he said.

But a 4-foot-long banner that draped his booth listed dozens of "Therapies" the EPFX could provide. Keough admitted the EPFX contains many therapies that go beyond what the FDA allows. "I don't know how Bill Nelson gets by with it," he said.

In Budapest, Nelson doesn't worry about the FDA. In the past year, he established companies that are bringing in new products and devices into the United States.

He also has produced a music video in which he sings in front of a giant image of FDA headquarters. Nelson's song ends with a taunt to the regulators: "You ain't seen nothing yet."

Staff reporter Sonia Krishnan and researchers David Turim and Gene Balk contributed to this report.

Michael J. Berens: 206-464-2288 or mberens@seattletimes.com; Christine Willmsen: 206-464-3261 or cwillmsen@seattletimes.com

***Christine Willmsen**: 206-464-3261 or cwillmsen@seattletimes.com; on Twitter: @christinesea.*

Michael J. Berens

Video by doctor that build a full-scale Dotto ring

https://vimeo.com/10631133

Dotto Ring Doctor.m4a

My comments on above video:

- Seems like if it was working, he would have demonstrated it in operation
- I would like to see the business end with the gap and constantan rod
- He wouldn't be sitting comfortable like that if the ring was heated to 700 to 800 deg F, as in the full spec to which he built it. Copper is the second-highest metal thermal conductor, after silver.

Nexus Magazine Article on Dotto Ring

THE DOTTO RING

A HEALING, AGE-REVERSAL DEVICE

Dr Gianni Dotto invented a device which recreates the Hunza Valley's special magnetic environment that he believes is responsible for the good health and longevity of the Hunza people.

Part 1 of 2

by Dr Gianni Dotto © 1972

(Introduction by unknown author)

From the KeelyNet website at:
http://www.keelynet.com/biology/dotto.htm

Editor's Note: The following article introduces a 1972 paper by Dr Gianni Dotto, but the name of its author and the original date of publication are unknown. Final commentary is provided by Jerry Decker, who has posted the complete text and some diagrams on the KeelyNet website, but this will appear in part two of the extract next issue. Note that several mentions to animal experiments are made in these articles. NEXUS does not agree with the practices of animal experimentation and vivisection, but we also don't want to censor the articles we publish.

Gianni A. Dotto was born in Venice, Italy, the son of a prominent engineer who was the designer of two hydro-electric generating plants on both the American and Canadian sides of Niagara Falls. His father was an Italian Marquis, and Gianni, the eldest son, would have inherited the title had he not become an American citizen. The family is directly descended from Galileo, and the Galileo coat of arms has been adopted for use as the Foundation's [*sic*] letterhead.

Before World War II, Gianni had received flight training, but Mussolini never did trust the Dotto family—so Gianni was drafted into the Italian Army as a paratrooper. When Italy surrendered, Gianni was able to join the American [Army] Air Force as a fighter pilot in time to participate in numerous engagements against the German Messerschmitts before the war ended.

After the war, Gianni became head of the racing division of Alfa-Romeo and started racing cars of his own design. His racing career ended when his wife Renata served him with an ultimatum to "give up racing". He is a prolific inventor, as he is owner of many Italian patents bearing on the automotive industry and, subsequently, just as many American patents. He is highly educated, holding the Italian equivalent of an American PhD in nuclear physics from Milan University and a degree in mechanical engineering from an Italian technical school. Subsequently, he received a degree in electrical engineering from Wayne University in Detroit, USA.

While Gianni was teaching at Milan University, the medical school requested the services of a physicist to collaborate with the doctors on a research project. This started him on a career as a biophysicist; that is, a physicist who specialises in the area of the science of physics that has bearing on the human body. This embraces an amazingly wide field, as it has to do with magnetic fields, polarity, the various vibrations and pulsations generated by the brain and, of course, the effect of the many facets of nuclear fission on the human body.

It was there that Gianni discovered that magnetic fields induced by an electric coil and by permanent magnets had a small effect on the human body, but that a mild magnetic field created by adjacent hot and cold areas was definitely beneficial. In other words, the thermal imbalance created a magnetic field that matched the natural field of the body.

The development of the "Dotto Ring" was Gianni's practical way of producing a piece of equipment that could impress the beneficial magnetic field on the body. The Ring is 27 inches in diameter, made of heavy copper and has adjacent heated and refrigerated areas. Through the Ring he has reproduced in a compact, accessible form the same magnetic environment responsible for the good health and longevity of the Hunza people.

Visitors to Hunza land always attribute this great advantage to the Hunzas' diet, air and water, but Gianni could not accept this belief because there are many valleys in the Himalaya Mountains where the diet, air and water are similar to that of the Hunza region,

but the inhabitants of these valleys are devoid of the same health and longevity manifestations as in the Hunza Valley.

With the principle of the Dotto Ring in mind, a panoramic view of the Hunza Valley makes Gianni's theory easy to understand. At the head of the valley there is a huge glacier or ice mass and in the valley itself the temperature becomes quite warm, thus creating the thermal imbalance mentioned previously and which is recreated in the principle of the Dotto Ring. When the Hunzas travel across this valley, they receive a beneficial treatment from a mild magnetic field. The similarity of the Dotto Ring to the Hunza Valley is interesting, to say the least.

Gianni has written what he describes as a "simple explanation of just how the Ring works". Simple for a physicist, perhaps, but difficult for a layperson to understand! Consequently, the following preliminary explanation has been outlined for the purpose of clarification.

The nucleus of each cell contains a material known as the DNA, which is an abbreviation for deoxyribonucleic acid. This substance contains the life or genetic code. The presence and function of the DNA had long been suspected by our doctor-scientists and had been presented as a theory, but it was only about seven years ago with the development of the electron microscope that the presence of the DNA was confirmed. Now it can be seen, photographed and sketched.

Imagine a tiny ladder twisted together in a coil fashion until the unit forms a double helix. The DNA is pliable and rubbery and is never still, as it constantly vibrates in resonance with brain signals and even outside influences. The DNA is polarised, one end being plus and the other being minus. A healthy DNA reproduces healthy cells and aids the body naturally to overcome and eliminate an invasion of bacteria or toxins. This, of course, adds up to good health. When the body lands within the beneficial magnetic field of the Dotto Ring, polarisation of the DNA is oriented properly and resonance is synchronised to that of a healthy cell.

When the body lands within the beneficial magnetic field of the Dotto Ring, polarisation of the DNA is oriented properly and resonance is synchronised to that of a healthy cell.

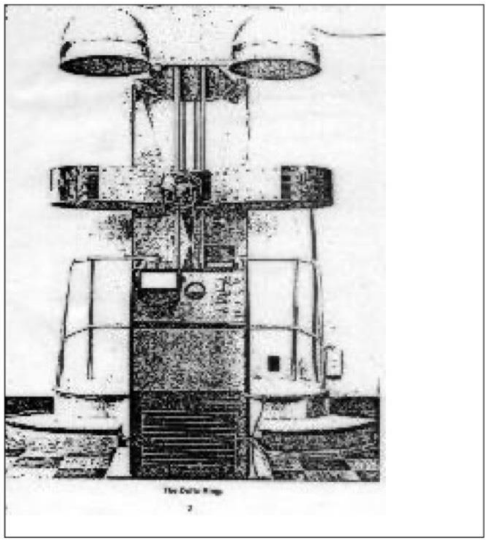

Illustration showing the Dotto Ring device.

Important animal tests required by the medical authorities have been underway for the past three years, culminating in seven official tests that were conducted under rigidly controlled conditions. The tests were conducted by Professor Gerald L. Willis, Biology Professor at the University of Dayton, and Dr Robert E. Zipf, PhD. Dr Zipf is owner of a group of biological laboratories and has been Coroner for Montgomery County, Ohio, for 20 years. The room in which the tests were conducted was kept under triple lock so that only Professor Willis had access to the area. Dr Zipf performed the pathology on the test mice.

The mice—six per cage and eight cages per test—were injected with cancer cells. In three tests, C-37 cancer cells were used, and in two other tests, Krib-type carcinoma cells were used. The most recent tests were conducted on mice that had induced leukaemia. Results have been very good indeed. The untreated mice died in about seven days, while, with a few exceptions, the treated mice survived. When the treated mice were finally sacrificed, they showed no evidence of cancer. These tests, as well as actual experience using the Ring on the human body, prove definitely that there are no side effects.

Gianni Dotto has now had five years of experience in the use of his Ring. For the past two years, the Ring has been in operation in his Bio-Physics Laboratory in Kettering, Ohio. Results have been uniformly good.

Following is the scientific paper prepared by Dr Gianni Dotto.

BACKGROUND ON THE "DOTTO RING" THEORY

Most of the external physical factors which have been implicated in the evolution of life are of an electromagnetic nature. It has now been established that, throughout the reviewable geological period, the biosphere has been a region of electromagnetic fields and radiations of all the frequencies known to us—from slow periodic variations of the Earth's magnetic and electric fields to gamma rays.

It is fundamentally possible on the basis of general considerations that any of the ranges of the electromagnetic spectrum could have played some role in the evolution of life and are involved in the vital processes of organisms. This has already been demonstrated for a considerable region of the spectrum: for electromagnetic radiations in the infrared range (photobiology) and from X-rays (radiobiology).

The situation is different with the vast remaining region of the spectrum, which includes electromagnetic fields (EMFs) of superhigh, ultra-high, high, low and infra-low frequencies. Experimental investigations and theoretical considerations suggest that EMFs can have a significant biological action only when their intensity is fairly high, and that such action can be due to only one process: conversion of the electromagnetic energy to heat, or vice-versa.

There is an increasing amount of reliable experimental data which indicates that EMFs can have non-thermal effects and that

living organisms of diverse species, from unicellular organisms to man, are extremely sensitive to EMFs.

Finally, it has been found that very weak, natural EMFs can affect organisms of various species. All this indicates the necessity for a fundamentally new approach to the problem of the biological action of EMFs and for the need to reconsider the question of the possible role of EMFs in the vital activity of organisms (Parin).

It is believed that my work is not the first attempt at such an approach to the problem on the basis of the concept of the informational role of EMFs in the evolution and vital activity of organisms. There are three kinds of "biological activity of EMFs":

1) the effect of natural environment EMFs on the regulation of vital processes;
2) the role of internal fields in the organisms in the coordination of physiological processes;
3) the interaction between organisms by means of EMFs.

It is not sufficient to consider only the energetic aspect of the interaction of EMFs with biological systems, and in a portion of my past investigations I have dealt with the informational functions of these fields in living nature.

I have constructed equipment necessary to conduct my cancer research. A substantial databank of case histories has been accumulated. Not all case histories are well defined, but general results are amazingly good. This is understandable, however, since I am in the process of establishing the first formulation of a new biological problem.

My concept of the informational functions of EMFs in living organisms and the hypothesis expressed in this respect will undoubtedly rouse interest in a wide circle of the medical readers.

The objectives of this research project are to:

1) prove that the human body responds favourably when exposed to EMFs;
2) establish what type of EMFs are more effective.
3) determine the specific frequency of EMFs for different types of disease.

Dr Gianni Dotto

WORKING THEORY OF THE "DOTTO RING"

There are four basic major, but disparate, theories explaining the development of cancerous tissues:

1) Virus (theory supported by scientists of Sloan-Kettering, New York);
2) Low negative voltage across cancer cell skin (Cone, NASA);
3) Excess of base pairs per turn on the DNA double helix (Dotto);
4) Alteration of the DNA code due to a certain type of virus (Temin).

The first theory would be correct if we are to accept the hypothesis that all the viruses of the four groups responsible for the manufacture of the nuclei (even if similar in size, shape and crystal form) are tuned to a different frequency, according to the location in the human body of different groups of cells. In this case, a virus out of position can create the Temin phenomenon of mixing up the sequence of the DNA code. (If this is the case, the theory that some day immunisation against cancer will be as simple as polio immunisation is unrealistic. The variety of cancer immunisation viruses will be in the numerical magnitude of trillions.)

Theory #2 (Cone, NASA) would be acceptable if we consider a cancerous cell a parasite cell, to some extent.

According to theory #3 (Dotto), the magnetic charge of the genetic code is maintained at the proper level by the electrical property of the double helix, which functions as a common transformer, where the voltage of the primary and the secondary windings is proportional to the number of the turns of the coils.

If the DNA double helix of a cancer cell has a lesser number of turns than the DNA double helix of a normal cell, consequently the number of base pairs per turns will be greater. A greater number of base pairs per turn of the double helix and eagerness to complete the outer electron orbiting of the atomic structure of the nucleus leads to a greater capability of reproduction of the DNA.

The second and third theories, then, are similar in principle but explained from a different observer's viewpoint. One explains the result, the other explains the cause.

Theory #4 (Temin) is a consequence of theory #1 (Sloan-Kettering, NY)—however, with an incorrect interpretation of the phenomenon. Due to the tremendous variety of viruses classified in eight distinct groups—four RNA types and four DNA types—there is no way in which to resolve the immunisation capability unless the immunisation factor can be obtained with the natural method described in the second Dotto patent application #42,301, filed June 1, 1970:

"Milk taken from the right breast of a nursing mother is maintained separate from the milk taken from the left breast. On high 'g' centrifuge, viruses are separated from proteins and fats. Immunisation will start with oral or injection methods by using RNA-type viruses from the right breast, and be repeated two months later with DNA-type viruses from the left breast. In the

human breast, there are all the variety of viruses necessary for the immunisation."

Why, then, the electronic reactor (Dotto Ring device) and not chemistry to resolve the problem?

To begin with, in the normal process of life of a healthy body, when a new cell is produced the orbital electron spinning of the new cell assumes a direction opposite to the one of the mother cell in order to maintain the mutual attraction.

When the increasing kinetic electron energy of the new cells overcomes the energy of the mother cell, the orbital electron spinning of the mother cell is forced to change direction and mutual rejection occurs. In the process, the entire energy of the mother cell collapses (in the same fashion as a transformer core) and its energy is absorbed entirely by the new cells.

However, if the energy potential and derived magnetic field in the human body is diminished or unbalanced, the new cell loses the body support to increasing kinetic energy and the dying cell never changes directional electron spinning. The dying cell, then, maintains enough residual energy to be attracted by the newborn cell and becomes its parasite.

The DNA of the new cell now must perform double work: support the new cell and the parasite cell, with the result that the life-span of the new DNA will be shortened. The oncoming new DNA must now have enough energy to support the dying cell and the parasite cell. Furthermore, it cannot rely any longer on the body's support due to a weak or unbalanced magnetic field.

In a desperate attempt to be liberated of the parasite cell, the DNA sends a message to the enzymes. Most of the time, the enzymes are too busy in the assimilation of the processed food of modern civilisation, with the result that the DNA of the new cell now has to support two parasite cells, and so on... When the combined energy of the parasite cells becomes greater than the energy of the new cell, the new DNA loses control over the RNA in the formation of protein. The RNAs are then formed by the combined genetic code of the DNA of the parasite cells. This will occur when enough or greater genetic code in the summation of the parasite cells overcomes the control of the normal DNA.

The DNA code so completed may have all the information necessary to sustain life, but in the wrong sequential order—and a new, strange life in the life is born. This phenomenon is known as *cancer*. From the above explanation, it is quite obvious that a cell in the dying process must lose its entire energy to be removed by the blood or lymphatic system, otherwise the body must have enough enzyme supply to destroy the cells before they become parasites.

To prevent and control cancer, several methods can be applied.

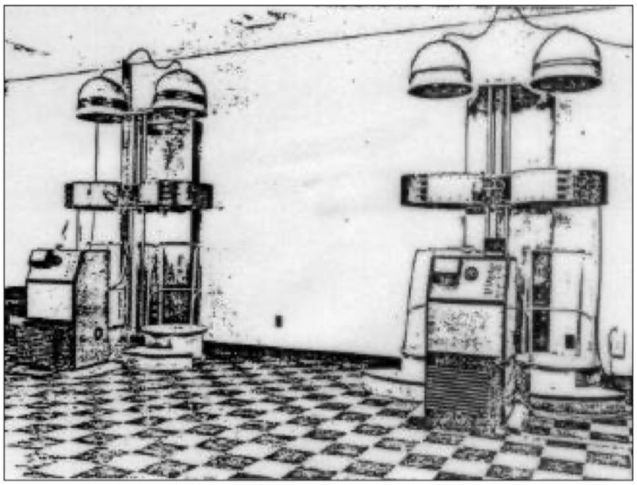

Illustration showing installed Dotto Ring devices.

1) Magnetic intensity, homogeneity and orientation in the human body must always be maintained at the optimum level.

2) Mineral balance and proper distribution are essential. The cell needs copper to convert AC impulses from the nervous system to DC energy; this energy is necessary to maintain the DNA in the proper oscillation frequency. Aluminium and zinc are necessary to maintain the voltage level. Iron is necessary to accumulate inductive energy EMF. The most important elements, magnesium and oxygen, are necessary to ensure the total collapsing effect of the iron when the electron orbital spinning in the nucleus reverses.

In modern civilisation, where the entire environmental surrounding is bound to destroy humanity, the above conditions are essential for survival. While natural food consumption maintains the proper mineral balance and may maintain the enzyme proportion in the high level, the most important factor is to supply the body with enough energy to maintain the magnetic field as described above. However, we must clarify that we call *magnetic force* any energy capable of attracting or repelling matter.

In reality, there are four different types of magnetic force, each one caused by a different physical phenomenon.

1 – Permanent magnet

If we try to magnetise a bar of copper we will never succeed because, in the copper, the outer orbit of the electrons increases in kinetic energy without shifting electrons from one orbit to another. The same effect we will obtain if we try to magnetise a bar of nickel.

Now, let's take a copper-nickel alloy, such as alnickel, and expose it to the EMF of a high-inductive coil. The directional spinning of the electrons' orbit in the nickel does not change, but the orbital spinning of the electrons in the copper reverses its direction. Result: any atom of nickel strongly attracts an atom of copper, creating a bipole.

The energy summation of all bipoles combined creates one of the strongest permanent magnets on the market: alnickel V. Every permanent magnet, then, must be composed of at least two different atoms, one of which is willing to change the orbital spinning direction of the electrons. This type of permanent magnet is not recommended for any therapeutic purpose for the human body.

While, in mice tests, this type of permanent magnet seems to be very promising (Barnothy, Pressman *et al.*), the physical working principle is similar to the H-bond's attraction that holds together the DNA. The tumour in the mouse disappears due to the disassembly of the DNA in the affected cell by the demagnetisation effect of the H-bonds. At the same time, the genetic code of the

healthy cell is also altered and the consequences in the following generations could be very undesirable.

2 – Electromagnetic field

This type of magnetic field obeys the third Newtonian law of motion: for every action, there is always an equal and opposite reaction.

If an iron bar is inserted in the centre of an inductive coil, every electron travelling along the coil wire forces one electron in the iron bar to travel in the opposite direction. This type of magnetic field is not recommended for any therapeutic purposes. Indeed, it has been proven to be detrimental even in mice tests.

Electrons flowing along the magnetic coil will shift electrons from one part of the body to another. In this process, RNA-type viruses of negative polarity will be shifted from diseased cells to healthy cells in the same fashion as the electrons.

Furthermore, the shifting of electrons deprives the healthy cells of the energy necessary to support life and will produce severe side effects of dizziness that will last for several days thereafter.

3 – Electrostatic attraction

When we rub a bar of hard rubber or a bar of amber, one acquires electrons in excess and the other loses electrons from the outer shell orbit. Consequently, one will attract particles rich in electrons, the other will attract particles poor of electrons. This type of magnetic attraction is not recommended because one will weaken the energy of normal cells, the other increase the negative potential of the skin of the cancer cell, thus facilitating the growth of the cancer.

…in the normal process of life, when a new cell is produced, the orbital electron spinning of the new cell assumes a direction opposite to the one of the mother cell in order to maintain the mutual attraction.

4 – Thermomagnetic field

The thermomagnetic field is the product of the Thompson–Peltier effects combined, known in physics as the Seebeck effect.

The thermomagnetic field is responsible for the general gravitational system: heat (sun) attracts cool (planet) and vice versa.

According to Dotto law:

$$F = G \frac{M/M^{11} \Big/ \sqrt{1 - \left(\frac{K/\text{Famu}}{K^{1}/\text{Famu}} \frac{4}{3}\pi\right)^{2}}}{R^{2} \Big/ \sqrt{1 - \left(\frac{K^{1}}{K^{11}}\right)^{2}}}$$

K^{11} = warmest body
K^{1} = coolest body
Famu = 1.00759
famu = 0.000055
$G = 6.66 \times 10^{-8}$ cm³ g⁻¹ sec⁻²

The Newton Law of Attraction $F = G \frac{M/M^{11}}{R^{2}}$

can be applied only between two masses having the same temperature.

This type of magnetic field is the only type of energy proven to be beneficial to animals and humans. Since humans for millions of years have lived in this constant magnetic or gravitational field, the body has become very sensitive to any variation.

• Thompson effect

One end of a copper rod is heated and the other is cooled. If the hot side is heated high enough, it will thermally increase the kinetic energy of the outer orbit electrons to a point where their kinetic energy (1/2 mv^2) will be greater than the work function and allow them to discharge into space.

Due to the copper conductivity, the electrons, instead of dissipating into the air, will shift in tremendous quantity toward the cool side in straight lines, following the heat propagation velocity. By reaction, excited electrons from the cool side will travel in the opposite direction at the speed of a particle (1/2 mv^2) toward the hot side, encircling the copper rod by gyroscopic phenomenon and following Fleming's rule.

The product is very low voltage (a few millivolts) as a resultant of the electrons travelling in circular motion. But, as in any electrical circuit, the EMF in the copper rod is governed by Ohm's law (E/R = I) and will be in the range of several thousand amperes.

• Peltier effect

In a metal alloy bar (such as constantan, 60% Cu, 40% Ni), one end is heated and the other is maintained cold. When the hot end is heated enough, electrons of nickel and copper atoms become excited. The electrons of nickel force the electrons of copper to reverse orbital spinning (as described in section 1 on the permanent magnet). By centripetal force, electrons from the cool side shift toward the hot side. The hot side becomes negative in respect to the cold positive side—exactly opposite to the Thompson effect.

Of course, the Thompson and Peltier effects are temporary; they last only until the proportion between the cool and the hot side reaches the electrons' numerical balance.

• Thompson–Peltier effect

Let's now combine the Thompson and Peltier effects together in the thermocouple fashion. In the Thompson effect, the electrons move from the hot side toward the cold side. In the Peltier effect, the electrons travel from the cold toward the hot side, and back to the hot side of the copper to complete the circuit. The temporary phenomenon of the Thompson–Peltier effect now combined becomes permanent for as long as the temperatures of the hot and cold junction are maintained unbalanced. In physics, this is known as the Seebeck effect.

Let's now reduce the Peltier effect rod to the minimum possible length according to the equation Con R = Cu Rx *pi*. The electrons, in the reaction phenomenon described in the Thompson effect, instead of travelling toward the copper hot junction will be attracted by the centripetal force of the electrons spinning in the Peltier effect, and the free electrons in the Peltier effect will be attracted by the hot junction of the Thompson effect.

Furthermore, to obtain a sawtooth effect of a unijunction transistor, a silicon pellet is added between the two cold junctions and the EMF becomes unidirectional, with oscillatory frequency of approximately 1.9 megacycles.

In this condition, 95 per cent of the EMF travelling in linear velocity motion equal to the heat propagation will be accelerated time and time again by the hot side of the Ring, and the resulting kinetic energy in the orbital electron spinning will be so great that the various electron shells will travel on the same orbital plane. As a result, portions of the atom proton energy will be exposed toward the centre of the Ring. The phenomena, then, that occur in

Continued on page 82

THE DOTTO RING

A HEALING, AGE-REVERSAL DEVICE

Dr Gianni Dotto applied his understanding of DNA to his Ring device, which acted as an inductive coil to recharge the cells to their correct energy level and promote longevity.

Part 2 of 2

by Dr Gianni Dotto © 1972

Notes by
Jerry Decker of KeelyNet

From the KeelyNet website at:
http://www.keelynet.com/
biology/dotto.htm

Editor's Note: This edition we continue the 1972 paper by Dr Gianni Dotto on his Ring device. Commentary is provided at the end of the paper by Jerry Decker, who has posted the complete text and some diagrams on the KeelyNet website (at http://www.keelynet.com/biology/dotto.htm). Note that several mentions are made to animal experiments. NEXUS does not agree with the practices of animal experimentation and vivisection, but we also don't want to censor the articles we publish.

THE AGEING PROCESS

To understand the human ageing process, let's now examine the structure and the function of the DNA. Imagine a flexible ladder one metre (39 inches) long, composed of six billion steps. Each step has the form of two capital Ts facing each other. The horizontal line of the T has 70% of its length made of sugar and 30% of phosphate. The vertical line is of a different composition: adenine or guanine, or thymine or cytosine.

At the vertical ends of the T, there are atoms of hydrogen. (The hydrogen, first element in the atomic chart, is composed of one proton and one electron.) At the end of the phosphate rod, the orbital electrons spin clockwise. At the end of the sugar rod, the orbital electrons spin counter-clockwise. In the hydrogen atoms at the end of adenine and thymine, the electrons spin clockwise; and in the hydrogen atoms at the end of guanine and cytosine, they spin counterclockwise. This type of T is called a *base* or *nucleotide*.

The DNA is then formed by 12 billion nucleotides facing each other and connected in a straight line to form the double helix—deoxyribonucleic acid, or DNA. This is the genetic code, and every one of the 6.3 trillion cells of the human body has at least one. To form a new cell, the DNA must repeat itself. This is accomplished by splitting the ladder along the middle of the step and reforming two DNAs absolutely identical and in the same sequence. To form two DNAs, another 12 billion nucleotides are necessary.

Inside the cell nucleus there are constantly at least eight different types of virus: four RNA types (negative charge), and four DNA types (positive charge). Every pair of virus (one RNA and one DNA type) attracts each other to form a bipole. They do so, first, to protect themselves against any external magnetic disturbance, and, second, to accumulate energy in the following manner… Inactive viruses are crystal forms, but in active status, such as inside the cell nucleus, they reveal one RNA or DNA core covered with protein. Of course, even in active status they still maintain all the properties of a crystal, and as a crystal they are very sensitive to the high sound frequency.

Under sound frequency up to five megacycles, the two viruses continuously strain each other and produce energy due to the piezoelectric effect (the same principle is used in the energy conversion effect of the supersonic generator). In the ultra-high sound frequency over five megacycles, an isolated inactive virus can be excited to alter the transition temperatures or Curie point and disintegrate (Ruben). The human DNA (like a Yagi antenna, one metre long) is tuned to any radio emission between 375 and 385 megacycles.

Furthermore, the DNA is under the constant influence of charged ions travelling through the nervous system and acting as a modulation frequency. The combined action of the two physical phenomena force the DNA to emit a high-frequency sound in the range of 1.9–2.0 megacycles in order to detect, by returning echo, what type of protein is missing in the cell. These sound frequencies are not only necessary to the DNA in scanning the type of RNA to produce, but they also maintain active the virus in bipole form by means of the strain effect.

To control the energy level from the piezoelectric effect, the RNA-type virus covers itself with phosphate and the DNA-type virus with sugar. In forming this special type of coating, the virus—like any living organism—produces waste. These wastes are accumulated in the centre of the rod just formed and will be called adenine, guanine, thymine or cytosine according to the type of virus in the bipole. The process to make the coating is accomplished at the expense of the electrical charge accumulated by the piezoelectric effect. At the end of the charge, to remain active the group of viruses removes the coating that now is in the form of a capital T and exposes itself to the high-frequency sound produced by the DNA, and the process starts all over again.

Due to the described phenomena, the DNA has always enough bases available to produce RNA strains and to reproduce itself.

Now, let's go back to the flexible ladder composed of six billion steps. Suppose we twist this strange ladder so many times as to have only a few steps for every turn of the coil so formed (these steps are called *base pairs per turn*). Since every base has different polarity according to the code formed by past generations, the DNA can be compared to the multi-polarity rotor of an alternator. In the alternator, the speed is inversely proportional to the number of poles and the output power is directly proportional to the energy applied.

At every electrical impulse flowing through the nervous system, the DNA moves back and forth as many degrees as one base is separated from the next one. The more base pairs per turn, the less degree the DNA has to move and the less energy is required to make it vibrate.

Then there are three controlling factors for the DNA to reproduce itself and create a new cell:

1) the kinetic energy of the electron in the H-bonds;
2) the number of the base pairs per turn in the double helix (DNA);
3) the energy and the frequency of charged ions travelling along the nervous system.

That is, the DNA of the embryo cell in the mother womb has 46 base pairs per turn, the kinetic energy of the electrons in the H-bond is weak, and charged ions coming from the mother's body are strong. Result: the DNA produces one cell per second.

After six weeks of pregnancy, the DNA in the cell of the embryo has 34 base pairs per turn; the kinetic energy of the electrons in the H-bonds increases, the charged ions from the mother are unchanged, the DNA produces one cell every minute, and so on. By the time the foetus is in the 10th lunar month, the single DNA (half from the mother, half from the father) has already reproduced itself more than six trillion times.

When the baby is born, the slowing process of reproduction increases. At the age of two, the DNA winds again to have 22 base pairs per turn, 14 at the age of 21, and 10 at the age of 35. From the age of 35 to 55, the 10 base pairs per turn in the DNA do not change. At approximately the age of 55, the base pairs per turn are reduced to six. By this time, the kinetic energy of the electron in the H-bond and the energy of the charged ion become very weak, the DNA stops reproducing itself and the ageing process begins.

To slow down the body ageing process, three factors must be considered:

1) Ways of stretching the DNA to increase the base pairs per turn back to 10, by means of energy in motion up and down along the body, as in the Ring device.
2) Ways of increasing the electron kinetic energy in the H-bonds by means of proton pulling force. The proton energy available (as previously explained) toward the centre of the Ring is high enough to attract (in the vacuum) one electron 20 feet away.
3) Ways of increasing the energy of the charged ions in the nervous system by means of exercise and proper diet.

By this time, the kinetic energy of the electron in the H-bond and the energy of the charged ion become very weak, the DNA stops reproducing itself and the ageing process begins.

Cancer Cell Formation

At this point, it is necessary to clarify one important factor that is the basic secret of life creation. Without explaining the working principle of this secret, we will never understand the vital importance of the homogeneity and orientation of the magnetic field in the human body.

All the 6.3 trillion DNAs of the human body are absolutely identical; all are tuned to the same resonance frequency; all have exactly the same genetic sequence code. Yet the 6.3 trillion cells in the human body, where each DNA is enclosed, are all different, and each one of these cells fits exactly the proper place and functionality in the human system. How is this possible?

The human DNA, as mentioned before, is approximately one metre (39 inches) long and has six billion steps formed by 12 billion bases. The entire length of the DNA is necessary to maintain and transmit from generation to generation the entire genetic code. Yet only a portion of the DNA (different in every cell) is used to create a specific cell. How is this accomplished?

Suppose we have a thread one metre long. On this thread we insert 46 nylon light beads half an inch long. Let's insert, now, this strange chain in the centre of an electrostatic tube with bipole orientation. After a few seconds, all the nylon beads will be charged with the same electrostatic energy and they will repel each other, leaving an interspace between them. They will repel each other, but not with the same force. The interspace between the static charge will be shorter; gradually, toward the opposite polarity of the tube, the interspace will be longer. The only part of the thread we see is the part not hidden by the beads.

Let's now call the thread DNA and the 46 beads chromosomes. Since the chromosomes act as a shield, the only portion of the DNA that controls a specific cell is the one of the interspace between the chromosomes, which for every cell has a different length according to different magnetic intensity, polarity and orientation in the human body. Each chromosome encloses 1,250 DNA lengths (genes), and each gene is formed of 100,000 base pairs (microgene). Of the total six billion steps of the ladder (DNA), only 250 million are really controlling the cell life.

The chromosomes appear immediately after the DNA is formed and they disappear when the cell is completed and just before the DNA is ready to repeat itself, to appear again only in the new DNA. If the chromosomes of the new DNA, due to the phenomena previously explained have the wrong interspace sequence, it is quite possible that the DNA will produce, say, in the neck, a cell that belongs to the kidney or vice versa. This can be called *cancer*.

Furthermore, like in a musical instrument, the sound produced

by the DNA in the scanning system has different harmonics according to the chromosome's interspace. The virus responsible for the creation of nucleotides in a different group of cells of different harmonics, adjusts the equilibrium potentials of the component charges in the crystal lattice. This pressure effect in the electrical field distribution governs the final crystal structure of the many compounds of the virus.

If a group of RNA-type virus with a final crystal structure as a result of harmonics of one group of cells is transferred by means of electromagnetic reaction in a different group of cells, under the influence of the new harmonics, it will alter the transition temperature (Curie point). In this transaction, it will lose the protein coating and release the core RNA to control the protein creation in the new cell (Ruben). As a result, a new type of cell will be created that is different from any surrounding cell, and this also will be a cancer cell.

From the above-described phenomena, well known in physics, the Temin theory that the RNA-type virus uses its own RNA core as a template to modify the structure of the genetic code and create the reversal of the DNA is absurd. If the phenomenon exists, it could not be a creation of the present civilisation but has existed from the beginning of time. And there are no records available of claims of apes deriving from humans.

Theories #1 and #4 of the introductory explanation support the principle that some forms of cancer and leukaemia are caused by isolated virus. In this case, a physical principle known as the *pyro-piezoelectric effect* will be the solution to the problem.

If a Rochelle salt crystal is rapidly cooled from 25°C to 0°C, the polarisation increases so fast that the normal conductivity cannot bring about equilibrium, and a transient potential as great as a thousand volts can be produced between the two electrodes contacting the crystal (Ruben).

Since, in the isolated virus crystal, the RNA- or DNA-type core acts as an electrode between the two poles, when the voltage potential overcomes the core's DC resistance the energy discharged across it will be so great as to disintegrate the virus core as a common electric fuse.

The same phenomenon, of course, is applied to the joint virus (one DNA type and one RNA type) existing in the cell nucleus and responsible for the DNA creation. Because of the electrical principle that, in an inductance, two joint EMFs opposite and contrary eliminate each other, no voltage will appear across the joint virus.

In an experiment with dying AKR mice (mice carrying leukaemia), a constant laboratory temperature of 35°C was maintained. The cage containing the mice was placed two times a day for 20 minutes each time in a small refrigerator where temperature was kept at 0°C. After five days of treatments the mice were sacrificed, and pathological studies revealed no evidence of lymphosarcoma. A piezobaric chamber, where a temperature body change of 25°C can be obtained in less than one minute, is under construction to repeat the experiment.

Reorienting the Magnetic Field with the Dotto Ring

By evenly re-establishing the orientation of the body's magnetic field, the virus groups responsible for the manufacture of the nuclei (necessary to the reproduction of the DNA) are bound to stay only in the specific group of cells tuned to their own resonance frequency, with no chance of spreading to other parts of the body. With the correction of the environmental resonance frequency of a group of cells, a virus out of position will become inactive in the same fashion as a portion of a variable capacitor not facing the stator.

In theory #3 (Dotto), the Ring re-establishes the proper number of base pairs per turn on the DNA double helix due to the phenomenon known as the *Wunder effect*.

In a vacuum, a suspended secondary coil inserted in a primary coil of a fixed number of turns adjusts itself to the same primary number of turns when voltage is applied, with capability proportional to the current intensity and inversely proportional to the square of the spring reaction strength of the secondary coil. This principle is widely applied in automatic tuning devices for modern colour televisions.

By applying to the human body voltage, EMF and magnetic intensity similar to the value existing in the DNA of normal cells (in the human between the ages of 35 and 55), a voltage of 45 to 70 millivolts maintains a linearity of 10 base pairs per turn in the double helix (Crick and Watson). The DNA of the cancer cell adjusts itself to the proper level of functionality, regardless of cell condition, since absorbed energy will be inversely proportional to the existing cell energy level. In the case of six base pairs per turn in the double helix (humans over 55), when the DNA stops the reproduction capability the base pairs per turn are triggered back to 10, and so remain as long as the magnetic intensity is reapplied at least once every 14 days. This results in slowing down the ageing process.

The DNA of the cancer cell adjusts itself to the proper level of functionality, regardless of cell condition, since absorbed energy will be inversely proportional to the existing cell energy level.

Another important factor must be clarified. In widely known mice experiments (Pressman, Barnothy), a combined action of a constant permanent magnetic field and microwaves in the gigacycle range proved to be very efficient in causing tumour recession in mice. This phenomenon is caused by the disturbance action of the microwaves on the normal orbital spinning of electrons in the DNA H-bonds. But we must not forget that to humans we must give the right to live, not merely to survive.

However, frequencies in the range of 1 to 3 megacycles and modulation frequencies of 80 to 200 kilocycles are known to penetrate deeper into the human body and be capable of breaking the thin skin of the cancer cell without jeopardising the DNA code of normal cells (Pressman).

For this reason, the Ring is pretuned on the Peltier junction to the average frequency of 1.8 megacycles and modulation frequency of 100 kilocycles to obtain a current fluctuation chopping effect similar to a unijunction transistor. The Ring is also a 350- ohm television antenna, where the lower band resonance is tuned to a VHF (Thompson effect junction) and the upper band (Peltier junction) is tuned to a UHF resonance. The upper frequency then maintains, on the correct level, the activity of the normal cell, while the penetrating low frequency neutralises the activity of the cancer cells.

Theory #2, which postulates that cancer cells to some extent may be considered as parasitic cells, is proved correct as far as the Ring is concerned.

The Ring is an inductive coil. In the motion along the body, the

Ring recharges the cells to the proper, desired level. While the normal cells retain the charge, the cancer cells behave like a faulty battery. At the passage of the Ring, the temporary magnetic charge collapses in the same fashion as transformer lamination. This collapsing effect is detectable by electrodes of an EEG sensitive to electrical brain impulses. By synchronising a recorder to the Ring velocity, the location of the collapsing tumour can be detected with a five-centimetre accuracy.

Many years of investigation have proved the Ring to have no detrimental or side effects. On the contrary, it has proved to be very helpful for people who have suffered from exposure to radiation, cobalt, linear accelerators, etc.

For all the reasons stated above, the Ring should be considered primarily as a tool for physicians in disease prevention and disease control rather than as a cure.

[Signed] Dr Gianni A. Dotto
Montgomery County, State of Ohio

The above document was signed before me, a notary public, by the said Dr Gianni A. Dotto, this 8th day of February, 1972.
[Photocopied signature unreadable] – Notary Public

NOTES FROM JERRY DECKER OF KEELYNET

Years ago I had the pleasure of knowing Arthur Coleman, at one time a key research scientist in Research and Development at Rockwell International. Arthur had a small research lab in Rockwall, Texas, and he was part of our group in Dallas. Arthur was a brilliant engineer and scientist, having developed an iontophoretic device for treating all kinds of disease conditions. In his lifetime, he had been involved with many unusual experiments, some he could only hint about.

Other reports claim that Sloan-Kettering removed all funding and destroyed the machines because they actually cured cancer!

One of these was this mysterious Dotto Ring which was said to heal cancer and reverse ageing. After two years of teasing, one day he called me about meeting for brunch, saying he had something for me. We met and he said he had decided to give me a copy of the Dotto papers, explained them and asked me not to post them publicly as they had been handed to him in confidence on a trip to Washington for consulting. I promised.

About five years later, I happened to be at a conference where my friend Dr George Friebott was speaking. After his presentation, we went to lunch and I asked if he'd ever heard of the Dotto Ring. George said he had, and later showed me a copy of the same papers Arthur had given me.

On my return to Dallas, I called Arthur and told him about it. He said that now that it was finally out, I could do with them as I pleased. They were then shared with friends and other networks as well as presented on several occasions over the eight years of the Dallas Roundtable meetings.

NEXUS printed a version of them some years ago [see vol. 2, no. 9, August–September 1992]. I'd mailed out many copies to people who requested them but I never found time to put them online, so here they are. I do see they're being sold elsewhere.

Some correlations and concepts you might find of interest:

• David Hudson claims that monoatomic elements are superconductive and so can store energy. He believes that, when ingested, they lodge in the tissues and enhance the energy of the "aura", or Kirlian field, which in his opinion is a result of dynamic superconductivity. I like to call it an *attenuated dynamic Meissner field*. It turns out that new, growing tissues are in fact superconducting, so, over time, ingestion of this material is supposed to heal and change your body. I have no direct experience or trustworthy reports about this, but I remain intrigued that a *pure current*, as superconductors possess and which has little if any voltage (produced by resistance), is exactly what Dr Dotto produces with his Ring.

• Nature tends to seek equilibrium; therefore, immersing a body in a high-energy DC magnetic field would cause an energy transfer which would "pull up" the energy in the body due to the "enriched" background. In this case, I think it could well "brighten" the aura or the Meissner field, which is produced by superconductivity.

• Nordic people have been reported to sit in a hot sauna for a period, then run out naked and roll in the snow. Others jump into freezing water after a hot sauna. Note Dotto's mention of the piezoelectric effect where high voltage can be produced inside the body from drastic, rapid, temperature changes. Arthur told me he had bought a metal coffin with the idea of lying in a bath of hot water, then rapidly flushing it with cold water and repeating it as with the mice experiment quoted above. The mice were exposed to 0°C for 20 minutes, but humans might take longer because of the thickness of the body. The point is to create as rapid a temperature change as possible.

There are reports that the Ring technology was suppressed because the machines would levitate from the floor due to the high magnetic field repelling against the Earth's field. Other reports claim that Sloan-Kettering removed all funding and destroyed the machines because they actually cured cancer! We can't have that: cancer is a very lucrative business!

The last I heard, Dr Dotto had moved back to his family castle in Italy, was now in his 80s and, shall we say, immersed in religion.

Arthur Abraham Coleman passed away at 73 years of age on October 23, 1997 in Rockwall, Texas. He is best remembered for his invention of the chemical milling process for bonding metals together (which is used on most airplane wings) as well as his remarkable electrotherapy device (used by many doctors).

The Dotto Ring US patent number is 3,839,771 (Method for Constructing a Thermionic Couple). Dotto's Electrostatic Wand patent number is 3,785,383. If you have additional information or updates regarding the Dotto Ring or related technology that you would be willing to share online, please contact Jerry Decker. Thanks!

If you found this file useful or interesting, please consider a donation or a purchase to help keep KeelyNet online and providing free information. Even a dollar will help. Others sell it; we prefer to share it! ∞

Editor's Note:
This file was posted on December 17, 2001, and is reproduced with permission from Jerry Decker of KeelyNet. Contact: KeelyNet, PO Box 111786, Carrollton, Texas 75011-1786, USA, email jdecker@keelynet.com, website http://www.keelynet.com.

The Dotto Ring: A Healing, Age-Reversal Device

Continued from page 41

the Ring Device are unique in their nature and not replaceable by any artificial means.

In the Ring Device, the following phenomena can be detected:

1) The voltage is maintained at a minimum of 25 to 45 millivolts. This EMF will produce 120 gauss at the Ring circumference and 10 gauss at the centre of the Ring. This is approximately five times the Earth's magnetic field. This magnetic field is sufficient to maintain the orientation of the human body, but too weak to jeopardise the orbital spinning in the H-bonding of the DNA.

2) In the electromagnetic field and permanent magnet, the electrons travel from the south toward the north pole. If this type of magnetic field is applied to the human body, it will have the same deteriorating effect as if the jumper used to start a car is connected to the opposite polarity of the battery. In the Ring, the EMF travels from the positive pole toward the negative in the same fashion that dry batteries are instantly charged by inductive methods.

3) Like in any electrical circuit, the energy across the Ring is regulated by Ohm's law, where E = .045 volt, R = 5 x 10 to the negative 6th, and I = 9,000 amps, as explained before.

It is quite obvious that there is enough energy to supply every one of the 6.3 trillion human cells the proper energy needed. The energy from the Ring is transferred to the body by an inductive method similar to the one used to instantly charge a dry battery. During the treatment, the Ring is maintained at constant slow motion of 1.5 inches per second. This velocity is sufficient to cause energy transfer from the Ring to the body by inductive method, but not fast enough to create any disturbance to the electron orbital spinning in the DNA H-bonds. In the process, the parasite cells (cancer cells) are also charged to the energy level of the healthy cells, and like a faulty car battery they release the energy and reverse polarity at each end of the inductive effect.

Four to five passages of the Ring near the tumour are sufficient to deprive the cell energy and to reverse the orbital spinning of the electrons in the phosphate bonds. In this condition, the bases of the DNA repel each other and the DNA dissolves. At the end of the cell life-span, the tumour disappears. Of course, for the Ring to be effective, the treatment must start when the disease is first detected. Radiations of any nature prior to the Ring treatment will accelerate the orbital electron spinning in the DNA H-bonds and will jeopardise the benefit of the Ring treatment.

From the above clarification it is quite evident that the Ring Device does not remagnetise, reorient and homogenise the magnetic field in the body by external magnetisation, but by energy transfer in the inductive fashion. Let's explain with an example. Consider an electric generator where the rotor is formed of a plurality of magnetic poles. If the rotor is rotated by external means, the coil winding of the stator absorbs and transfers EMF at the expense of the magnetic pole (electric generator). If EMF is supplied to the stator winding, the rotor generates power (electric motor) at the expense of external EMF, while the magnetic pole of the rotor will gain intensity.

The human body is like a rotor with an infinite number of poles, DNA frequencies, field orientations, etc. By applying energy from the stator (Dotto Ring), the body will create power while the magnetic level,

Book on Dotto (only available in Australia)

The Amazing Story of Dr. Gianni Dotto and the Dotto Ring / John West

REQUEST ORDER A COPY

Bib ID:

2087706

Format:

Book

Author:

West, John (John E.)

Description:

- Bundaberg, Qld : Veritas Press, c1994
- 14 leaves : ill., ports. ; 30 cm.

ISBN:

0958813175

Notes:

- Includes bibliographical reference.
- NLq 615.845 W518 copy Digital master available National Library of Australia

Subject:

- Dotto, Gianni
- Thermomagnetism
- Magnetotherapy

Copyright:

In Copyright

The Amazing Story of Dr. Gianni Dotto and the Dotto Ring

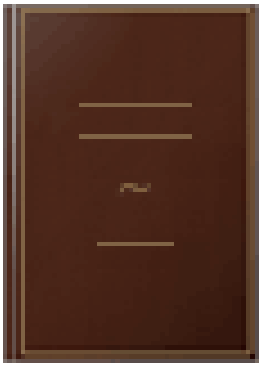

John E. West

Veritas Press, 1994 - Science - 28 pages

Bibliographic information

Title	The Amazing Story of Dr. Gianni Dotto and the Dotto Ring
Author	John E. West
Publisher	Veritas Press, 1994
ISBN	0958813175, 9780958813174
Length	28 pages
Subjects	Science › General

Video on Dotto Ring and Possibiliy it Levitated

https://www.youtube.com/watch?v=CHwShnuIB_w

- Note: Current of 30,000 amps is assumed in the video analysis, and this is too high (see my analysis).
- He says that the ring width and thickness are not specified, but they are specified at the values he is using (9” wide and 0.5” thick).

Appendix K. Technical Autobiography

Below is a summary of my technical training and awards:

GE & Lockheed Martin Training Courses

- GE A, B, C Advanced Courses in Engineering
- Introduction to Sonar
- Sonar Adaptive Space-Time Signal Processing
- Advanced Matrix Theory and Adaptive Processing (1982)
- Discrimination and Classification
- Digital Signal Processing (MIT)
- A Second Course in Signal Processing, 1988 (Cornell University)
- Fundamentals of Turbulence (1991)
- Underwater Acoustic Modeling and Sonar Performance Prediction (1992)
- Submarine Operations
- C++ Programming
- Signal Classification and Recognition (1994)
- AN/SQQ-89 Sonar System (1999)
- Advanced Tracking Algorithms (2014)

General Awards & Memberships

- BSEE degree, Summa Cum Laude, 3.84 GPA, 1st in University Class, University of Hartford
- MSEE degree with 4.0 GPA - Syracuse University (SU), Syracuse, New York (1983)
- National Broadband Processing Working Group, Leader
- National Defense Industrial Association (NDIA) Technology Working Group
- Member, Syracuse NY Advanced Technology Working Group
- CRC Chemistry Award for Highest GPA in College Chemistry
- President of University of Hartford Microprocessor Club
- IEEE member
- Rube Goldberg Award in IEEE Energy Efficient Vehicle Contest (1977)

Lockheed Martin/Martin Marietta/General Electric, Syracuse, NY

- US Patent 8,816,632 B2 Award, 2011 (Jointly with D. Winfield and F. Rotundo, Radio Frequency Power Transmission System)
- Trade Secret Awards, 2009
- Named Lockheed Martin Fellow, 2006
- Special Recognition Awards, 2004, 2010
- USS SRA Team Award, DD(X) Integration, 2005
- Department Award - Tech Ops, 2001
- Program Manager's Awards, 1997 & 1998
- ASTECS Proposal Extra Effort Award, 1995
- Recognition Awards for Valued Employees (RAVE), 1991 & 1994

- Section Manager's Award, 1992
- Stock Option Award for Valued Technical Contributors, 1992
- General Manager's Award, 1991
- General Manager's Technical Excellence Award, 1988
- Named Engineer of the Year, 1988
- Graduated First in GE A, B & C Advanced Courses in Engineering (ACE)
- GE Edison Engineering Program Graduate

(Note: most awards and memberships in junior high, high school, and college are not listed)

Technical Autobiography Highlights – John Smigel

I first started having a passion for learning math, science, and English in about 6th grade (age 11). In 6th grade I was selected along with about 3 other students to form a special language skills class that met outside of normal classes. We trained outside normal class time on reading, information retention, and literacy.

However, I had a learning setback in 7th grade. I still remember the test we were given to determine which of the 3 "smartness" class levels to which we would be assigned. The levels were J, F, and K (for John F. Kennedy). J was for smartest, F was average, and K was below average. I do not do well with timed tests; I will not stop trying to answer a question until I'm sure it's correct. Therefore, I didn't finish all of the test. I knew my parents were extremely disappointed that I was not assigned to the smartest level, but only to the middle, F, level. However, I did achieve many scholastic awards in junior high school and was near the top of the class.

I became interested in quantum and atomic physics, avidly reading library books on these subjects. But I had a 7th-grade science project disaster. I created a simulation of an atomic chain reaction. This was a box containing mouse traps (set) and ping-pong balls, sealed with plastic wrap on top. Adding a single ball through a hole started the chain reaction. Unfortunately, before classes started, older students stole my project from the classroom before it was evaluated and had much fun with it. I was scolded, disciplined by the nuns, and failed the project because ping pong balls and mouse traps were all over the school!

I also started excelling in math in 7th grade, Mrs. Dufault's class (fortunately not a nun & I had a bit of a crush). Whenever she asked any question, I would raise my hand, anxious to answer. She eventually told me, "Don't raise your hand any more John, I know you know the answer." I'm pretty sure I would have been considered a "savant" in math and "on the spectrum", equally lacking in other skills, including social, geography, and art (the only D's I ever received were in geography and art from sister Nancy).

Unfortunately, the "smartness" group you were assigned in junior high (grades 7-9) also determined your placement in high school (grades 10-12). I was not initially assigned to the advanced, college-bound tier in high school, also to my parent's dismay. Rather quicky, my teachers recognized that was a mistake. I was only assigned to the basic

geometry class with Mr. Argassi. I was so much above the other students that it became a problem for him. I always immediately knew all the answers and scored perfect on every test. The other students became aware of this and constantly tried to copy my answers. Eventually, Mr. Argassi separated me from the class during tests and placed me in a different adjacent room. I graded other tests for him during the tests, rather than having to take any tests. He and my other teachers soon had me transferred to the advanced college-bound classes/curriculum.

I LOVED math, physics, chemistry, and biology in high school. I also developed a passion for computers and programming. At that time computers and programming were not used or taught in school; but the school was starting a plan to introduce them. There were not any "personal" computers yet, just some portable computers (basically large fancy calculators) and teletypes connected to remote main-frame computers using telephone dial-up modems. Apparently, teachers recognized my extreme nerdiness because I was singled out to try the new school computers. I did this after school. There was a stand-alone computer (probably a Wang, like my physics teacher, Mr. Leiper owned) in the back left of Mrs. Parton's room (my advanced algebra teacher). I was the only student taught and trained how to use it. There was also a teletype terminal at the front right of our physics classroom. Mr. Leiper taught me how to use that too. I was the only student trained on computers at that time (1974-1976).

As part of this training, I taught myself the BASIC computer language and became obsessed with a Star Trek program available on the teletype (being a Trekkie of course). The Star Trek game was originally developed in 1971: See history here: https://en.wikipedia.org/wiki/Star_Trek_(1971_video_game). You could enter commands like "Fire Phasors" and the program would tell you what happened. There was a random aspect to the game and what happened.

My obsession with computers and programming continued into college at the University of Hartford. I was in the Electrical Engineering program and quickly found the computer center that contained a Data General Eclipse minicomputer, 2 teletypes, a line printer, a card reader, and some card punch stations. I immediately started learning everything I could about the equipment. I lived at the computer center. I was there when it opened and they had to kick me out when it closed. I took the dozens of extra technical manuals home and had a stack of manuals about 4 ft high, and read them cover-to-cover. Fairly quickly, the computer center decided to hire me as a computer operator, my first real job. I helped start, shut down, and maintain the equipment. I also helped other students with programming and operating the equipment.

I wrote a Star Trek game version (based on my high school experience) that ran on the teletypes. At first there were no video terminals connected to the computer and all programs were entered with hole-punched cards. When I was working as computer operator, the center obtained a single new type of computer interface device called a video display terminal (VDT) that had a video/CRT text display and a keyboard. At first only the operators were allowed to use the one new VDT. I modified my Star Trek

program to run on the VDT and created video effects by writing and erasing characters all over the screen. The phasors were especially popular. I believe this was one of the first modern-style computer video games ever created. The head operator distributed my game (without asking me) to all other universities in the USA that had Eclipse minicomputers via the Eclipse user's group. I was told that my game (called Star T) became very popular at larger schools (including Northeastern) with multiple video terminals. Many years later, I went to a PC game exhibit at the Everson Museum in Syracuse, NY that featured what was credited as the first and most successful PC video game. It was a PC video Star Trek game that was suspiciously very similar to my Star T game.

I also started writing a visual computer chess game in assembly language, but never finished. I got to the point where I could draw a chess board on the VDT and determine all the valid moves. I probably would have needed more memory to make implementation practical; 64K bytes of core memory was a lot at that time. We started the minicomputer every day in the morning by entering a binary bootstrap program into core using 64 toggle switches on the front panel.

After graduating 1st in my university class, I got a job with General Electric in Syracuse in their 3-year Advanced Course in Engineering (ACE). The ACE was considered the most grueling and difficult engineering training program in the country. This included getting a master's degree in electrical engineering at Syracuse University (SU). I continued to over-achieve, getting the highest grade on every weekly project and course. My weekly reports were saved and stored as the "model correct answer" for most projects. Other students hated me, especially in classes at SU where grades were on a curve and the instructor showed the grades. In SU matrix algebra class, I single-handedly caused students to drop out (fortunately not ones in the ACE).

My first 6-month rotating job assignment was a blast. I worked in test equipment engineering for Al Landry. I became his personal pet because I was good at BASIC computer programming, a new tool for him. I developed several computer programs to help him manage the department, including an inventory manager and a construction lab scheduler/tracker. I designed and built (or had built by our model shop) many pieces of custom test equipment that were used to test the sonar and radar products we manufactured. I became the person interfacing with the model shop and tracking status using my BASIC programs.

My next assignment was developing a detailed combined radar and missile simulation to determine the most efficient radar techniques to use against anti-radiation missiles (ARMs). After that, I developed software specifications for sonar automated detection and tracking algorithms. I also worked on developing Enhanced Modular Signal Processor (EMSP) technology. I implemented and sized key algorithms in the new technology. My next assignment was in Solid State radar (SSR) systems engineering on the AN/TPS-59 final integration and test team. I wrote the final technical document for the radar and helped perform radar calibration and first article flight tests, required for

customer acceptance. Because of my job, I had special radar test data access that was output using a special connection to a time-share computer and stored on 9-track tapes. Radars at that time did not have the storage or processing power to do real-time automated detection and tracking. All detection and tracking were done manually by the operators on the plan position indicator (PPI) display. I obtained raw radar output data and developed an automated detect and track program for the radar output, based on my sonar experience. This was new technology for radar and it helped find some unknown problems with our new AN/TPS-59 radar.

For most of the rest of my career, I worked in Advanced Engineering for Don Winfield, responsible for developing and evaluating new technologies. I developed several new breakthrough technologies based on adaptive beamforming. This included a new algorithm for passive submarine detection and a technique for evaluating towed array self-noise. I was still very young and unknown. My adaptive beamforming mentor, Dr. Ayhan Vural, thought my algorithm was so good that he presented it to the Navy at the Naval Underwater Systems Center in Connecticut (at that time – later moved to Rhode Island). I was shocked at the number of people who attended the presentation of my new algorithm (in an auditorium). We were discouraged from publicly disclosing any of our new technology. I submitted a patent disclosure for my algorithm to our patent attorney; but unfortunately, it was too late by the time they discovered he was negligent and not processing any disclosures into patents. He was immediately fired. That is why I don't have more patents. Eventually, another Navy lab engineer who attended the above presentation developed a similar non-adaptive algorithm that was implemented in all the sonar systems. It was considered one of the best new algorithms and made him a rock star. It is probably still used. My version was even better. I'm not bitter.

I was assigned to a team working for the defense department to determine if a particular classified technology could be developed (and possibly used against us). We (GE) were responsible for the main design and construction. Another part of the team was from a government-contracted company (ARETE in beautiful La Jolla, CA) with the country's smartest people in signal processing (led by Dr. Craig Holt) who were tasked with developing an optimal (maximum likelihood) algorithm. I also developed our best algorithm and a detailed simulation to test the algorithms. I remember checking the math of ARETE's algorithm at home near Syracuse, NY on our picnic bench in my spare time. It required one equation that was several pages long. My algorithm performed as well as ARETE's "optimal" one (or even better), with much less computational requirements. I won. The head of ARETE soon flew across the country to meet me (at GE) and try to convince me to come work for them. I stayed with GE and was responsible for signal processing implementation. I did the successful field system installation and testing on a submarine out of San Diego.

I developed a reputation as an expert in advanced adaptive signal processing algorithms and able to perform seemingly impossible tasks. We teamed again with the Navy and GE corporate research and development to demonstrate a new massively parallel computer technology (iWARP). I was responsible for defining the adaptive algorithm

for the iWARP demonstration. It was successfully tested on a submarine. A classified journal reviewed my algorithm as "one of the most significant advances ever achieved." Most of the technology I have developed is classified, so I can't describe it here, except in vague, unclassified terms.

Due to my hard work and success, my boss let me replace him as GE's representative with both the Syracuse Advanced Technology working group and SU's Center for Advanced Technology. Here is SU's history blurb on that:

> The Center for Advanced Technology in Computer Applications and Software Engineering was created in 1984 under the leadership of Dr. Bradley J. Strait, professor of electrical engineering, who served as dean of the college from 1981-1984 and 1989-1992. The Northeast Parallel Architectures Center, an interdisciplinary center for high-performance computing, followed in 1987, and the Center for Hypersonics, supported by NASA to focus on studies in air and space travel, was created in 1993.

I participated in Syracuse and SU meetings discussing emerging technology. We worked with SU's Northeast Parallel Architectures Center (NPAC) and funded them for projects evaluating computing technology with our algorithms. SU's NPAC was on the team developing the World Wide Web (WWW) for the internet. I was able to communicate with them through something called email and they showed me how to access the WWW using a prototype Mosaic web browser they gave me. There was nothing on the WWW yet, but an empty site they called a web store. They had a person they called "The Oracle" who guided their vision of the future. His top-two visions for the WWW were on-line shopping and streaming media on demand rather than the broadcast channels of that time. These were revolutionary ideas at that time. Due to my background, I also envisioned multiplayer computer games and social media applications. I was a member of one of the amazingly-popular dial-up computer bulletin boards (social media of the time) and played a multiplayer game called Barren Realms Elite. I dreamed of creating multiplayer games and a social media app for the WWW. I started developing a graphical WWW social media app based on a free bulletin board package, but never had time to finish. I did recently finish a multiplayer WWW game app, JLMahJongg, in 2024.

Another project for which I received an award is a proposal effort for a new Navy shipboard electronic support measures (ESM) system (called ASTECS in 1995). This was a new business area that we were trying to break in to. An external team of ESM algorithm experts were called in to help define the algorithms and write the technical proposal. I was called in by the red team proposal reviewers to fix the technical proposal that was considered horrible. I worked with the experts to learn about ESM algorithms and rewrote the proposal. We won the proposal; and that started a major new multi-billion-dollar business in Syracuse that is still going.

When GE's defense business was sold to Martin Marietta, their San Diego office that developed new technology had just started a major joint program between the Navy and

industry to develop a lightweight, broadband, variable-depth sonar (LBVDS). Note the references to my joint-Navy publications in this link. I had already developed a prototype environmentally-adaptive sonar processor called the Environmental Evaluation Processor (EEP – now a Lockheed Martin product) on my own time and with GE IR&D funds. My processor was selected as the core of the LBVDS processing and I became the processing and analysis lead for the industry-side of this multimillion-dollar project (Sally Sutherland-Pieterzak replaced Matt Tattersall as my partner Navy lab lead). It was like I was a rock star for a few years because this was the only large technology project funded by the Office of Naval Research (ONR). My prototype processor was successfully built and demonstrated; leading to a full-scale production system that was also built and demonstrated. Unfortunately, the LBVDS technology was targeted for the new Zumwalt-class destroyer whose lead was won by our competitors, the Raytheon, Northrop Grumman & General Dynamics team.

Martin Marietta was later merged with Lockheed and became Lockheed Martin. Much of the sonar/radar technology and development was moved to other locations. I decided to switch from primarily sonar to primarily radar. This was difficult since I was not a radar expert at my job level. The most difficult and dreaded job is getting assigned as a large proposal author. I ended up assigned to 2 large radar proposals at the same time, a ballistic projectile classify radar (AN/TPQ-53) and a large surveillance radar (G/ATOR). The AN/TPQ-53 is an improved replacement for Raytheon's Firefinder radars. I was responsible for key parts of both proposals: the classification algorithm in one and the ESM (including anti-jamming) in the other. The current classification algorithm from a partner company was not meeting requirements; so I developed a new algorithm that is considered amazing. It is still used as a key component in this critical Army radar system. I was not an expert in radar ESM. I had to rapidly become an expert to write my assigned proposal sections. We won the projectile-classifying radar proposal, but not the one with ESM (G/ATOR). However, proposal sections were each rated with colors from red (bad), yellow, green, blue, to purple (outstanding). On the G/ATOR proposal we lost, all my ESM sections were the only ones rated purple.

I was scheduled to go away on vacation during this two-proposal period, but told my wife I could not go (In hindsight, a mistake). She went without me and it almost ended our marriage. On the positive side, my hard work and success on these proposals helped get me awarded a Lockheed Martin Fellowship. Being a Lockheed Martin Fellow is the highest technical honor awarded.

I continued working on new radar and sonar technology, including improving the new Space Fence radar algorithms and evaluating my classification algorithm performance for the ballistic projectile classifying radar mentioned above. I was also asked to develop improved technology for US ballistic missile defense systems. I was lead systems engineer for part of a large (multi-billion, decades-long) multi-national project (with Italy and Germany) for a new ballistic missile defense system (approved unclassified description here: Media Release (long), MEADS FT2 (short), and Ad). Part of my responsibility was the environmentally adaptive algorithms, including ESM and

algorithms in the surveillance radar (SR) to counter nuclear ballistic missile threats. The SR was my baby. MEADS was designed for the Army as a major improvement and replacement for the well-known and old Raytheon Patriot missile defense system. MEADS is not currently used (to my knowledge) for mostly-political reasons.

One other notable classified program I worked on was counter-IED technology with Lockheed's Manassas, VA location. I was tasked with developing a new improved device using a technology patented by someone else, but while not infringing on the patent. I quickly learned all about cell phone technology and designed a new counter-IED device for them; however, I did not see how we could not infringe on the patent and still do what they wanted.